43454

National Library of Canada
Canadian Theses Division
Ottawa, Canada
K1A 0N4

Bibliothèque nationale du Canada
Division des thèses canadiennes

PERMISSION TO MICROFILM — AUTORISATION DE MICROFILMER

• Please print or type — Écrire en lettres moulées ou dactylographier

Full Name of Author — Nom complet de l'auteur

BASIL DANIEL PETER KOZIAK

Date of Birth — Date de naissance	Country of Birth — Lieu de naissance
14 / 06 / 56	CANADA

Permanent Address — Résidence fixe

10445 - 85 AVE
EDMONTON
T6E 2K2

Title of Thesis — Titre de la thèse

ANALYSIS OF PRESTRESSED CONCRETE WALL SEGMENTS

University — Université

U/ ALBERTA

Degree for which thesis was presented — Grade pour lequel cette thèse fut présentée

M. Sc STRUCTURAL ENGINEERING

Year this degree conferred — Année d'obtention de ce grade	Name of Supervisor — Nom du directeur de thèse
1979	D. W. Murray

Permission is hereby granted to the NATIONAL LIBRARY OF CANADA to microfilm this thesis and to lend or sell copies of the film.

The author reserves other publication rights, and neither the thesis nor extensive extracts from it may be printed or otherwise reproduced without the author's written permission.

L'autorisation est, par la présente, accordée à la BIBLIOTHÈQUE NATIONALE DU CANADA de microfilmer cette thèse et de prêter ou de vendre des exemplaires du film.

L'auteur se réserve les autres droits de publication; ni la thèse ni de longs extraits de celle-ci ne doivent être imprimés ou autrement reproduits sans l'autorisation écrite de l'auteur.

Date	Signature
2 / 10 / 79.	Basil Koziak

NL-91 (4/77)

National Library of Canada

Cataloguing Branch
Canadian Theses Division

Ottawa, Canada
K1A 0N4

Bibliothèque nationale du Canada

Direction du catalogage
Division des thèses canadiennes

NOTICE

The quality of this microfiche is heavily dependent upon the quality of the original thesis submitted for microfilming. Every effort has been made to ensure the highest quality of reproduction possible.

If pages are missing, contact the university which granted the degree.

Some pages may have indistinct print especially if the original pages were typed with a poor typewriter ribbon or if the university sent us a poor photocopy.

Previously copyrighted materials (journal articles, published tests, etc.) are not filmed.

Reproduction in full or in part of this film is governed by the Canadian Copyright Act, R.S.C. 1970, c. C-30. Please read the authorization forms which accompany this thesis.

THIS DISSERTATION
HAS BEEN MICROFILMED
EXACTLY AS RECEIVED

AVIS

La qualité de cette microfiche dépend grandement de la qualité de la thèse soumise au microfilmage. Nous avons tout fait pour assurer une qualité supérieure de reproduction.

S'il manque des pages, veuillez communiquer avec l'université qui a conféré le grade.

La qualité d'impression de certaines pages peut laisser à désirer, surtout si les pages originales ont été dactylographiées à l'aide d'un ruban usé ou si l'université nous a fait parvenir une photocopie de mauvaise qualité.

Les documents qui font déjà l'objet d'un droit d'auteur (articles de revue, examens publiés, etc.) ne sont pas microfilmés.

La reproduction, même partielle, de ce microfilm est soumise à la Loi canadienne sur le droit d'auteur, SRC 1970, c. C-30. Veuillez prendre connaissance des formules d'autorisation qui accompagnent cette thèse.

LA THÈSE A ÉTÉ
MICROFILMÉE TELLE QUE
NOUS L'AVONS REÇUE

THE UNIVERSITY OF ALBERTA

ANALYSIS OF PRESTRESSED CONCRETE WALL SEGMENTS

BY

© BASIL DANIEL PETER KOZIAK

A THESIS

SUBMITTED TO THE FACULTY OF GRADUATE STUDIES AND RESEARCH

IN PARTIAL FULFILLMENT OF THE REQUIREMENTS FOR THE DEGREE

OF MASTER OF SCIENCE

IN

DEPARTMENT OF CIVIL ENGINEERING

EDMONTON, ALBERTA

(FALL, 1979)

THE UNIVERSITY OF ALBERTA

FACULTY OF GRADUATE STUDIES AND RESEARCH

The undersigned certify that they have read, and recommend to the Faculty of Graduate Studies and Research, for acceptance, a thesis entitled "ANALYSIS OF PRESTRESSED CONCRETE WALL SEGMENTS" submitted by BASIL DANIEL PETER KOZIAK in partial fulfilment of the requirements for the degree of Master of Science.

T. M. Hrudey, Supervisor

S. H. Simmonds

J. R. Colbourne

Date 19 JUNE 1979

ABSTRACT

An iterative numerical technique for analysing the biaxial response of reinforced and prestressed concrete wall segments subject to combinations of prestressing, creep, temperature and live loads is presented.

Two concrete constitutive relations are available for this analysis. The first is a uniaxially bilinear model with a tension cut-off. The second is a nonlinear biaxial relation incorporating equivalent uniaxial strains to remove the Poisson's ratio effect under biaxial loading.

Predictions from both the bilinear and nonlinear model are compared with observations from experimental wall segments tested in tension. The nonlinear model results are shown to be close to those of the test segments, while the bilinear results are good up to cracking.

Further comparisons are made between the nonlinear analysis using constant membrane force-moment ratios, constant membrane force-curvature ratios, and a nonlinear finite difference analysis of a test containment structure. Neither nonlinear analysis could predict the response of every wall segment within the structure, but the constant membrane force-moment analysis provided lower bound results.

ACKNOWLEDGEMENTS

This research project was initiated by and completed with the encouragement and guidance of Dr. D. W. Murray, Professor of Civil Engineering, whose assistance in the preparation of the report is greatly appreciated.

The assistance of Dr. T. M. Hrudey, Professor of Civil Engineering is also acknowledged.

Financial support was provided by the National Research Council of Canada and the University of Alberta.

The author would also like to thank his sister-in-law, whose patience and skilful typing was greatly appreciated.

TABLE OF CONTENTS

Title Page		i
Approval Sheet		ii
Abstract		iii
Acknowledgements		iv
Table of Contents		v
List of Tables		ix
List of Figures		x
List of Symbols		xiii
CHAPTER 1	INTRODUCTION	1
	1.1 Background	1
	1.2 Objectives and Scope	2
CHAPTER 2	THEORY	5
	2.1 Introduction	5
	2.2 Assumptions	5
	2.3 Fundamental Theory	6
	2.4 Solution Technique	13
	2.5 Creep and Thermal Loads	13
CHAPTER 3	CONSTITUTIVE RELATIONS	16
	3.1 Introduction	16
	3.2 Uniaxial Bilinear Elastic Concrete Relation	16
	3.3 Biaxial Nonlinear Elastic Concrete Relation	17
	3.3.1 Equivalent Uniaxial Strain	18
	3.3.2 Saenz Stress-Strain Curve	20
	3.3.3 Poisson's Ratio	22
	3.3.4 Ultimate Curves	23
	3.3.4.1 Ultimate Stress Curve	23

3.3.4.2 Equivalent Uniaxial Strain at Ultimate Stress 25

3.3.5 Tensile Declining Branch 28

3.3.6 Equivalent Uniaxial Strain Constants 29

3.3.7 Instability of the Declining Branch of the Stress-Strain Curves 30

3.3.8 Unloading 32

3.3.9 Crack Closure After Unloading 34

3.4 Reinforcing Steel Constitutive Relation 36

3.5 Prestressing Steel Constitutive Relation 36

CHAPTER 4 PROGRAM DEVELOPMENT 53

4.1 Description of Approach 53

4.2 Program Flowcharts 56

4.3 Convergence Difficulties 58

4.4 Solution Accuracy 60

4.5 Layering Technique 61

4.6 Example Problem 62

4.6.1 Segment Description 63

4.6.2 Loading Description 63

4.6.3 Discussion of Results 64

CHAPTER 5 APPLICATIONS 86

5.1 Comparison of Program with Wall Segment Tests 86

5.1.1 Wall Segments with Prestressing 88

5.1.1.1 Wall Segment No. 1 88

5.1.1.2 Wall Segment No. 3 89

5.1.1.3 Wall Segment No. 8 89

5.1.1.4 Wall Segment No. 5 90

5.1.1.5 Wall Segment No. 6 90

5.1.1.6 Wall Segment No. 12 90

5.1.2 Wall Segments Without Prestressing 92

5.1.2.1 Wall Segment No. 4 92

5.1.2.2 Wall Segment No. 7 93

5.1.3 General Results 93

5.2 Comparison of Concrete Constitutive Relations 94

CHAPTER 6 FURTHER APPLICATIONS 113

6.1 Introduction 113

6.2 Interpretation of Interaction Diagrams 113

6.3 Analysis of Containment Structure Segments 117

6.3.1 Segment 9-10 120

6.3.2 Segment 3-2 121

6.3.3 Segment 3-16 122

6.3.4 Segment 7-4 123

6.3.5 Summary of Results 124

CHAPTER 7 SUMMARY AND CONCLUSIONS 136

7.1 Summary 136

7.2 Conclusions 137

REFERENCES 139

APPENDIX A COWSAC USER'S MANUAL 142

A.1 Program Objectives 142

A.2 Input Deck 142

A.2.1 Data Deck Description 142

A.2.2 Explanation of Variables 143

A.2.3 Load Codes 147

A.2.4 Sign Convention 148

A.3 Output 149

APPENDIX B LISTING OF COWSAC 150

APPENDIX C SAMPLE INPUT AND OUTPUT 179

C.1 Sample Input 179

C.2 Sample Output 180

LIST OF TABLES

3.1 Comparison of Observed and Calculated Values of σ_{ic} and ε_{iuc}

4.1 Steel Layer Details - Segment UD1

4.2 Applied Loads for Load Steps

5.1 Summary of Wall Segment Data - Steel Details

5.2 Summary of Wall Segment Data - Concrete Details

5.3 Loading Sequence for Wall Segment No. 12

6.1 Test Structure Segment Details

6.2 Test Structure Segment Steel Details

6.3 Comparison of Test Structure Segment Ultimate Loads

LIST OF FIGURES

1.1 Wall Segment Showing Degrees of Freedom

3.1 Uniaxial Bilinear Elastic Stress-Strain Law

3.2 Typical Compressive Stress-Equivalent Uniaxial Strain Curve

3.3 Ultimate Stress Curve

3.4 Comparison of Saenz Equation and KHR Data for $\sigma_1 / \sigma_2 = 0 / -1$

3.5 Comparison of Saenz Equation and KHR Data for $\sigma_1 / \sigma_2 = -.5 / -1$

3.6 Comparison of Saenz Equation and KHR Data for $\sigma_1 / \sigma_2 = .22 / -1$

3.7 Comparison of Saenz Equation and KHR Data for $\sigma_1 / \sigma_2 = 1 / .5$

3.8 Comparison of Saenz Equation and KHR Data for $\sigma_1 / \sigma_2 = 1 / 0$

3.9 Equivalent Uniaxial Strains at Ultimate Stress

3.10 Stress-Equivalent Uniaxial Strain Curve in Tension

3.11a Concrete Stresses on Ascending Branch of σ-ε_{1u} Curve

3.11b Concrete Stresses on Descending Branch of σ-ε_{1u} Curve

3.12 Stress-Strain Curve for Reinforcing Steel

3.13 Stress-Strain Curve for Prestressing Strands

3.14 Linear Elastic Stress-Strain Curve for Concrete in Tension, with Tension Cut-off

4.1 Flow Chart of Main of COWSAC

4.2 Flow Chart of Load Control

4.3 Flow Chart of Load Application and Solution

4.4 Flow Chart of Nonlinear Concrete Constitutive Relation

4.5 Flow Chart of Bilinear Concrete Constitutive Relation

4.6 Wall Segment Showing Orientation of Layers

4.7 Segment UD1

4.8 Applied Axial Load vs. Strain - Segment UD1

4.9 Moment vs. Curvature - Segment UD1

4.10 Concrete Biaxial Stress Path on Inner Surface of Segment UD1

4.11 Concrete Biaxial Stress Path on Outer Surface of Segment UD1

4.12 Open Crack Depth vs. Live Axial Load in Direction 1 of Segment UD1

5.1 Typical Test Segment Cross-Section Orthogonal to Direction 1

5.2 Typical Test Segment Cross-Section Orthogonal to Direction 2

5.3 Concrete Stress Path for Test Segment No. 1

5.4 Force-Deflection Curve of Test Segment No. 1

5.5 Force-Deflection Curve of Test Segment No. 3

5.6 Force-Deflection Curve of Test Segment No. 8

5.7 Force-Deflection Curve of Test Segment No. 5

5.8 Force-Deflection Curve of Test Segment No. 6

5.9 Force-Deflection Curve of Test Segment No. 12, Face A

5.10 Force-Deflection Curve of Test Segment No. 12, Face B

5.11 Force-Deflection Curve of Test Segment No. 4

5.12 Force-Deflection Curve of Test Segment No. 7

6.1 Typical Interaction Diagram

6.2 Test Structure Segment 9-10

6.3 Test Structure Segment 3-2M

6.4 Test Structure Segment 3-2C

6.5 Test Structure Segment 3-16M

6.6 Test Structure Segment 3-16C

6.7 Test Structure Segment 7-4M

6.8 Test Structure Segment 7-4C

LIST OF SYMBOLS

ε	real mechanical strain
ε^c	creep strain
ε^e	elastic strain
ε^m	real mechanical strain in the minor direction (direction of lower absolute stress)
ε^{ms}	mid surface strain in direction i
ε^p	prestrain in prestressing tendons
ε^t	real total strain
ε^{temp}	temperature strain
ε_{io}	concrete strain at ultimate stress in uniaxial compression
ε_{iot}	concrete strain at ultimate stress in uniaxial tension
ε_{iu}	equivalent uniaxial strain in direction i
ε_{iuc}	equivalent uniaxial strain at maximum stress, in direction i
ε_u	ultimate concrete strain, biaxial reaction
υ_i	Poisson's ratio of concrete in direction i
υ_o	initial Poisson's ratio for concrete
σ^m	concrete stress in the minor direction
σ_i	concrete stress in direction i
σ_{ic}	ultimate concrete stress in direction i
σ_{pu}	ultimate stress of prestressing tendons
σ_y	yield stress of reinforcing steel
ϕ_i	wall segment change in curvature in direction i
Ψ_j	unbalanced load for degree of freedom j
A	accuracy of a solution
C	stiffness matrix of the wall segment relating forces {Q} and deformations {q}

ds	width of one layer of a wall segment
D_{ki}	stiffness matrix relating σ_k and ε_i
E^m	tangential modulus of concrete in the minor direction
E^s	short-term initial modulus of concrete
E^L	long-term initial modulus of concrete
E_i	tangential modulus of concrete, in direction i
E_o	initial Young's modulus of concrete
E_p	Young's modulus of prestressing strands
E_s	secant modulus of concrete
E_{st}	Young's modulus of steel
f'_c	maximum uniaxial compressive stress of concrete
f'_t	maximum uniaxial tensile stress of concrete
$\{F^d\}$	vector of dead loads
$\{F^L\}$	vector of live loads
$\{F^p\}$	vector of prestressing loads
F_i	specified load at degree of freedom i
m	number of degrees of freedom at which a force is specified in the load vector
M_i	moment on wall segment in direction i
N_i	axial force on wall segment in direction i
{q}	vector of wall segment deformations
{Q}	vector of wall segment loads
$\{\bar{Q}\}$	vector of internal resisting forces
rdθ	arc length of one layer of a wall segment
R_i	radius of curvature of the wall segment in direction i
υ	virtual strain energy of a body

δU	virtual strain energy
V	volume of a body
δW	virtual work done by external forces on a body
XINC	under relaxation factor
Z	location coordinate within the wall segment

1. INTRODUCTION

1.1 Background

During the last five years, the Department of Civil Engineering at the University of Alberta has been conducting a research program to aid in the understanding of the overload behavior and design problems associated with nuclear secondary containment structures. The structure is modelled as a segmented axisymmetric shell constructed of concrete, reinforced and prestressed in two directions. Due to the prestressing and the load carrying mechanisms of a shell, the walls and roof of the containment structure are subject to in-plane normal forces and out-of-plane moments in both directions simultaneously.

Under the overloads to which the walls and dome of the structure may be subjected, a large portion of the vessel would be stressed in tension, uniaxial or biaxial. This deviates from the usual stress state to which concrete is subjected at design loads and, therefore, the familiar assumptions and theory applied to concrete in tension may not give a realistic assessment of the behavior of the containment.

A previous study addressing the problem of analysing a wall segment from a containment vessel was conducted by Epstein and Murray (1976). In addition to computing the forces acting at design load on the wall segments variously located through the structure, Epstein and Murray (1976) attempted to establish load factors to various limit states by analysing the behavior of these segments. This analysis was elastic and one-dimensional, and considered the transformed area and moment of inertia, with due regard to cracking, to calculate the wall segment

response. The behavior of concrete in tension was assumed to follow the classical theory of being linearly elastic up to its fracture strength and to lose all stiffness after cracking. (This will be referred to as a "tension cut-off" analysis).

1.2 Objectives and Scope

The shell element to be analysed herein is similar to that discussed in the report of Epstein and Murray (1976) and is depicted in Fig. 1.1. The element is of arbitrary size, doubly curved and has two degrees of freedom in each of the two orthogonal directions associated with the principal radii of curvature. These degrees of freedom allow in-plane stretching deformations and out-of-plane curvatures. The analysis developed herein will accept the presence of reinforcing steel or prestressing steel running in the direction of either of the principal curvatures. These steel elements can be placed at any location within the thickness dimension of the wall.

The objective is to develop a computer-aided numerical analysis to predict the biaxial response of wall segments, using either a uniaxial bilinear elastic concrete constitutive relation, or a biaxial nonlinear concrete constitutive relation, and to compare the results obtained from this program, which shall be referred to by the acronym COWSAC (COWSAC is a short form of COntainment Wall Segment Analysis Code), with those from experimental tests of wall segments and from other nonlinear analyses.

Two concrete constitutive relations will be incorporated into the analysis. The first will be a bilinear elastic model with a tension

cut-off considering each dimension independently, similar to that employed by Epstein and Murray (1976). The second will be a two-dimensional nonlinear analysis including the softening behavior of the concrete stress-strain curve in both tension and compression. This unorthodox treatment of the behavior of concrete in tension is expected to allow simulation of problems where the wall segment is loaded in tension. The prestressing and reinforcing steel will be modelled with uniaxial piecewise linear stress-strain relations.

In the present work, the "load" applied to the wall segment associated with each degree of freedom can be either a force or a deformation. Thus, for the axial degrees of freedom, either a normal force, N_1 or N_2, or a normal strain ε_1^{ms} or ε_2^{ms}, can be imposed. For the rotational degrees of freedom, either a moment, M_1 or M_2, or a change in curvature, ϕ_1 or ϕ_2, may be imposed. With a total of four degrees of freedom, and a choice of two types of "loads" associated with each, sixteen possible types of loading patterns may be specified.

In addition to the live loads, the wall segment may be subject to prestressing loads, creep effects, and thermal loads. For each of these load states, the analysis can account, through the strain displacement equations, for nonuniform strains across the section.

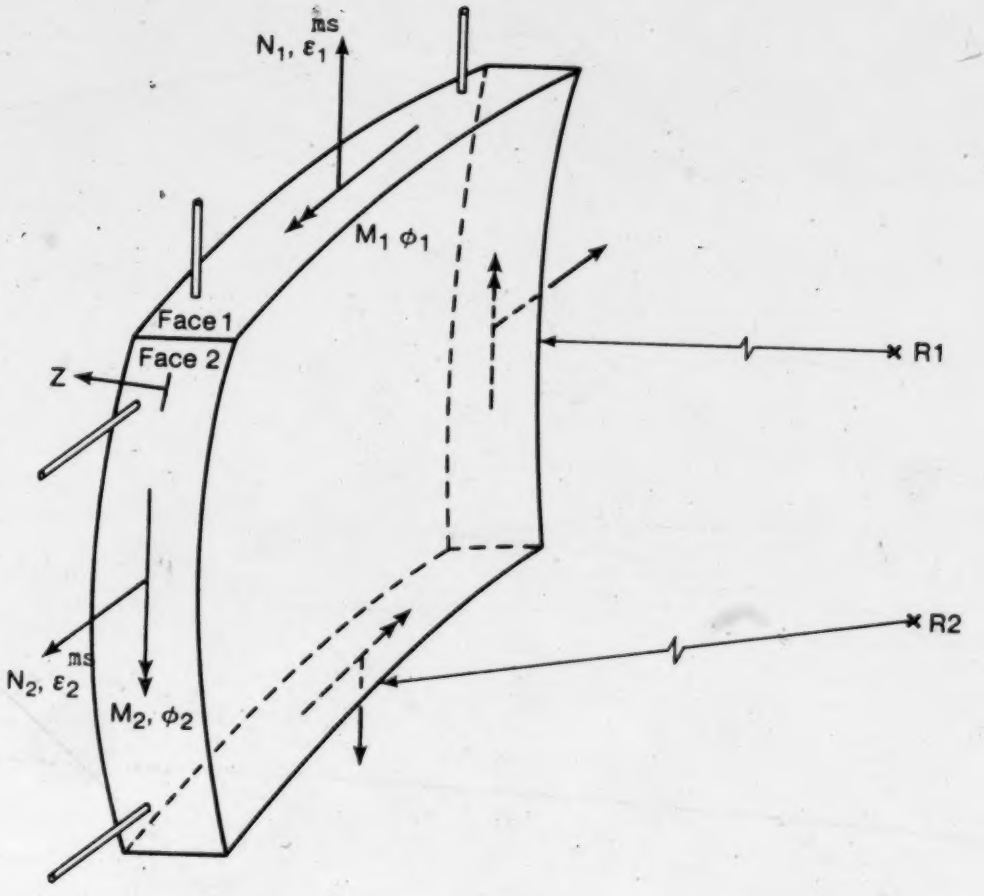

Fig. 1.1 Wall Segment Showing Degrees of Freedom

2. THEORY

2.1 Introduction

The fundamental theory used to model the wall segment is presented in this chapter. The assumptions which pertain to both the material stress-strain relationships of the steel and concrete, and the wall segment theory are first presented. The general theory for a wall segment is then discussed. Central to this theory are the wall segment equilibrium equations developed to include the segment layering, the interaction of the layers, and the response of the segment to either imposed forces or strains. The Newton-Raphson solution technique is then discussed relative to these equations. Finally, the specialized problems of thermal and creep loads are treated.

2.2 Assumptions

To simplify the mathematical formulation of the problem, the following assumptions regarding the plane-stress analysis of the wall segment are made.

1. The Love-Kirchhoff assumptions are valid. That is, normals to the reference surface remain straight and normal after deformation. Material layers can be considered to be in a state of plane stress.
2. No in-plane shear forces are present. That is, principal stresses and principal directions always coincide with the directions of principal curvature. This condition occurs when axisymmetric structures are loaded axisymmetrically.
3. Strain compatability is always maintained, in both elastic and inelastic regions, between the concrete and steel.

4. The steel layers carry uniaxial stress only.

5. The steel layers may be modelled as continuous layers of equivalent area extending across the width of the segment. The size and spacing of the steel bars or tendons have no effect other than determining the effective thickness of the layer.

2.3 Fundamental Theory

The development of equations parallels that for BOSOR5 (Bushnell, 1974) and is based on the principle of virtual work. The program simulates the relation between the force vector {Q} and the corresponding displacement vector {q}, where

$$\{Q\} = \langle N_1, M_1, N_2, M_2 \rangle \tag{2.3.1}$$

and

$$\{q\} = \langle \varepsilon_1^{ms}, \phi_1, \varepsilon_2^{ms}, \phi_2 \rangle \tag{2.3.2}$$

These forces and deformations are shown in Fig. 1.1.

The object of the program is, given a force, to find the resulting strain or, given a strain, to find the corresponding force, so that at the time of solution, both {Q} and {q} are known.

From the principle of virtual work

$$\delta U = \int_V \sigma_k \, \delta\varepsilon_k \, dV = Q_j \, \delta q_j = \delta W \tag{2.3.3}$$

where δU represents the virtual strain energy, V is the volume of the body, σ_k represents a vector (consisting of the stresses σ_1 and σ_2), ε_k represents a vector consisting of the corresponding strains ε_1 and ε_2, δW is the virtual work done by the external forces and δ is the

standard symbol denoting a change in the variable which it precedes. Thus the summation convention is used in Eq. 2.3.3, with a range of 2 for k, and a range of 4 for j.

If the matrix, D_{ki} is now introduced which relates σ_k and ε_i by the following equation

$$\sigma_k = D_{ki} \quad \varepsilon_i \tag{2.3.4}$$

then Eq. 2.3.3 can be written as

$$\delta U = \int_V D_{ki} \quad \varepsilon_i \quad \delta\varepsilon_k \quad dV = Q_j \, \delta q_j = \delta W \tag{2.3.5}$$

Equilibrium requires that the external forces on a body must be resisted by equal forces developed within the body. By defining Ψ_j, a variable force which represents the difference between the internal and external forces, one can write

$$\Psi_j = \int_V \sigma_k \frac{\partial \varepsilon_k}{\partial q_j} \, dV - Q_j = 0 \tag{2.3.6}$$

Since the internal and external forces are equal, Ψ_j should always equal zero in an equilibrium condition.

An increment in Ψ_j can be represented by

$$\Delta\Psi_j = \frac{\partial \Psi_j}{\partial q_i} \, \Delta q_i = 0 \tag{2.3.7}$$

or from Eq. 2.3.6 by

$$\Delta\Psi_j = \int_V \left(\frac{\partial \sigma_k}{\partial q_i} \frac{\partial \varepsilon_k}{\partial q_j} + \sigma_k \frac{\partial^2 \varepsilon_k}{\partial q_i \partial q_j} \right) dV \Delta q_i - \Delta Q_j = 0 \tag{2.3.8}$$

If the unbalanced forces Ψ_j are not zero then corrections to q_i can be obtained by requiring

$$\Delta\Psi_j = -\Psi_j \tag{2.3.9}$$

Equations 2.3.9 are simultaneous non-linear equations which are known as the Newton-Raphson equations. Using Eq. 2.3.7, Eq. 2.3.9 may be rewritten as

$$\frac{\partial\Psi_j}{\partial q_i}\ \Delta q_i = -\Psi_j \tag{2.3.10}$$

where the subscripts i and j have a range of N, where N equals the number of degrees of freedom, which in this case is four.

The above equations are applied to a wall segment which is layered through the wall thickness and which has concrete, reinforcing steel and prestressing steel layers. The contribution of each layer towards the stiffness of the entire segment is found individually and by integrating through the volume of the body, the stiffness of the segment as a whole can be found.

Assuming a unit length, the strains for each layer are (Bushnell, 1974)

$$\varepsilon_{11} = \frac{(\varepsilon_1^{ms} - Z\,\phi_1)}{(1 + Z/R_1)}$$

$$\varepsilon_{22} = \frac{(\varepsilon_2^{ms} - Z\,\phi_2)}{(1 + Z/R_2)} \tag{2.3.11}$$

$$\varepsilon_{12} = 0$$

where Z is a distance coordinate measured from the centre of the segment thickness, positive being outward from the centres of curvature, and R_1 and R_2 are the principal radii of curvature of the segment in the principal directions as shown in Fig. 1.1.

The element of volume of one layer is

$$dV = r\,(1 + Z/R_1)\;\;(1 + Z/R_2)\;\;dZ\;\;d\theta\;\;ds \qquad (2.3.12)$$

where dZ is the thickness of the layer and ds and rdθ are the width and arc length of the layer, r being the radius of the parallel circle of the reference surface.

By defining three new terms k_1, k_2 and k_3 such that

$$\begin{aligned} k_1 &= (1 + Z/R_1) \\ k_2 &= (1 + Z/R_2) \\ k_3 &= k_1 k_2 \end{aligned} \qquad (2.3.13)$$

and by assuming that ϵ_i is associated only with the mechanical strains, i.e.

$$\epsilon_i = \epsilon_i^{\,t} - \epsilon_i^{\,c} - \epsilon_i^{\,temp} \qquad (2.3.14)$$

where $\epsilon_i^{\,t}$ are the real total strains, $\epsilon_i^{\,c}$ are the creep strains and $\epsilon_i^{\,temp}$ are the temperature strains, then differentiation of Eq. 2.3.11 yields

$$\left[\frac{\partial \epsilon}{\partial q}\right] = \begin{bmatrix} \frac{\partial \epsilon_{11}}{\partial \epsilon_1^{ms}} & \frac{\partial \epsilon_{22}}{\partial \epsilon_1^{ms}} \\ \frac{\partial \epsilon_{11}}{\partial \phi_1} & \frac{\partial \epsilon_{22}}{\partial \phi_1} \\ \frac{\partial \epsilon_{11}}{\partial \epsilon_2^{ms}} & \frac{\partial \epsilon_{22}}{\partial \epsilon_1^{ms}} \\ \frac{\partial \epsilon_{11}}{\partial \phi_2} & \frac{\partial \epsilon_{22}}{\partial \phi_2} \end{bmatrix} - \begin{bmatrix} \frac{1}{k_1} & 0 \\ \frac{-Z}{k_1} & 0 \\ 0 & \frac{1}{k_2} \\ 0 & \frac{-Z}{k_2} \end{bmatrix} \tag{2.3.15}$$

$$\frac{\partial^2 \epsilon_k}{\partial q_i \partial q_j} = 0 \tag{2.3.16}$$

Substituting Eqs. 2.3.12, 2.3.13, 2.3.15 and 2.3.16 into Eq. 2.3.6 and carrying out the multiplication

$$\langle Q^I \rangle = \int_{Z=-\frac{t}{2}}^{\frac{t}{2}} \left\langle \frac{\sigma_{11}}{k_1} \quad \frac{-Z\sigma_{11}}{k_1} \quad \frac{\sigma_{22}}{k_2} \quad \frac{-Z\sigma_{22}}{k_2} \right\rangle k_1 k_2 \, r d\theta \, ds \, dZ \tag{2.3.17}$$

where $\langle Q^I \rangle$ are the internal forces developed to resist the external forces $\langle Q \rangle$. Assuming a unit length along the reference surface, define the size of the segment as

$$\begin{aligned} r d\theta &= 1 \\ ds &= 1 \end{aligned} \tag{2.3.18}$$

which results in

$$\langle Q^I \rangle = \langle N_1 \; M_1 \; N_2 \; M_2 \rangle = \int_{-\frac{t}{2}}^{\frac{t}{2}} \langle k_2\sigma_{11}, \; -Zk_2\sigma_{11}, \; k_1\sigma_{22}, \; -Zk_2\sigma_{22} \rangle \, dZ \tag{2.3.19}$$

Applying Eq. 2.3.15 and 2.3.16 to Eq. 2.3.8, the incremental equilibrium expression becomes

$$\int_V \begin{bmatrix} 1/k_1 & 0 \\ -Z/k_1 & 0 \\ 0 & 1/k_2 \\ 0 & -Z/k_2 \end{bmatrix} \begin{bmatrix} \frac{\partial \sigma_{11}}{\partial \varepsilon_1^{ms}} & \frac{\partial \sigma_{11}}{\partial \phi_1} & \frac{\partial \sigma_{11}}{\partial \varepsilon_2^{ms}} & \frac{\partial \sigma_{11}}{\partial \phi_2} \\ \frac{\partial \sigma_{22}}{\partial \varepsilon_1^{ms}} & \frac{\partial \sigma_{22}}{\partial \phi_1} & \frac{\partial \sigma_{22}}{\partial \varepsilon_2^{ms}} & \frac{\partial \sigma_{22}}{\partial \phi_2} \end{bmatrix} dV \begin{bmatrix} \Delta\varepsilon_1^{ms} \\ \Delta\phi_1 \\ \Delta\varepsilon_2^{ms} \\ \Delta\phi_2 \end{bmatrix} - \begin{bmatrix} \Delta N_1 \\ \Delta M_1 \\ \Delta N_2 \\ \Delta M_2 \end{bmatrix} = 0 \qquad (2.3.20)$$

Assuming that

$$\sigma_{11} = f_{11}(\varepsilon_{11}, \varepsilon_{22}) \qquad (2.3.21)$$

$$\sigma_{22} = f_{22}(\varepsilon_{11}, \varepsilon_{22})$$

where ε_{11} and ε_{22} are the mechanical strains as defined by Eq. 2.3.14 then

$$\frac{\partial \sigma_{11}}{\partial \varepsilon_1^{ms}} = \frac{\partial f_{11}}{\partial \varepsilon_1^{ms}} = \frac{\partial f_{11}}{\partial \varepsilon_{11}} \frac{\partial \varepsilon_{11}}{\partial \varepsilon_1^{ms}} + \frac{\partial f_{11}}{\partial \varepsilon_{22}} \frac{\partial \varepsilon_{22}}{\partial \varepsilon_1^{ms}} = \frac{1}{k_1} \frac{\partial f_{11}}{\partial \varepsilon_{11}}$$

Similarly

$$\begin{aligned}
\frac{\partial \sigma_{11}}{\partial \varepsilon_1^{ms}} &= \frac{1}{k_1} \frac{\partial f_{11}}{\partial \varepsilon_{11}} & \frac{\partial \sigma_{22}}{\partial \varepsilon_1^{ms}} &= \frac{1}{k_1} \frac{\partial f_{22}}{\partial \varepsilon_{11}} \\
\frac{\partial \sigma_{11}}{\partial \phi_1} &= \frac{-Z}{k_1} \frac{\partial f_{11}}{\partial \varepsilon_{11}} & \frac{\partial \sigma_{22}}{\partial \phi_1} &= \frac{-Z}{k_1} \frac{\partial f_{22}}{\partial \varepsilon_{11}} \\
\frac{\partial \sigma_{11}}{\partial \varepsilon_2^{ms}} &= \frac{1}{k_2} \frac{\partial f_{11}}{\partial \varepsilon_{22}} & \frac{\partial \sigma_{22}}{\partial \varepsilon_2^{ms}} &= \frac{1}{k_2} \frac{\partial f_{22}}{\partial \varepsilon_{22}} \\
\frac{\partial \sigma_{11}}{\partial \phi_2} &= \frac{-Z}{k_2} \frac{\partial f_{11}}{\partial \varepsilon_{22}} & \frac{\partial \sigma_{22}}{\partial \phi_2} &= \frac{-Z}{k_2} \frac{\partial f_{22}}{\partial \varepsilon_{22}}
\end{aligned} \qquad (2.3.22)$$

Substituting Eqs. 2.3.22 into 2.3.20 results in the following

$$\begin{bmatrix} C_{11} & C_{12} & C_{13} & C_{14} \\ C_{21} & C_{22} & C_{23} & C_{24} \\ C_{31} & C_{32} & C_{33} & C_{34} \\ C_{41} & C_{42} & C_{43} & C_{44} \end{bmatrix} \begin{bmatrix} \Delta\xi_1 \\ \Delta\phi_1 \\ \Delta\xi_2 \\ \Delta\phi_2 \end{bmatrix} = \begin{bmatrix} \Delta N_1 \\ \Delta M_1 \\ \Delta N_2 \\ \Delta M_2 \end{bmatrix} \tag{2.3.23}$$

or

$$[C] \quad \{\Delta q\} \quad = \quad \{\Delta Q\} \tag{2.3.24}$$

where the coefficients of the matrix C are defined as

$$C_{11} = \int_{-\frac{t}{2}}^{\frac{t}{2}} \frac{\partial f_{11}}{\partial \varepsilon_{11}} \frac{k_2}{k_1} \, dZ \qquad C_{12} = \int_{-\frac{t}{2}}^{\frac{t}{2}} -Z \frac{\partial f_{11}}{\partial \varepsilon_{11}} \frac{k_2}{k_1} \, dZ$$

$$C_{13} = \int \frac{\partial f_{11}}{\partial \varepsilon_{22}} \, dZ \qquad C_{14} = \int -Z \frac{\partial f_{11}}{\partial \varepsilon_{22}} \, dZ$$

$$C_{21} = \int -Z \frac{\partial f_{11}}{\partial \varepsilon_{11}} \frac{k_2}{k_1} \, dZ \qquad C_{22} = \int Z^2 \frac{\partial f_{11}}{\partial \varepsilon_{11}} \frac{k_2}{k_1} \, dZ$$

$$C_{23} = \int -Z \frac{\partial f_{11}}{\partial \varepsilon_{22}} \, dZ \qquad C_{24} = \int Z^2 \frac{\partial f_{11}}{\partial \varepsilon_{22}} \, dZ$$

$$C_{31} = \int \frac{\partial f_{22}}{\partial \varepsilon_{11}} \, dZ \qquad C_{32} = \int -Z \frac{\partial f_{22}}{\partial \varepsilon_{11}} \, dZ \tag{2.3.25}$$

$$C_{33} = \int \frac{\partial f_{22}}{\partial \varepsilon_{22}} \frac{k_1}{k_2} \, dZ \qquad C_{34} = \int -Z \frac{\partial f_{22}}{\partial \varepsilon_{22}} \frac{k_1}{k_2} \, dZ$$

$$C_{41} = \int -Z \frac{\partial f_{22}}{\partial \varepsilon_{11}} \, dZ \qquad C_{42} = \int Z^2 \frac{\partial f_{22}}{\partial \varepsilon_{11}} \, dZ$$

$$C_{43} = \int -Z \frac{\partial f_{22}}{\partial \varepsilon_{22}} \frac{k_1}{k_2} \, dZ \qquad C_{44} = \int Z^2 \frac{\partial f_{22}}{\partial \varepsilon_{22}} \frac{k_1}{k_2} \, dZ$$

By solving Eq. 2.3.24 for the unknown quantities $\{\Delta q\}$ successive corrections can be made to $\{q\}$ until $\{\Psi\}$ equals zero at which point the solution has converged.

2.4 Solution Technique

As stated in Section 2.3, the Newton-Raphson iterative technique is used to solve the non-linear coupled equations and follows the general outline below.

1. Given an estimate of $\{q\}$, calculate the forces $\{Q^I\}$ from Eq. 2.3.19
2. Find the unbalanced forces $\{\Delta Q\} = \{Q\} - \{Q^I\}$
3. If $\{\Delta Q\}$ is small, then the solution is correct. If $\{\Delta Q\}$ is large, go to step 4
4. Evaluate $[C]$ from Eqs. 2.3.25
5. Find $\{\Delta q\} = [C]^{-1} \{\Delta Q\}$
6. New $\{q\} = \{q\} + \{\Delta q\}$
7. Go to 2

2.5 Creep and Thermal Loads

Strains resulting from creep and temperature changes are removed from the total strains in a layer, i.e.

$$\varepsilon_i = \varepsilon_i^t - \varepsilon_i^c - \varepsilon_i^{temp}$$

where ε_i^t are the total real strains, ε_i^{temp} are the strains resulting from a temperature change, ε_i^c are the strains in the concrete due to creep and ε_i are the resulting mechanical strains. It is the mechanical

strains which are then used to find stresses, tangential moduli, and Poisson's ratios.

The variation in temperature changes through the wall thickness can be specified by one of the following equations.

$$\begin{aligned} &1. \quad \Delta T = T1 + T2 \cdot Y + T3 \cdot Y^2 \\ &2. \quad \Delta T = T1 + T2 \cdot Y^{T3} \\ &3. \quad \Delta T = T1 + T2 \cdot e^{Y \cdot T3} \end{aligned} \tag{2.5.1}$$

T1, T2 and T3 are user defined constants and Y is the location coordinate. The origin for Y (Y = 0) is at the inside surface of the wall segment (Z = -t/2).

Depending upon the location and orientation of the wall segment in a structure, one or more of the degrees of freedom of the wall may be restrained from temperature movements. For this reason, a program variable must be input to specify which degrees of freedom are fixed against thermal movement.

Creep strains are found by using a 'long-term' Young's modulus. During the creep step, this reduced modulus replaces the normal or 'short-term' modulus and under constant load, the strains increase to maintain resistance to this load. The 'long-term' modulus is related to the 'short-term' modulus by the following.

$$F_c = \frac{E^s}{E^L} = \frac{\varepsilon^c + \varepsilon^e}{\varepsilon^e}$$

where F_c is the creep factor, E^s is the 'short-term' or normal Young's modulus, and E^L is the 'long-term' modulus. The third term applies for

a plain concrete section where ε^c would be the creep strains and ε^e the initial elastic strains before creep.

The creep factor, F_c, can be related to the C.E.B. creep coefficient ϕ_t (C.E.B., 1969) by the expression

$$F_c = \phi_t - 1 \qquad (2.5.3)$$

where

$$\phi_t = K_c \quad K_b \quad K_d \quad K_e \quad K_t \qquad (2.5.4)$$

and the value K_c is a function of the relative humidity, K_b is a function of the water - cement ratio, K_d is a function of the age at loading, K_e is a function of the fictitious thickness, and K_t is a function of the duration of load. The values of these parameters may be obtained from graphs by C.E.B. (1969).

The creep factor ϕ_t was developed under the assumption of constant load. While the program considers the load on the wall segment to be kept constant during the creep step, the load on the concrete layers decreases as stress is transferred to the steel layers. Equation 2.5.2 therefore overestimates the creep strain ε_c. This is corrected after returning the tangential modulus back to the short term E by adjusting ε_c in the concrete layers by successive iterations to compensate for the reduced concrete stress. The increase in strains in the steel layers which accompany the creep step are real; the mechanical strains in the steel layers equal the total strains.

3. CONSTITUTIVE RELATIONS

3.1 Introduction

This chapter deals in detail with the constitutive relations for concrete and steel. Two constitutive relations for concrete are presented. The first is a uniaxial bilinear elastic relation incorporating a tension cut-off with crack closure but no crack healing. Although both directions on the wall segment can be analysed using this relation, they are essentially independent of each other. The stress-strain curve of this uniaxial concrete relation is based on mechanical strains. The second relation is a non-linear two-dimensional concrete constitutive relation which some authors label hypoelastic (Schnobrich, 1977). This relationship is based on the equivalent uniaxial strain theory (Darwin and Pecknold, 1974) and uses the Saenz equations (Saenz, 1964) to define the stress-strain law, in terms of equivalent uniaxial strains. Finally, details of the uniaxial stress-strain curves for both the reinforcing steel and the prestressing steel are discussed.

3.2 Uniaxial Bilinear Elastic Concrete Relation

The first approximation of the concrete stress-strain curve used in this study is a uniaxial bilinear elastic law which requires the specification of: E, Young's modulus, f'_c, the ultimate strength of concrete in uniaxial compression, f'_t, the ultimate strength of concrete in uniaxial tension, ε_u, ultimate concrete strain in uniaxial compression, ε_c, which equals f'_c/E and ε_t which equals f'_t/E. It has been shown (Murray, 1979; Whitney, 1943) that the post ultimate portion of the concrete stress-strain curve which can be measured experimentally

is a function of the stiffness of the testing machine. Therefore, published data concerning this property is affected by the testing procedure. For this model, it was assumed that $\varepsilon_u = -.0038$ (Hognestad et al., 1955).

The following mathematical equations then describe the constitutive relation, which does not account for any Poisson's ratio effects.

$$\sigma = E \cdot \varepsilon \qquad E = E \qquad \varepsilon_c < \varepsilon < \varepsilon_t \tag{3.2.1}$$

$$\sigma = 0 \qquad E = 0 \qquad \varepsilon_t < \varepsilon \tag{3.2.2}$$

$$\sigma = f'_c \qquad E = 0 \qquad \varepsilon_u < \varepsilon < \varepsilon_c \tag{3.2.3}$$

$$\sigma = 0 \qquad E = 0 \qquad \varepsilon < \varepsilon_u \tag{3.2.4}$$

This curve is shown graphically in Fig. 3.1. For these and the following equations, f'_c has a value less than zero.

When ε exceeds ε_t, cracking occurs, and for that particular layer, the value of ε_t is then changed so that ε_t equals 0. Therefore, the concrete can no longer develop tensile stresses but its behavior in compression is assumed to be unaffected. The crack in this layer can close and compression stresses can form but no subsequent tensile stresses can occur if the strains were to become positive a second time.

In compression, the stress-strain curve is elastic up to ε_u. Beyond this point however, the concrete in this layer is assumed to have crushed and can no longer develop any stresses in tension or compression regardless of the level of strain.

3.3 Biaxial Nonlinear Elastic Constitutive Concrete Relation

There are currently many theories available for predicting the

nonlinear biaxial behavior of plain concrete (Chen and Chen, 1975; Liu et al., 1972; Romstad et al., 1974; Kupfer and Gerstle, 1973; Bazant and Bhat, 1976; Darwin and Pecknold, 1977; Argyris, 1973). Common to most of these models is the assumption of linear elastic behavior of concrete in tension with a tension cut-off. Once cracked, the concrete is assumed to have zero stiffness in tension. In a reinforced concrete specimen however, the cracks which form relieve the tensile stress in the uncracked concrete and the concrete between the crack continues to contribute some stiffness to the specimen. To account for this additional stiffness, a few investigators have gone beyond the simple tension cut-off model and have proposed a concrete stress-strain curve in tension complete with a declining branch. (Lin and Scordelis, 1975; Scanlon and Murray, 1974; Murray et al, 1978; Elwi and Murray, 1979).

The proposed biaxial model incorporates the concepts of equivalent uniaxial strain developed by Darwin, Bashur and Pecknold (Darwin and Pecknold, 1974, 1977; Bashur and Darwin, 1978), the nonlinear stress-strain curve of Saenz (1964) and the stress failure surface of Kupfer and Gerstle (1973).

3.3.1 Equivalent Uniaxial Strain

The concept of equivalent uniaxial strains was developed to remove the Poisson's ratio coupling of strains in two (or three) dimensions, and therefore result in a set of strains which are independent of each other, and which can be simply applied to a chosen stress-strain law. In this manner, it is assumed that biaxial stress-strain curves can be

derived from uniaxial curves. (Darwin and Pecknold, 1974).

The incremental stress-strain relations for an orthotropic material not subject to shear take the form

$$\begin{bmatrix} d\sigma_1 \\ d\sigma_2 \end{bmatrix} = \frac{1}{(1-\upsilon_1\upsilon_2)} \begin{bmatrix} E_1 & \upsilon_2 E_1 \\ \upsilon_1 E_2 & E_2 \end{bmatrix} \begin{bmatrix} d\varepsilon_1 \\ d\varepsilon_2 \end{bmatrix} \tag{3.3.1}$$

From Maxwell's reciprocal theorem the stiffness matrix should be symmetric, which gives rise to

$$\upsilon_1 E_2 = \upsilon_2 E_1 \tag{3.3.2}$$

To simplify the expression further, the concept of an 'equivalent Poisson's ratio' is introduced whereby

$$\upsilon^2 = \upsilon_1\upsilon_2 \tag{3.3.3}$$

Equation 3.3.1 now takes the form

$$\begin{bmatrix} d\sigma_1 \\ d\sigma_2 \end{bmatrix} = \frac{1}{(1-\upsilon^2)} \begin{bmatrix} E_1 & \upsilon\sqrt{E_1E_2} \\ \upsilon\sqrt{E_1E_2} & E_2 \end{bmatrix} \begin{bmatrix} d\varepsilon_1 \\ d\varepsilon_2 \end{bmatrix} \tag{3.3.4}$$

The incremental equivalent uniaxial strains are defined as

$$d\varepsilon_{1u} = \frac{d\sigma_1}{E_1}$$

$$d\varepsilon_{2u} = \frac{d\sigma_2}{E_2} \tag{3.3.5}$$

which upon substitution into Eq. 3.3.4 gives the equivalent uniaxial strains in terms of the true strains, the elastic moduli and the equivalent Poisson's ratio.

$$\begin{bmatrix} d\varepsilon_{1u} \\ d\varepsilon_{2u} \end{bmatrix} = \frac{1}{(1-\upsilon^2)} \begin{bmatrix} 1 & \upsilon\sqrt{E_2/E_1} \\ \upsilon\sqrt{E_1/E_2} & 1 \end{bmatrix} \begin{bmatrix} d\varepsilon_1 \\ d\varepsilon_2 \end{bmatrix} \qquad (3.3.6)$$

The total equivalent uniaxial strains can now be defined as

$$\varepsilon_{iu} = \int \frac{d\sigma_i}{E_i} \qquad i = 1, 2 \qquad (3.3.7)$$

where the summation convention is not used.

The equivalent uniaxial strains are not real strains. They cannot be observed and cannot be transformed under rotation of the coordinate axis in the same manner as stresses and true strains. Equivalent uniaxial strains are accumulated in the principal directions which can change during loading. This theory does, however, recognize stress-induced orthotropic behavior. Fundamentally, it allows the use of curves similar to that representing the uniaxial stress-strain curve to describe the biaxial stress-strain curves.

3.3.2 Saenz Stress-Strain Curve

The uniaxial stress-strain relationship of Saenz will be extended to cover biaxial response, paralleling the procedure used by Darwin and Pecknold (1977). The same curve, with some modification, will be used to describe behavior in both tension and compression.

In a uniaxial test, real strains and equivalent uniaxial strains are equal. With this knowledge, the Saenz equation will be modified to cover biaxial response by substituting equivalent uniaxial strains for real strains. The Saenz relation then becomes for the direction i

$$\sigma_i = \frac{E_o \, \varepsilon_{iu}}{1 + (R + R_E - 2)\left(\frac{\varepsilon_{iu}}{\varepsilon_{iuc}}\right) - (2R - 1)\left(\frac{\varepsilon_{iu}}{\varepsilon_{iuc}}\right)^2 + R\left(\frac{\varepsilon_{iu}}{\varepsilon_{iuc}}\right)^3} \qquad (3.3.8)$$

where

$$R_E = E_o / E_s \qquad (3.3.9)$$

$$E_s = \sigma_{ic} / \varepsilon_{iuc} \qquad (3.3.10)$$

$$R_\sigma = \sigma_{ic} / \sigma_{if} \qquad (3.3.11)$$

$$R_\varepsilon = \varepsilon_{if} / \varepsilon_{iuc} \qquad (3.3.12)$$

$$R = \frac{R_E (R_\sigma - 1)}{(R_\varepsilon - 1)^2} - \frac{1}{R_\varepsilon} \qquad (3.3.13)$$

and where ε_{iu} is the current accumulated equivalent uniaxial strain in direction i; σ_{ic} is the maximum stress on the stress-strain curve in direction i for the current principal stress ratios; ε_{iuc} is the equivalent uniaxial strain at σ_{ic}; σ_{if} and ε_{if} are the coordinates of a point on the declining branch of the current stress-equivalent uniaxial strain curves; and E_o is the initial modulus of elasticity from a uniaxial test.

The type of curve described by Eq. 3.3.8 is shown in Fig. 3.2.

As required by Eq. 3.3.4, the incremental elastic moduli must be determined. From Eq. 3.3.5 it can be shown that for direction i

$$E_i = \frac{d\sigma_i}{d\varepsilon_{iu}} \qquad (3.3.14)$$

Differentiating Eq. 3.3.8 with respect to ε_{iu} results in

$$\frac{d\sigma_i}{d\varepsilon_{iu}} = E_i \frac{E_o\left[1 + (2R-1)\left(\frac{\varepsilon_{iu}}{\varepsilon_{iuc}}\right)^2 - 2R\left(\frac{\varepsilon_{iu}}{\varepsilon_{iuc}}\right)^3\right]}{\left[1 + (R+R_E-2)\left(\frac{\varepsilon_{iu}}{\varepsilon_{iuc}}\right) + (1-2R)\left(\frac{\varepsilon_{iu}}{\varepsilon_{iuc}}\right)^2 + R\left(\frac{\varepsilon_{iu}}{\varepsilon_{iuc}}\right)^3\right]^2} \quad (3.3.15)$$

Having determined the value of E_i, the change in equivalent uniaxial strain, $d\varepsilon_{iu}$, can be calculated and accumulated to find the total equivalent uniaxial strain, ε_{iu} which is required to compute the stress, σ_i.

3.3.3 Poisson's Ratio

In addition to the incremental elastic moduli, Eq. 3.3.4 requires the values of Poisson's ratio for various locations on the loading path. The equation describing Poisson's ratio was taken from similar studies (Elwi and Murray, 1979) which used the uniaxial compression curves of Kupfer, Hilsdorf and Rusch (1969). From this data, the Poisson's ratio was determined and expressed as a function of equivalent uniaxial strains.

The value for Poisson's ratio, υ_i in direction i is

$$\upsilon_i = \upsilon_o\left[1 + 1.3763\left(\frac{\varepsilon_{iu}}{\varepsilon_{iuc}}\right) - 5.360\left(\frac{\varepsilon_{iu}}{\varepsilon_{iuc}}\right)^2 + 8.586\left(\frac{\varepsilon_{iu}}{\varepsilon_{iuc}}\right)^3\right] \quad (3.3.16)$$

$$\upsilon_i \leq 0.50 \quad (3.3.17)$$

where υ_o is the initial value of Poisson's ratio. The limitation placed on υ_i is present to prevent the dilatency phenomena observed in concrete when reaching ultimate strength. The equivalent Poisson's ratio, υ,

is now found from Eq. 3.3.3.

3.3.4 Ultimate Curves

To define the stress-strain curve described by Eq. 3.3.8, the additional parameters accompanying this equation must be determined. These parameters are σ_{ic}, σ_{if}, ε_{iuc} and ε_{iuf}. σ_{ic} and ε_{iuc} will be expressed as failure curves which are direct or indirect functions of the current principal stress ratio, and σ_{if} and ε_{if} will be functions of σ_{ic} and ε_{iuc}.

3.3.4.1 Ultimate Stress Curve

The stress failure curve of Kupfer and Gerstle (1973) was used to determine the values of σ_{ic}. This curve is composed of three parts which are functions of the stress ratio and is illustrated in Fig. 3.3.

In the compression-compression quadrant of the biaxial stress space, the strength envelop is described by

$$\left(\frac{\sigma_{1c}}{f'_c} + \frac{\sigma_{2c}}{f'_c}\right)^2 - \frac{\sigma_{2c}}{f'_c} - 3.65\,\frac{\sigma_{1c}}{f'_c} = 0 \qquad (3.3.18)$$

for which σ_1 is greater than or equal to σ_2, and σ_1, σ_2 and f'_c are values less than zero.

By defining the ratio α as

$$\alpha = \frac{\sigma_1}{\sigma_2} \qquad (3.3.19)$$

Eq. 3.3.18 can be solved to express σ_{1c} and σ_{2c} in terms of α, as

$$\sigma_{2c} = \frac{1 + 3.65\,\alpha}{(1+\alpha)^2}\, f'_c \qquad (3.3.20)$$

$$\sigma_{1c} = \alpha\,\sigma_{2c} \qquad (3.3.21)$$

In this case, σ_{2c} is the major direction (the direction of higher absolute stress).

In the tension-compression quadrants, the following straight line is used.

$$\frac{\sigma_{1c}}{f'_t} = 1 - 0.8\,\frac{\sigma_{2c}}{f'_c} \qquad (3.3.22)$$

which can be restated as

$$\sigma_{2c} = \frac{f'_c\, f'_t}{\alpha f'_c + 0.8 f'_t} \qquad (3.3.23)$$

$$\sigma_{1c} = \alpha\,\sigma_{2c} \qquad \sigma_{1c} > 0 \qquad (3.3.24)$$

There is a small region of overlap where Eqs. 3.3.20 and 3.3.21 are used in the tension-compression quadrants.

For the tension-tension quadrant, a constant tensile strength is used.

$$\sigma_{1c} = f'_t \qquad (3.3.25)$$

$$\sigma_{2c} = \frac{\sigma_{1c}}{\alpha} \qquad (3.3.26)$$

3.3.4.2 Equivalent Uniaxial Strain at Ultimate Stress

The equations which were derived for this section are based on the data from the biaxial tests of Kupfer (1973). A program developed by A. A. Elwi, using the stress-strain relations for an orthotropic material, the Saenz (1964) stress-strain equations and the Poisson's ratio equation of A. A. Elwi, has been used to mathematically model the constant stress ratio experiments of Kupfer. By varying the input value of ε_{iuc} into this program, the optimum ε_{iuc} which provided a reasonable correlation between the predicted and observed stress-strain curves was found for each stress ratio. Figures 3.4 through 3.8 compare the curves of Kupfer, for a few stress ratios, with those obtained using the above technique and the optimum values of ε_{iuc}.

The values of ε_{iuc} determined to optimize the correlation with the specific set of stress-strain curves provided by Kupfer (1973), were then generalized to define an equivalent uniaxial strain curve in biaxial space. That is, from the expressions of ε_{iuc} which were found, expressions were developed to relate the current stress ratio to the associated value of ε_{iuc}, where ε_{iuc} is the equivalent uniaxial strain when the stress, σ_i equals the maximum, σ_{ic}, for that particular stress ratio. Figure 3.9 contains a diagram of the ε_{iuc} envelop.

In the compression-compression region, a new variable β was defined where

$$\beta = \frac{\varepsilon_{1uc}}{\varepsilon_{2uc}} \qquad (3.3.27)$$

A new material constant ε_{io}, is now required to define the curve

in Fig. 3.9, where ε_{io} is the equivalent uniaxial strain in the stressed direction at ultimate stress for a uniaxial compression test. ε_{iuc} can now be calculated using

$$\varepsilon_{2uc} = \frac{\varepsilon_{io}\,(1 + 7.75\beta)}{(1 + 4\beta)} \tag{3.3.28}$$

$$\varepsilon_{1uc} = \beta\,\varepsilon_{2uc} \tag{3.3.29}$$

$$\beta = \alpha^3 - 1.8\,\alpha^2 + 1.8\,\alpha \tag{3.3.30}$$

When σ_2 equals f'_c and σ_1 equals zero, then ε_{2uc} equals ε_{io}.

A second material constant, ε_{iot} is required where ε_{iot} equals the equivalent uniaxial strain, in the stressed direction, at ultimate stress, for a uniaxial tension test. In the tension-compression quadrants, the following relationship is suggested.

$$\varepsilon_{1uc} = \varepsilon_{iot}\left[1 - (1 - \sigma_{ic} / f'_t)^4\right] \tag{3.3.31}$$

$$\varepsilon_{2uc} = \varepsilon_{io}\left[0.9\left(\frac{\sigma_{2c}}{f'_c}\right) - 1.4\left(\frac{\sigma_{2c}}{f'_c}\right)^2 + 1.5\left(\frac{\sigma_{2c}}{f'_c}\right)^3\right] \tag{3.3.32}$$

When σ_1 equals f'_t and σ_2 equals zero, $\varepsilon_{iuc} = \varepsilon_{iot}$

For the tension-tension quadrant, ε_{iuc} is found by

$$\varepsilon_{1uc} = \varepsilon_{iot}\,(1 + 0.5\,\beta_t - 0.25\,\beta_t^2) \tag{3.3.33}$$

$$\varepsilon_{2uc} = \varepsilon_{iot}\,(0.75\,\sqrt[3]{\beta_t} + 0.5\,\beta_t^3) \tag{3.3.34}$$

$$\beta_t = 1 / \alpha \tag{3.3.35}$$

Table 3.1 gives a comparison of the observed values of σ_{ic} and ε_{iuc} against calculated values for a medium strength concrete. In this table, the stress and strain values are nondimensionalized with the values of f'_c, f'_t, ε_{io} and ε_{iot}, which for this concrete were -4650 psi, 423 psi, -.00219 in./in. and .00009 in./in. respectively. The observed values are those taken from Kupfer (1973). The calculated values of σ_{ic} / f'_c and σ_{ic} / f'_t are the values which would be found using the equations in Section 3.3.4.1 and the given stress ratios. Two sets of the values $\varepsilon_{iuc} / \varepsilon_{io}$ and $\varepsilon_{iuc} / \varepsilon_{iot}$ are then listed. The first set, calculated from the predicted σ_{ic} represent the values which would be found starting only with the knowledge of the stress ratio, and include any errors which may be included when calculating σ_{ic}. The second set are calculated using the observed values of σ_{ic}. However, there is no difference in the strain values obtained using the predicted or observed σ_{ic} in the compression-compression or tension-tension quadrants as the strain values in these quadrants are calculated directly from the stress ratio and independently of the ultimate stresses. Only in the compression-tension region are the ultimate stresses used to calculate ε_{iuc}.

The values of σ_{if} and ε_{if} are used to define the shape of the declining branch of the stress-strain curve. At the present time, there are few existing studies on the declining branch of concrete stress-strain curves (Evans and Morathe, 1968; Hughes and Chapman, 1966) and the following assumptions, made by Elwi and Murray (1979) will be used.

$$\varepsilon_{if} = 4 \quad \varepsilon_{iuc} \tag{3.3.36}$$

$$\sigma_{if} = \sigma_{ic} / 4 \tag{3.3.37}$$

These are the last values required to calculate σ_i and E_i from Eqs. 3.3.8 and 3.3.15.

3.3.5 Tensile Declining Branch

Chapter 5 contains a detailed comparison of the experimental observations of test wall segments and of the analytical results obtained from COWSAC on models of these test segments. From these comparisons, it became clear that the declining branch of the Saenz stress-strain curve was too steep for tensile stresses. As a result, the declining branch previously described by the Saenz equation was replaced by a straight-line of negative slope with a minimum residual strength. This curve is shown graphically in Fig. 3.10. Up to ε_{iuc}, in both the major and minor directions, the $\sigma - \varepsilon_{iu}$ curves follow the Saenz relation. Beyond these points, the stress decrease $\Delta\sigma_i$, is linearly related to the increase in equivalent uniaxial strain, $\Delta\varepsilon_{iu}$.

For the major direction, (direction 1, $\sigma_1 > \sigma_2$) the declining slope E_1 is

$$E_1 = \frac{6.5\ \sigma_{1c}}{7.5 \times 30\ \varepsilon_{iuc}} \qquad (3.3.38)$$

In the minor direction, the slope E_2 equals

$$E_2 = \frac{6.5\ \sigma_{2c}}{7.5 \times 30\ \varepsilon_{iuc}} \qquad (3.3.39)$$

In both directions the minimum residual stress is σ_{1c} / 7.5.

As the Saenz equation was developed for concrete subject to compression forces, and no test wall segments were tested in axial compression, there was no necessity to change the postultimate portion of the Saenz curve in compression. For tension-compression stress combinations, the tensile stresses are assumed to follow the $\sigma - \varepsilon_{iu}$ curve of the major direction shown in Fig. 3.10 while the compressive stresses follow the Saenz equation.

3.3.6 Equivalent Uniaxial Strain Constants

To accurately describe the concrete constitutive relations, two additional constants over and above the normally obtainable values of f'_c, f'_t, E_o and υ_o are required to help shape the concrete stress-strain curves in compression and tension. These are ε_{io}, the strain at maximum stress in uniaxial compression, and ε_{iot}, the strain at maximum stress in uniaxial tension. For uniaxial tension or compression, the equivalent uniaxial strains equal the real strains.

If these strains cannot be provided to the program, the following default equations are invoked (Saenz, 1964)

$$\varepsilon_{io} = \frac{-1 \times f'^{\,1/4}_c (31.5 - f'^{\,1/4}_c)}{100{,}000} \qquad (3.3.40)$$

$$\varepsilon_{iot} = \frac{f'_t}{E_o} \qquad (3.3.41)$$

For Eq. 3.3.40, f'_c must be in units of psi. The value of ε_{iot} from Eq. 3.3.41 assumes that the $\sigma - \varepsilon_{iu}$ curve in tension is linear up to the ultimate stress whereas the program follows the curved Saenz equation,

whose slope starts at E_o from a strain of zero and then declines to zero at a strain equaling ε_{iot}. Therefore, it is suggested that the default value of ε_{iot} be overridden when using COWSAC. A better value of ε_{iot} would be larger than that suggested by Eq. 3.3.41, possibly by a factor of 1.2 or 1.3.

3.3.7 Instability Arising From the Declining Branch of the Stress-Strain Curve

The use of the concept of equivalent uniaxial strains, and of the stress ratio, σ_1 / σ_2 as the basis for defining the failure curves, in conjunction with an iterative numerical procedure, leads to instabilities on the declining branches of the $\sigma - \varepsilon_{iu}$ curves. This instability manifests itself in the degeneration of the minor stress-strain curve (smaller absolute magnitude) to a point at the origin of the stress-equivalent uniaxial strain space.

To describe this problem, some of the solution procedures will be described for test wall segment No. 1, detailed in Table 5.1 and Fig. 5.4. This is a typical prestressed and reinforced wall segment tested at a load ratio of 2:1. For this specimen, the direction with the greater load will be called direction 1. This direction also corresponds with the major direction (direction of greater absolute stress) of the concrete layers.

As indicated by the test results in Fig. 5.4, each of the two load-extension curves can be divided into two distinct parts: the first, of large constant stiffness up to cracking, in which both the stress in the steel and the concrete increase, and the second of smaller stiffness

(slope) after cracking, in which the stress in the concrete decreases.

On the first portion of these curves, when the total specimen displays a large stiffness, the concrete is on the ascending branch and the minor direction is stable. If a greater stress is required in direction 2, the strains in that direction are increased. When this occurs, the stress point of the concrete in an individual layer, which is originally at location B on the solid curve of Fig. 3.11a moves up and along this solid curve to increase the stress in direction 2. Since this stress has increased relative to the major direction, the stress ratio changes and the final location of the stress-strain point in direction 2 is at B' on the dashed line. Since the total strains have increased, the stress in the steel layers also increases. For the entire segment, the response to an increase in load in direction 2 is, due to the positive stiffness of the segment, an increase in strain in direction 2. This results in greater stress in the steel layers, and greater stress in the concrete as the concrete stress moves from B to B' in Fig. 3.11a.

On the second branch of the curves in Fig. 5.4, when the total specimen displays a smaller positive stiffness, the concrete is on the declining branch of the stress-strain curves and the minor direction is unstable. If a greater stress is required in direction 2, the strains in direction 2 are increased, as the overall segment has a positive stiffness. When this occurs, the stress-strain point of the concrete in an individual layer which is originally at location B of Fig. 3.11b moves down along the stress-strain curve. Since the stress-ratio has changed, the final location of the stress-strain point in the minor direction is

at B' on the dashed curve of Fig. 3.11b. The overall segment response indicates an increase in steel stresses, but a large decrease in concrete stresses. To compensate for the decrease in concrete stresses, the strains in direction 2 are increased further. The cycle is repeated and the minor direction degenerates to zero.

To prevent this degeneration, the stress loss in absolute terms in the minor direction on the descending branch has been limited to

$$|\Delta\sigma^m| \leq |E^m \times \Delta\varepsilon^m| \qquad (3.3.42)$$

where $\Delta\sigma^m$ is the change in stress in the minor direction, E^m is the tangent modulus on the declining branch in the minor direction, and $\Delta\varepsilon^m$ is the change in real mechanical strains in the minor direction.

If the stress loss calculated by the normal procedure is greater than that calculated by Eq. 3.3.42, then the results are overridden by Eq. 3.3.42. This action prevents the stress ratio on the declining branch from decreasing, but will not inhibit an increase in the stress ratio, which is updated twice during every increment in real strains. (See Chapter 4).

3.3.8 Unloading

In a generally accepted definition of unloading as used in plasticity (Fung, 1965) a loading surface exists which is a function of the stress state, plastic strains and a strain hardening parameter, on which the current biaxial stress state is located. It can be assumed that the shape of this curve in two dimensions before plastic strains have occurred is similar to that describing the stress failure curve, and that if the

distance from the point of zero stress to the failure curve in any one direction is L_f, and if the distance from the point of zero stress to the loading curve in this same direction is L_1, then the ratio L_1 / L_f is a constant (less than or equal to one) for any particular loading curve. Knowing the shape of the loading curve then, in the elastic range if the next stress point is on the outside of the loading curve, the material is being loaded. If the next stress point is on the inside of the loading curve, then the material is being unloaded.

To reduce the complexity of applying this definition in programming, the failure curve used was the curve of equivalent uniaxial strains at ultimate stress, Fig. 3.9, and the loading curve contained the current equivalent uniaxial stresses. Unloading again occurs when the next point is within the current loading curve. The unloading condition is then approximated by the following.

$$\left|\frac{\varepsilon_{iu}}{\varepsilon_{iuc}}\right|_{\text{present load state}} - \left|\frac{\varepsilon_{iu}}{\varepsilon_{iuc}}\right|_{\text{previous load state}} < 0 \qquad (3.3.43)$$

If Eq. 3.3.43 is satisfied in both directions, then an unloading condition is assumed to have occurred. If the material is on the ascending portion of the stress-strain curve, then unloading follows the nonlinear Saenz relation. However, if unloading occurs when on the descending branch of the stress-strain curve, then the stresses and stiffness drop to zero. When this happens on a compression curve, that layer of concrete is assumed to have crushed and will take no further compressive or tensile loads. When this occurs on a tensile curve, that layer of concrete is

assumed to have cracked and will take no further tensile stresses. This cracked layer can take full compressive load after the crack closes. The example problem discussed in Chapter 4 discusses unloading behavior in further detail.

3.3.9 Crack Closure After Unloading

In a reinforced concrete wall segment subjected to tensile loads, the average response of the concrete appears to follow the stress-strain curve exhibited in Fig. 3.10. However cracks open up in the specimen, across which no stresses can exist, even though the 'average' stress-strain curve predicts some load carrying capacity. It can be assumed that the classical brittle linear elastic curve with a tension cut-off shown in Fig. 3.14 more closely represents the concrete behavior on a microscopic level in a normal test situation. With this model, no inelastic strains will accumulate in the concrete even though the 'average' strains are greater than the strain at maximum stress. The additional strains predicted by Fig. 3.10 result from the opening and widening of cracks. The concrete in between the cracks behaves linearly and elastically. Therefore we can predict the point at which the concrete accepts compressive stresses (crack closure) with elastic theory, as follows.

If the concrete is cracked in both directions, then the concrete will close in one direction when

$$\varepsilon_i \leq 0 \tag{3.3.44}$$

where ε_i are the real mechanical strains in direction i. This then

reduces the problem to one of cracking in one direction.

If the concrete is cracked in only one direction, the point at which the cracks close can be found by determining the conditions under which the concrete will develop compression in this direction.

If direction 1 is the cracked direction, then at crack closure, Eq. 3.3.4 can be evaluated by assuming that E_2, the tangent modulus in the stressed direction, is approximately equal to the secant modulus, and hence

$$E_1 = E_o \qquad \sigma_1 = 0 \qquad (3.3.45)$$

$$E_2 = E_2 \qquad \sigma_2 = \sigma_2 \qquad (3.3.46)$$

Then Eq. 3.3.4 becomes

$$\sigma_1 = \frac{1}{(1-\upsilon^2)} \left[E_1 \varepsilon_1 + \upsilon \sqrt{E_1 E_2}\ \varepsilon_2 \right] \qquad (3.3.47)$$

Setting σ_1 to zero in Eq. 3.3.47, the strain, ε_1, at which cracks in direction 1 close can be determined as

$$\varepsilon_1 = -\upsilon \sqrt{E_2 / E_o}\ \varepsilon_2 \qquad (3.3.48)$$

If the second direction is in compression and has progressed significantly along the stress-strain curve, some inelastic strains will have occurred, violating the assumption of elastic behavior and reducing the accuracy of this relation.

3.4 Reinforcing Steel Constitutive Relation

The reinforcing steel is modelled as a uniaxial layer, contributing its stiffness to the wall segment only along its length, and replacing the concrete in that direction. In the transverse direction, the presence of the steel has no effect and the concrete stiffness and stresses are used, making no modification for the steel. Due to its one-dimensional contribution, a simple elastic-plastic stress-strain curve can be used for the reinforcing steel as shown in Fig. 3.12.

The steel has an initial constant stiffness up to yield, beyond which the tangent stiffness becomes zero and the stress is maintained at the yield stress. This is described by the equations

$$\sigma = -\sigma_y \qquad \varepsilon < -\varepsilon_y \qquad (3.4.1)$$

$$\sigma = E_{st} \times \varepsilon \qquad -\varepsilon_y \leq \varepsilon \leq \varepsilon_y \qquad (3.4.2)$$

$$\sigma = \sigma_y \qquad \varepsilon_y < \varepsilon \qquad (3.4.3)$$

where σ_y is the yield stress of the steel, E_{st} is the Young's modulus for the steel and ε_y equals σ_y / E_{st}. This curve is followed for both loading and unloading.

3.5 Prestressing Steel Constitutive Relation

The prestressing strands are also one-dimensional elements and are treated similarly to the reinforcing steel elements. The stress-strain curve for the strands was derived from tests taken in conjunction with the wall segment tests discussed in Chapter 5 and is composed of 6 straight lines as shown in Fig. 3.13.

The equations describing the curve, again applicable to both loading

and unloading, are

$$\sigma = E_p \times \varepsilon \qquad \varepsilon < \varepsilon_{sy} \qquad (3.5.1)$$

$$\sigma = 0.777\,\sigma_{pu} + \frac{(.087\,\sigma_{pu})(\varepsilon - \varepsilon_{sy})}{.0084-\varepsilon_y} \qquad \varepsilon_{sy} < \varepsilon < .0084 \qquad (3.5.2)$$

$$\sigma = 0.864\,\sigma_{pu} + 20\,\sigma_{pu}\,(\varepsilon - .0084) \qquad .0084 < \varepsilon < .010 \qquad (3.5.3)$$

$$\sigma = 0.896\,\sigma_{pu} + 6.5\,\sigma_{pu}\,(\varepsilon - .010) \qquad .010 < \varepsilon < .012 \qquad (3.5.4)$$

$$\sigma = 0.909\,\sigma_{pu} + 4.75\,\sigma_{pu}\,(\varepsilon - .012) \qquad .012 < \varepsilon < .020 \qquad (3.5.5)$$

$$\sigma = 0.947\,\sigma_{pu} + \frac{.053\,\sigma_{pu}}{.23}\,(\varepsilon - .020) \qquad .020 < \varepsilon < .25 \qquad (3.5.6)$$

$$\sigma = 0 \qquad .25 < \varepsilon \qquad (3.5.7)$$

where E_p is the initial Young's modulus of the prestressing strands, σ_{pu} is the ultimate strength of the prestressing strands and ε_{sy} equals $0.777\,\sigma_{pu} / E_p$.

	Observed Values				Calculated Values					
							From Predicted σ_{ic}		From Observed σ_{ic}	
$\frac{\sigma_1}{\sigma_2}$	$\frac{\sigma_{ic}}{f'_c}$	$\frac{\sigma_{ic}}{f'_t}$	$\frac{\varepsilon_{iuc}}{\varepsilon_{io}}$	$\frac{\varepsilon_{iuc}}{\varepsilon_{iot}}$	$\frac{\sigma_{ic}}{f'_c}$	$\frac{\sigma_{ic}}{f'_t}$	$\frac{\varepsilon_{iuc}}{\varepsilon_{io}}$	$\frac{\varepsilon_{iuc}}{\varepsilon_{iot}}$	$\frac{\varepsilon_{iuc}}{\varepsilon_{io}}$	$\frac{\varepsilon_{iuc}}{\varepsilon_{iot}}$
$\frac{-1}{-1}$	1.15 1.15		1.735 1.735		1.16 1.16		1.750 1.75		1.750 1.750	
$\frac{-0.52}{-1}$	0.645 1.240		0.890 1.667		0.652 1.25		0.978 1.658		0.978 1.658	
$\frac{-0.22}{-1}$	0.262 1.19		1.594 1.575		0.269 1.21		0.488 1.526		0.488 1.526	
$\frac{0}{-1}$	0. 1.00		0 1.00		0 1.00		0 1.00		0 1.00	
$\frac{0.052}{-1}$	0.850	0.484	0.653	1.11	0.729	0.417	0.493	0.884	0.675	0.929
$\frac{0.070}{-1}$	0.770	0.594	0.557	1.11	0.637	0.490	0.393	0.932	0.548	0.973
$\frac{0.103}{-1}$	0.620	0.704	0.388	0.667	0.518	0.586	0.299	0.971	0.377	0.992
$\frac{0.202}{-1}$	0.370	0.824	0.210	0.773	0.331	0.735	0.199	0.995	0.217	0.999
$\frac{1}{0}$		1.00 0		1.00 0		1.00 0		1.00 0		1.00 0
$\frac{1}{0.23}$		1.077 0.253		1.17 0.556		1.00 0.230		1.10 0.466		1.10 0.466
$\frac{1}{0.54}$		1.033 0.561		1.11 0.667		1.00 0.540		1.20 0.689		1.20 0.689
$\frac{1}{1}$		1.00 1.00		1.22 1.22		1.00 1.00		1.25 1.25		1.25 1.25

TABLE 3.1 Comparison of Observed and Calculated Values of σ_{ic} and ε_{iuc}

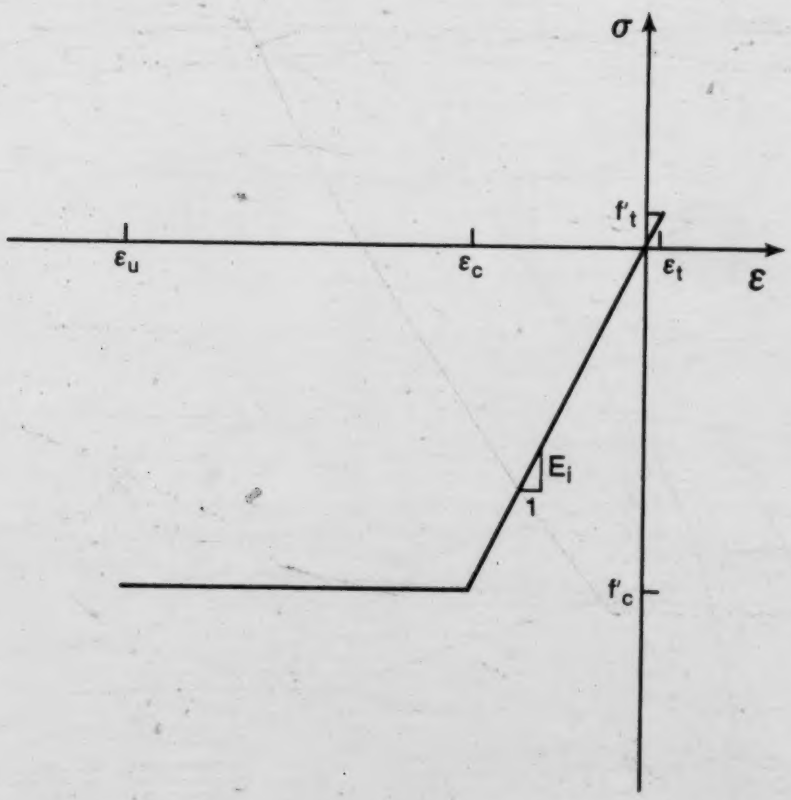

Fig. 3.1 Uniaxial Bilinear Elastic Stress-Strain Law

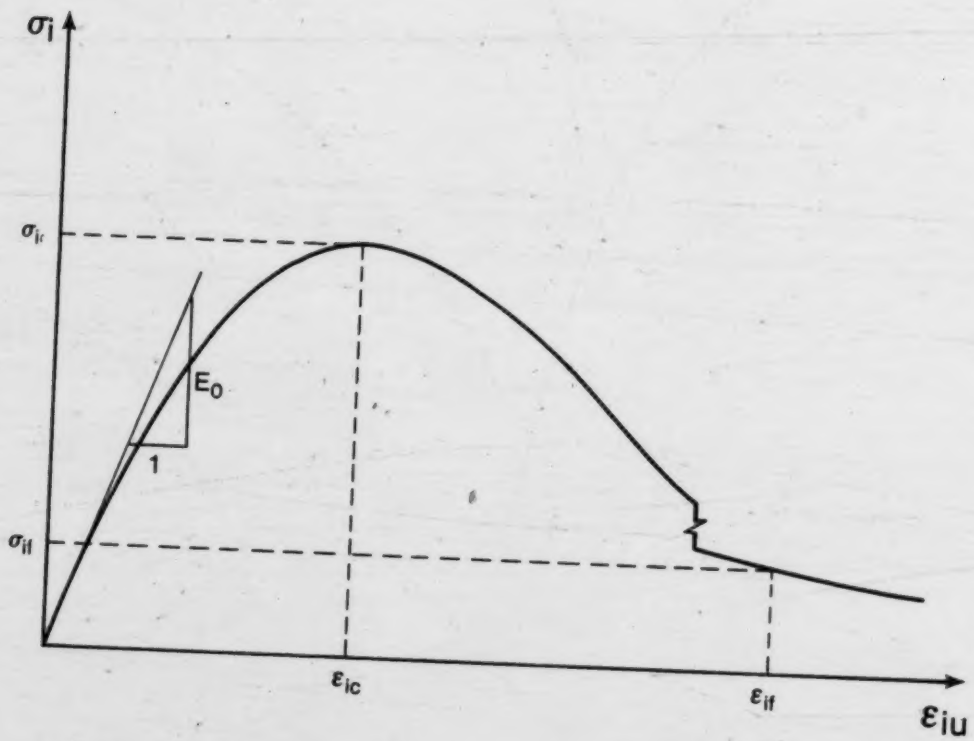

Fig. 3.2 Typical Compressive Stress-Equivalent Uniaxial Strain Curve

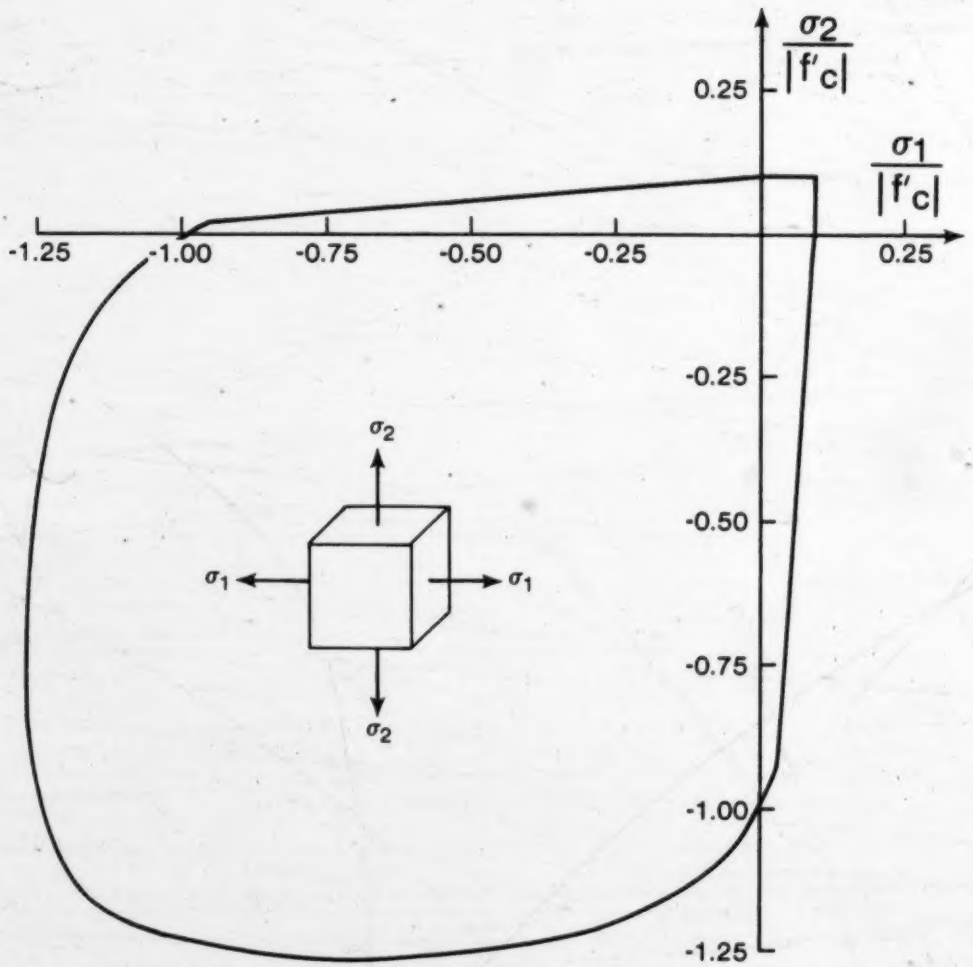

Fig. 3.3 Ultimate Stress Curve

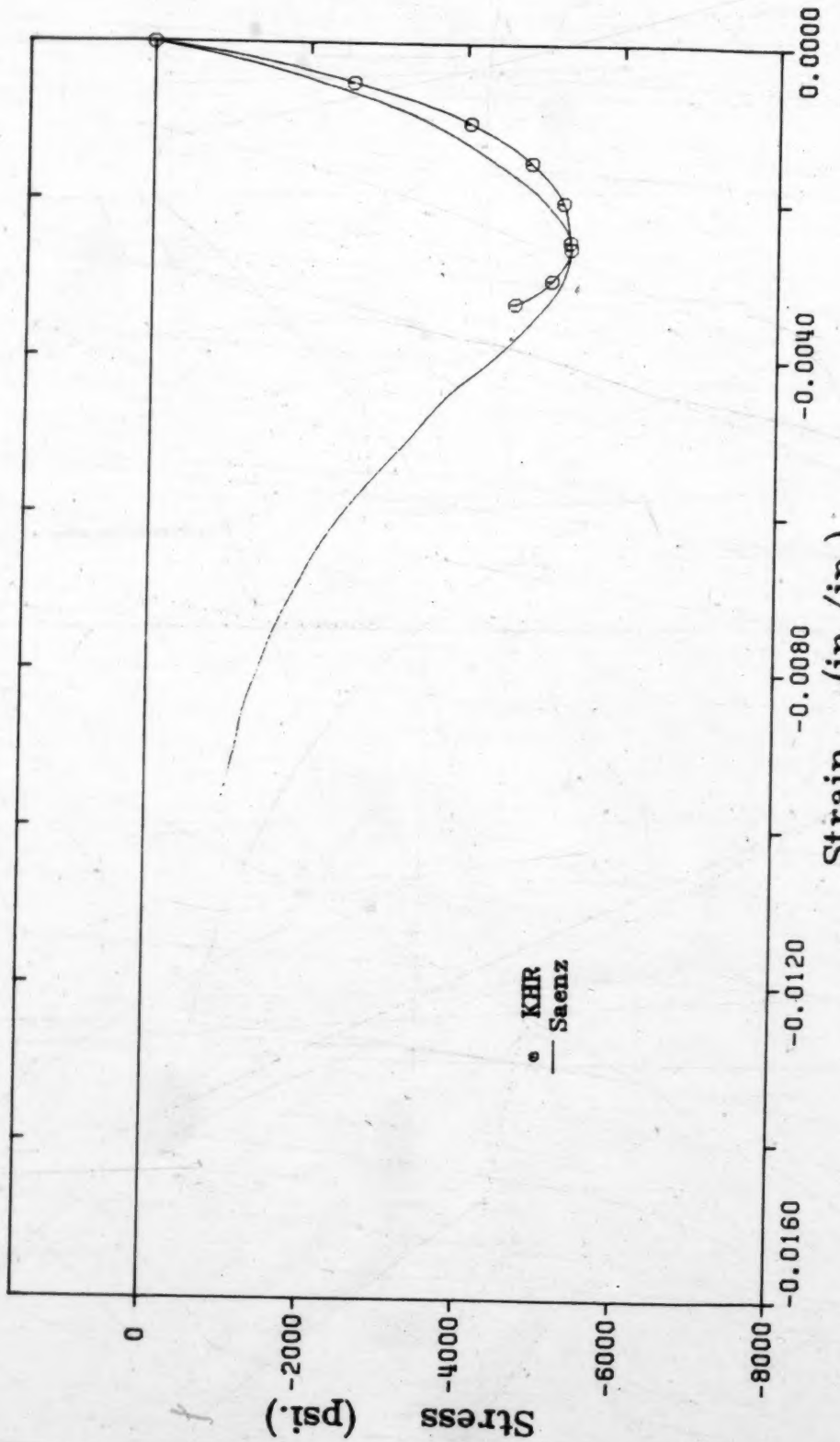

Fig. 3.4 Comparison of Saenz Equation and KHR Data for $\sigma_1 / \sigma_2 = 0 / -1$

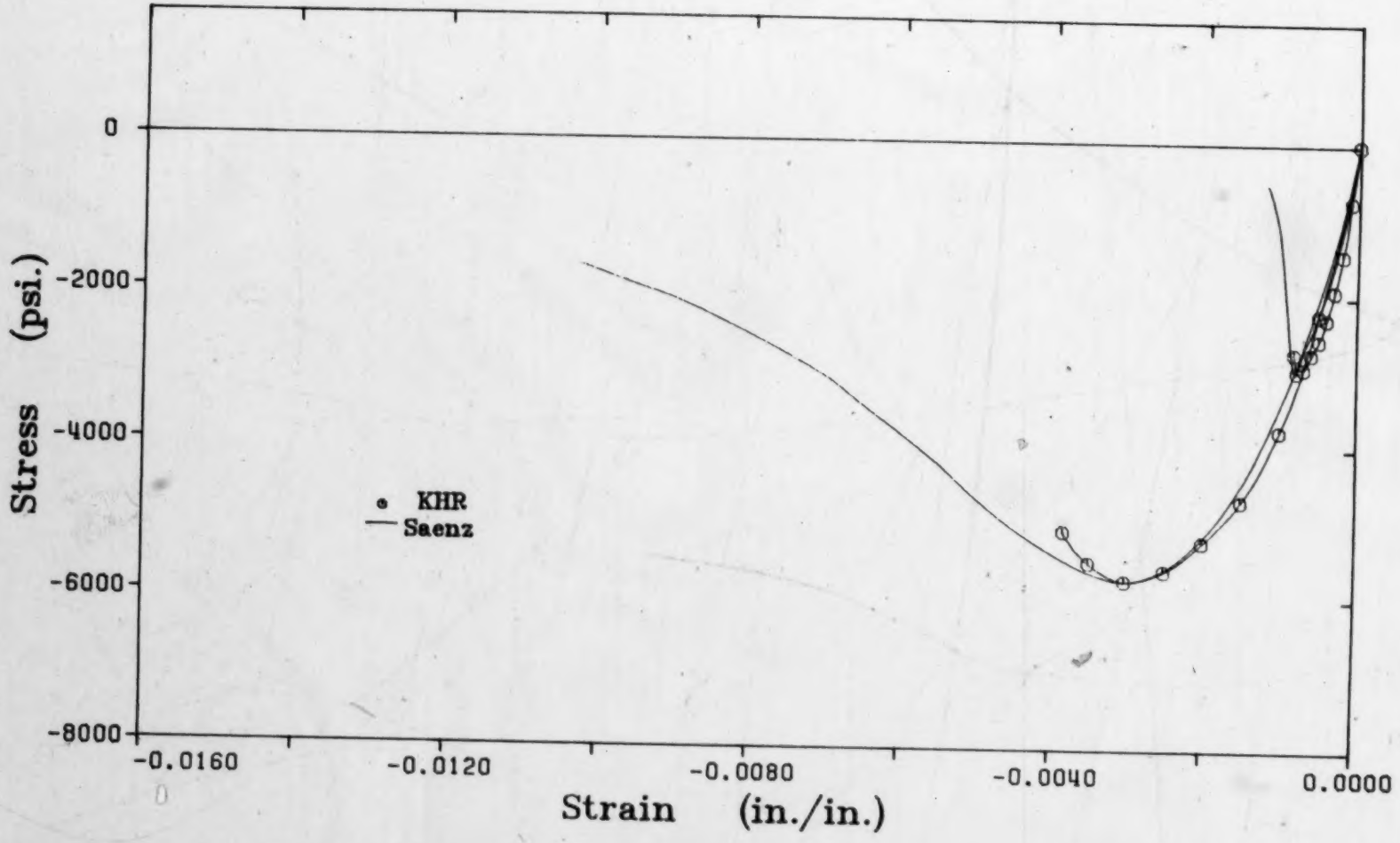

Fig. 3.5 Comparison of Saenz Equation and KHR Data for $\sigma_1 / \sigma_2 = -.5 / -1$

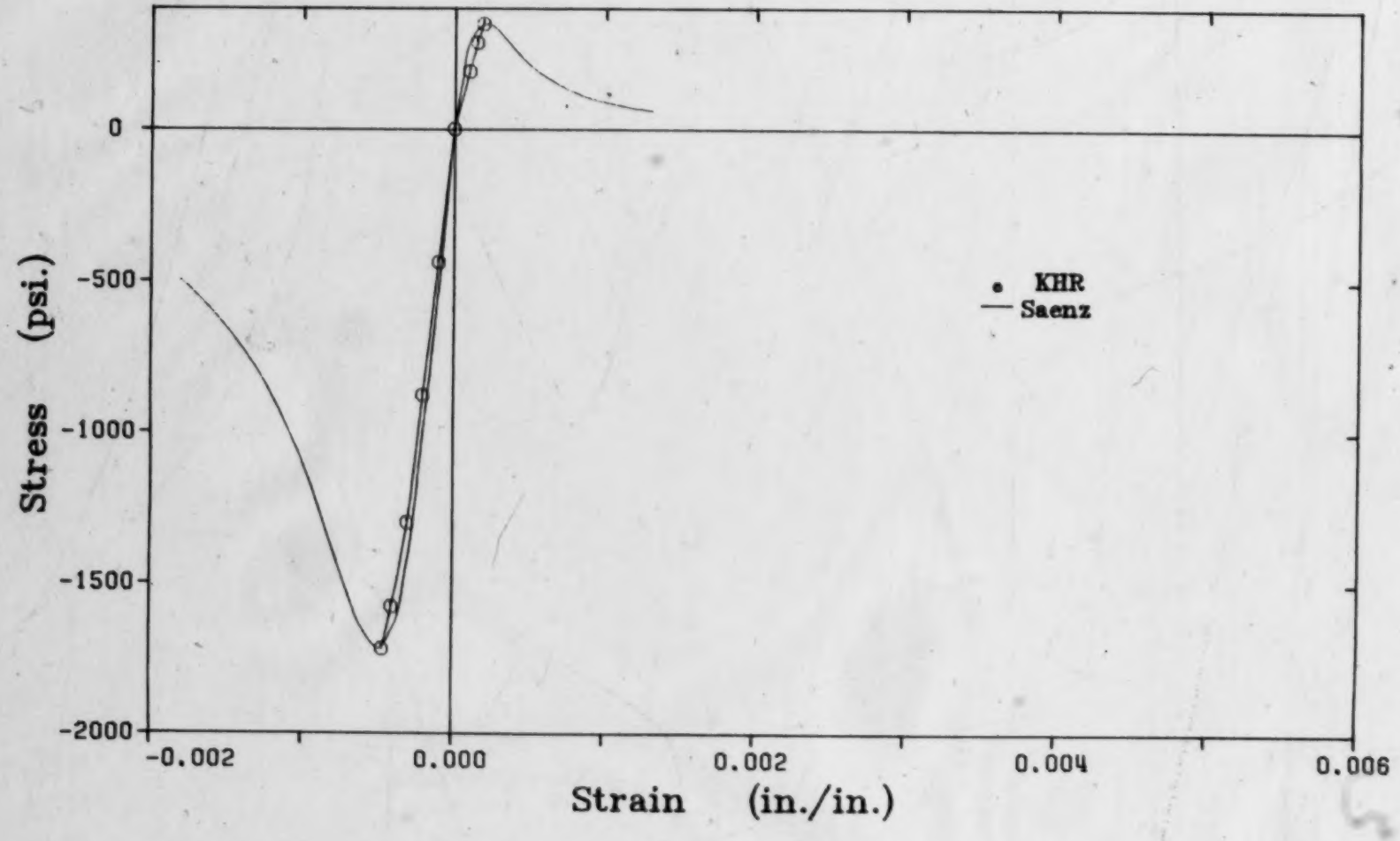

Fig. 3.6 Comparison of Saenz Equation and KHR Data for $\sigma_1 / \sigma_2 = .22 / -1$

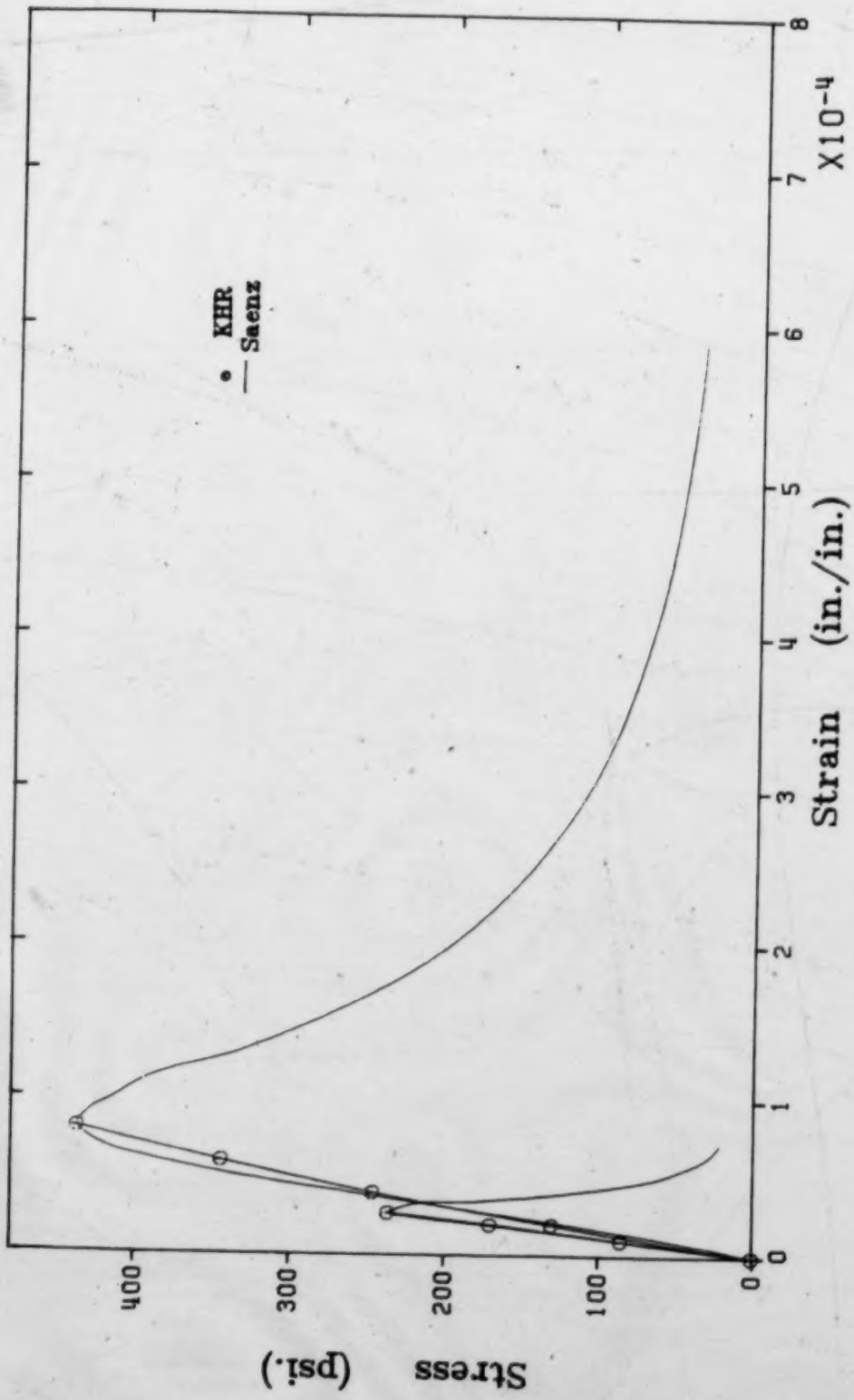

Fig. 3.7 Comparison of Saenz Equation and KHR Data for $\sigma_1 / \sigma_2 = 1 / .5$

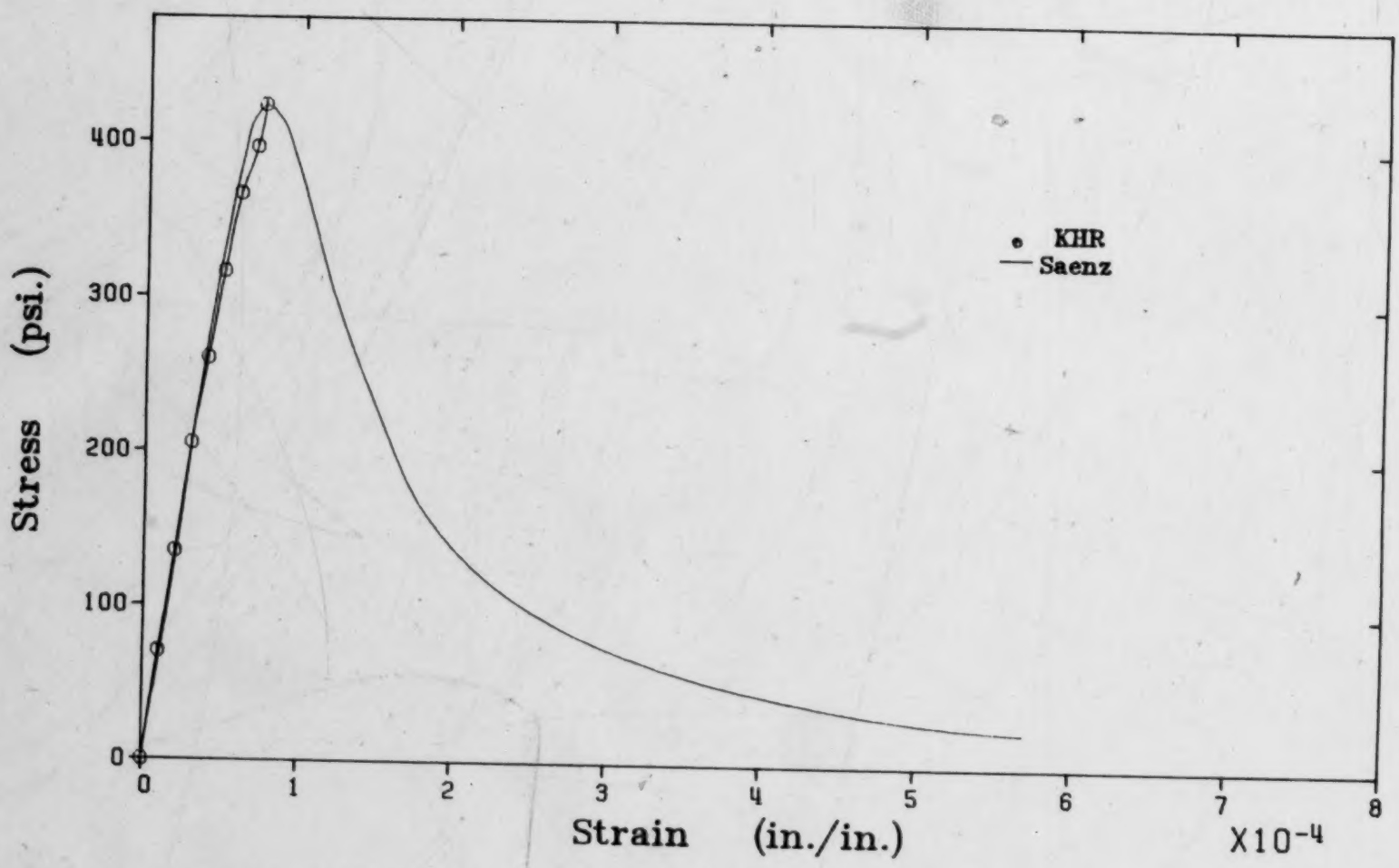

Fig. 3.8 Comparison of Saenz Equation and KHR Data for $\sigma_1 / \sigma_2 = 1 / 0$

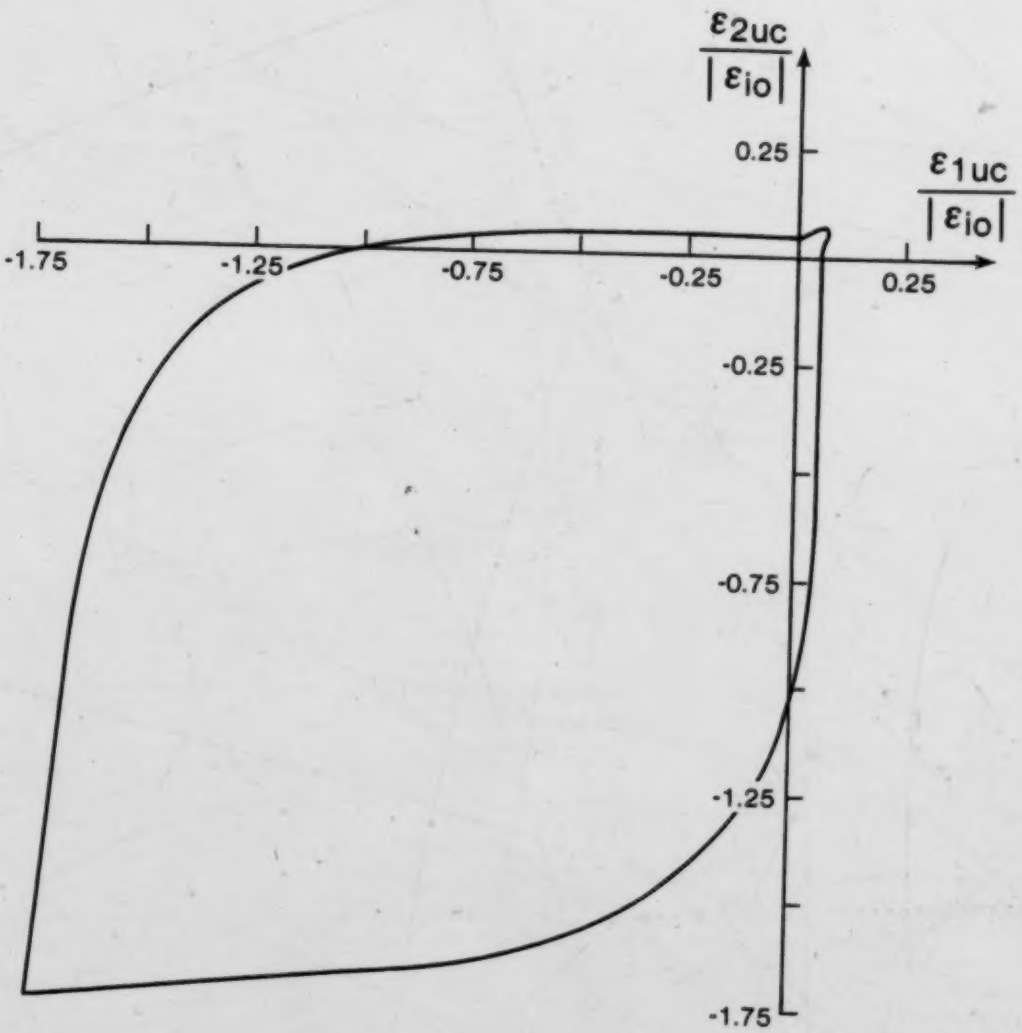

Fig. 3.9 Equivalent Uniaxial Strains at Ultimate Stress

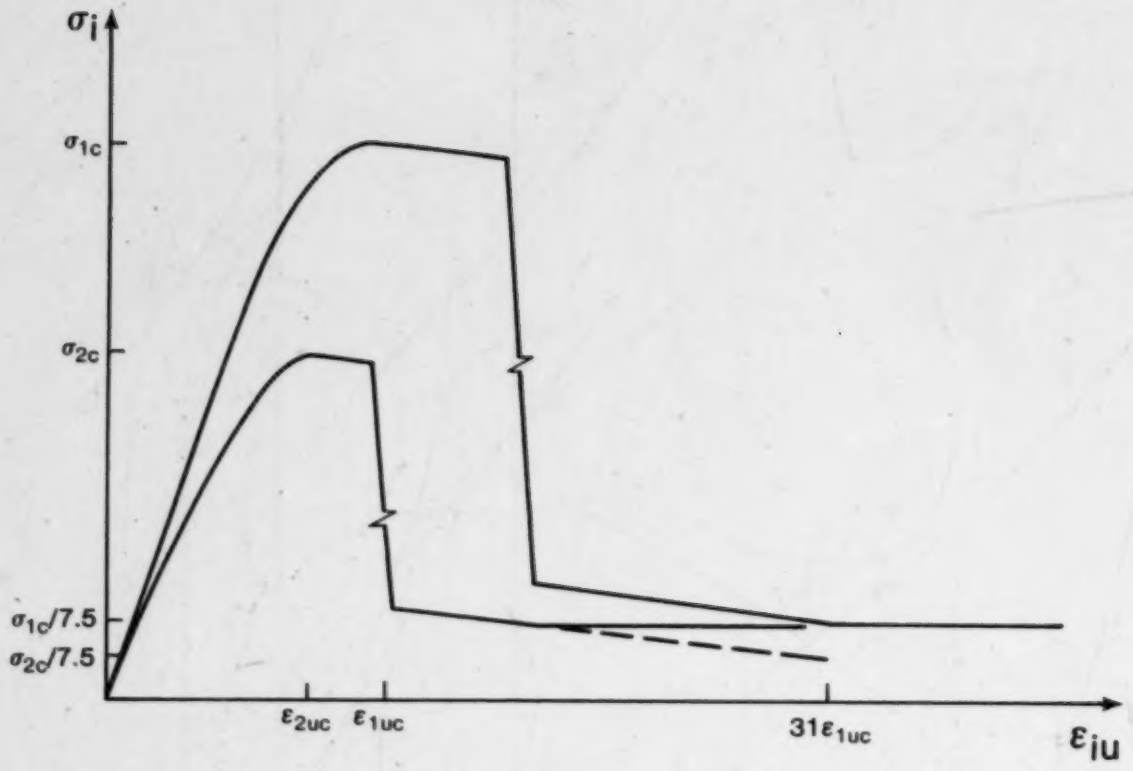

Fig. 3.10 Stress-Equivalent Uniaxial Strain Curve in Tension

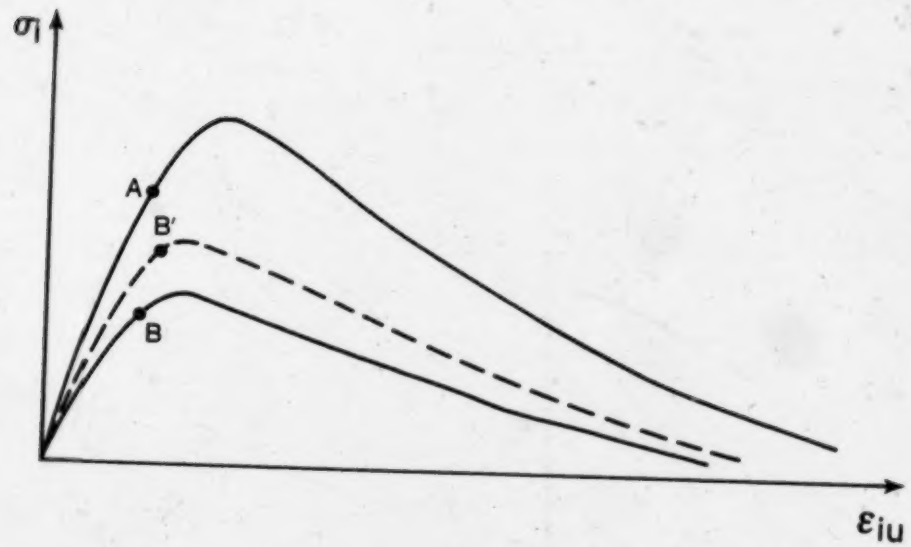

Fig. 3.11a Concrete Stresses on Ascending Branch of σ-ε_{iu} Curve

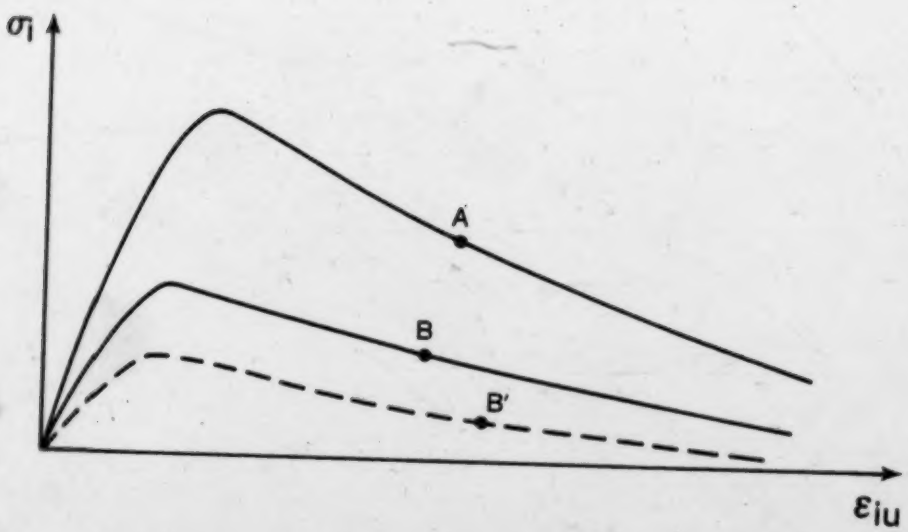

Fig. 3.11b Concrete Stresses on Descending Branch of σ-ε_{iu} Curve

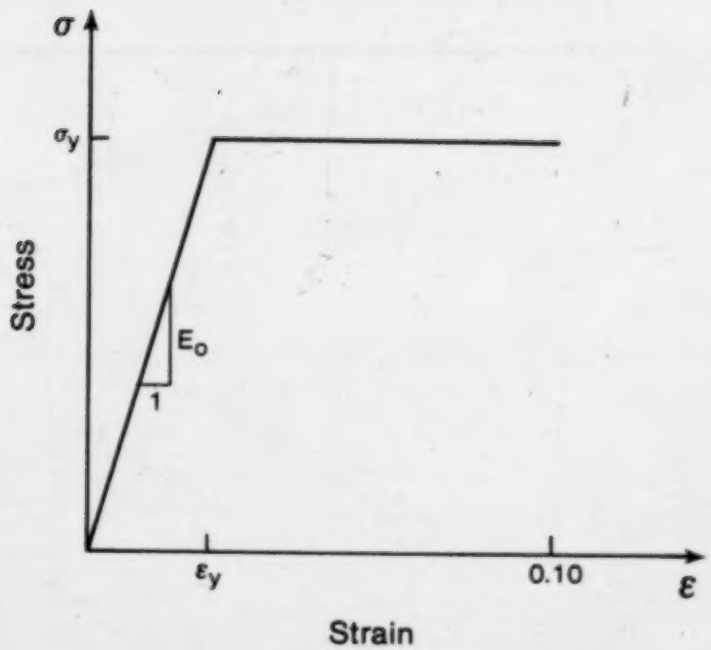

Fig. 3.12 Stress-Strain Curve for Reinforcing Steel

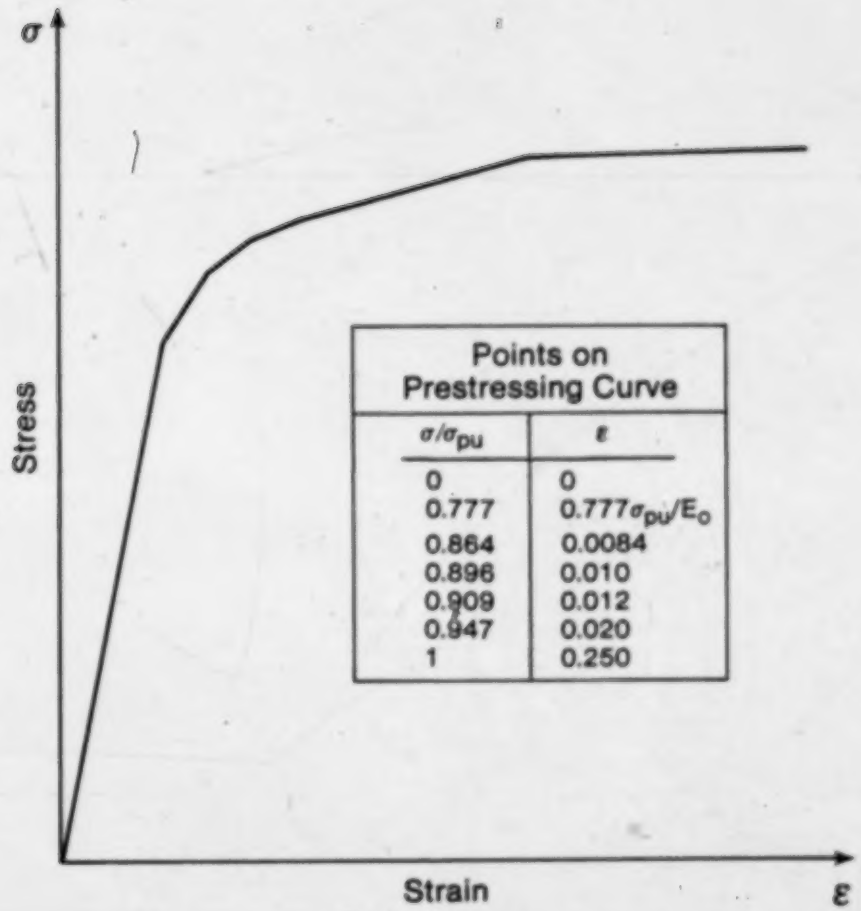

Points on Prestressing Curve	
σ/σ_{pu}	ε
0	0
0.777	$0.777\sigma_{pu}/E_o$
0.864	0.0084
0.896	0.010
0.909	0.012
0.947	0.020
1	0.250

Fig. 3.13 Stress-Strain Curve for Prestressing Strands

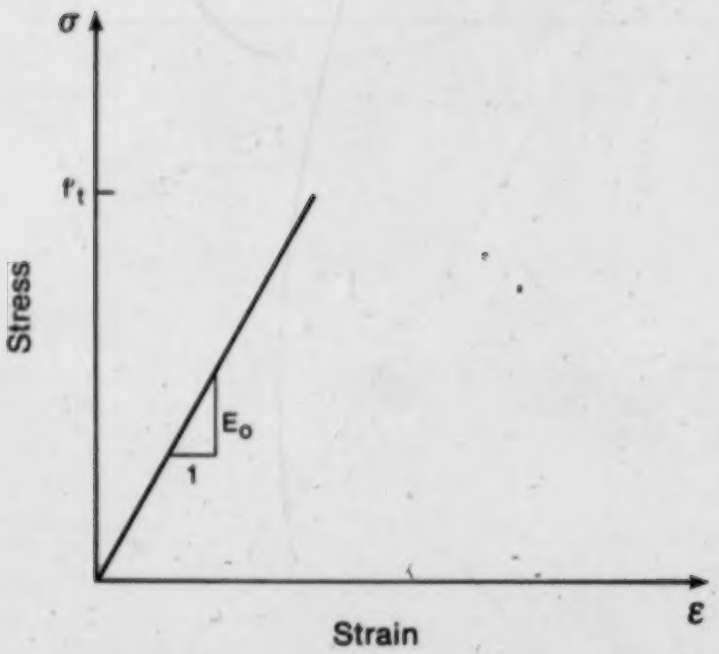

Fig. 3.14 Linear Elastic Stress-Strain Curve for Concrete in Tension, with Tension Cut-off

4. PROGRAM DEVELOPMENT

4.1 Description of Approach

The computer coding which was developed to solve the range of problems outlined in Chapter 1, was designed to be user oriented. To satisfy this requirement, the successful operation of the program must be accomplished with a minimum of input, and the data requests must be sufficiently flexible to handle a wide variety of problems. To help provide the needed versatility, no restrictions are placed on the specimen dimensions or steel layer locations. A variety of loading schemes are available, which can be mixed. Any consistent system of units may be used to specify the problem; the program output will follow in consistent units.

Before the live load is applied, there is opportunity to place four different types of load on the wall segments in the following order, which is based on a possible construction sequence. Before the prestressing is applied, a dead load can be placed on the segment. This load will stress the concrete and reinforcing steel, but not the prestressing steel. For this load step, the area occupied by the prestressing steel will be assumed to have no stiffness and no strength, so effectively the prestressing strands are considered to be absent, with empty holes at their designated locations. For this and all load steps, the concrete strength is expected to have the set of material properties which are specified by the user. No reduction in strength due to concrete immaturity is here allowed or accounted for.

After the dead load, the prestressing can be applied. The pre-

stressing force (rather than stress) can be specified as a value to be achieved either before or after the elastic response of the specimen to the prestressing forces has taken place. In addition, the option exists to sequence the prestressing. The tendons can be stressed either individually, in groups, or all at once, according to the order specified by the user. As each of the prestress steps is applied, a load must be specified which is the load on the segment at the conclusion of each prestress increment. This load is in addition to the internal load resulting from the prestressing. For example, the test wall segments which are discussed in Chapter 5 are prestressed but are not subjected to any external forces. Therefore, the load on the segment at the conclusion of prestressing of these test wall segments would be zero forces and zero moments. However, the wall segments discussed in Chapter 6, which form part of the containment structure, have gravity loads upon them. The segment must be in equilibrium with the prestressing and these specified gravity loads.

Once the dead load and prestressing effects have been determined, the specimen can be allowed to creep if desired. This is accomplished by changing the elastic modulus of the concrete from the original short-term modulus to the long-term values, by means of a creep factor which is discussed in Chapter 3. The loads on the specimen at the time of prestressing are maintained and the creep strains which accumulate in the concrete are recorded. After the creep step, the elastic modulus of the concrete returns to its short-term value and the creep strains of each concrete layer are subtracted from the total strains to result in the net mechanical strains. The additional strains in the steel

layer which result from the creep process remain as the total strains and are used to calculate the steel stresses.

The first type of live load which can now be applied is a thermal load. Three different types of thermal gradients, each being defined by three specified constants as indicated in Eqs. 2.5.1 are available to describe most expected temperature distributions. The temperature change (from zero) calculated at each layer is then multiplied by the appropriate thermal expansion coefficient to find the thermal strain for that layer. The thermal effects can occur under boundary conditions of constant load or constant strain, as specified by the user.

The final loads to be applied are the live loads. These loads can be specified either as the total loads on the segment, or as additional loads to be added to the previous total loads. The type of load, either total or incremental, can be changed for each live load. Each live load can be subdivided into load increments so that a solution will be found at intervals between loads. The number of these subdivisions can be changed for each live load. If so desired, a loading procedure can be invoked where the load consists of axial forces and curvatures, the two being linearly dependent, and the curvature being calculated from initial force and moment data. This is the type of loading employed by Epstein and Murray (1976).

The above loading sequence of dead loads, prestressing loads, creep loads, thermal loads and live loads cannot be altered. However, not all of the loads must be included.

4.2 Program Flowcharts

The flowcharts in Figs. 4.1 to 4.5 serve to provide a general description of logical flow within the program, and to disclose the main iterative loops and subincrement generators. A detailed User's Manual, specifying input requirements, is contained in Appendix A, and a program listing is contained in Appendix B.

The main routine calls for the solution of the loads described above in the stated sequence. This is illustrated in Fig. 4.1. The solution of each type of load is similar and can be traced through the flowcharts of load control and load application, Fig. 4.2 and 4.3.

The flowchart of load control, shown in Fig. 4.1, describes the prime generator of load subincrements. If the bilinear elastic concrete constitutive relation is used for the solution, the load is not subdivided. If the nonlinear concrete constitutive equations are specified however, then the load is subdivided to restrict the change in overall segment strains to a set value. Once the load is subdivided, all the values describing the current status of the material layers are noted. These values are known to be correct and shall be used until the solution has converged at the next load subincrement. The method of solution is described in the flowchart of load application Fig. 4.3, which is discussed later. Once the solution has been found for the last subincrement of the current load step, the overall change in strain for the wall segment is checked to see if this change is too large for the number of subincrements. If this is true, the solution is rejected and the process returns to the start of the load application, with the values of the material parameters for each layer recalled from the end of the last

load step. The number of subincrements is increased and the solution process begins again.

The method of solution for a load subincrement is described in the flowchart of load application shown in Fig. 4.3. First the segment stiffness matrix is compiled from the results of the last trial solution. The program loops over all the layers calling for the appropriate constitutive relations, finds the stiffness of each layer and integrates these. Then with the current estimate of the segment strains, the biaxial strains for each layer are found, the stresses in each layer computed, and the load resistance of the wall segment calculated. The load resistance is then compared to the applied load. If the difference is small, the solution has been found. If the difference is large, a correction is made to the segment strains, and the loop repeated.

The constitutive relations for the steel layers and the bilinear elastic constitutive relation for the concrete are straight forward. However, the nonlinear concrete constitutive relation is more complex and is described in Fig. 4.4. This relation, if specified, is called separately for each concrete layer for every trial solution. The solution for the layer stiffness and stress begins by again checking the change in real strains. If this change is too large, the strain change is subdivided. For the current subdivision, an initial estimate is made of the change in equivalent uniaxial strains, $\Delta\varepsilon_{iu}^{1}$, using the values of the tangential moduli, E_i, the stresses, σ_i, and Poisson's ratio, υ from the previous subdivision. This initial estimate, $\Delta\varepsilon_{iu}^{1}$ is added to the previous total equivalent uniaxial strains, ε_{iu}, to find an estimate of the new total, ε_{iu}^{1}. Using σ_i and ε_{iu}^{1}, the failure para-

meters σ_{ic}^{1} and ε_{iuc}^{1} which are the ultimate stresses for the current stress ratio and the equivalent uniaxial strains at ultimate stresses for the current stress ratio, are calculated. New values for the stress σ_i^1, tangential modulus E_i^1 and Poisson's ratio υ^1, are found based on ε_{iu}^{1}, σ_{ic}^{1} and ε_{iuc}^{1}. A second estimate of $\Delta\varepsilon_{iu}$ is made, based on E_i^1 and υ^1. This new estimate $\Delta\varepsilon_{iu}^{2}$ is averaged with $\Delta\varepsilon_{iu}^{1}$ to find $\Delta\varepsilon_{iu}^{a}$. This averaged value, $\Delta\varepsilon_{iu}^{a}$ is added to the value of ε_{iu} from the last subdivision to obtain the new total equivalent uniaxial strain, ε_{iu}^{n}. Based on σ_i^1 and ε_{iu}^{n}, the failure parameters are revised to σ_{ic}^{n} and ε_{iuc}^{n}. These are then used to calculate the final values of σ_i^n, E_i^n and υ^n. This process is repeated for all of the strain subdivisions.

In total then, there is a hierarchy of three subdivision loops. The increment generator divides each load into load steps. This number is user controlled. The second subdivision occurs when the change in strains to solve a load step is too large. Here the load step is subdivided into load increments. The final increment generator is within the nonlinear concrete subroutine. If the strain change for the solution of a load increment is too large, then this strain change is subdivided. If however, the bilinear concrete equations are specified, only the first subdivision generator, which is user controlled, is operative.

4.3 Convergence Difficulties

Three different types of convergence problems may be encountered when using the program. The most common type of convergence difficulty involves a trial solution for the concrete which is so far from the correct solution that subsequent corrections to this trial lead to

greater error in the solution. The end result of this incorrect solution path may be either convergence on an incorrect solution which is in equilibrium with the loads, or no convergence at all. The three main levels of increment generators are designed to minimize the stray movement of the solution path by keeping the strain change between solutions small. After the solution of each load increment, the strain change is calculated and if this change is too large, the process returns to the last load increment, and this load increment is subdivided into load subincrements.

This type of convergence difficulty was most often encountered when the concrete stress is moving across the peak of the stress-strain curve or in other words, from the ascending to the descending branch. However it also occurred at the time of changes in the stiffness of the reinforcing bars or the prestressing strands. This type of convergence is not experienced when using the bilinear elastic concrete relation.

The second type of convergence problem which may be encountered can occur with either the bilinear or nonlinear concrete relations. This problem occurs when the program is only able to find solutions which bracket the correct solution, but which do not satisfy the accuracy requirements. This problem occurs most frequently when a layer of steel yields. To reduce the frequency of this, and also the first type of convergence problem, an under-relaxation factor is used which is applied to and reduces the calculated strain corrections. The under-relaxation factor is calculated to maintain the strain corrections below a set value. If, however, a solution which meets the accuracy requirements of 0.1%

is not found within 90 attempts, the accuracy requirement is reduced to 5%, and if this limit is satisfied, the solution is accepted and the next load increment is attempted. The determination of the accuracy of a solution is discussed in the next section.

If strains rather than forces are specified, none of these difficulties will occur. If a segment response curve contains a portion of overall negative stiffness, then again no difficulties will occur if strains are specified. However if forces are specified, then portions of negative stiffness for the wall segment can cause difficulties. To force the segment to accept increasing loads, after 20 strain corrections have been applied, the strains are constrained to move in the same direction as the loads. Thus, if the axial force in Direction 1 is increasing, then the strains in this direction are not allowed to decrease. This mechanism can be successful in jumping small dips in the response curve.

A fourth convergence problem which always occurred after the concrete response had moved into the post ultimate region of the stress-strain curves, involved the degeneration of the stress-strain curve in the minor direction. This problem has been effectively eliminated. The technique employed to overcome this problem is dealt with in Section 3.3.7.

4.4 Solution Accuracy

The accuracy of a solution is approximated by the following equation

$$A = \sqrt{\left[\sum_{i=1}^{4} (\Delta Q_i / F_i)^2\right] / m} \qquad (4.4.1)$$

where ΔQ_i is the unbalanced load at degree of freedom i, F_i is the specified load at degree of freedom i, m is the number of degrees of freedom where a force rather than a deformation is specified, and the result A is the calculated accuracy of the solution. Only those degrees of freedom at which forces are specified are included in this equation so that $(\Delta Q_i / F_i)$ is set to zero for those degrees of freedom at which deformations are specified. The accuracy limit which A must satisfy for solutions determined in ninety trials or less is .001. For solutions found between the ninety-first and the one hundred and twentieth trial, A must be less than or equal to .05.

4.5 Layering Technique

The concrete wall segment, when subjected to a curvature, does not react uniformly across the wall thickness because of the imposed strain gradient. In addition, the presence of the steel layers causes further differences in the response of the segment, from that of a plain concrete section. To account for these effects, the wall segment has been subdivided into layers through the wall segment as shown in Fig. 4.6. Within each layer, the material is assumed to have uniform properties and individual layers are not influenced by adjoining layers. By then integrating across all of the concrete and steel layers, the composite response of the wall segment, including any nonlinear results, will be assessed. The values of the elements in the matrix $[C]$ of Eq. 2.3.25 and in the vector of Eq. 2.3.19 are found by calculating separately for each concrete and steel layer, the values of σ_i, Z and $\partial f_i / \partial \varepsilon_i$. The integration of these values through the entire thickness of the wall

gives the complete wall properties.

This integration is organized into two parts. First, the wall segment is modelled ignoring the steel. Second, the steel is added. The integration of the plain concrete follows the stated technique without complication. The advantage of the technique is that the number of the plain concrete layers, and their thicknesses are uniform, not being affected by the steel. The steel layers, at any location in the segment, and of any thickness, are simply added into the sum. To account for the concrete which was displaced by the steel, but has been included in the integrated properties, a negative concrete layer is associated with each steel layer. The results obtained from this negative concrete layer are subtracted from the integration of the wall segment. Because of the unidirectional contribution of the steel, the negative concrete layer subtracts only in the same direction as the steel. The materials quantities of the negative concrete layer, however, are calculated in a manner consistent with the plain concrete layers.

4.6 Example Problem

The example segment which shall be examined is taken from the elastic stress analysis report by Epstein and Murray (1976), henceforth referred to as the EM report, and the segment is labelled in this report as UD1. This doubly-curved segment is located in the upper dome, next to the ring beam of the Gentilly-type structure which in part consists of the outside dome and an inner dome which together form a water reservoir. Although in the actual structure, the dome is thickened where it meets the ring beam, in this analysis it is assumed that this thickening is not present and the analysis will ignore any extra strength

that the thickening may provide. It does not, therefore, accurately reflect the response which would be expected in the prototype structure.

4.6.1 Segment Description

The geometry of the segment and the locations of the reinforcing steel and prestressing steel are shown in Fig. 4.7. The area of the steel layers and the prestressing forces are listed in Table 4.1. The reinforcing layers have a yield stress of 60 ksi and have a Young's modulus of 29000 ksi. The prestressing steel has an ultimate strength of 255 ksi with an initial modulus of 29600 ksi.

The concrete strength in uniaxial compression for this example was assumed to be 5 ksi. Using this value and the A.C.I. recommendations (American Concrete Institute, 1971) the initial concrete modulus was calculated to be 4030 ksi. The tensile strength of 0.424 ksi was computed using $6\sqrt{f'_c}$. An initial Poisson's ratio was selected to be 0.15. The default value provided in the program was used for ε_{io}. The value of ε_{iot} was input as 0.000126 or $1.2\, f'_t / E_o$. For both the concrete and steel, the coefficient of thermal expansion was assumed to be 0.65×10^{-5} in. / in. F .

4.6.2 Loading Description

To determine the forces and moments to which the segment will be subjected, the containment vessel was analysed using a linear elastic finite difference program based on the classical thin shell equations (Epstein and Murray, 1976). From this program the forces and moments resulting from dead loads, prestressing loads, and live loads were found. Table 4.2 lists the total applied load vectors to which the dome segment

was subjected for each load step. As part of modelling the construction sequence, a small dead load was applied before prestressing. After prestressing, a period of time will pass before the live loads due to overpressure are applied, and therefore a creep step is provided. The creep factor is set to 2.50. The thermal loads are simulated by a linear temperature gradient varying from $+26^{\circ}F$ on the inner surface to $-50^{\circ}F$ on the outer surface, the same temperature distribution as used in the EM report. For this example, it was assumed that the segment would be restrained against curvatures resulting from the temperature gradient, but that axial movement would not be restricted. In other words, the temperature change would affect the in-plane axial deformations and out-of-plane moments, but would not change the axial forces or curvatures. The live loads are the last to be imposed. The moments and axial forces resulting from a unit of internal pressure are listed in the EM report and were calculated using the classical shell analysis. It was then assumed that the ratio of axial force to curvature resulting from the unit of internal pressure would remain constant up to the ultimate load of the segment. By specifying the live load to be of this type, as was used in the EM report, the ratio of N_1 / M_1 and N_2 / M_2 can be input to COWSAC and the necessary curvatures are calculated using a linear elastic uncracked section.

4.6.3 Discussion of Results

Figure 4.8 contains the axial load-axial strain curves for both directions one and two. The various points labelled 1.1 - 1.5 and 2.1 - 2.5 are the results from the various applied loads up to and

including the live loads. Points 1.1 and 2.1 represent the segment response to the dead load in directions 1 and 2 respectively. Points 1.2 and 2.2 describe the response to the prestressing. The prestressing forces are internal to the segment but the external axial forces are not constant therefore both the strains ϵ_1^{ms} and ϵ_2^{ms} and the applied forces N_1 and N_2 change. Points 1.3 and 2.3 show the results of the creep step. During this operation, the loads are assumed to remain constant and therefore only the strains change. Locations 1.4 and 2.4 exhibit the results of the temperature changes. Since the axial degrees of freedom are not restrained against thermal movement, the axial forces remain constant while the axial strains change.

After the solution to the thermal effects has been determined, the live loads are applied. As previously stated, the linear elastic response of containment vessel to a unit of internal pressure was computed by the authors of the EM report, who then assumed that the axial forces and the curvatures which resulted from this analysis would vary in a linear manner to higher internal pressures. This loading path was also employed here to obtain the results shown for this example.

The solid lines of Fig. 4.8 trace the load-strain curves for the segment in both directions, for a set of loads consistent with the above hypothesis. The direction labelled $N_1 - \epsilon_1^{ms}$ starts at an external load level near zero and then moves into the tension zone. The response is linear up to approximately 200 kips whereupon the segment begins to soften gradually. If the segment were loaded uniformly with no moment, then it would be expected that this initial linear behavior would persist up to the cracking load, or about 450 kips. The overall segment stiffness

would then change abruptly after the concrete had cracked in tension. This type of behavior is demonstrated by Segment UD3 in the EM report. However, the presence of the large moment in direction 1 of this example segment, UD1, causes some of the concrete to crack at lower loads and the sudden break in the load-strain curve that would be expected under these conditions is replaced with the smooth transition shown in Fig. 4.8.

In the second direction, labelled $N_2 - \epsilon_2^{ms}$, the segment begins in tension but then moves into compression. A large moment is present in this direction at lower loads, but the applied moment disappears as the compressive axial force increases. Since the applied axial loads are well under the capacity of the segment, the response curve in this direction is linear.

Also shown in Fig. 4.8 are the response curves in both directions that are obtained using the same loading conditions but with the bilinear elastic model. These results are designated with the dashed-dotted lines, and are the results which would be expected from the EM report. These curves indicate that there are no significant differences between the results obtained from the nonlinear or the bilinear concrete constitutive equations as described. However, the results obtained from this particular problem are not general in that the very high moment reduces the significance of the tensile behavior of the concrete. The uniqueness of these results is demonstrated by the results in Chapter 5, which do not exhibit a close comparison between the nonlinear and bilinear solutions for the test segments. In fact, the EM report showed no differences in response for UD1 when the tensile strength of the concrete was reduced to zero

from $6\sqrt{f'_c}$.

The moment-curvature diagram for Segment UD1 when subjected to the above loading sequence is illustrated in Fig. 4.9. The points labelled 1.1 to 1.5 and 2.1 to 2.5 are similar to those in the axial force-strain diagram. Points 1.1 and 2.1 show the moment and curvature in directions 1 and 2 respectively, after the application of dead load. With the application of the prestressing forces, a large moment is placed on direction 1 and a small moment is placed on direction 2. These moments are not directly the result of the prestressing but are applied moments which the finite difference analysis of the EM report predicts will accompany the prestressing. The results of the prestressing is indicated by the points labelled 1.2 and 2.2. After the prestressing, the segment is allowed to creep. This step is shown by locations 1.3 and 2.3. The applied moments M_1 and M_2 are assumed to remain constant, but due to creep, ϕ_1 and ϕ_2 change from the previous step. During the calculation of the thermal effects however, it was assumed that the segment was restrained so that the curvatures were kept constant and the moments allowed to vary. The results of the linear temperature variation are shown at points 1.4 and 2.4. The effect of increasing the temperature on the inner surface and decreasing the temperature on the outer surface was a large negative moment in both directions.

The locations where live loading begins are indicated by points 1.5 and 2.5 which differ from the previous solution at 1.4 and 2.4. This discrepancy is due to the fact that some of the outside concrete layers unloaded after they reached their maximum tensile stress and were on the declining branch of the stress-strain curve. This unloading, the defini-

tion of which is given in Chapter 3, is the consequence of the live load moment opposing the moment after the application of the thermal effects. When unloading is detected in a concrete layer which is on the declining branch of a tensile stress-strain curve, the stresses and stiffness in that concrete layer drop to zero and remain there until that layer goes into compression. These layers can no longer resist any tensile loads. Since these layers now do not contribute strength to the segment, a sudden reduction in moment resistance is experienced.

Beginning at locations 1.5 and 2.5, the solid lines trace the response of the segment to the live loads. The curve of M_1 - ϕ_1 begins with an initial section of increasing stiffness. The stiffness continues to increase until all of the cracked layers are closed and are accepting stresses. From this point, the curve is linear up to the region where the concrete layers behave inelastically. Here the slope of the curve declines to zero, at which point the maximum moment is reached. Since the loading is curvature controlled, the moment now begins to decrease with increasing curvature.

The behavior of the moment-curvature trace in the second direction is similar to that in the first direction. Again, there is the jump from the thermal load solution to the start of live loading, dictated by the unloading model. After this, the moments increase linearly up to the point where loading stops, at a value comparable to the maximum moment in the first direction. Since the two directions of Segment UD1 are similar in details of construction any apparent difference in moment capacity between directions 1 and 2 is a result of the axial loading.

Also shown in Fig. 4.9 are the response curves in both directions

from the bilinear elastic analysis using the same loading conditions. These results are denoted by the dashed-dotted lines. Again, as for the axial force-strain diagram, the bilinear and nonlinear solutions compare well. The only characteristic not displayed by the linear analysis is the jump from the thermal solution to the start of live loading. However this jump could not be expected from the bilinear solution as this concrete model has no post ultimate portion, and therefore no unloading from this region. However in direction 1, the nonlinear solution exhibits extra moment capacity after a curvature of approximately .00002 in./in.

Some of the characteristics displayed by the M - ϕ plots can be further understood by examining the stress path of the concrete. Figure 4.10 shows the concrete stress path for the concrete on the inner surface of the segment, and Figure 4.11 for the concrete on the outer surfaces. Locations 1 - 4 indicate the solutions to the dead, prestressing creep and thermal loads. The solid line from positions 4 to 5 marks the stress path followed during the application of the live load. For the concrete on the inner surface of Segment UD1, Fig. 4.10, the direction of this path results in an initially constant σ_2, as σ_1 moves toward the σ_2 axis. After σ_1 becomes positive, the $\sigma_1 - \sigma_2$ stress path touches the failure envelop and σ_1 decreases to its minimum value.

The consequence of unloading on the declining branch of a stress-strain curve which is discussed in Chapter 3, are shown in Fig. 4.11. After the creep solution has been found, shown at location 3 in Fig. 4.11, the outside layer of concrete has positive stiffness. When the thermal strains are added, the stresses hit the failure envelope and start to

decline. Both directions are now on the declining branch of their $\sigma - \varepsilon_{iu}$ curves. Under the application of internal pressure the applied moment now reverses and the outer concrete layers begin to unload. The response of the nonlinear concrete constitutive model to unloading from the declining branch is to set the concrete stresses to zero, and so the next point in Fig. 4.11 after point 4 is at the origin of the stress plot. As the loading continues, the real strains continue to decrease and eventually the cracks close in direction 1, and this direction picks up compressive stresses, and the stress path begins to move along the σ_1 axis. Further in the loading, the cracks transverse to direction 2 close and this direction accepts compressive stresses. At this point the stress path leaves the σ_1 axis. As the tensile axial load N_1 increases, the stress σ_1, again moves toward the tensile region. However, because of the prior cracking, this layer of concrete cannot accept any tensile stresses and the stress path is restricted to the σ_2 axis.

Figure 4.12 details the depth of open cracks transverse to direction 1 as the axial live load N_1 increases. At the start of live loading, the open cracks on the exterior of the segment exist through 12 % of the segment thickness. As the live load increases, these cracks close until the live axial load reaches 75 kips, at which point no open cracks exist on the outside of the segment. At a line axial load of 200 kips, cracks begin to appear on the interior side of the segment. The depth of these open cracks increases with increasing live load until this load reaches 575 kips, at which point open cracks penetrate through the wall segment. Also shown in Fig. 4.12 are the cracking results obtained by Epstein and Murray for Segment UD1. The results by the two different analysis agree,

the difference usually being less than 50 kips.

Steel Layer	Area (in^2)	Prestress Force (kips)
A_{11}	1.1	-
A_{12}	1.1	-
A_{21}	1.27	-
A_{22}	1.69	-
P_1	2.33	374.0
P_2	2.33	200.0

TABLE 4.1 Steel Layer Details - Segment UD1

Load Step	N_1	M_1	N_2	M_2	$\frac{M_1}{N_1}$	$\frac{M_2}{N_2}$
	(kips)	(in kips)	(kips)	(in kips)	(in)	(in)
Dead Load	-15.4	-302.0	21.9	-46.7	-	-
Prestress Load	0.6	-1258.8	72.8	-165.1	-	-
Creep Load	0.6	-1258.8	72.8	-165.1	-	-
Live Load	635.2	-	510.1	-	19.7132	-3.9332

TABLE 4.2 Applied Loads for Load Steps

MAIN OF COWSAC

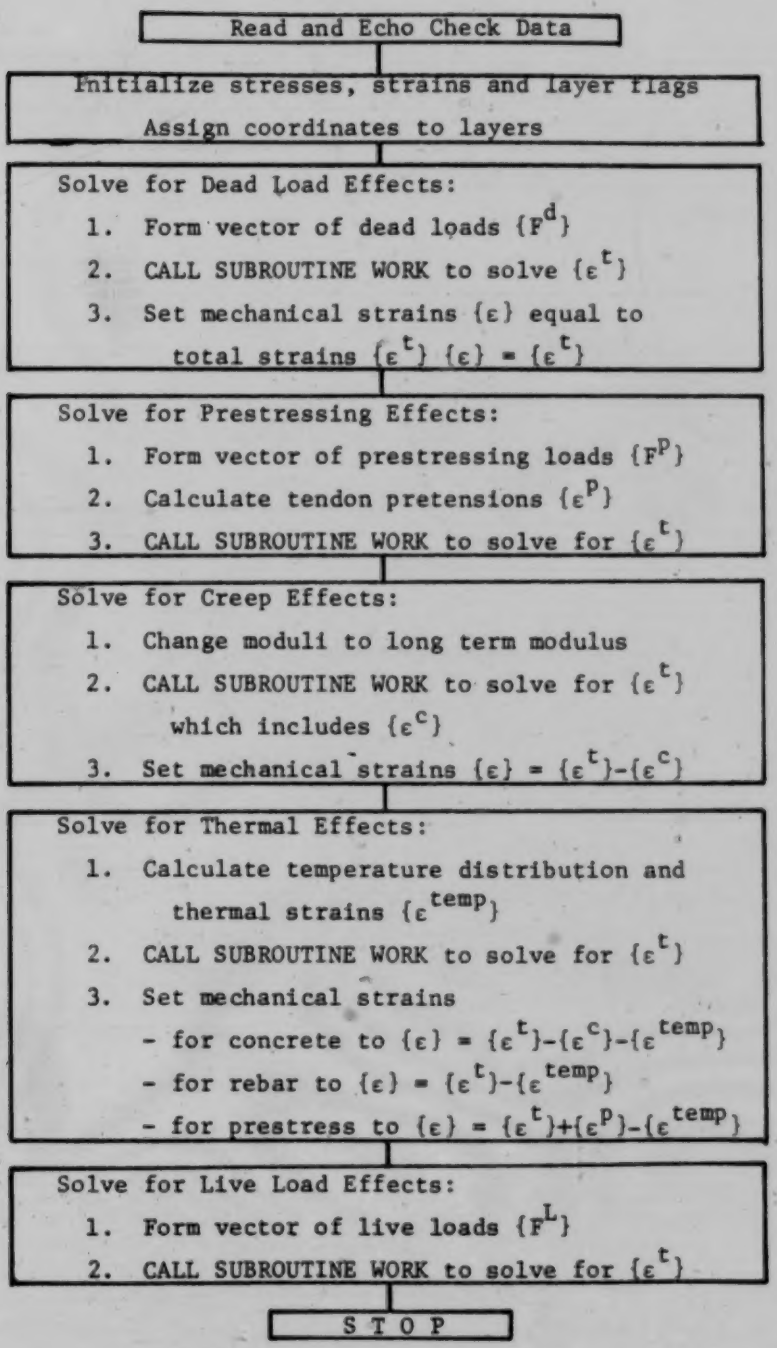
Read and Echo Check Data
Initialize stresses, strains and layer flags
Assign coordinates to layers
Solve for Dead Load Effects:
1. Form vector of dead loads {F^d}
2. CALL SUBROUTINE WORK to solve {ε^t}
3. Set mechanical strains {ε} equal to total strains {ε^t} {ε} = {ε^t}
Solve for Prestressing Effects:
1. Form vector of prestressing loads {F^p}
2. Calculate tendon pretensions {ε^p}
3. CALL SUBROUTINE WORK to solve for {ε^t}
Solve for Creep Effects:
1. Change moduli to long term modulus
2. CALL SUBROUTINE WORK to solve for {ε^t} which includes {ε^c}
3. Set mechanical strains {ε} = {ε^t}-{ε^c}
Solve for Thermal Effects:
1. Calculate temperature distribution and thermal strains {ε^temp}
2. CALL SUBROUTINE WORK to solve for {ε^t}
3. Set mechanical strains
- for concrete to {ε} = {ε^t}-{ε^c}-{ε^temp}
- for rebar to {ε} = {ε^t}-{ε^temp}
- for prestress to {ε} = {ε^t}+{ε^p}-{ε^temp}
Solve for Live Load Effects:
1. Form vector of live loads {F^L}
2. CALL SUBROUTINE WORK to solve for {ε^t}
STOP

Fig. 4.1 Flowchart of Main of COWSAC

SUBROUTINE WORK

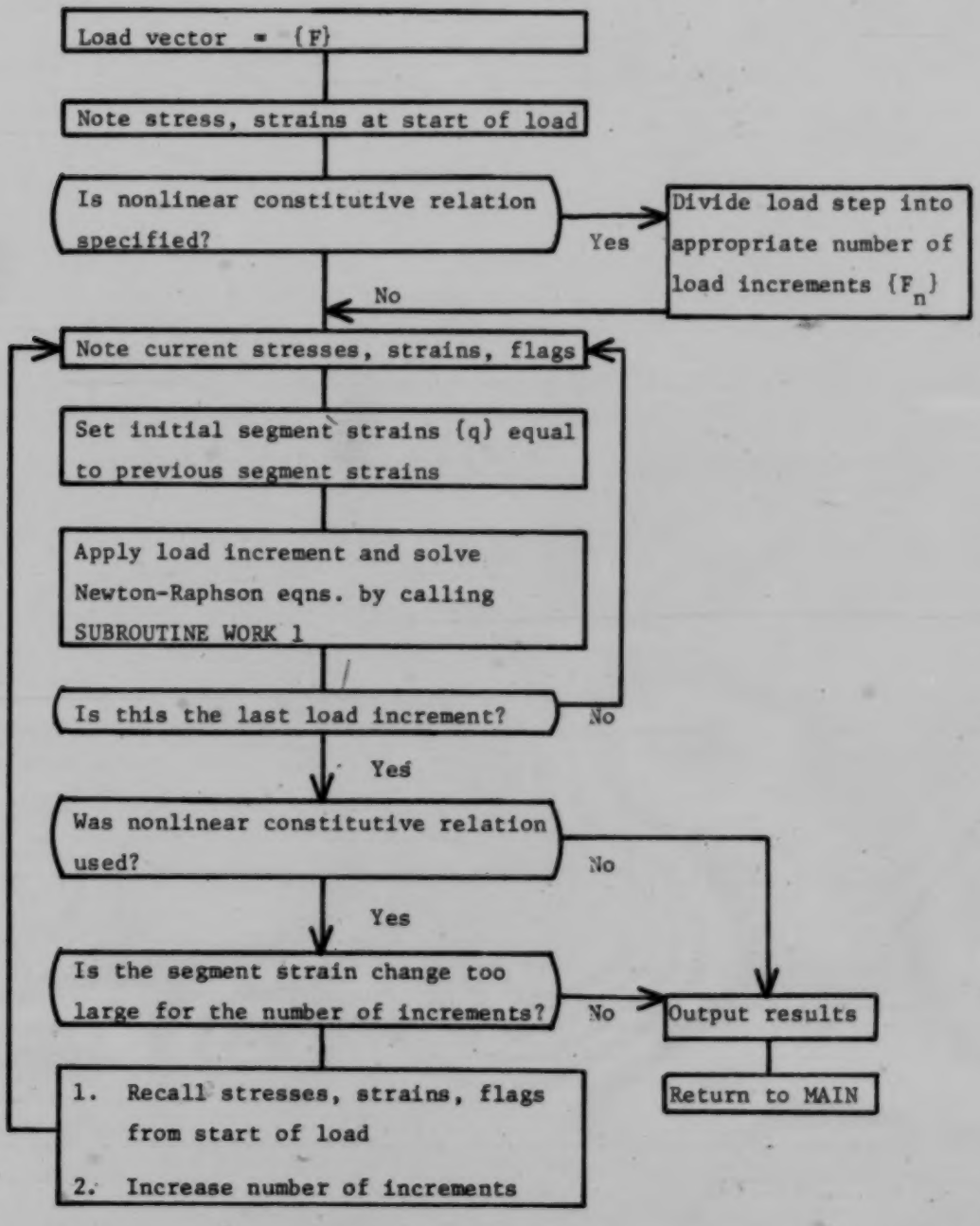
Load vector = {F}
Note stress, strains at start of load
Is nonlinear constitutive relation specified?
Yes
Divide load step into appropriate number of load increments {F_n}
No
Note current stresses, strains, flags
Set initial segment strains {q} equal to previous segment strains
Apply load increment and solve Newton-Raphson eqns. by calling SUBROUTINE WORK 1
Is this the last load increment?
No
Yes
Was nonlinear constitutive relation used?
No
Yes
Is the segment strain change too large for the number of increments?
No
Output results
Return to MAIN
1. Recall stresses, strains, flags from start of load
2. Increase number of increments

Fig. 4.2 Flowchart of Load Control

SUBROUTINE WORK 1

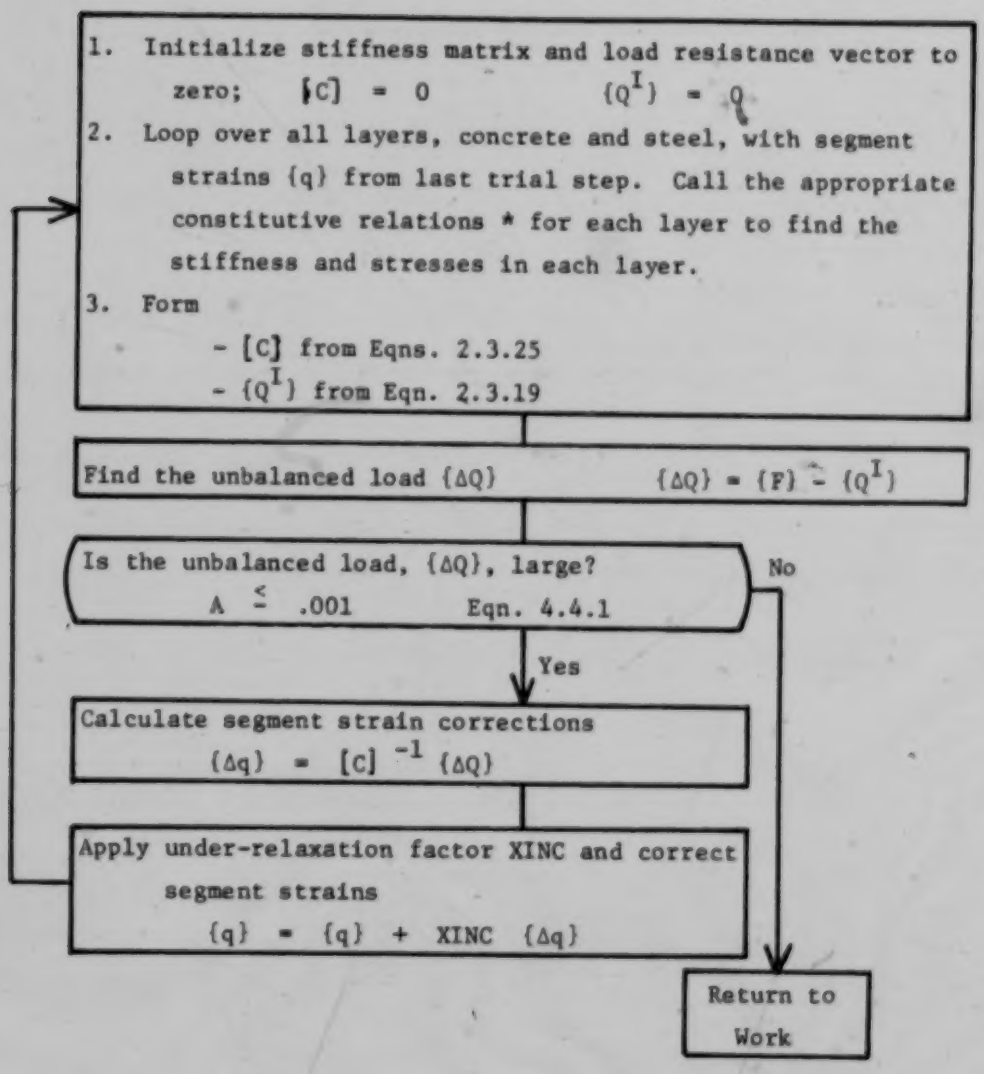
1. Initialize stiffness matrix and load resistance vector to zero; [C] = 0 {Q^I} = 0
2. Loop over all layers, concrete and steel, with segment strains {q} from last trial step. Call the appropriate constitutive relations * for each layer to find the stiffness and stresses in each layer.
3. Form
- [C] from Eqns. 2.3.25
- {Q^I} from Eqn. 2.3.19
Find the unbalanced load {ΔQ} {ΔQ} = {F} - {Q^I}
Is the unbalanced load, {ΔQ}, large?
A ≤ .001 Eqn. 4.4.1
No
Yes
Calculate segment strain corrections
{Δq} = [C]^-1 {ΔQ}
Apply under-relaxation factor XINC and correct segment strains
{q} = {q} + XINC {Δq}
Return to Work

* For bilinear concrete material, call SUBROUTINE LINELC
For nonlinear concrete material, call SUBROUTINE SAENZ

Fig. 4.3 Flowchart of Load Application and Solution

SUBROUTINE SAENZ

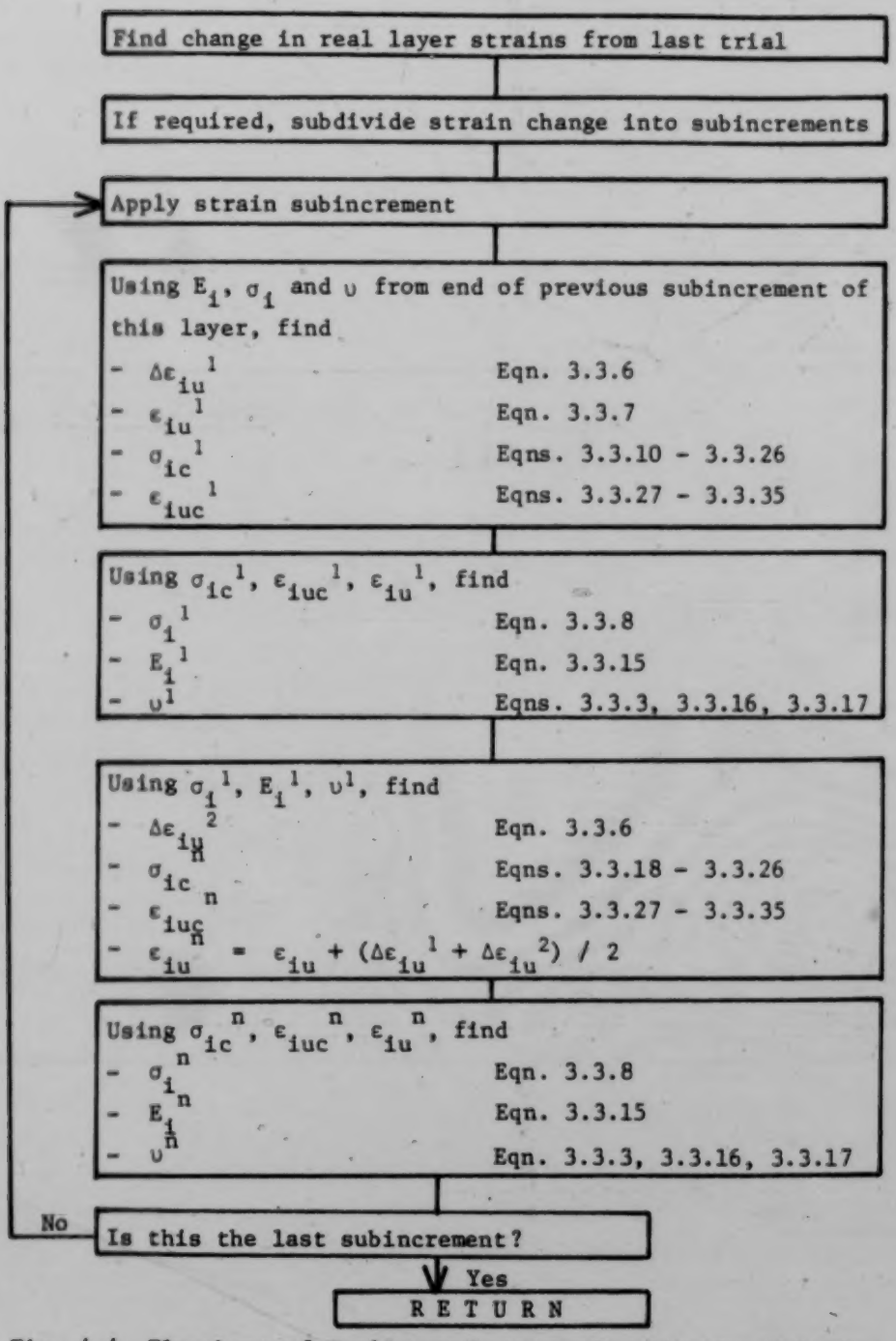
Find change in real layer strains from last trial
If required, subdivide strain change into subincrements
Apply strain subincrement
Using E_i, σ_i and υ from end of previous subincrement of this layer, find
- $\Delta\varepsilon_{iu}^{1}$ Eqn. 3.3.6
- ε_{iu}^{1} Eqn. 3.3.7
- σ_{ic}^{1} Eqns. 3.3.10 - 3.3.26
- ε_{iuc}^{1} Eqns. 3.3.27 - 3.3.35
Using σ_{ic}^{1}, ε_{iuc}^{1}, ε_{iu}^{1}, find
- σ_i^{1} Eqn. 3.3.8
- E_i^{1} Eqn. 3.3.15
- υ^{1} Eqns. 3.3.3, 3.3.16, 3.3.17
Using σ_i^{1}, E_i^{1}, υ^{1}, find
- $\Delta\varepsilon_{iu}^{2}$ Eqn. 3.3.6
- σ_{ic}^{n} Eqns. 3.3.18 - 3.3.26
- ε_{iuc}^{n} Eqns. 3.3.27 - 3.3.35
- $\varepsilon_{iu}^{n} = \varepsilon_{iu} + (\Delta\varepsilon_{iu}^{1} + \Delta\varepsilon_{iu}^{2}) / 2$
Using σ_{ic}^{n}, ε_{iuc}^{n}, ε_{iu}^{n}, find
- σ_i^{n} Eqn. 3.3.8
- E_i^{n} Eqn. 3.3.15
- υ^{n} Eqn. 3.3.3, 3.3.16, 3.3.17
No
Is this the last subincrement?
Yes
RETURN

Fig. 4.4 Flowchart of Nonlinear Concrete Constitutive Relation

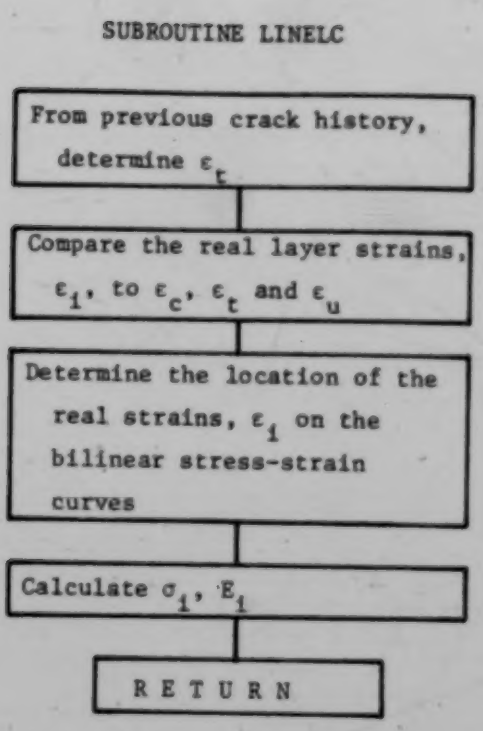
SUBROUTINE LINELC
From previous crack history, determine ε_t
Compare the real layer strains, ε_i, to ε_c, ε_t and ε_u
Determine the location of the real strains, ε_i on the bilinear stress-strain curves
Calculate σ_i, E_i
RETURN

Fig. 4.5 Flowchart of Bilinear Concrete Constitutive Relation

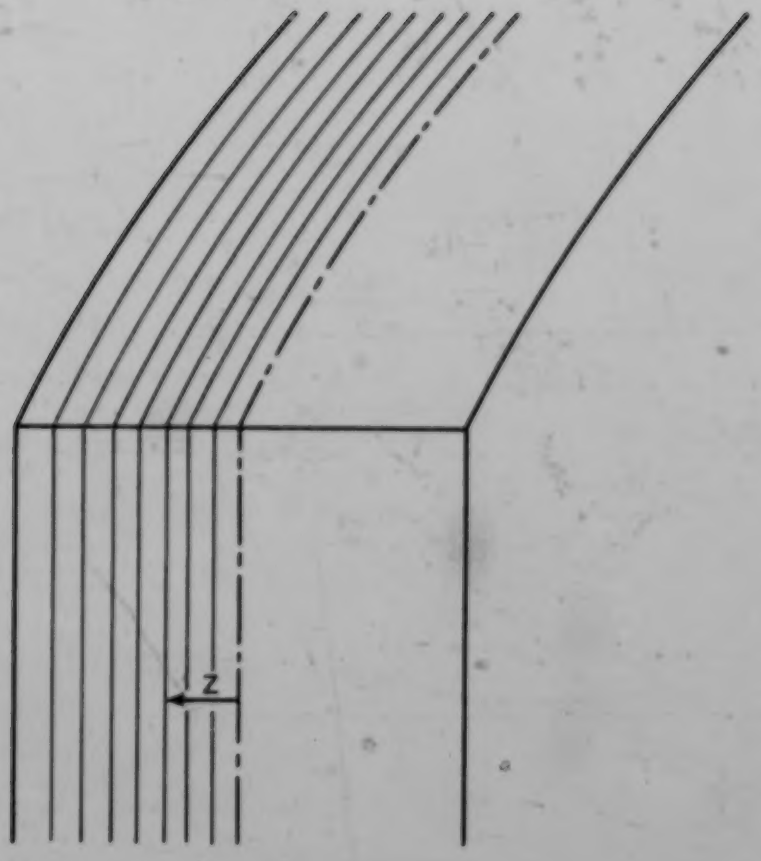

Fig. 4.6 Wall Segment Showing Orientation of Layers

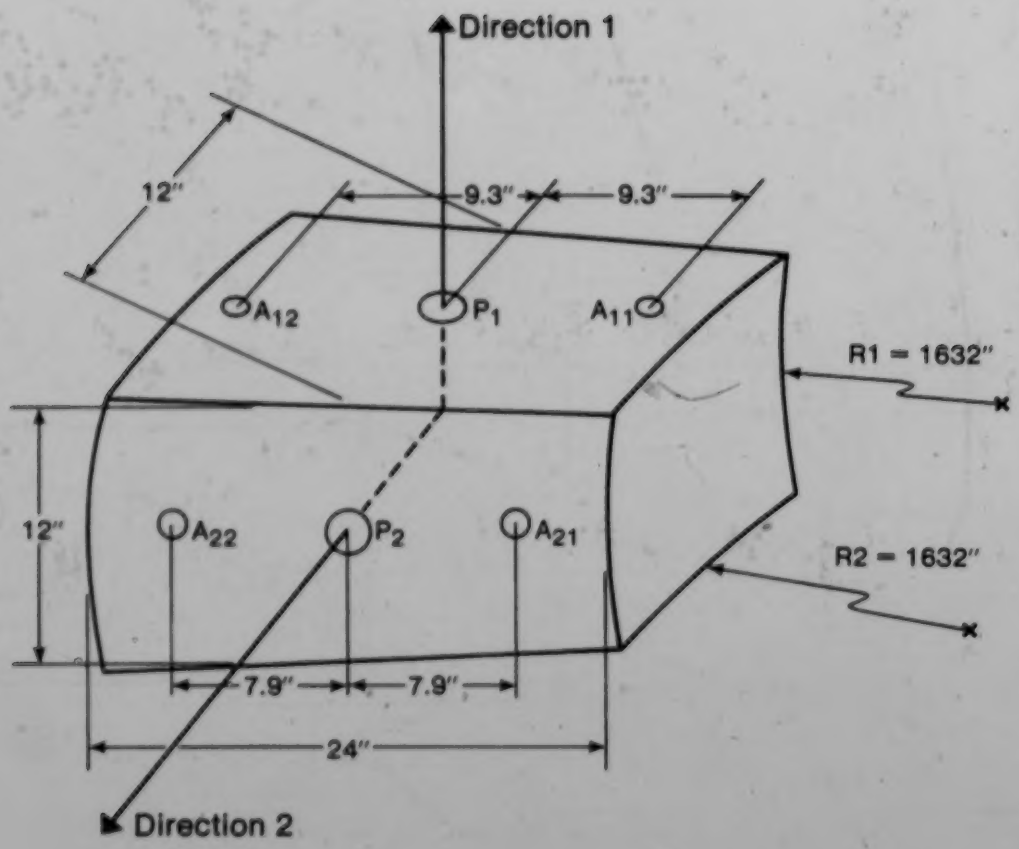

Fig. 4.7 Segment UD1

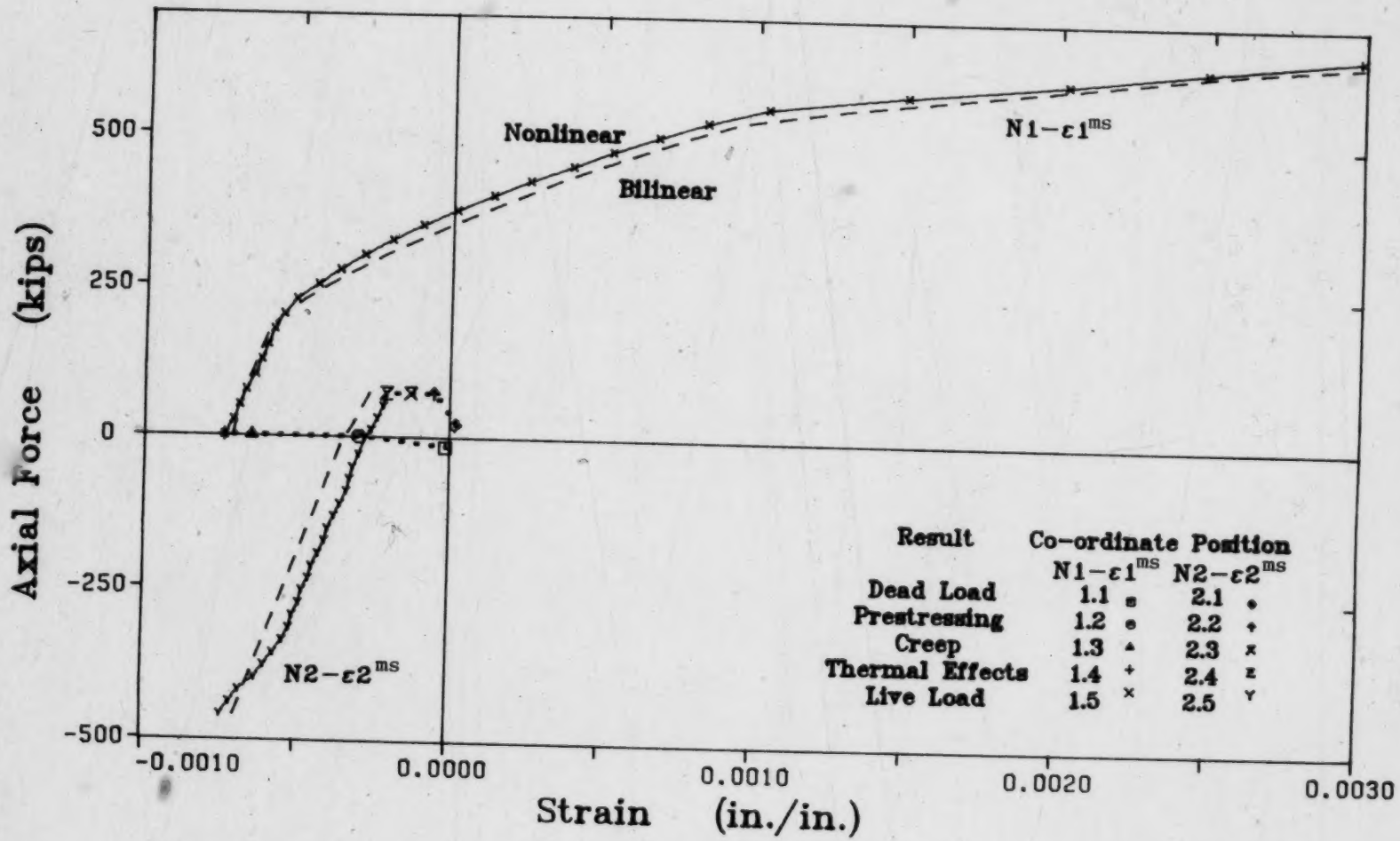

Fig. 4.8 Applied Axial Load vs. Strain - Segment UD1

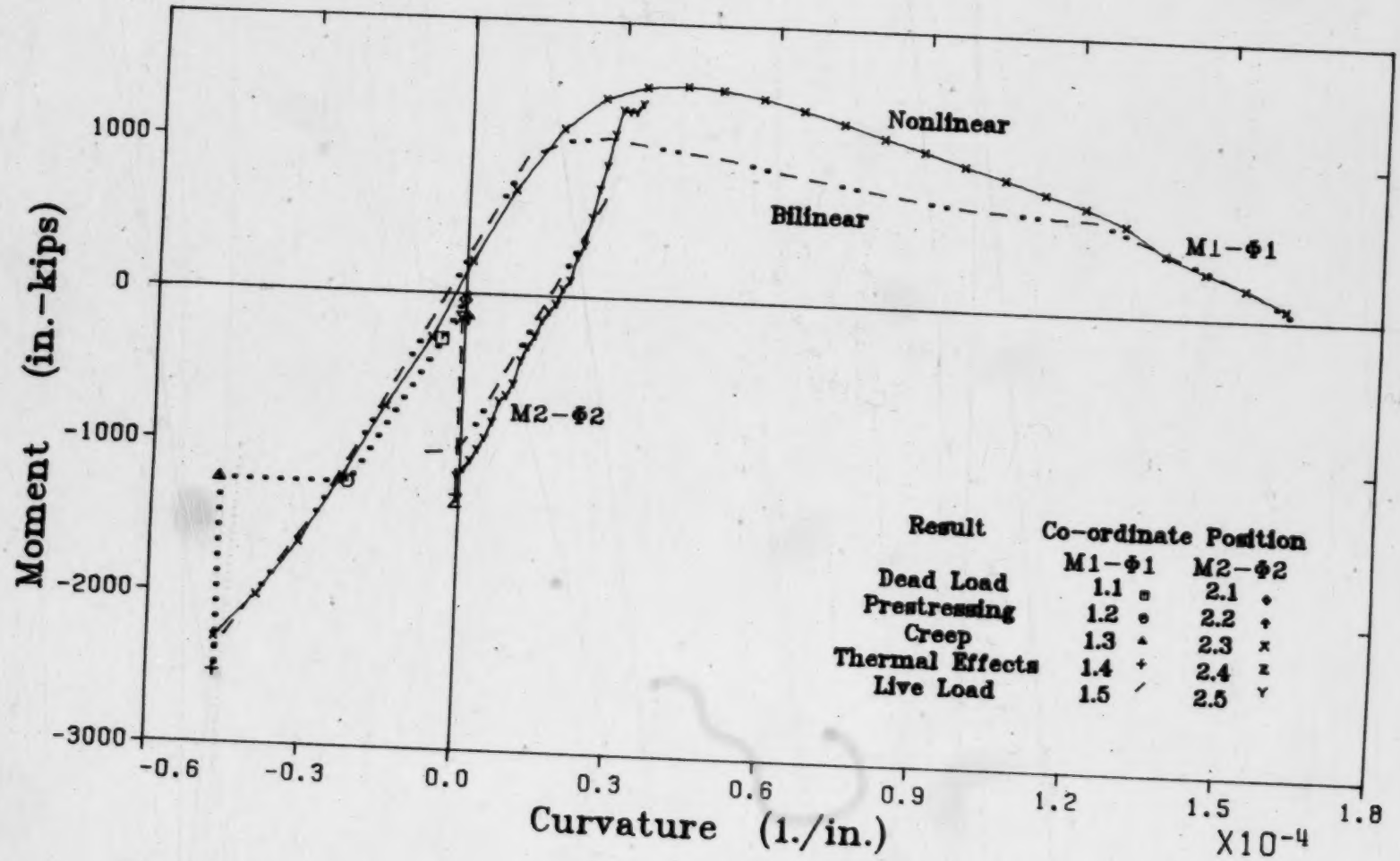

Fig. 4.9 Moment vs. Curvature - Segment UD1

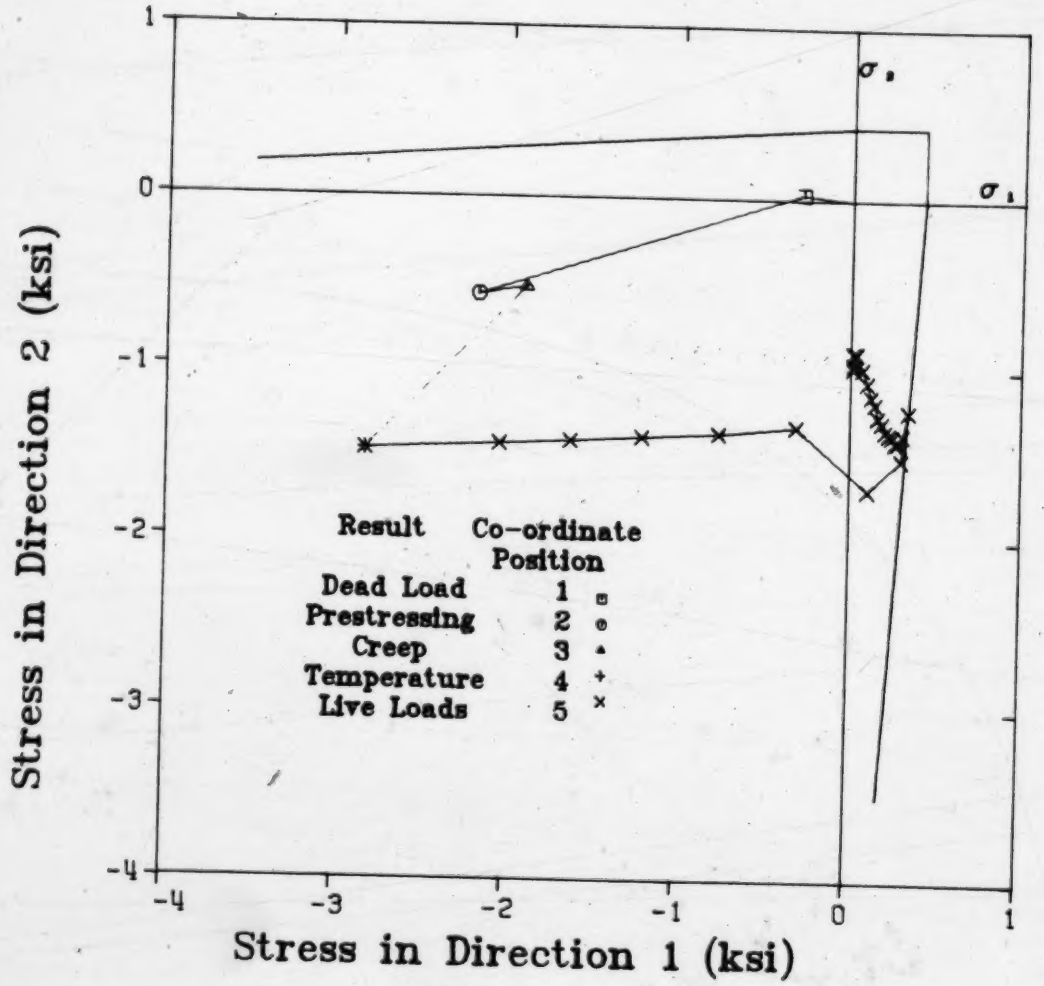

Fig. 4.10 Concrete Biaxial Stress Path on Inner Surface of Segment UD1

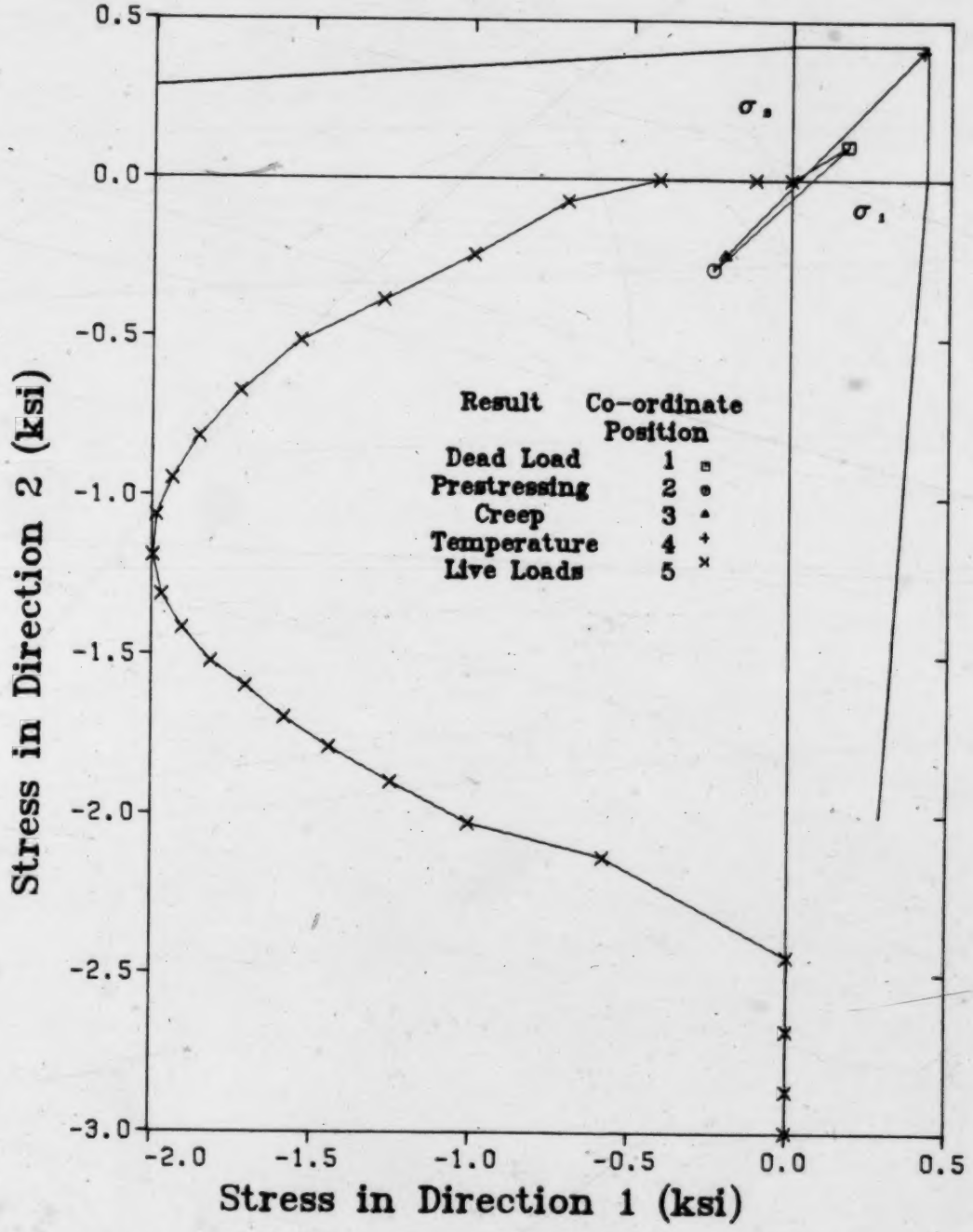

Fig. 4.11 Concrete Biaxial Stress Path on Outer Surface of Segment UD1

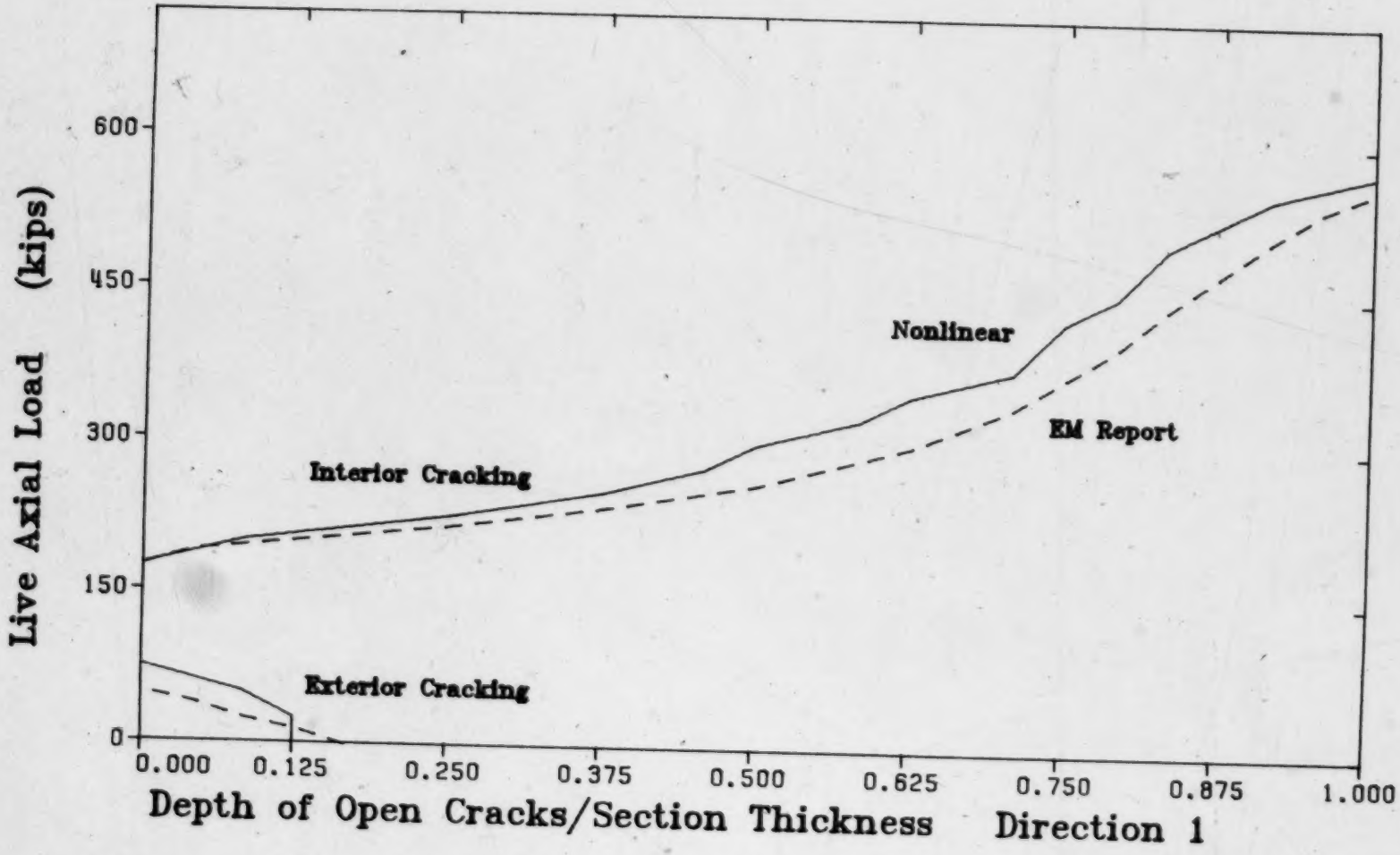

Fig. 4.12 Open Crack Depth vs. Live Axial Load in Direction 1 of Segment UD1

5. APPLICATIONS

5.1 Comparison of Program with Wall Segment Tests

The ultimate test of the accuracy and adequacy of a computer program and the theory on which it is based is the comparison between test results and predicted results. To test this computer model, the program output was compared with the observations from eight wall segment tests, one including imposed moments (Rizkalla, et al, 1979). The wall segments, of common width and length, were cast in two different thicknesses, with a varying amount of reinforcing steel, and in some specimens, with prestressing steel. Three different load ratios were used. The two cross-sections of interest for Specimen No. 1 are shown in Fig. 5.1 and 5.2. Tables 5.1 and 5.2 contain a summary of the pertinent information of all the wall segments. Of the data presented in this table, it should be noted that the value of f'_t for each specimen was obtained from a Brazilian tensile test. The best value to be used as the ultimate tensile strength for the test segments was found to be $0.6\ f'_t$ (Murray, et al, 1978). This value shall be accepted in the following analyses. The value for the initial elastic modulus of the concrete was assumed (Rizkalla, et al, 1979) to be 3800 ksi for all the specimens. Similarly, the initial value of Poisson's ratio was fixed at 0.2.

The tests which were conducted on these specimens were primarily tension tests, since tensile live loads were placed on the wall segments and all of the walls failed in tension. Although this provides sufficient data to verify the degrading stiffness used for concrete in tension data are not available to check the failure curves of the concrete in

tension-compression and compression-compression, or to accurately assess the declining branches of the Saenz stress-strain curve in compression. The presence of the prestressing, however, allows the opportunity to check the program in the compression-compression and tension-compression quadrants at levels of stress below the maximum, since after the application of the prestress, the wall segment is subjected to biaxial compression. As the tensile loads increase, the stresses move into the tension-compression quadrant, and finally into the biaxial tension quadrant. This path is typified by the stress path of Specimen No. 1 shown in Fig. 5.3.

To produce the tensile loads on the segment, the specimen was attached to the loading machine by fixing the loading heads onto the ends of the prestressing strands and reinforcing bars. There was no direct connection between the testing apparatus and the concrete. All forces had to be transferred from the loading jacks to the concrete through the steel elements. Due to the assumptions made in the analysis, this system of loading cannot be modelled and it will be assumed that the entire face of the segment, rather than only the steel layers, will be loaded.

In these tests, the major contribution to strength is made by the reinforcing and, if present, the prestressing steel. For this reason, the specimen axial force-strain response plots contain curves which represent the capacity at a given strain, of the steel only.

5.1.1 Wall Segments with Prestressing

Segments Nos. 1, 3, 8 and 12 contained prestressing in both directions and were tested at load ratios of 2:1, 1:1, 2:1 and 2:1 respectively, the latter specimen including a moment in one direction. Segments Nos. 5 and 6 contained prestressing in one direction only and were both tested at load ratios of 1:0.

5.1.1.1 Wall Segment No. 1

This segment was tested at a load ratio of 2:1 with the larger imposed force being in direction 1, as designated in Table 5.1, which is the direction containing the greater area of prestressing tendons. The tensile strength of the concrete was found by the Brazilian test to be 490 psi. The effective tensile strength was taken to be six-tenths of this value or 294 psi.

Up to the initial cracking load of the concrete in either direction, the program results predict a stiffer response than observed, as shown in Fig. 5.4. This however, is highly dependent upon the chosen value for the initial elastic modulus of the concrete. More accurate data for this variable may provide closer agreement. In the major direction (direction 1), the model predicts a higher cracking load than that observed, and that additional concrete strength continues to influence the response in the major direction until the concrete strength is exhausted. However, the stiffness of the model is close to that of the test specimen after cracking. In the minor direction, the predicted curve is very close to the observed points.

5.1.1.2 Wall Segment No. 3

Specimen No. 3, containing the same steel and prestressing as Specimen No. 1, was tested at a load ratio of 1:1 up to 375 kips, after which direction 1 was loaded further, keeping the load on direction 2 constant. The tensile strength of the concrete was 426 psi, giving an effective strength of 256 psi.

Up to cracking there is good agreement between the response curves of the model and the test specimen, which are shown in Fig. 5.5. In direction 2, a close correlation exists between the predicted and observed curves, the model predicting an extra load capacity of about 20 kips at a given strain. Again however, the specimen stiffness of the model after cracking is very close to the observed results. In direction 1, there is a slow change in stiffness at the 'cracking load', and this is predicted by the model. After the change in loading ratio, the response curve of the model is more flexible than that shown by the test specimen.

5.1.1.3 Wall Segment No. 8

This specimen again contains the same steel and prestressing arrangement as Specimens Nos. 1 and 3, and was tested at a load ratio of 2:1, as was Segment No. 1. The tensile strength of the concrete was 424 psi resulting in an effective tensile strength of 254 psi.

Up to cracking, the agreement between the model and the specimen is good in both directions, the choice of the initial elastic modulus of the concrete being the most significant factor. In direction 1, the cracking load of the model and test specimen are similar, with the response of the model about 20 kips below the curve of the specimen.

These curves are shown in Fig. 5.6. Both curves have similar slopes after cracking. In direction 2, the agreement of the cracking load and of the stiffness after cracking between the model and the test specimen is very good.

5.1.1.4 Wall Segment No. 5

Specimen No. 5 contains prestressing steel only in one direction and it was loaded only in the prestressed direction, for a load ratio of 1:0. The concrete tensile strength was 420 psi, the effective tensile strength, 252 psi.

The model and the test again provide reasonable agreement, with the model predicting load-carrying capabilities of about 20 kips less after cracking. The stiffness after cracking of the model and the test segment are similar. The results from this segment are shown in Fig. 5.7.

5.1.1.5 Wall Segment No. 6

Segment No. 6, like Specimen No. 5, contains prestressing in only one direction, but more reinforcing steel is present. The load is again applied only in the direction of the prestressing. The measured tensile strength was 361 psi for an effective strength of 217 psi.

The model and the test segment agree reasonably well, both sharing a common total stiffness after cracking, but with the model predicting a curve about 30 kips above that measured (See Fig. 5.8).

5.1.1.6 Wall Segment No. 12

This wall segment, similar in construction to Segments Nos. 1, 3 and 9, has axial loads applied in the ratio of 2:1 and additionally a

moment across the wall face orthogonal to the minor direction. The applied load on this specimen is complicated by the method in which forces are transferred from the testing machine to the wall segment. Since this transfer occurs through the prestressing steel and the reinforcing steel, strain measurements on the exposed lengths of the steel were used to compute the actual loading history in the direction with moment. The loading sequence for this analysis is listed in Table 5.3, and it should be noted that the curvature in the first direction, ϕ_1, was assumed to be constant at zero. For the purposes of discussion, Face A shall be the inside face of the segment, so that the applied positive moment produces tensile strains on this face.

The presentation of the test observations and the results of both the linear and nonlinear analysis are shown in Fig. 5.9 and 5.10. On Face A, the predicted response curve of the nonlinear analysis in direction 1 lies above that observed during the test. It appears from the test results that the concrete is not contributing to the segment stiffness in this direction, as the test observations follow the response of the linear elastic tension cut-off curve after cracking. In direction 2, the curve produced by the nonlinear analysis closely follows the test observations up to 250 kips. After this point, at a strain of approximately .002 in./in., the steel in the analytical model yields and the stiffness of the section is reduced. This reduction in stiffness did not occur in the test specimen.

On Face B of Specimen No. 12, the predicted load-strain response of the nonlinear analysis is close to the response of the test specimen for direction 1. However, as in the curves of Face A, direction 2, the

analytical model softens at the yield strain of .002 while the test specimen does not. There is close agreement again in direction 2, up to a load of 270 kips. Beyond this point, the predicted response diverges from the actual response.

The close agreement between the analytical results and the test results in direction 2 for both Face A and Face B indicates that the predicted moment-curvature relationship, M_2-ϕ_2, should correspond accurately with the observed results. Since zero curvature in direction 1 was imposed in the loading conditions, the results of the nonlinear analysis show the response curves in direction 1 on Face A and Face B to be the same. However, the test results indicate the presence of a strain gradient in this direction. Reanalysis of the section setting M_1 equal to zero, as opposed to setting ϕ_1 equal to zero during loading, does not significantly alter the results. The strain gradient from Face A to Face B in direction 1 must then have been produced by some detail of the testing procedure.

5.1.2 Wall Segments Without Prestressing

5.1.2.1 Wall Segment No. 4

Specimen No. 4 was tested at a load ratio of 1:1, and the computed effective strength of the concrete was 322 psi. The comparison between the model and the specimen is poor. The cracking load was measured to be about 50 kips whereas the model predicts a cracking load of 100 kips. This difference in cracking loads of 50 kips is equivalent to approximately 150 psi in concrete stress. After cracking, the concrete in the test specimen maintains its strength in one direction, as the observed

load-strain curve remains parallel to the steel only curve, while the strength decreases in the orthogonal direction. Both curves eventually cross under the steel only curve. These curves are shown in Fig. 5.11.

5.1.2.2 Wall Segment No. 7

Specimen No. 7 was tested at a load ratio of 1:1. The effective concrete strength was calculated to be 203 psi. In contrast to the previous segments, this specimen was constructed to a thickness of 15.75 inches.

This segment also compares poorly with the predictions of the model as shown in Fig. 5.12. The analytical response curve follows the expected pattern of a large constant stiffness up to cracking, followed by a softer constant stiffness composed of the addition of the positive stiffness contributed by the steel elements, and the negative stiffness of the concrete. The specimen results lack the initial large stiffness, the high cracking load, and the second slope of smaller stiffness. The greatest strength contribution by the concrete is only approximately 40 kips, equivalent to 80 psi, whereas the model predicts the concrete will carry up to 100 kips, and the concrete strength of the test segment is exhausted at a small strain, leaving only the steel to resist the load.

5.1.3 General Results

The results for the specimens with prestressing were generally good. The model response curves displayed no trend in being either above or below the response curves of the test specimens and therefore it is assumed that a more accurate determination of the effective concrete tensile strength as it would vary between specimens would provide yet

closer agreement. The stiffness of both the model and the test specimen after cracking were close, indicating that the postulated declining branch of the concrete stress-strain curve in tension provides results that comply with the test observations.

The results for the segment with an applied moment were comparable in accuracy with the results for the segments without moments. Based on the available test data, the predicted moment-curvature curves would show a similarly close agreement.

The results for the specimens without prestressing were poor, although the sampling may be small. Compared to the model predictions, the actual specimens were soft. Between the two tests, inconsistencies were also present. One exhibited a definite cracking load, the other did not. One showed the concrete to persist in carrying load long after "cracking", while the other displayed a rapid decline in strength. The presence of shrinkage cracks, which would not be a factor in the prestressed specimens, may have affected the strength of these specimens. Nevertheless, on the basis of these two tests, it appears that the effective concrete tensile strength for reinforced concrete is substantially lower than that for prestressed concrete.

5.2 Comparison of Concrete Constitutive Relations

The test wall segments were also analysed using the uniaxial, bilinearly elastic, tension cut-off constitutive relations described in Chapter 3. The results of these analyses are also shown in Figs. 5.4 - 5.12. In addition, the diagrams contain the contribution of the steel, without concrete, including prestressing, towards the capacity of the

wall segment as the "steel only" curves.

In the major direction of Specimen No. 1, Fig. 5.4, the predicted cracking load from the tension cut-off analysis is the same as that from the nonlinear analysis, and both are above the observed results. After cracking, the concrete no longer contributes any strength by the tension cut-off theory, and the segment response by this theory follows the "steel-only" solution, which is lower than both the test results and the nonlinear results. In the minor direction, the predicted cracking load is much higher than the results from both the nonlinear analysis and the tests. Again, after cracking, the tension cut-off solution follows the "steel-only" curve, which is below the test and nonlinear results.

The predictions from the tension cut-off analysis are high in one direction of Specimen No. 3 (Fig. 5.5) and low in the other. In the stiffer direction, the cracking load is lower and occurs at a lower strain than the test and nonlinear results show. In the second direction, the cracking load is higher than that from the test or nonlinear analysis.

Specimen No. 8 (Fig. 5.6) is similar in both section details and loading to Specimen No. 1. The comparison between the bilinear, nonlinear and test results are also similar. The cracking loads of the two analyses and the test in the major direction are close. Again, in the minor direction, the cracking load of the tension cut-off analysis is much higher than that of the nonlinear analysis or that of the test itself.

The predicted cracking loads of the nonlinear and tension cut-off analyses are the same for Specimens No. 5 and 6 shown in Figs. 5.7 and 5.8. For Specimen No. 5, this cracking load is below that of the test and for Specimen No. 6 the predicted cracking load is above that of the

test.

For the segment with moment, the tension cut-off analysis predicts the correct cracking load for direction 1 on Face B (Fig. 5.10) and for direction 2 on Face A (Fig. 5.9). After cracking the results of this analysis are below the observed results for both curves, as most of the concrete does not contribute to the stiffness of the segment after this point, and only the steel remains to resist the loads. Based on Segment Nos. 1, 3, 5, 6 and 8, these results followed the expected pattern. However in direction 1, Face A, the results of the tension cut-off analysis, after cracking, are close to the test results, implying that the concrete of the test segment does not contribute any strength. Contradicting this, it is shown from Face B, direction 1 that the concrete is stressed, leading to the conclusion that other factors may have been active during the test which influenced the results. In direction 2 on Face B, the tension cut-off results closely model the test results.

The cracking loads for Specimen Nos. 4 and 7 (Figs. 5.11 and 5.12) are again the same from both analyses. These loads are significantly above the cracking loads observed from the tests on these specimens.

By the bilinear elastic, tension cut-off constitutive relations once the concrete has cracked in tension, the concrete loses all its strength. As a result, in the tension cut-off analysis of each specimen, once the segment has reached its cracking load, the capacity of the segment drops off to the "steel-only" strength, which can be computed in a very simple manner. The predicted amount of energy which the segment can absorb is therefore lower by the tension cut-off analysis than by the nonlinear analysis.

The bilinear elastic constitutive relations formulated here are independent, with no interaction on a failure curve. Both directions are allowed to reach the full tensile cracking load, which is not usually the case in the nonlinear analysis. If the segment is loaded in only one direction, then the cracking load of both the nonlinear and linear analyses are comparable. For the segments loaded in both directions, the predicted cracking loads in the direction of maximum stress will be the same from both analyses. These comparable results will be from the direction where the concrete stresses at failure, in the nonlinear analysis reach the full tensile strength. In the orthogonal direction, the cracking load of the tension cut-off analysis will be greater than that of the nonlinear analysis. So in general, the linear elastic, uniaxial tension cut-off analysis will predict cracking loads equal to or greater than those of the nonlinear analysis. However, exceptions to this rule can occur as established by Specimen No. 3.

Reinforcing and Prestressing Steel

Specimen No.	Direction No. 1 Rebar Area (in^2)	Direction No. 1 Prestress Area (in^2)	Direction No. 1 Tendon Prestress (ksi)	Direction No. 1 Rebar Area (in^2)	Direction No. 1 Prestress Area (in^2)	Direction No. 1 Tendon Prestress (ksi)	Rebar Yield (ksi)	Rebar E_o (ksi)
1	2.2	1.676	134.6	2.2	1.077	124.0	58.2	28500
3	2.2	1.676	134.6	2.2	1.077	124.0	58.2	28500
4	3.2			3.2			55.0	29300
5	2.2	1.077	124.0	2.2			58.2	28400
6	3.2	1.077	124.0	3.2			55.0	29300
7	5.28			5.28			52.9	28400
8	2.2	1.676	134.6	2.2	1.077	124.0	58.2	28900
12	2.2	1.676	134.6	2.2	1.077	124.0	58.2	28500

Prestressing Tendon E_o = 29400 ksi

Tendon σ_{pu} = 264 ksi

TABLE 5.1 Summary of Wall Segment Data - Steel Details

Specimen No.	Thickness (in.)	f'_c (ksi)	f'_t (ksi)	0.6 f'_t (ksi)	Load Ratio $N_1:N_2$
1	10.5	5.093	.490	.294	2:1
3	10.5	5.694	.426	.256	1:1
4	10.5	5.79	.537	.322	1:1
5	10.5	5.69	.420	.252	1:0
6	10.5	4.54	.361	.217	1:0
7	15.75	3.50	.339	.203	1:1
8	10.5	4.92	.424	.254	2:1
12	10.5	5.93	.487	.292	2:1

Wall segment width = 31.5 in.

Wall segment length = 31.5 in.

Concrete E_o = 3800 ksi

Concrete υ_o = 0.20 ksi

TABLE 5.2 Summary of Wall Segment Data - Concrete Details

N_1 (kips)	ϕ_1 (1/in)	N_2 (kips)	M_2 (kip-in)
84.0	0.0	42.0	54.1
382.0	0.0	141.0	163.4
535.0	0.0	267.5	236.8
535.0	0.0	300.0	268.2
535.0	0.0	340.0	268.2

TABLE 5.3 Loading Sequence for Wall Segment No. 12

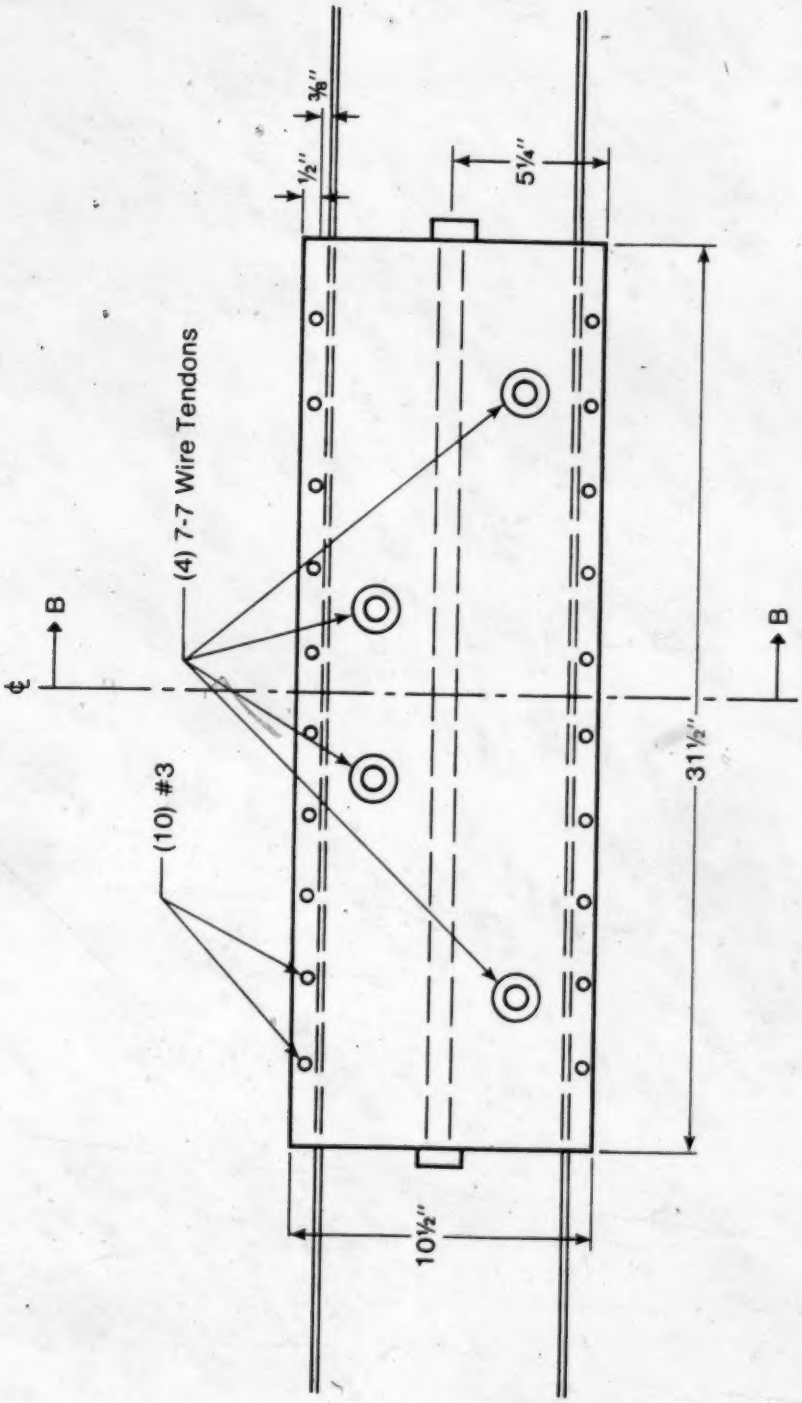

Fig. 5.1 Typical Test Segment Cross-Section Orthogonal to Direction 1

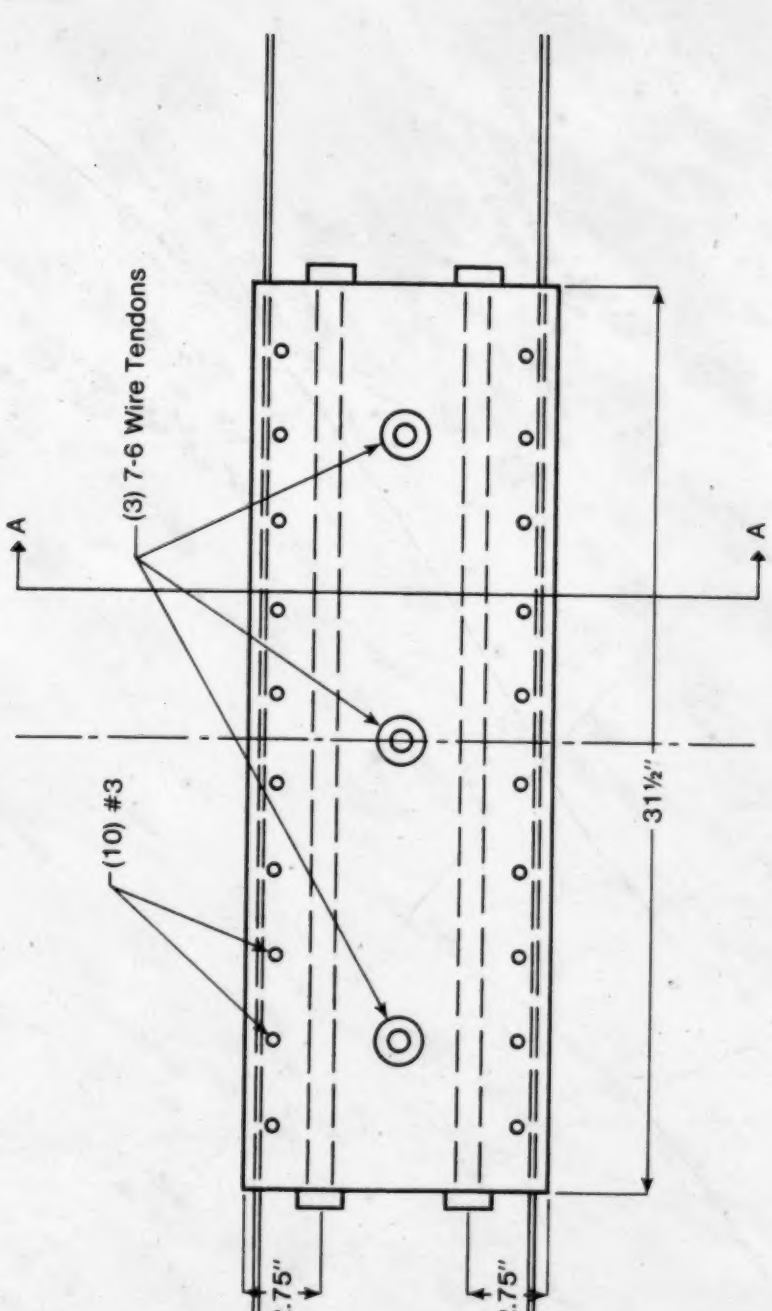

Fig. 5.2 Typical Test Segment Cross-Section Orthogonal to Direction 2

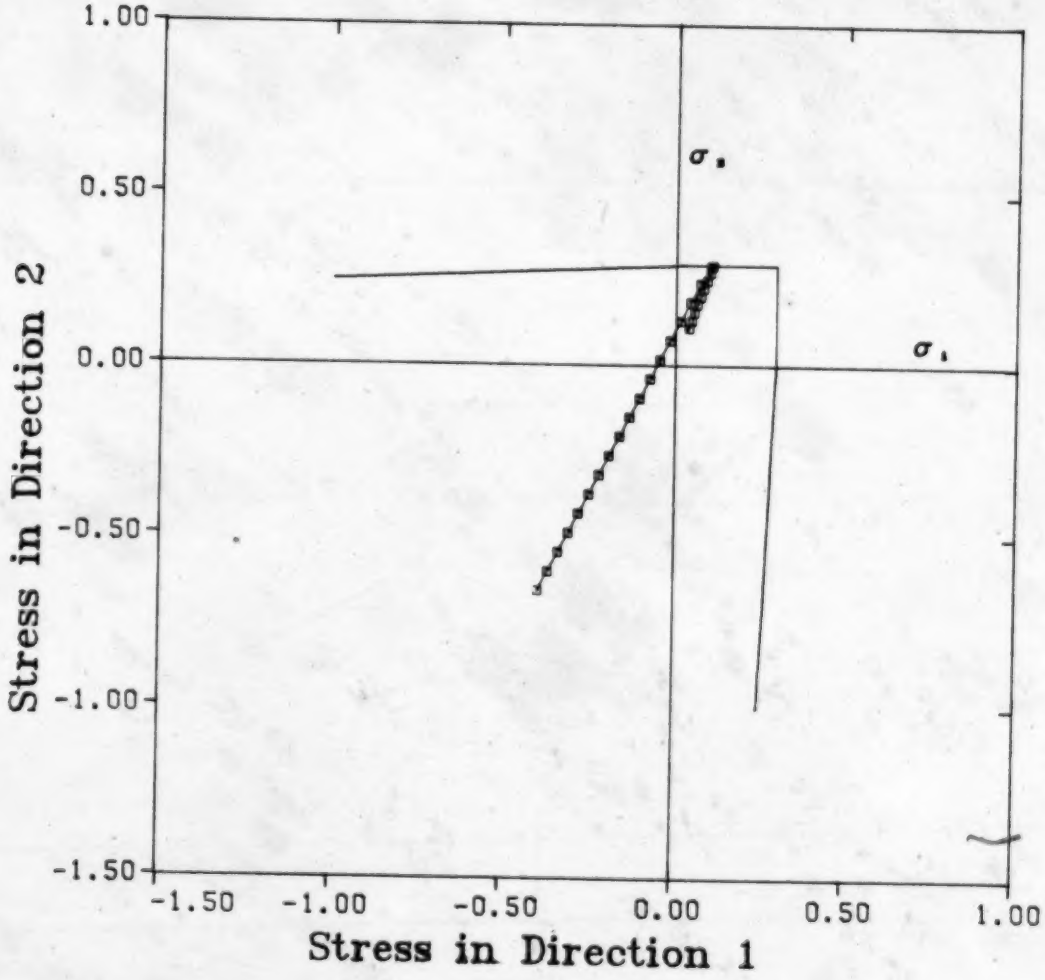

Fig. 5.3 Concrete Stress Path for Test Segment No. 1

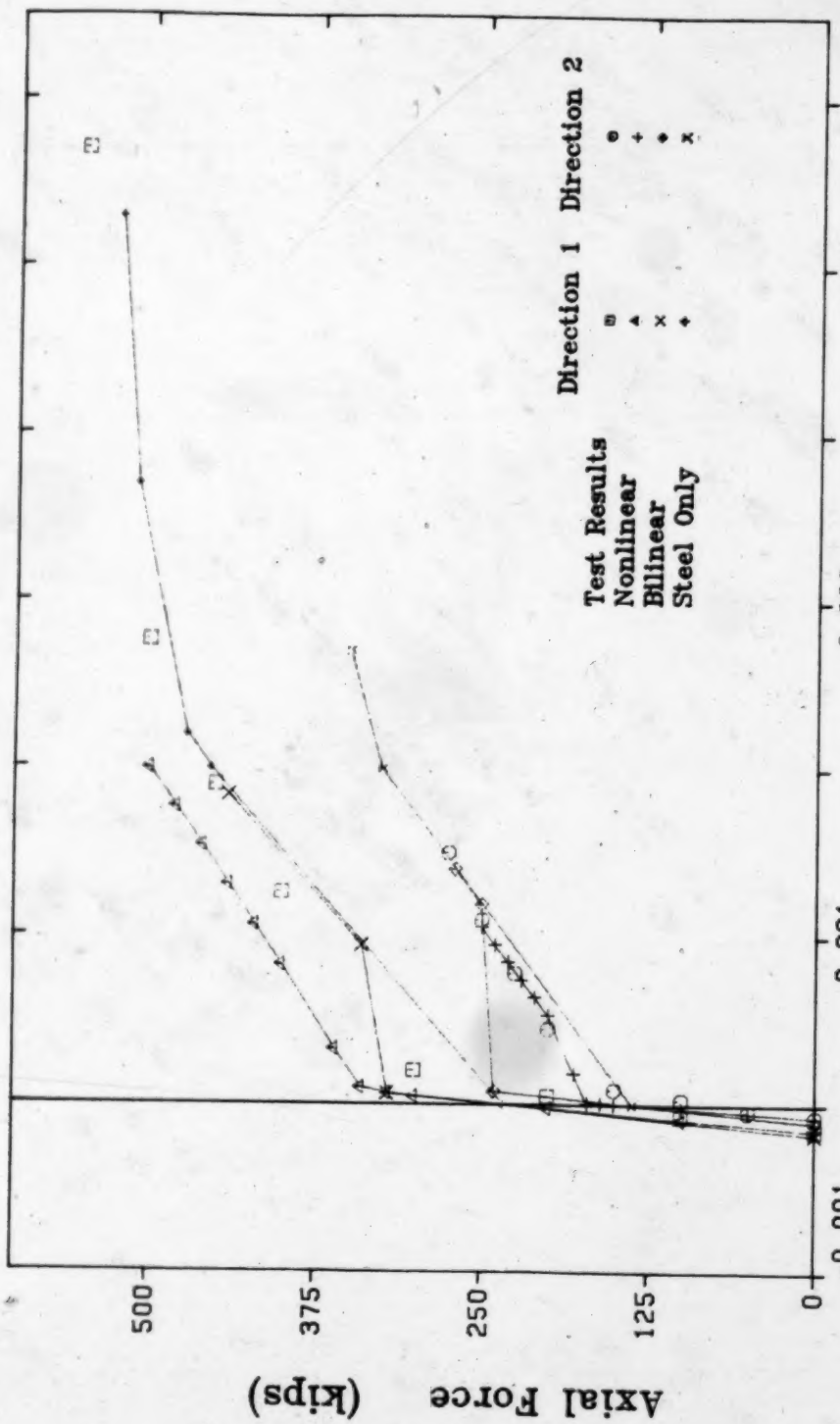

Fig. 5.4 Force-Deflection Curve of Test Segment No. 1

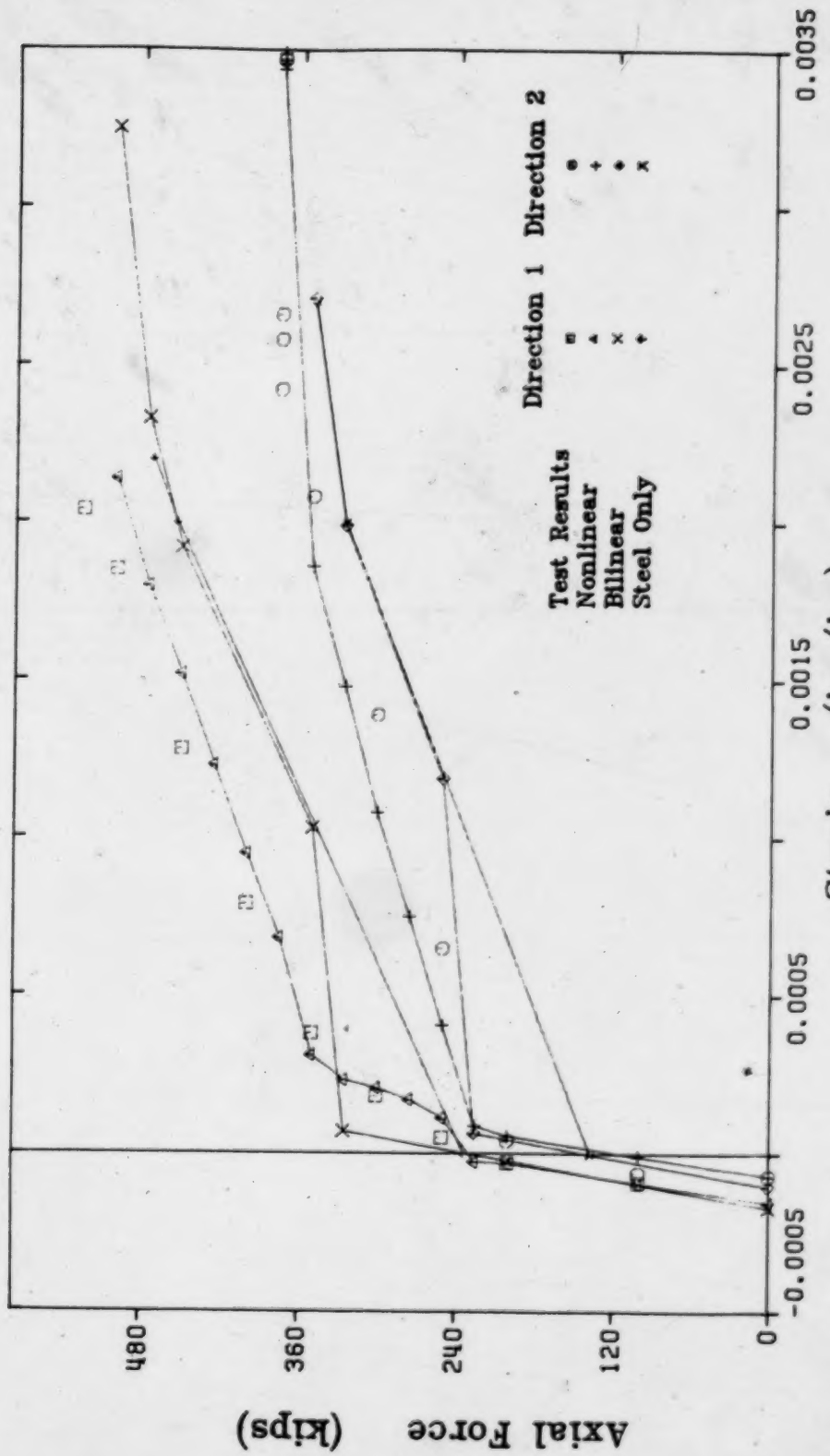

Fig. 5.5 Force-Deflection Curve of Test Segment No. 3

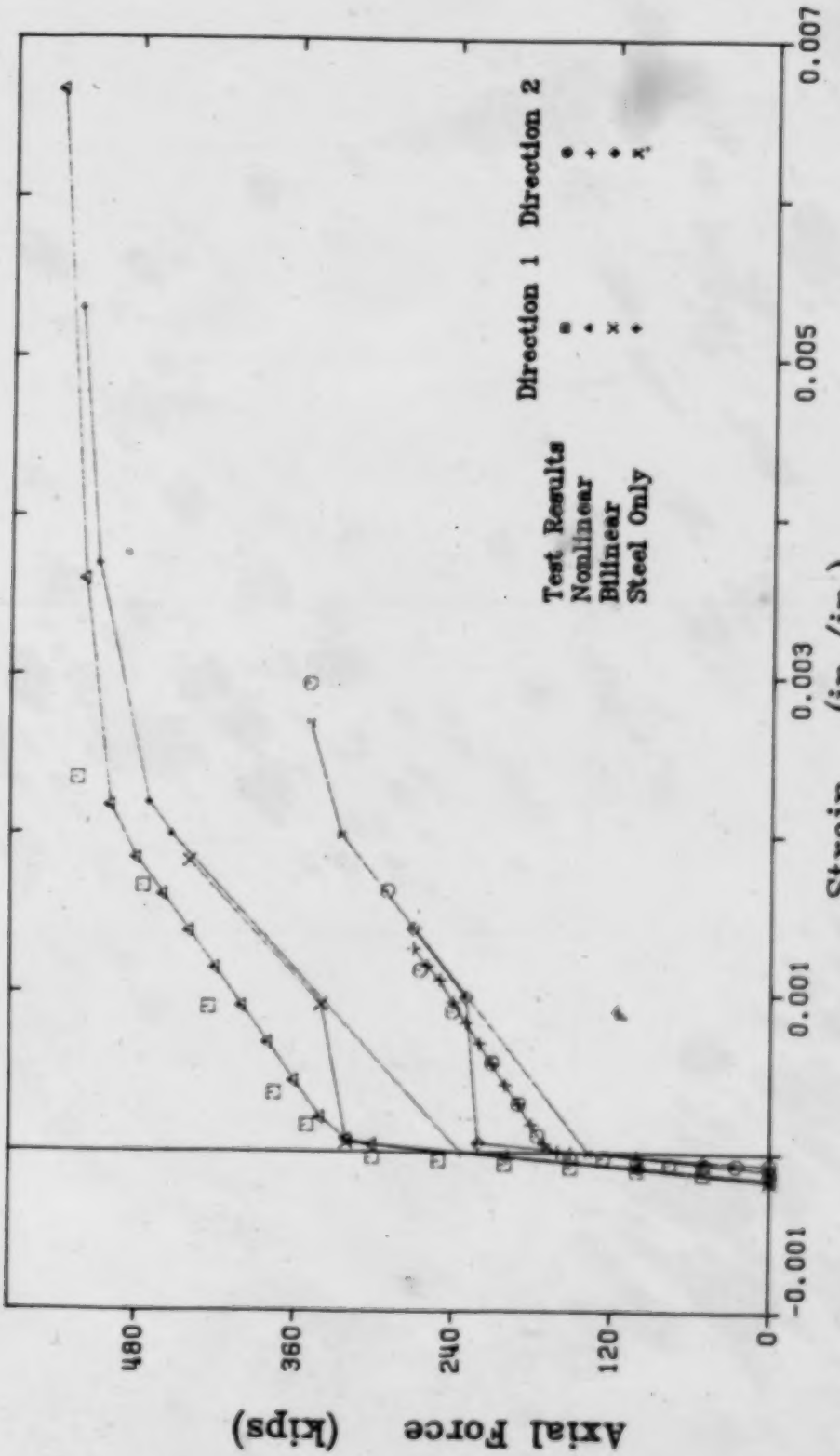

Fig. 5.6 Force-Deflection Curve of Test Segment No. 8

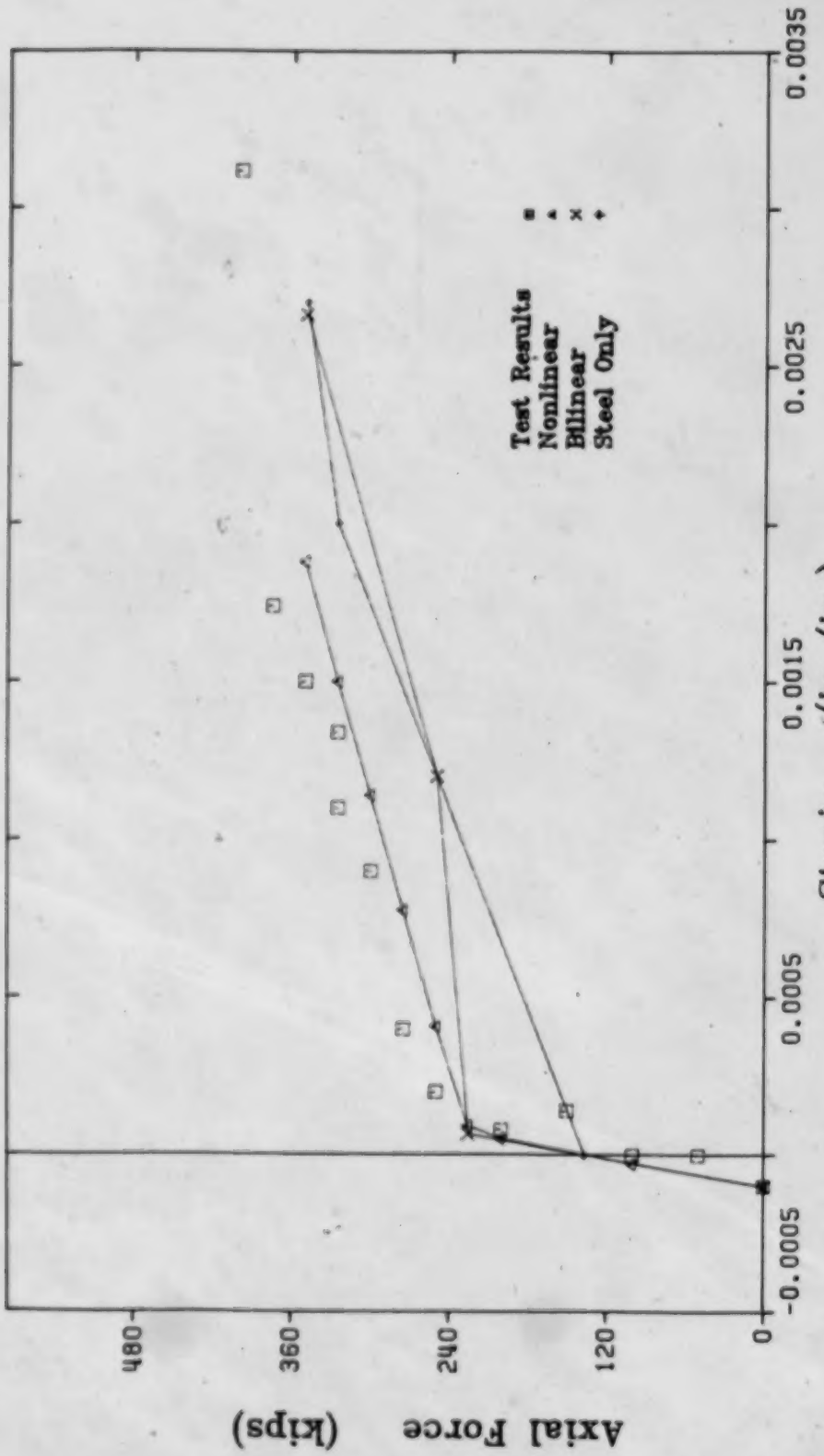

Fig. 5.7 Force-Deflection Curve of Test Segment No. 5

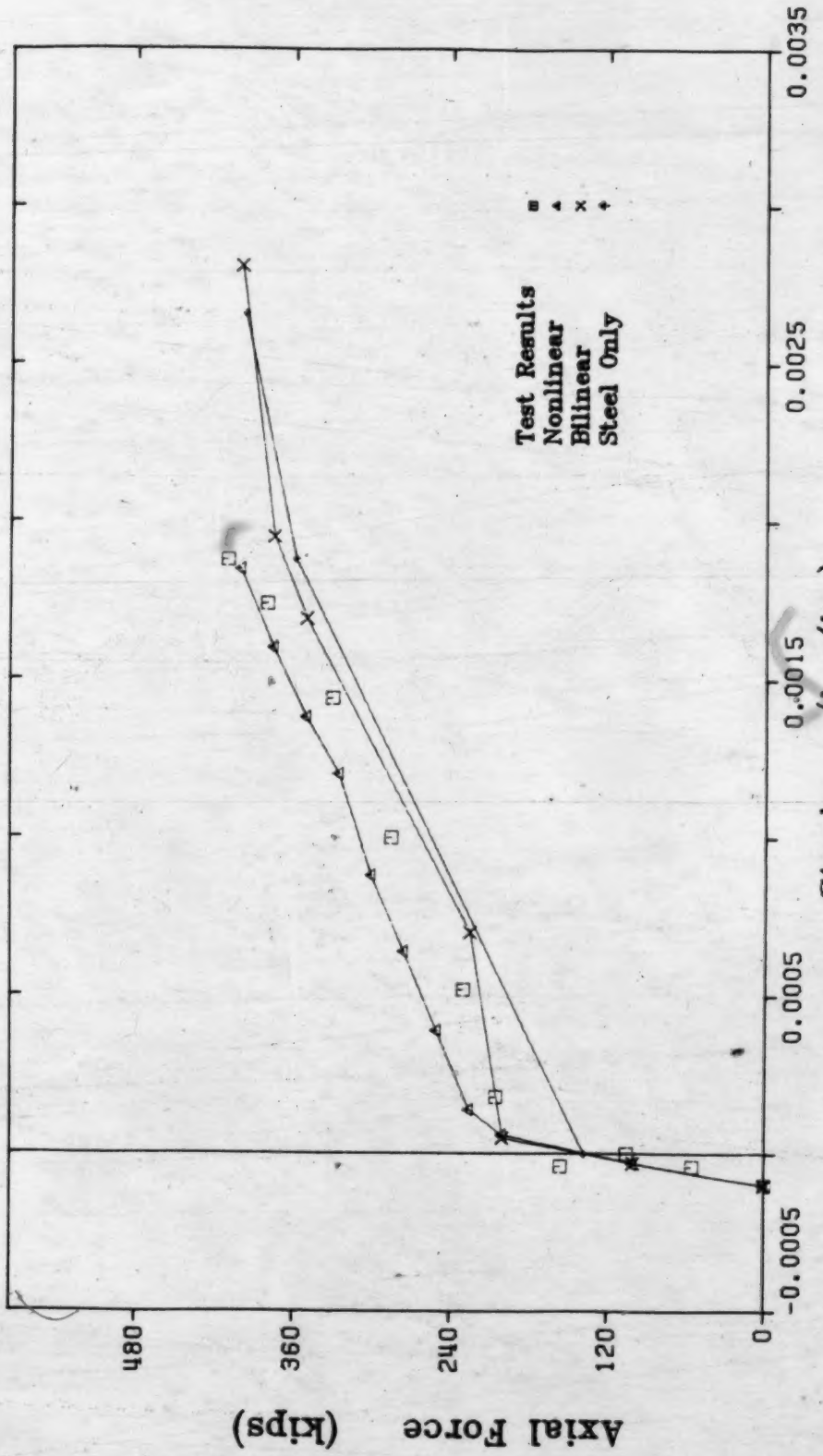

Fig. 5.8 Force-Deflection Curve of Test Segment No. 6

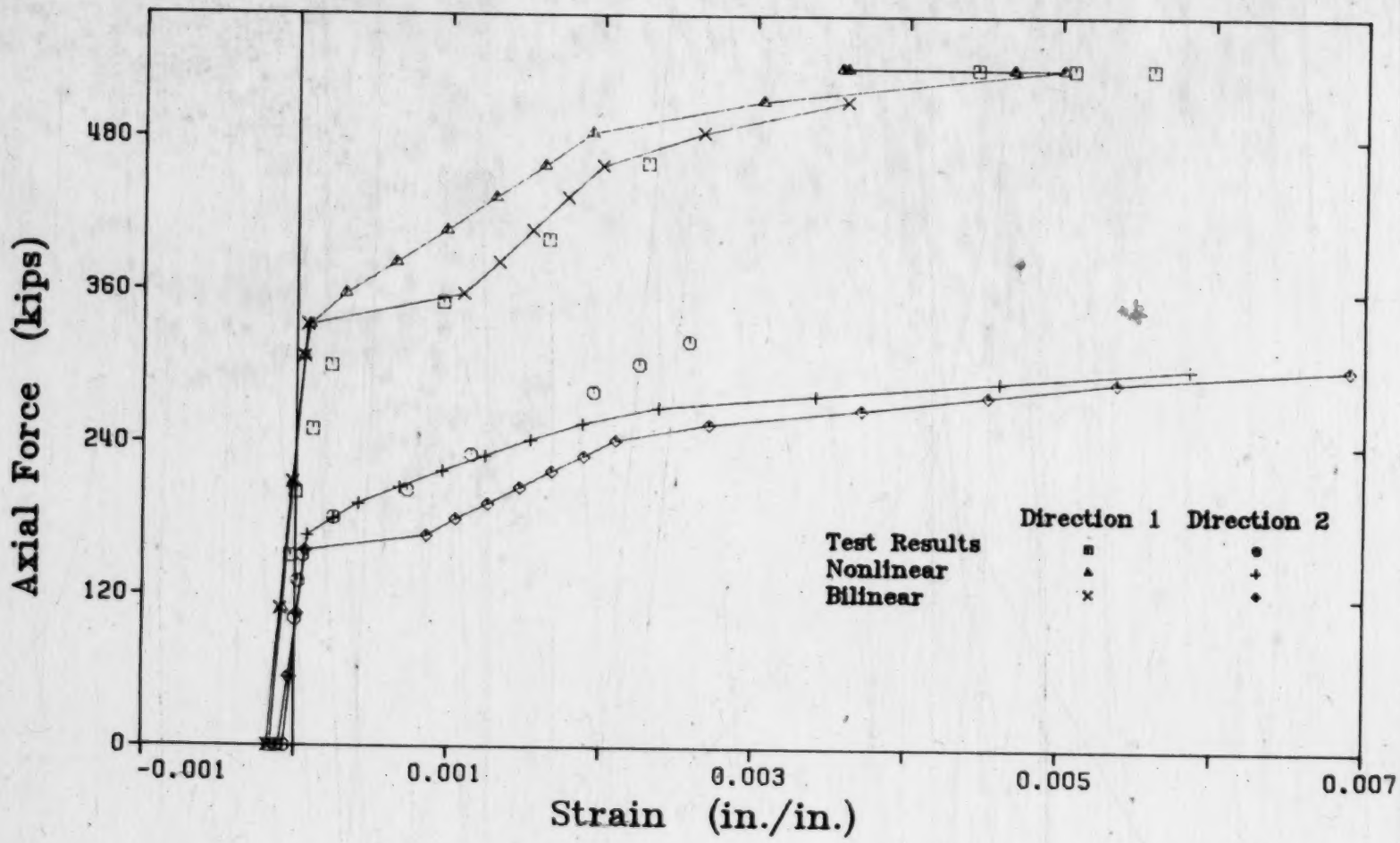

Fig. 5.9 Force-Deflection Curve of Test Segment No. 12, Face A

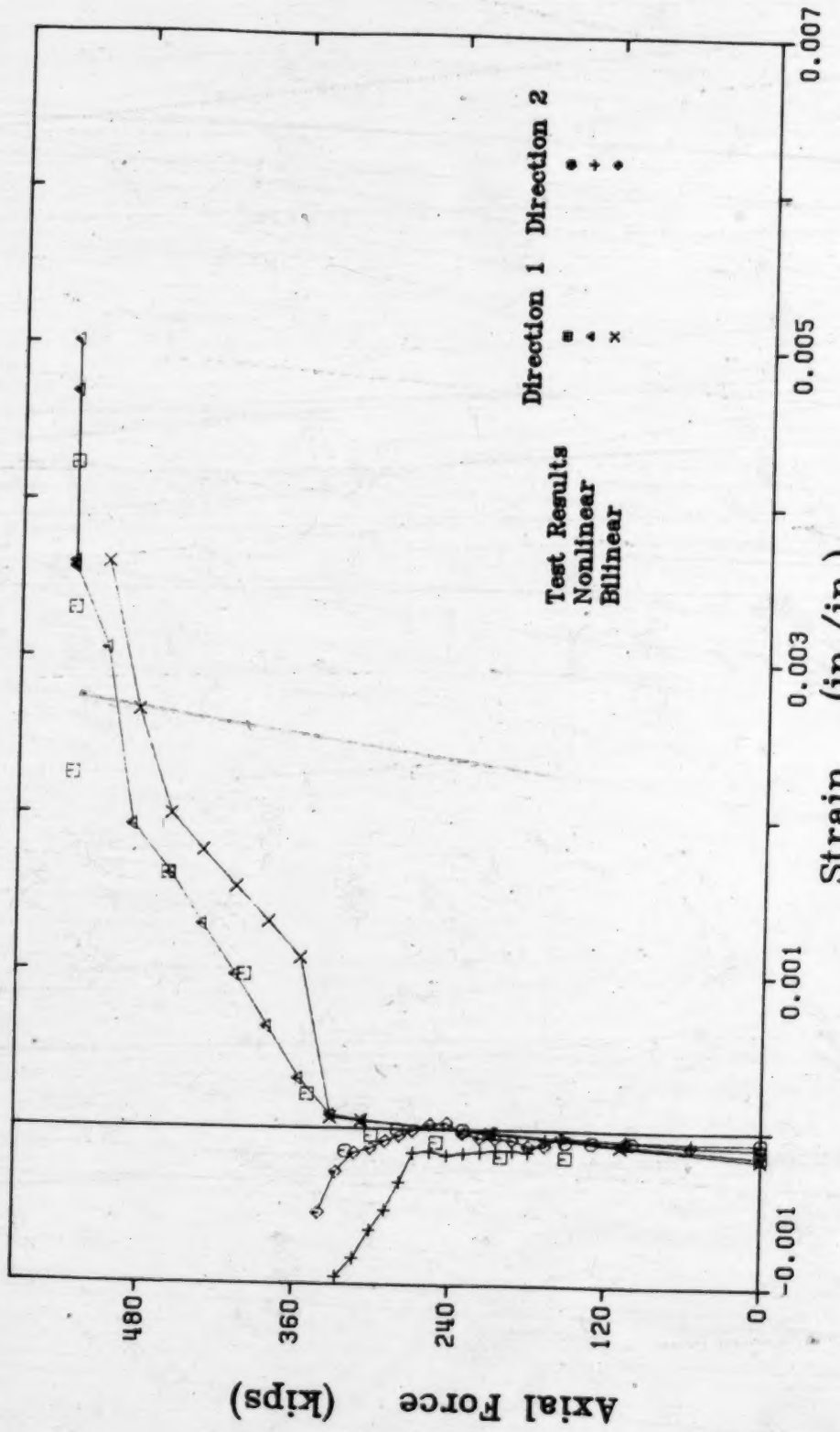

Fig. 5.10 Force-Deflection Curve of Test Segment No. 12, Face B

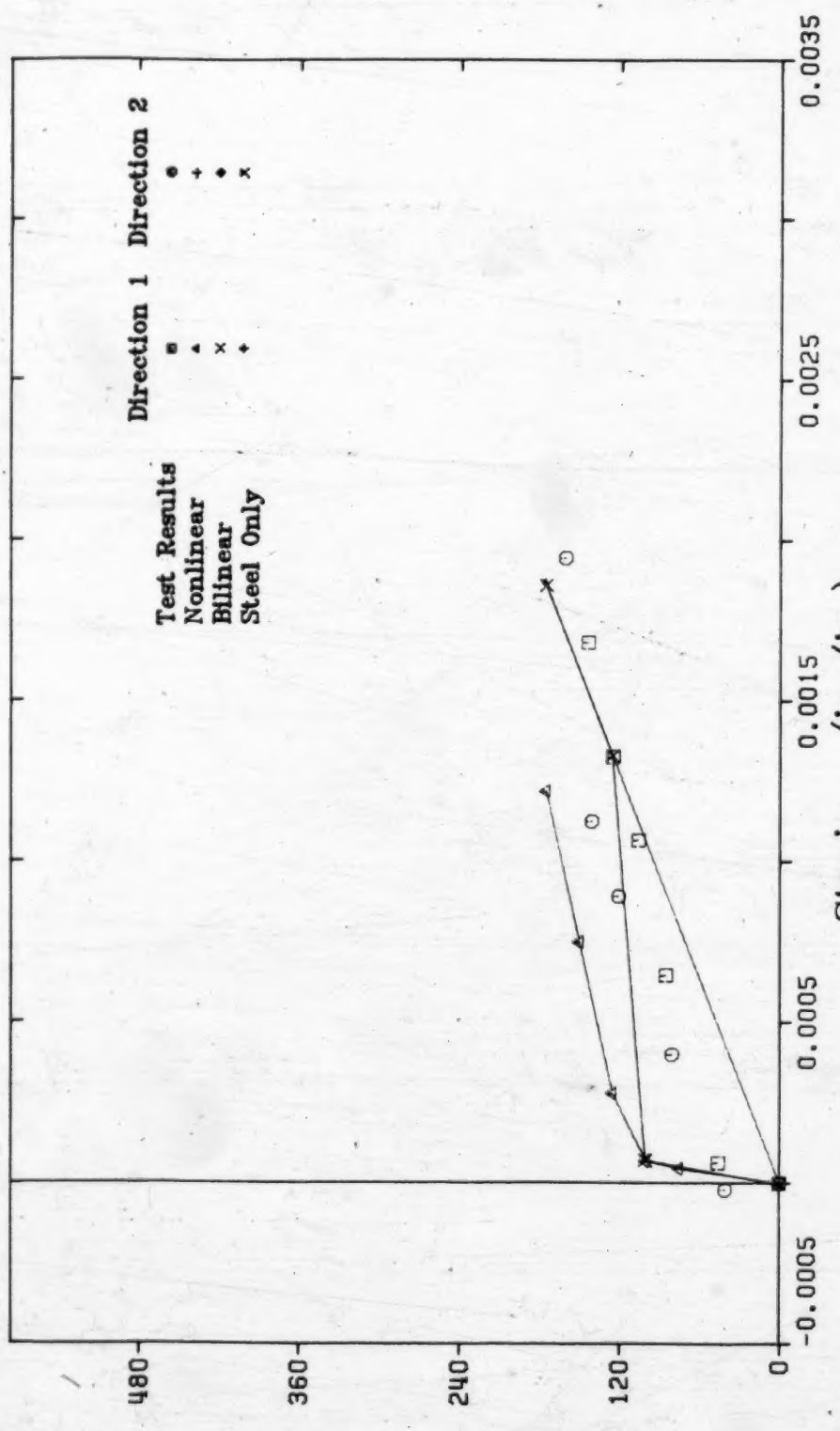

Fig. 5.11 Force-Deflection Curve of Test Segment No. 4

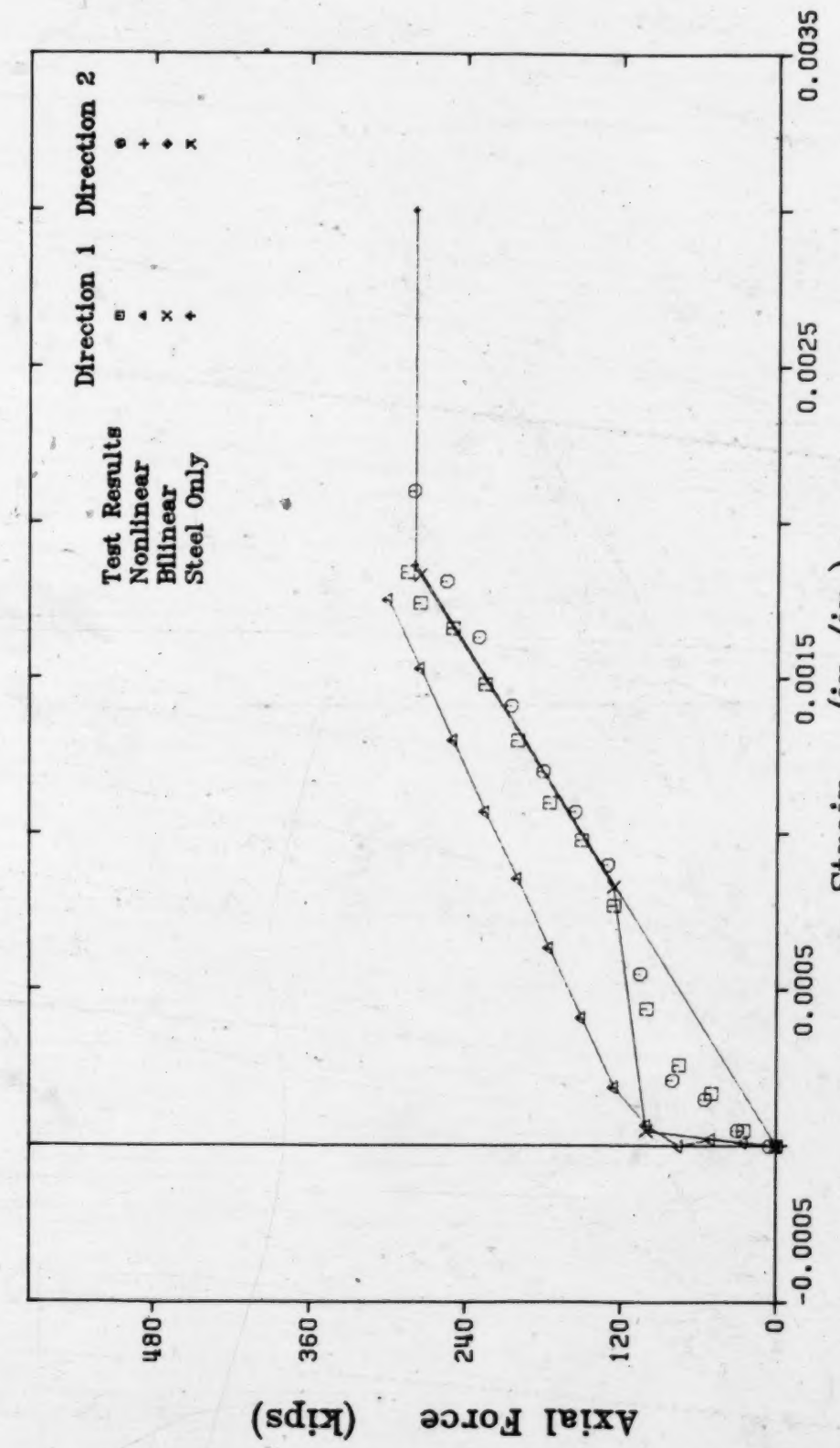

Fig. 5.12 Force-Deflection Curve of Test Segment No. 7

6. FURTHER APPLICATIONS

6.1 Introduction

A rigorous and widely acceptable method of analysing a concrete containment vessel would involve a nonlinear finite element or finite-difference technique. However, this type of analysis, if used as a design tool can be costly and time consuming. In this chapter, two simplified alternative design checking techniques will be investigated, the first being the theory and resultant program developed in the previous chapters of this report, which considers one segment of the total structure, and the second being the interaction diagrams presented by Epstein and Murray (1976), which considers only one direction of one segment. These two methods will then be compared with the results obtained from a BOSOR5 analysis, which considers the entire structure and for which the program was modified to include an elastic-plastic constitutive model for concrete. Before making these comparisons, an explanation of the construction and interpretation of the interaction plots will be given.

6.2 Interpretation of Interaction Diagrams

As an alternative to the type of analysis discussed in this report, in which a segment is subjected to a prescribed loading sequence, Epstein and Murray (1976) constructed interaction diagrams. From those diagrams, plotted in axial force-moment space, the various conditions of first cracking, first yield, through cracking, second yield, tendon rupture and crushing of the concrete can be predicted, not just for a single combination of loads, but for any combination. Figure 6.1 contains a typical

interaction diagram from that report.

In constructing the interaction plots, a nonlinear one-dimensional concrete constitutive relation was employed. Each plot ignores biaxial effects and is restricted to a given set of parameters, namely: the concrete strength, steel strength and the segment geometry. In addition, no thermal or creep conditions could be considered, and it was assumed that no prior cracking had occurred due to thermal or shrinkage stresses.

To use the interaction plots the effects of prestressing must be included as an external load, even though the strains in the tendons resulting from prestressing are implicitly considered in each diagram. From the location representing the axial load and moment induced by the prestressing, the live loads are added. Due to the nature of the plot, the live loads must be in the form of axial loads and moments, not in the form of imposed strains. Predictions from the interaction diagrams can be made for a load path in which the ratio of axial load to moment is kept constant. Since the actual loading history in a structure is a curved load path, especially after first cracking, the straight line assumption may lead to erroneous results.

As presented by Epstein and Murray (1976), the interaction diagrams may create some confusion. This can be illustrated by constructing the load paths Nos. 1 and 2 as shown in Fig. 6.1. If the segment loading follows path No. 1, then the predictions of the plots are clear. The prestressing brings the loading condition to point A. As the live load is applied, the segment begins to crack at B. Loading continues and at point C, one of the layers of reinforcing steel begins to yield. Failure of the segment occurs at point D when crushing of the concrete is first

experienced on the outside layer.

When following load path No. 2 however, the nature of the response is not so evident. Again beginning at point A, the first limit state encountered is through cracking at point E, indicating that open cracks exist completely through the section. As the loading continues from point E, first cracking is observed at point F. First yield occurs at point G, through cracking is again indicated at point H, second yield at point I and final failure results from tendon rupture at point J. This apparent sequence, in which first cracking occurs after open through cracking, is obviously incorrect, and a proper interpretation requires a consideration of the load history.

The area of the diagram bounded by the through cracking envelop is the only location where load history must be considered. If the section had not yet been subject to any loads, the following events would occur along load path No. 2. The first limit state to be encountered after leaving A would again be open through cracking, but now at location F. As the loading continues, first yield would be observed at point G, and open through cracking again at point H. At point H, the segment no longer contains open through cracks as the moment has forced one side of the segment into compression. This condition however, is accompanied by large strain gradients. The lines labelled through cracking form an envelop within which the condition of open through cracks exist. Therefore at location H, the loading leaves the open through cracking envelop and the cracks on one side of the segment close. After point H, second yield occurs at point I and as before, failure is the result of tendon rupture at point J.

Load reversal, however, will lead to different results. Once the loading has brought the forces and moments to some location after point F, where first cracking and open through cracking occur simultaneously, if some of the load is removed the cracks will not close until the through cracking envelop is reached at point E. If the segment has not previously been cracked, then first cracking and open through cracking occur simultaneously at F. However, once the segment has cracked, the cracks will not close until E or H is reached and with reloading, the open cracks will appear again at E.

Within the open through cracking envelop, only the two layers of reinforcing steel and the prestressing steel are resisting the axial forces and moments. This results in three other characteristics of the interaction diagrams. First, the vertical line which extends from the lower corner of the through cracking envelop to the tendon rupture line is part of the through cracking envelop. If the load combination is on this vertical line, then open through cracks exist, and both layers of steel have yielded. Secondly, the change in slope of the through cracking line below the first yield line results from yielding of the prestressing strands. The stress-strain law considered for the prestressing is linear up to $0.7\ \sigma_{pu}$. After this, the tangential modulus declines to zero at σ_{pu}. Therefore, at the "kink" in the through cracking line, the prestressing strands have reached the yield stress. Third, both of the steel layers have yielded on the vertical line extending from the junctions of the first yield lines to the second yield lines, and this line should also be labelled second yield. As this example section has steel layers of unequal area, this line is not on the moment axis (M=0).

The interaction diagrams presented by Epstein and Murray (1976) are correct but must be used with care, especially in the region bounded by the through cracking lines. If the section is previously uncracked, cracking will not occur anywhere on the diagram until the first cracking line is reached. If this line is reached within the through cracking envelop, then first cracking and through cracking occur simultaneously. If the segment has already been cracked, then the concrete has no strength in tension and through cracks will exist if the load state is anywhere within the through cracking envelop.

6.3 Analysis of Containment Structure Segments

To further assess the abilities of the segment analysis as developed herein, comparisons were made indirectly with a scale model test structure which was tested at the University of Alberta in 1978. This test structure was first analysed using BOSOR5 which provided an energy finite difference solution of the axisymmetric containment vessel subject to internal pressure. For this analysis of the test structure, one slice of the structure, composed of 102 segments, was examined (Simmonds, et al, 1979). The results of the BOSOR5 analysis compare well with the test structure and shall therefore be assumed to correctly represent the test model. The segment analysis technique of this report is now applied to segments from the test structure and the results compared to the BOSOR5 analysis.

For the comparison, four segments were taken from the BOSOR5 analysis. These segments are labelled 9-10, 3-2, 3-16 and 7-4. (The notation, of the form m-n, arises from the BOSOR5 model, in which m is

the shell component, and n is the station within the component.) Segment 9-10 is at the top of the dome, Segment 3-2 is at mid height in the cylinder wall, Segment 3-16 is at the junction of the cylinder with the ring-beam and Section 7-4 forms the junction of the ring-beam with the dome. The details of the segment geometrics are listed in Tables 6.1 and 6.2, along with pertinent material parameters.

The results of the segment analyses are presented such that the forces and moments on orthogonal load-carrying faces are examined individually. These faces are designated as meridional (or vertical) by M, and circumferential by C. That is, the forces on face C act in the circumferential direction and face C is orthogonal to these forces. For Segment 9-10, at the top of the dome, the segment geometry and loads are similar for both faces and therefore only the meridional face is discussed. The results of the circumferential face are similar.

The graphical results of the various solutions are shown in Figs. 6.2 - 6.8. These figures deviate from the sign convention adhered to in previous pages herein in that compressive axial forces are considered positive. The solid lines which form the interaction diagrams represent the uniaxial elastic solutions of the Epstein and Murray report (1976). The solutions of the two-dimensional nonlinear analysis, and of the BOSOR5 nonlinear analysis are shown as discrete points plotted on the interaction diagram. Each point represents an increment of 10 psig of internal pressure within the vessel starting from the reference state which includes prestressing, gravity, and the weight of the water which fills the structure. The points for the BOSOR5 analysis are plotted up to 130 psig. By the BOSOR5 analysis, the predicted failure load occurs

at approximately 134 psig.

While the live loading required for the BOSOR5 solution is specified as an internal pressure, the wall segment analysis developed in this report requires a loading history in terms of axial forces or strains, moments or curvatures. The source of this loading path must come from a solution which considers the entire structure, not just its elements in isolation. For the following comparisons, the results of the BOSOR5 analysis up to an internal pressure of 30 psig, at which point all of the materials were behaving elastically, were used to define the loading history required by the wall segment analysis. Two different loading histories were used. The first considers a constant ratio of the moments to axial forces on a face which result from the internal pressures, and these loads are added to the reference state. This shall be called the N-M analysis. The second loading history considers that the axial forces and curvatures, resulting from the internal pressure have a constant ratio. This method shall be called the N-ϕ analysis. For both of these loading histories, the ratio of the change in axial force to the change in internal pressure was assumed to be constant for the entire loading sequence.

The load path for a direct analysis by the interaction plots must also be specified in terms of axial forces and moments. Here the axial force to moment ratio resulting from the elastic response will be extrapolated until a failure condition is reached on the interaction plot, and knowing the increase in loads for a given increase in internal pressure, the pressure at which this failure condition has been reached

will be estimated. The results of this and the other procedures are listed in Table 6.3. This table lists the maximum possible internal pressure that can be reached by each analysis, along with the axial force and moment at this level of internal pressure. Since the BOSOR5 analysis deals with the entire structure, the maximum load to which any segment can be subjected is the load at which the weakest segment fails. The BOSOR5 analysis failed to converge at pressures above 134 psi. BOSOR5 values shown on Table 6.3 are extrapolated pressures required to produce failure of the tendons at the segment location. For the N-M and N-ϕ analyses, the maximum load to which any segment can be subjected is that load at which the weaker direction of the segment fails. Since the interaction plots are uniaxial, each direction of a segment fails at different load levels. If the smallest ultimate load of the four segments is taken from each of the analyses, the maximum loads as predicted by the BOSOR5, N-ϕ, N-M and interaction analyses are 138, 120, 95 and 100 psig.

6.3.1 Segment 9-10

The results from segment 9-10 are shown in Fig. 6.2. Since the segment details and loads are the same in both directions, this figure represents the results for both load-carrying faces of segment 9-10. The solid lines represent the familiar interaction diagram while the other analyses are shown by their designated symbols. All the segments have been analysed assuming the dimensions are one inch wide by one inch long, and this is reflected in the units of the axes. The thicknesses of the segments vary and are listed in Table 6.1.

The straight line load paths of the N-M segment analyses and the constant ratio extrapolations on the interaction plots will always have the same direction, and in this instance both indicate failure at an internal pressure of 110 psi. This agreement in results will not always occur but it is more likely to happen when the orthogonal load-carrying faces of the segment have similar loadings and details. However, the solutions obtained by assuming a constant ratio of axial force to moment do not follow the BOSOR5 solution as well as the N-ϕ analysis. After crossing the first cracking line of the interaction diagram, both the N-ϕ and BOSOR5 results predict that the moments decrease to almost zero. However, the N-ϕ analysis, which assumes that the axial force increases linearly with the internal pressure predicts failure of the segment at 120 psig whereas the BOSOR5 solution, which is not restricted by this assumption, indicates that the segment can withstand at least 138 psig. The assumption of linearity between membrane force and pressure is reasonably accurate in this instance but it is not sufficiently precise to make the agreement in internal pressures at failure between these two methods any closer.

6.3.2 Segment 3-2

The results of the forces and moments in the meridional direction of segment 3-2 are shown in Fig. 6.3 and the circumferential direction is shown in Fig. 6.4. Segment 3-2 is located half-way up the cylindrical wall of the structure and is little affected by the base or the ring-beam at the top. In the meridional direction the section is only subjected to tensile forces; the moments are very small. As a result all of the

analyses have similar predictions. The points of the BOSOR5, N-M and N-ϕ analysis do not reach the outer edge of the interaction plot as the failure occurs first in the orthogonal circumferential direction. In this direction, the N-M analysis again has moments close to zero. However, after cracking both the N-ϕ and BOSOR5 analyses predict increasing moments across this section which is eccentrically loaded by the prestressing. Failure occurs in this direction when the prestressing tendons fracture.

For this segment, as in segment 9-10, the closest agreement with the BOSOR5 results is obtained from the N-ϕ analysis. Also, in common with segment 9-10, this segment is not located close to any discontinuities.

6.3.3 Segment 3-16

Segment 3-16 is located at the top of the cylindrical wall immediately next to the top ring beam. The forces and moments applied to the segment in the meridional direction are shown in Fig. 6.5 and in the circumferential direction in Fig. 6.6. Arising from the proximity of this segment to the ring beam, large moments must be resisted in the meridional direction. Whereas the N-ϕ analysis indicates that the moments are reduced after cracking, the BOSOR5 analysis shows that these moments must be carried past the initiation of cracking and beyond the point of first yielding. For this section, the N-M analysis provides better agreement with the BOSOR5 results than does the N-ϕ analysis.

In the circumferential direction, the comparatively large and consequently stiff ring beam absorbs the majority of the forces and therefore the results are centred near the origin of the interaction plot, away

from any failure modes. Here again though, like the meridional direction, the N-M analysis provides results which are closer to the BOSOR5 results than the results of the N-ϕ analysis.

6.3.4 Segment 7-4

This segment is located near the bottom of the dome which is linked to the cylinder through the ring beam. This segment therefore also reflects many of the effects that were seen in segment 3-16. The results for the meridional direction, shown in Fig. 6.7 parallel those in the meridional direction of segment 3-16. After first cracking, the moments predicted by the N-ϕ analysis drop off. It is apparent though, that these moments must be resisted, as the BOSOR5 analysis shows their presence after the initiation of cracking, after first yielding, up to crushing. This behavior is closer to the response demonstrated by the N-M assumptions than by the N-ϕ assumptions.

The results in the circumferential direction, shown in Fig. 6.8 are also similar to those of section 3-16C. The large adjoining ring beam attracts a large proportion of the forces during the initial stages of loading. However, the BOSOR5 results do not adhere to the assumption made for the N-M and N-ϕ analyses that the axial force is proportional to the internal pressure. As shown by the BOSOR5 points plotted in Fig. 6.8, which represent increments of 10 psig of internal pressure, the change in axial force for a constant change in internal pressure increases at higher pressures. As a result of this assumption, changing ratios of axial force to internal pressure cannot be predicted.

6.3.5 Summary of Results

Two different types of behavior were observed. When the segment investigated is removed from any discontinuities, then the N-ϕ analysis gave results which most closely approximate the BOSOR5 results. However, when the segment was close to a discontinuity, then the N-M analysis was the more accurate. For the most part, the BOSOR5 results were bounded by the N-M and N-ϕ analyses on the interaction curve. The N-M analysis gave an underestimate for ultimate load in every instance whereas the N-ϕ analysis could predict higher or lower ultimate loads. The results obtainable from the uniaxial nonlinear elastic interaction charts are nearly identical to those of the biaxial nonlinear N-M analyses.

SEGMENT	THICKNESS	R_1	R_2	CONCRETE PROPERTIES					
				f'_c	ε_{io}	f'_t	ε_{iot}	E_o	υ_o
	in	in	in	ksi		ksi		ksi	
9-10	4.0	118	118	3.360	-.00217	.2225	.00012	3100	.20
3-2	5.0	∞	60.5	2.142	-.00238	.215	.00012	1800	.20
3-16	5.0	∞	60.5	2.142	-.00238	.215	.00012	1800	.20
7-4	7.22	118	118	3.360	-.00217	.2225	.00012	3100	.20

TABLE 6.1 Test Structure Segment Details

Section	Steel Layers						Prestress Layer				
			No. 1		No. 2						
	Yield Stress (ksi)	Young's Modulus (ksi)	Area (in^2)	Location 'Z' (in)	Area (in^2)	Location 'Z' (in)	Area (in^2)	Location 'Z' (in)	Initial Stress (ksi)	σ_{pu} (ksi)	E_o (ksi)
9-10	72.5	30500	.0128	-1.2564	.0128	1.2564	.0232	0.	110.8	260	30300
3-2M	51.0	29300	.0170	-1.616	.0170	1.617	.008	0.	95.8	270	30300
3-2C	51.0	29300	.0367	-1.643	.0367	1.643	.0152	.750	116.0	270	30300
3-16M	51.0	29300	.0170	-1.616	.0170	1.617	.008	0.	95.8	270	30300
3-16C	51.0	29300	.0367	-1.643	.0367	1.643	.0152	.750	116.0	270	30300
7-4M	72.5	30500	.0129	-2.8663	.0285	2.8611	.0214	-.200	110.8	260	30300
7-4C	72.5	30500	.0128	-2.8535	.0128	2.8427	.0232	-.177	110.8	260	30300

TABLE 6.2 Test Structure Segment Steel Details

Segment No.	BOSOR5	Analyses Types [1, 2] N - ϕ			N - M			Interaction Plots		
	p (psi)	p (psi)	N (kips)	M (in kips)	p (psi)	N (kips)	M (in kips)	p (psi)	N (kips)	M (in kips)
9-10	138	120	4.92	-.03	110	4.27	-1.37	110	4.4	-1.4
3-2M		140[4]	3.18	-.08	110[4]	2.33	.12	160	3.8	.20
3-2C	142	140	5.561	-1.46	110	4.08	-.083	130	5.2	-.10
3-16M	152	140[4]	3.21	-.084	95[4]	1.93	2.79	100	2.1	3.0
3-16C		140	.143	-.122	95	-.259	.505	470	3.1	3.1
7-4M	161	160[3]	2.49	.709	100[4]	.48	12.07	100	0.5	12.6
7-4C		160[3]	-5.45	.203	100	-4.62	3.25	760	-13.8	20.4

1. Forces and moments shown are per inch of segment width, and include the internal loads due to prestressing
2. Positive axial forces are tensile
3. Failure not yet reached
4. Failure initiated in this direction

TABLE 6.3 Comparison Test Structure Segment of Ultimate Loads

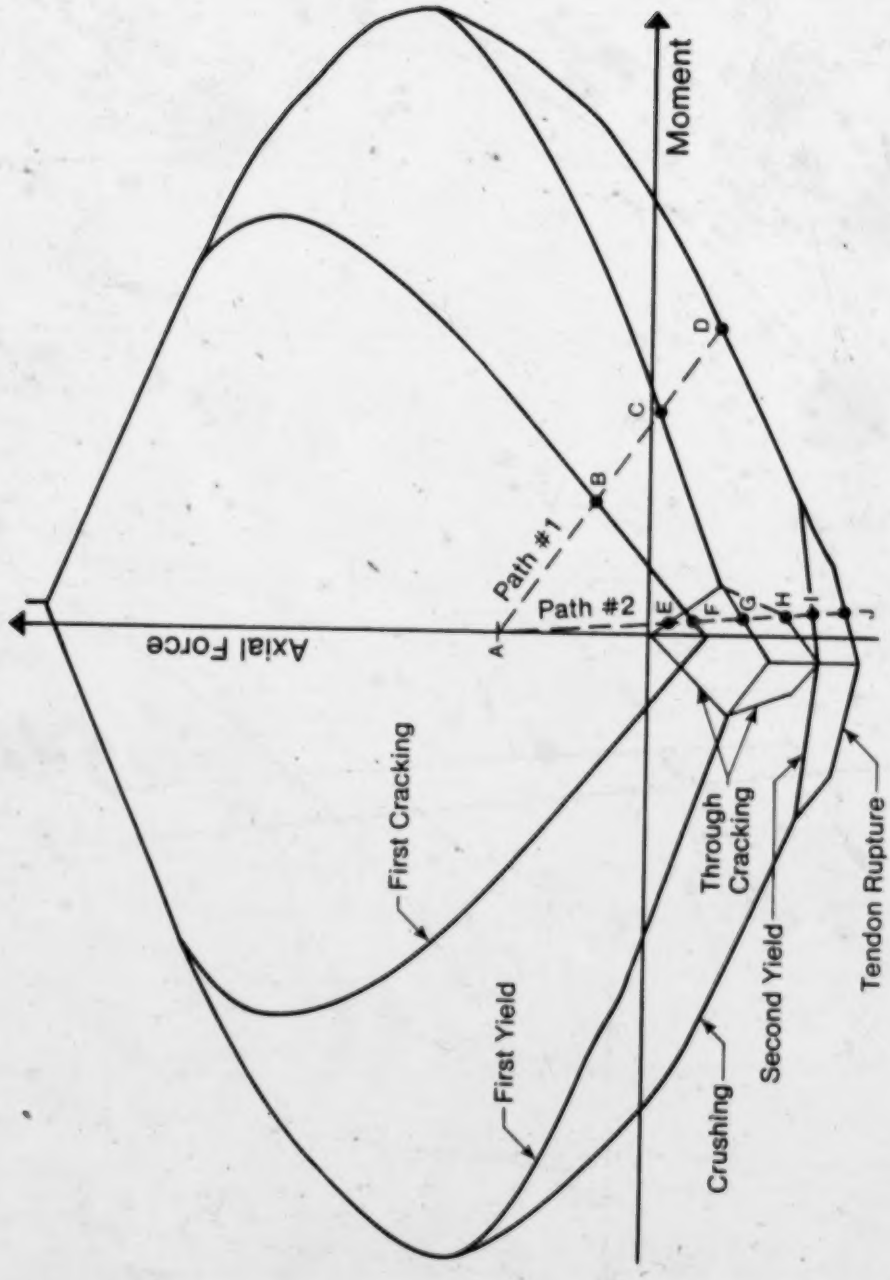

Fig. 6.1 Typical Interaction Diagram

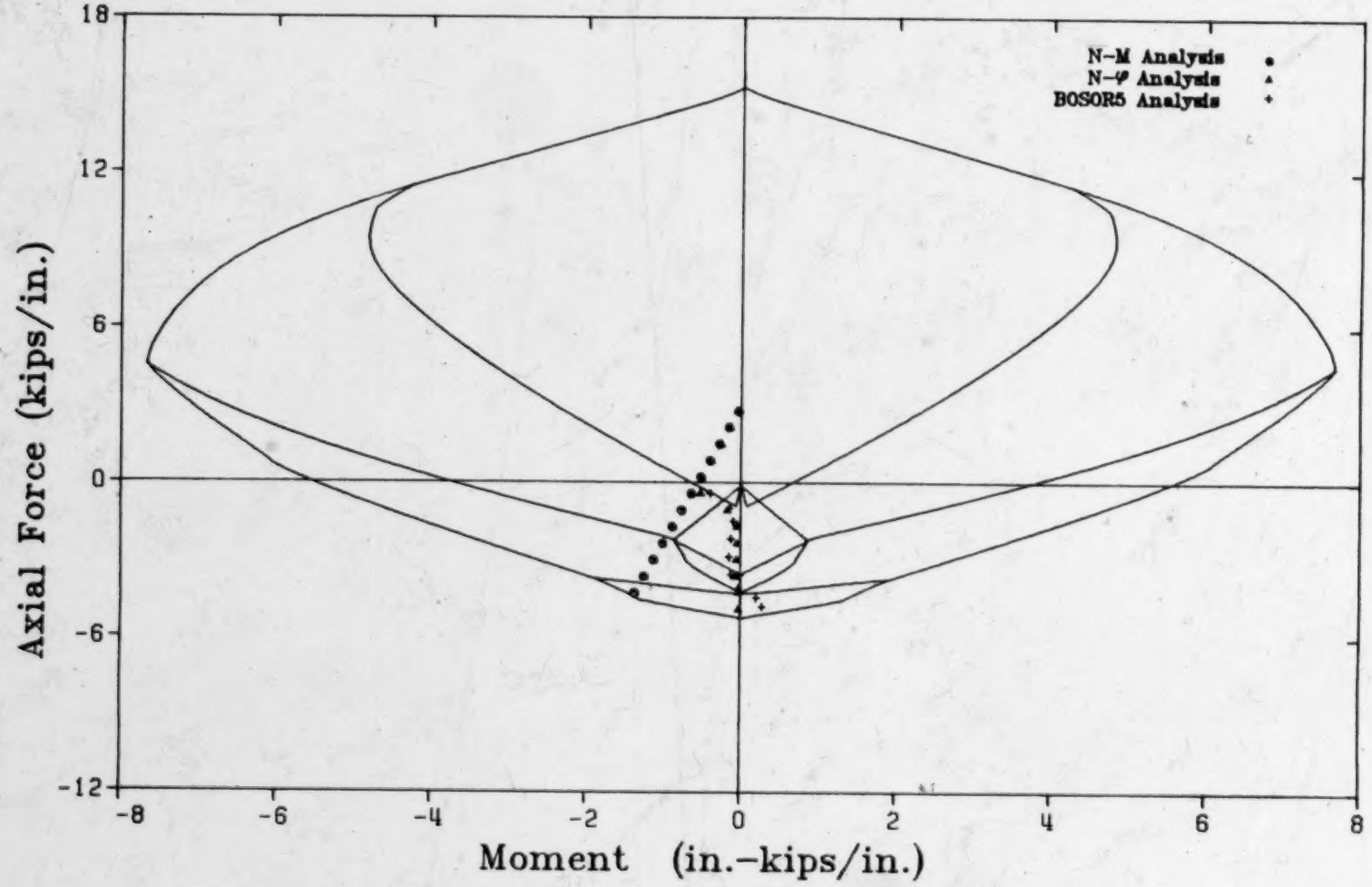

Fig. 6.2 Test Structure Segment 9-10

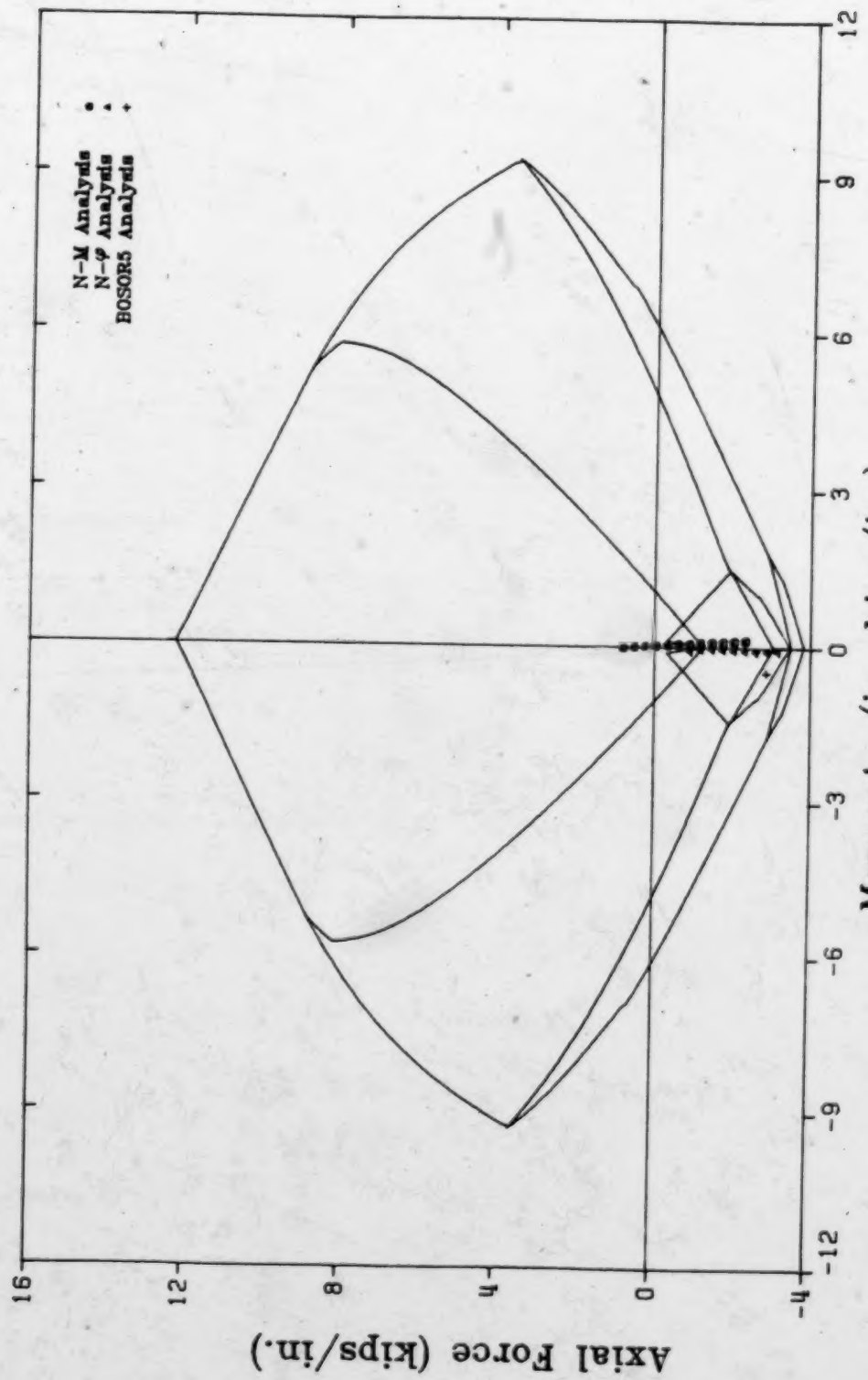

Fig. 6.3 Test Structure Segment 3-2M

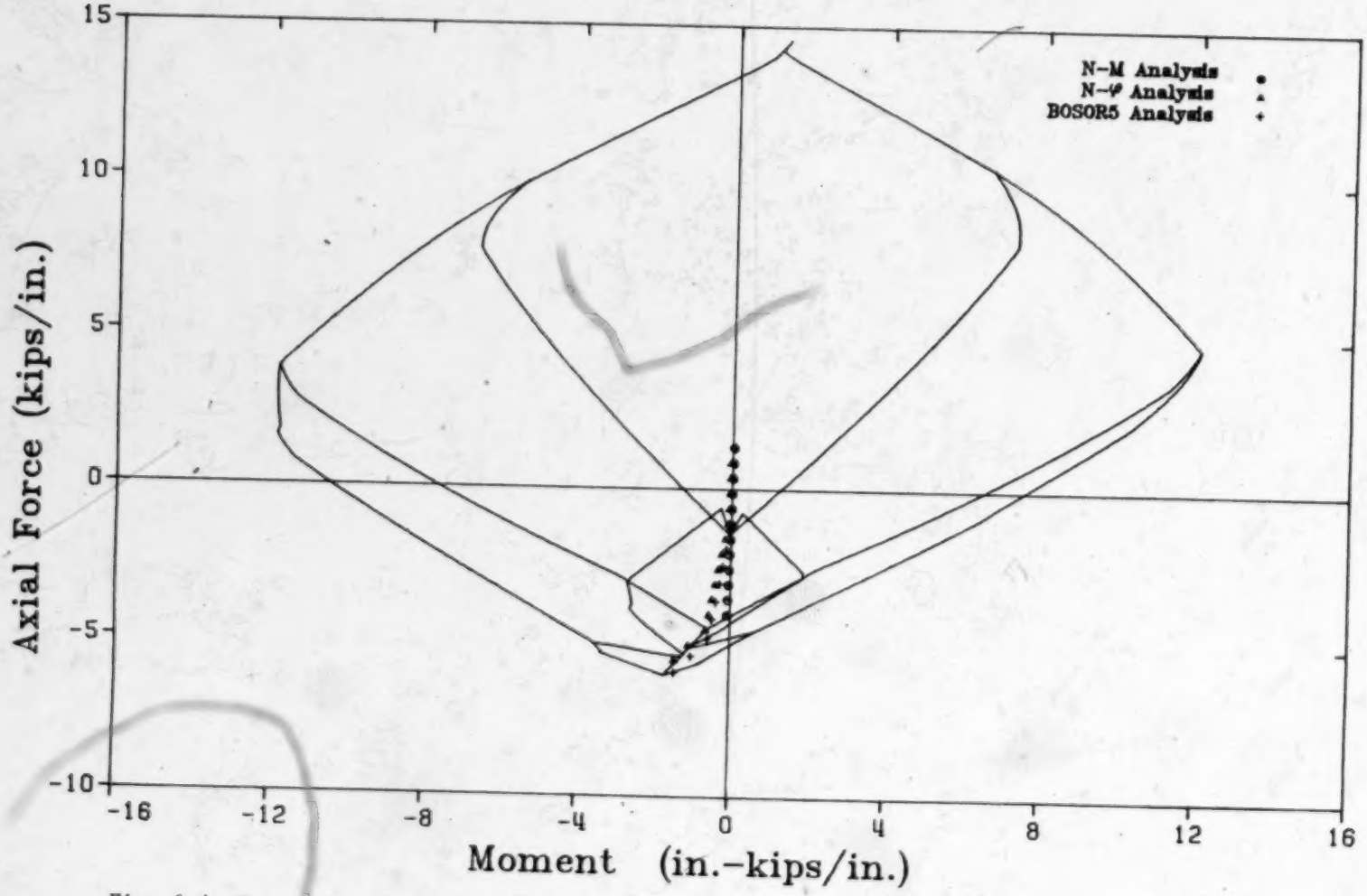

Fig. 6.4 Test Structure Segment 3-2C

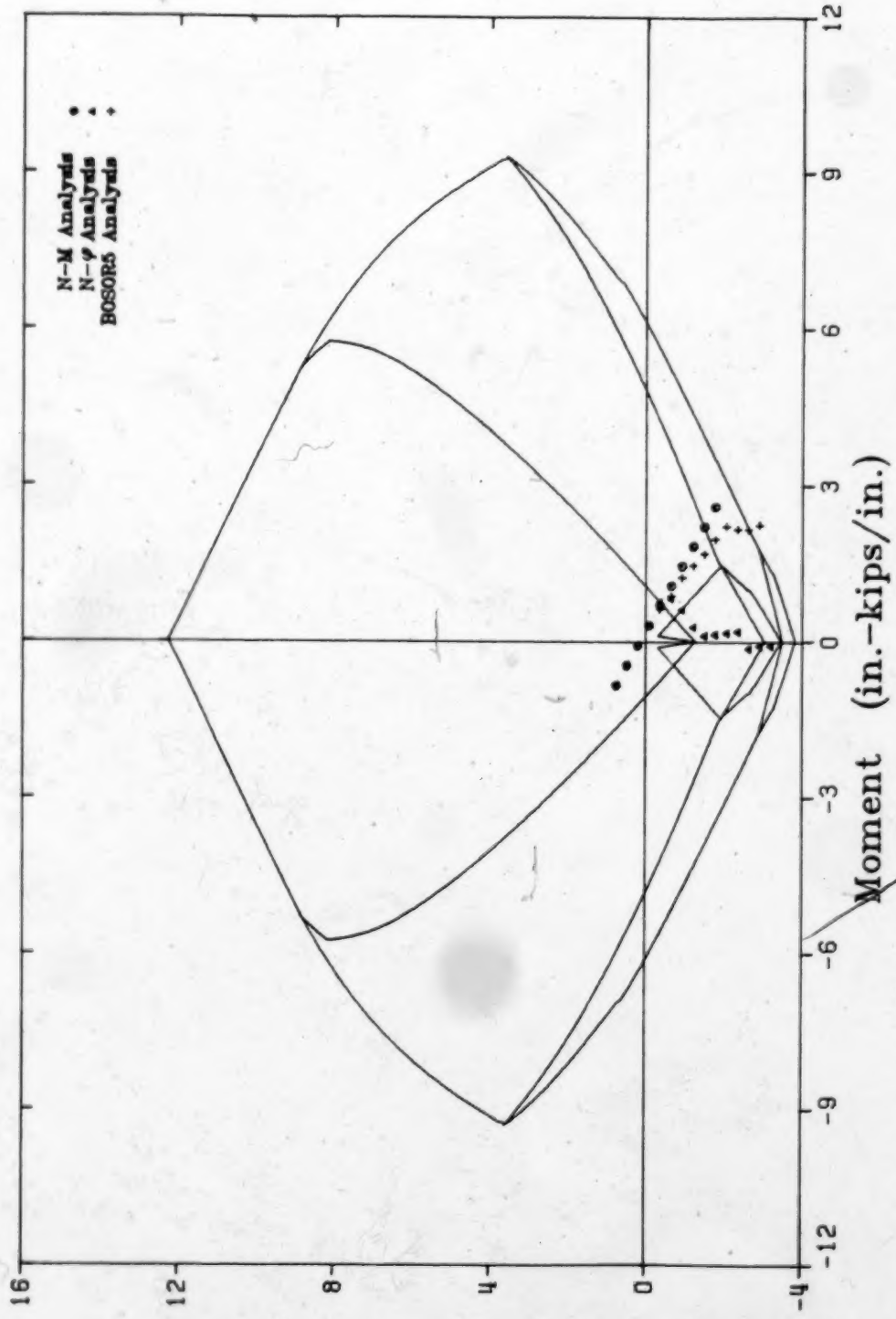

Fig. 6.5 Test Structure Segment 3-16M

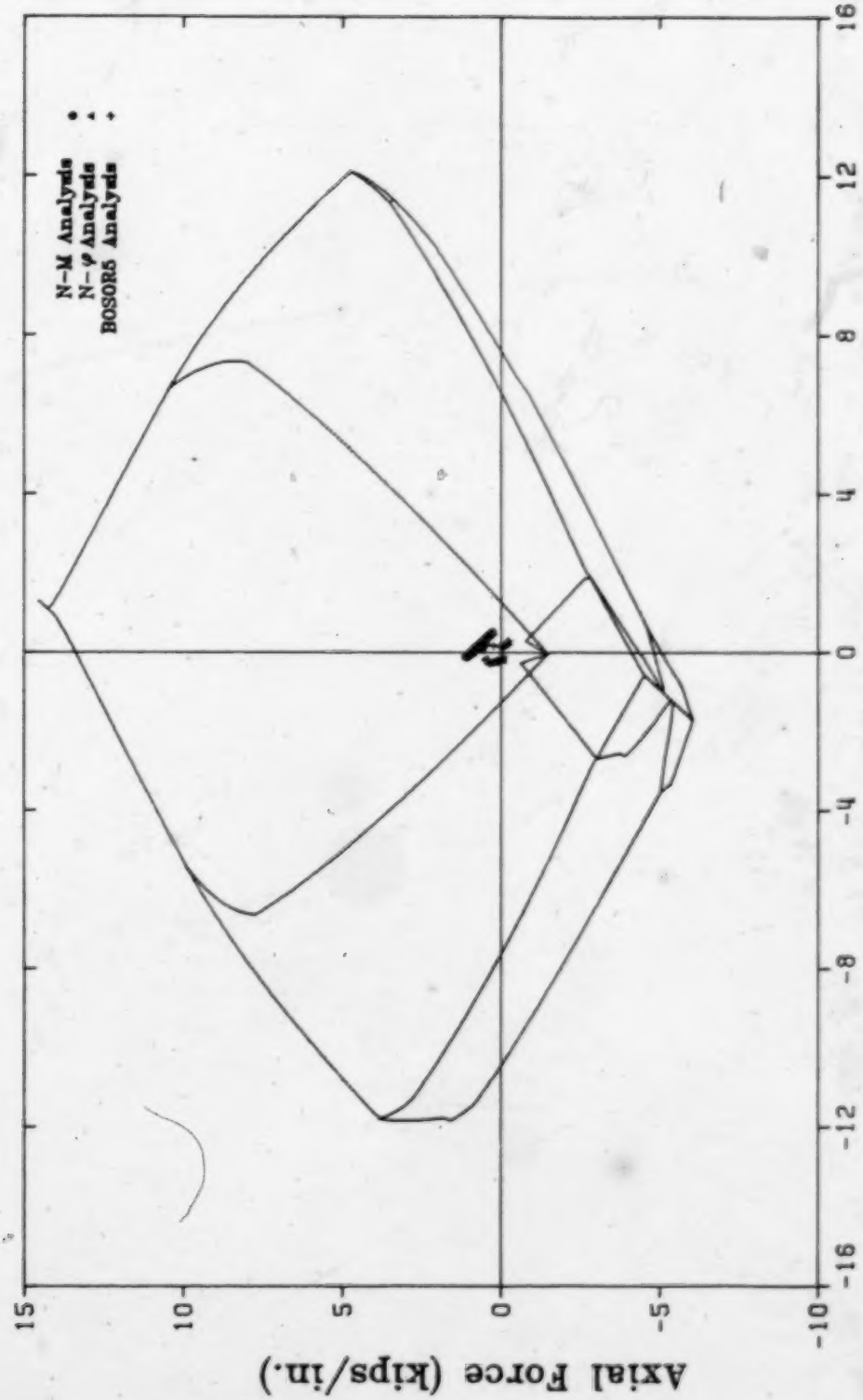

Fig. 6.6 Test Structure Segment 3-16C

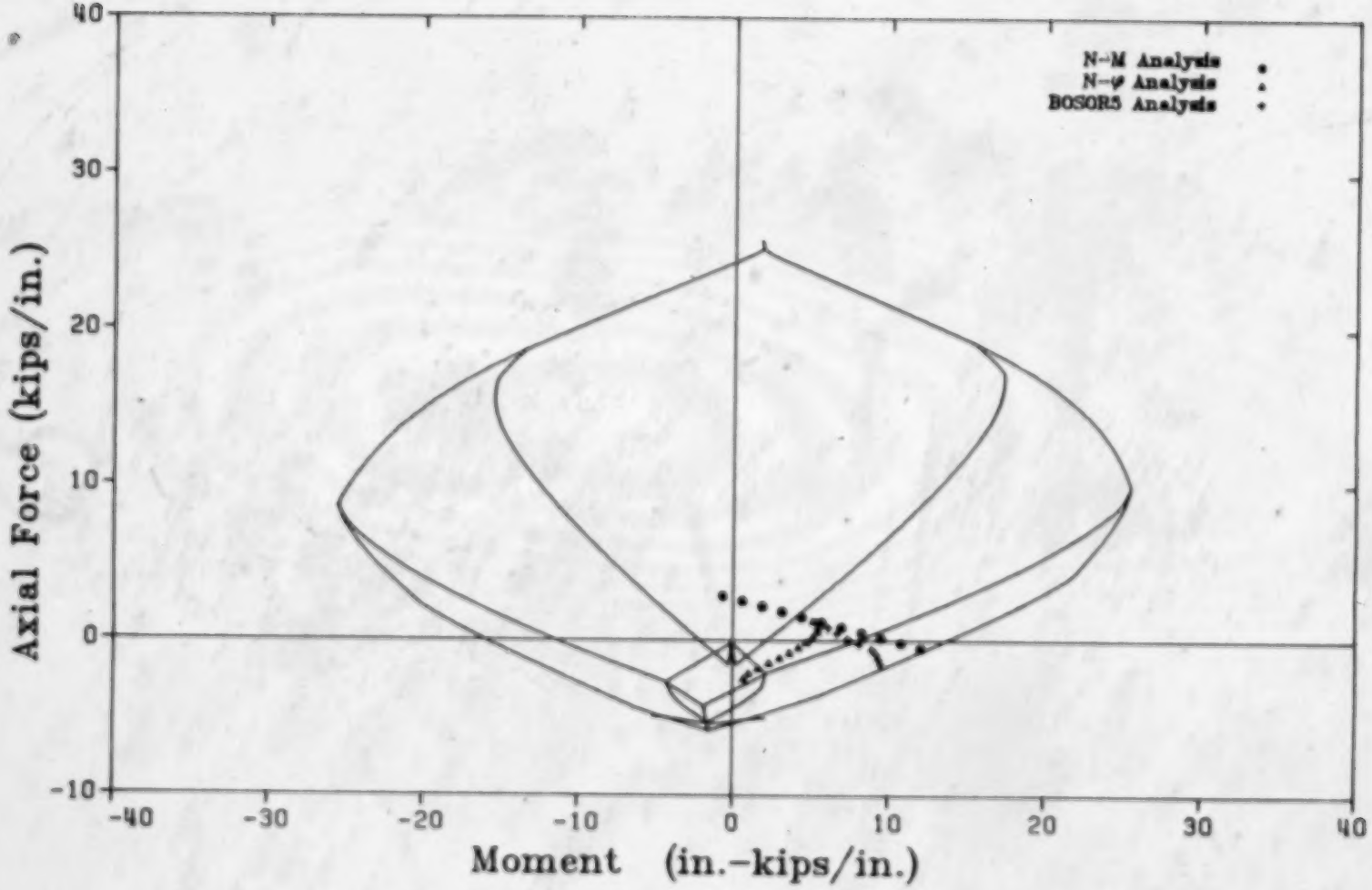

Fig. 6.7 Test Structure Segment 7-4M

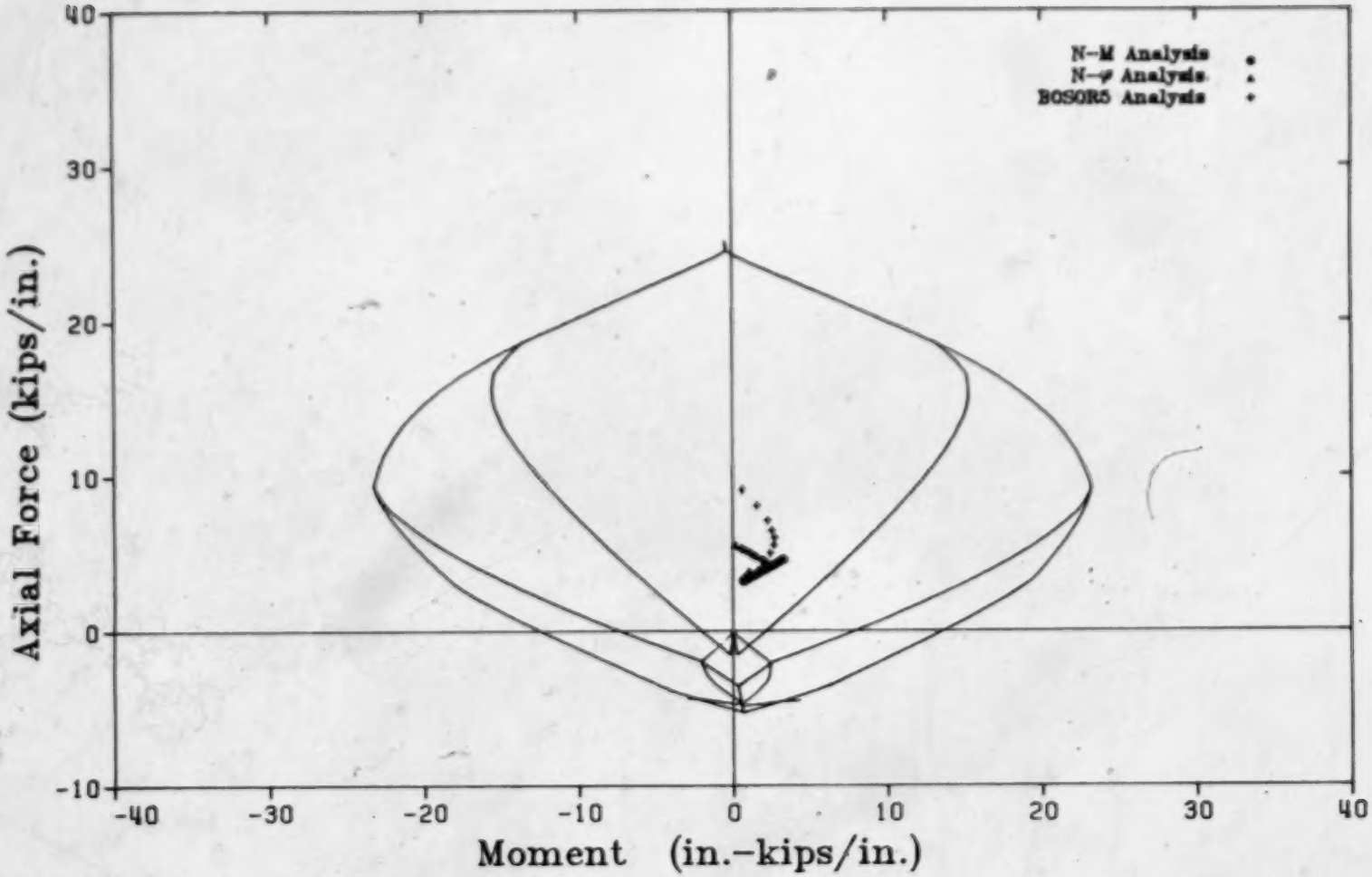

Fig. 6.8 Test Structure Segment 7-4C

7. SUMMARY AND CONCLUSIONS

7.1 Summary

A computer model was formulated to analyze a concrete wall segment containing two degrees of freedom in the direction of each of the two principal curvatures. In addition to the concrete matrix, the segment may include uniaxial elements of reinforcing bars and prestressing strands.

The segment analysis can be accomplished with either one of two available concrete constitutive relations. The first is a bilinear elastic uniaxial relation incorporating a two-part stress-strain curve in the compression region, and a tension cut-off. The second concrete constitutive relation is a biaxial nonlinear elastic type. In this relation, the real strains are first converted to equivalent uniaxial strains (Darwin and Pecknold, 1974). Then for a given stress ratio the corresponding point on the failure curve is found (Kupfer and Gerstle, 1973), the appropriate value for Poisson's ratio is determined (Elwi and Murray, 1979), and from curves developed in this report, the equivalent uniaxial strains at ultimate stress are ascertained. The current stresses are then computed from a stress-strain equation which includes a softening branch (Saenz, 1964).

The constitutive relation of the reinforcing steel consists of the conventional two-part elastic-perfectly plastic curve whereas the response of the prestressing steel is described by a piece-wise linear stress-strain curve.

The segment can be subjected to four different types of load.

These loads include prestressing forces, creep effects, thermal effects and live loads. The solutions under these loads are found by the Newton-Raphson technique. The response of the segment to a given set of strains is found by layering the segment, giving each layer appropriate properties and then integrating the responses from the individual layers to find the segment response. Corrections are made to this set of strains and the process repeated.

Comparisons were then made between this mathematical model and results from wall segment tests. Both the bilinear and nonlinear solutions were compared with seven test segments involving combinations of pure axial loads, and one test segment subject to axial loads and a moment.

The model was then applied to predict the nonlinear response of wall segments from a containment vessel test structure. Using the results of the BOSOR5 computer program, the initial axial force to moment ratios and the initial axial force to curvature ratios were determined. It was then assumed that either of these relations would remain constant during the entire loading sequence. These assumptions formed the basis of the N-M and N-ϕ analyses of Chapter 6. The results from these simplified analyses were then compared with those from a nonlinear BOSOR5 analysis of the entire structure.

7.2 Conclusions

The mathematical model, complete with the nonlinear biaxial concrete constitutive relation, which has been presented in this report to analyse reinforced and prestressed wall segments will predict with

acceptable accuracy the response of a prestressed wall segment to biaxial membrane forces, biaxial moments, or both. The predicted response of reinforced wall segments, as opposed to prestressed wall segments is not close to the test results. However these discrepancies may be the result of a conflict between the method of loading and the assumptions of the segment loading analysis. More importantly, it is probable that there are shrinkage cracks and stresses in the reinforced segments which were not present in the prestressed segments.

The wall segment model used with the bilinear elastic, tension cut-off concrete constitutive relation provides results which may or may not be accurate up to the cracking load, and which underestimate the post cracking stiffness of the wall segment in all cases.

The models were not verified in the compressive failure zones and no conclusions can be drawn as to their performance under compressive loading.

Although the wall segment analyses labelled N-M and N-ϕ bracket the results obtained from a nonlinear finite element program on an interaction diagram, neither analysis provides good agreement for all segments which might be extracted from the structure. For the wall segments unhindered by boundary elements, the N-ϕ analysis generates the best results. For the segments closer to the boundary elements, the N-M analysis provides better results. In all cases, the N-M analysis provides an underestimate of the maximum strength.

LIST OF REFERENCES

1. American Concrete Institute (1971). Building Code Requirements for Reinforced Concrete. American Concrete Institute ACI 318-71.

2. Argyris, J.H. (1973). Recent Developments in the Finite Element Analysis of Prestressed Concrete Reactor Vessels. ISD Report No. 151, University of Stuttgart.

3. Basur, F.K. and Darwin, D. (1978). Nonlinear Biaxial Law for Concrete. Journal of the Structural Division, ASCE, Vol. 104, No. ST1.

4. Bazant, Z.P. and Bhat, P.D. (1976). Endochronic Theory of Inelasticity and Failure of Concrete. Journal of the Engineering Mechanics Division, ASCE, Vol. 102, No. EM4.

5. Bushnell, D. (1974). BOSOR5 A Computer Program for Buckling of Elastic Plastic Complex Shells of Revolution Including Large Deflections and Creep. Published by Lockheed Missiles and Space Company.

6. Chen, A.C.T. and Chen, W-F. (1975). Constitutive Relations for Concrete. Journal of the Engineering Mechanics Division, ASCE Vol. 101, No. EM4.

7. Cohen, A.M., Cutts, J.F., Fielder, R., Jones, D.E., Ribbans, J. and Stuart, E. (1973). Numerical Analysis. Wiley and Sons, New York.

8. Comite Europeen du Beton (1969). (C.E.B.). Recommandations Internationales Pour le Calcul et l'Execution des Ouvrages en Beton. Commission "Recommandations Internationales", Paris.

9. Darwin, D. and Pecknold, D. (1974). Inelastic Model for Cyclic Loading of Plane Reinforced Concrete Structures. Structural Research Series No. 409, University of Illinois.

10. Darwin, D. and Pecknold, D. (1977a). Analysis of Cyclic Loading of Plane Reinforced Concrete Structures. Computers and Structures, Vol. 7, Pergammon Press.

11. Darwin, D. and Pecknold, D. (1977b). Nonlinear Biaxial Law for Concrete. Journal of the Engineering Mechanics Division, ASCE, Vol. 103, No. EM4.

12. Elwi, A. and Murray, D. (1979). A 3D Hypoelastic Concrete Constitutive Relationship. Will appear in the Journal of the Engineering Mechanics Division, ASCE, Vol. 105, No. EM4

13. Epstein, M. and Murray, D.W. (1976). An Elastic Stress Analysis of a Gentilly Type Containment Structure. Vol. 1, Structural Engineering Report No. 55, Department of Civil Engineering, University of Alberta.

14. Evans, R.H. and Morathe, M.S. (1968). Microcracking and Stress-Strain Curves for Concrete in Tension. Materials and Structures, Vol. 1, No. 1.

15. Fung, Y.C. (1965). Foundations of Solid Mechanics. Prentice-Hall, New Jersey.

16. Hognestad, E., Hanson, N.W. and McHerney, D. (1955). Concrete Stress Distribution in Ultimate Strength Design. ACI Journal Proceedings, Vol. 52, No. 12.

17 Hughes, B.P. and Chapman, B.P. (1966). The Complete Stress-Strain Curve for Concrete in Direction Tension. RILEM Bulletin No. 30.

18. Kupfer, H.B. (1973). Das Verhalten des Betons unter mehrachsiger Kurzzeitbelastung unter besonderer Berucksichtigung der Zweiachsigen Beanspruchung. Deutscher Ausschuss Fur Stahlbeton, Heff 229.

19. Kupfer, H.B. and Gerstle, K.H. (1973). Behavior of Concrete Under Biaxial Stresses. Journal of the Engineering Mechanics Division, ASCE, Vol. 99, No. EM4

20. Kupfer, H.B., Hilsdorf, H.K. and Rusch, H. (1969). Behavior of Concrete Under Biaxial Stresses. ACI Journal, No. 8, Vol. 66.

21. Lin, C.S. and Scordelis, A.C. (1975). Nonlinear Analysis of Reinforced Concrete Shells of General Form. Journal of the Structural Division, ASCE, Vol. 101, No. ST3.

22. Liu, T.C.Y., Nilson, A.H. and Slate, F.O. (1972). Biaxial Stress-Strain Relations for Concrete. Journal of the Structural Division, ASCE, Vol. 98, No. ST5.

23. Murray, D.W. (1979). A review of Explosive Characteristics of Secondary Containments Near Ultimate Load. Nuclear Engineering and Design, Vol. 52.

24. Murray, D.W., Chitnuyanondh, L., Wong, C. and Rijub-Agha, K.Y. (1978). Inelastic Analysis of Prestressed Concrete Secondary Containments. Structural Engineering Report No. 67, Department of Civil Engineering, University of Alberta.

25. Rizkalla, S., Chitnuyanondh, L., Murray, D.W. and MacGregor, J.G. (1979). An Effective Uniaxial Tensile Stress-Strain Relationship for Prestressed Concrete. Technical Report to the Atomic Energy Control Board, University of Alberta.

26. Romstad, K.M., Taylor, M.A. and Horrmann, L.R. (1974). Numerical Biaxial Characterization for Concrete. Journal of the Engineering Mechanics Division, ASCE, Vol. 100, No. EMS.

27. Saenz, I.P. (1964). Discussion of "Equation for the Stress-Strain Curve of Concrete" by Desayi, P. and Krishnan, S. ACI Journal, Proceedings, Vol. 61, No. 9.

28. Scanlon A. and Murray, D.W. (1972). Time Dependent Deflections of Reinforced Concrete Slabs. Ph.D. Thesis, Department of Civil Engineering, University of Alberta.

29. Schnobrich, W.C. (1977). Behavior of Reinforced Concrete Structures Predicted by the Finite Element Method. Computers and Structures, Vol. 7, Pergammom Press.

30. Simmonds, S.H., Rizkalla, S. and MacGregor, J.G. (1979). Test to Failure of a Prestressed Concrete Containment Structure. Part of the Atomic Energy of Canada Board Study, to be published as a Structural Engineering Report, Department of Civil Engineering, University of Alberta.

31. Whitney, C.S. (1943). Discussion of "The Plasticity Ratio of Concrete and Its Effect on the Ultimate Strength of Beams", by Jensen, V.P. ACI Journal, Supplement Proceedings, Vol. 39, No. 11.

APPENDIX A

COWSAC USER'S MANUAL

A.1 Program Objectives

This program is designed to predict the biaxial response of an arbitrarily prestressed and steel reinforced concrete wall segment of any dimension, in a plane stress condition, including out-of-plane curvatures with respect to creep, temperature and live loads. Given a force or moment on any face orthogonal to the principal radii of curvature, the program will find the resulting strains and curvatures, or vice versa. Thus, inputting any combination of forces and/or displacements on the two faces of the segment will result in the solution of the unknown displacements and/or forces.

A.2 Input Deck

Input is to be read from unit 5 and shall conform to the description given below. With the MTS system, data can be free-format with commas separating entries, or shall follow the specific format given. All input quantities should be in consistant units.

A.2.1 Data Deck Description

NUMBER OF CARDS (or lines)	FORMAT	VARIABLES
1	20A4	TITLE
1	I3, 5F10.4	NLAYER, T, WIDTH, HEIGHT, R1, R2
1	I3, 2E12.5	NREBAR, ER, FYR
NREBAR	I3, 2F10.4	NRD(I), AREAR(I), RCEN(I)

NUMBER OF CARDS	FORMAT	VARIABLES
1	I5, 4E12.7	NFLAGD, ALOADD(1), ALOADD(2), ALOADD(3), ALOADD(4)
1	I3, 2E10.5, 4I3, F10.5	NPRE, EP, FYP, KP, NPSTEP, KDO, NCRP, FCRP
NPRE	I3, 3F10.4, I3	NPD(J), AREAP(J), PCEN(J), PFORCE(J), NPN(J)
NPSTEP	I5, 4E12.7	NFLAGL(I), ALOADL(I,1), ALOAD(I,2) ALOAD(I,3), ALOAD(I,4)
1	5I4	NLOADS, NJUMPX, NPDO, NTHERM, NEPSTE
1, if NTHERM ≠ 0	5E12.5, I4	T1, T2, T3, ALPHAC, ALPHAS, NTCODE
1	I5, 4E12.5, I5	NFLAG(I), ALOAD(I,1), ALOAD(I,2), ALOAD(I,3), ALOAD(I,4), NINC(I)
the next two cards are to be repeated NLOAD - 1 times		
1	I4	NJUMPX
1	I5, 4E12.5, I5	NFLAG(I), ALOAD(I,1), ALOAD(I,2), ALOAD(I,3), ALOAD(I,4), NINC(I)
the last card shall always be		
1	4F10.4, 2I5, 2E12.7	FC, FTC, POISS, CEMOD, NTYPE, NSUB, EIO, EIOT

A.2.2 Explanation of Variables

1. TITLE — any alphanumeric string of 80 or less characters.
2. NLAYER — number of concrete layers into which the wall segment thickness is to be subdivided.
3. T — wall segment thickness.
4. WIDTH — dimension of wall segment parallel to direction 2.
5. HEIGHT — dimension of wall segment parallel to direction 1 .

6.	R1	radius curvature of wall about a line parallel to direction 1. If no curvature is desired (i.e. a flat wall) give R1 a negative value.
7.	R2	radius curvature of wall about a line parallel to direction 2. If no curvature is desired give R2 a negative value.
8.	NREBAR	total number of reinforcing steel layers.
9.	ER	elastic modulus of reinforcing steel. If NREBAR equals 0, ER and EYR may be omitted.
10.	FYR	yield stress of reinforcing steel.
11.	NRD(I)	either 1 or 2; specifies the direction parallel to the steel bars, for layer I.
12.	AREAR(I)	the total area of steel bars in layer I.
13.	RCEN(I)	the distance from the centre line of the concrete wall to the middle of the steel layer, a positive distance measured moving away from the centre of curvature.
14.	NFLAGD	load code for dead load (see Section A.2.2 entitled Load Codes). To NFLAGD only, add 1000.
15.	ALOADD(J)	the 4 dead load forces or strains to be put on the wall segment. The loads shall be forces or strains as specified by NFLAGD.
16.	NPRE	the number of prestressing layers.
17.	EP	elastic modulus of the prestressing strands.
18.	FYP	the ultimate strength of the prestressing strands. From this and EP, a stress-strain curve for the strands is calculated.
19.	KP	either zero (0) or one (1). If KP = 0, then the input prestressing force is before elastic response. If KP = 1, then the input prestressing force is after elastic response.
20.	NPSTEP	the number of steps required to apply prestressing. If five tendons are released individually, not simultaneously, then there would be five prestressing steps.
21.	KDO	if KDO = 999, do not apply prestress.

22. NCRP — if NCRP is not equal to zero, then apply creep under constant load after prestressing steps are complete.

23. FCRP — creep factor FCRP = $E_{\text{long term}} / E_{\text{short term}}$.

24. NPD(J) — either 1 or 2; specifies the direction which the prestressing strands parallel, for layer J.

25. AREAP(J) — the total area of prestressing strands in layer J.

26. PCEN(J) — the distance from the centre line of the concrete wall to the middle of the strand layer, positive away from the centre of curvature.

27. PFORCE(J) — prestressing force applied to layer J consistent with the value of KP above.

28. NPN(J) — the position in the prestressing sequence in which prestressing is applied to the layer J, i.e. if NPN(J) is 4, then the prestressing force is applied to this layer in the fourth step out of NPSTEP steps.

29. NFLAGL(I) — load code for prestressing loads ALOAD(I,J).

30. ALOADL(I,J) — the load vector to which the segment is subject after each prestress step I.

31. NLOADS — the number of live loads.

32. NJUMPX — the number of increments into which the following live load is to be divided.

33. NPDO — if NPDO is set equal to 0, then a summary of the stresses in each layer is output after each load increment.

34. NTHERM — if set equal to 1, 2, or 3, then thermal loads are applied to the segment before the live loads. The temperature distribution can be one of three:

NTHERM = 1, $\Delta T = T1 + T2 \cdot Z + T3 \cdot Z^2$

NTHERM = 2, $\Delta T = T1 + T2 \cdot Z^{T3}$

NTHERM = 3, $\Delta T = T1 + T2 \cdot e^{Z \cdot T3}$

For these equations only, the distance coordinate Z is defined as zero on the inside surface, positive moving towards the outside.

35.	NEPSTE	if NEPSTE = 1, then a ratio of axial force to moment should be input where curvatures are expected in the load vector. The curvature for a unit applied moment is calculated, and the force-moment ratio is converted to a force-curvature ratio. From this ratio an applied curvature for a given force is calculated and the load vector of axial forces and curvatures is constructed.
36. to 38.	T1, T2, T3	thermal load constants applicable in the equations above. The entire card containing T1 through NTCDDE must be omitted if thermal loads are not desired.
39.	ALPHAC	thermal coefficient of expansion for concrete.
40.	ALPHAS	thermal coefficient of expansion for steel.
41.	NTCODE	load code for thermal loads.
42.	NFLAG(I)	load code for live loads.
43.	ALOAD(I,J)	the four loads, (J = 1,4) which shall be the target live load, subdivided into NJUMPX increments.
44.	NINC(I)	NINC(I) = 0 ALOAD(I,J) is the target load to be reached NINC(I) = 1 add this load to the previous target load to get the new target load.
45.	NJUMPX	the number of increments into which the next load step is to be subdivided.
46.	FC	ultimate uniaxial compressive strength of concrete, entered as a positive number.
47.	FTC	ultimate uniaxial tensile strength of concrete, entered as a positive number.
48.	POISS	initial Poisson's ratio.
49.	CEMOD	initial uniaxial elastic modulus.
50.	NTYPE	concrete constitutive relation NTYPE = 1 - linear uniaxial concrete model NTYPE = 3 - nonlinear biaxial concrete model.

51.	NSUB	the number of subincrements within each load increment; if NSUB = -25, then the program will automatically choose the correct number of sub-increments.
52.	EIO	the strain at the maximum stress in uniaxial compression, a negative number. If a positive value is specified, the program will calculate a value for this variable. However, to use this and the following default, the units of input quantities must be pounds or inches.
53.	EIOT	the strain at maximum uniaxial tension, a positive number. If a negative number is specified, the program will calculate a value for this variable.

A.2.3 Load Codes

This section deals with specifying the type of loads to be applied, either as forces or strains. Load codes are used to specify dead loads, prestress loads, thermal loads and live loads and the specific variables are NFLAGD, NFLAGL, NTCODE and NFLAG respectively.

There are four degrees of freedom for this element. These degrees of freedom are shown in Fig. 1.1. When a load is to be applied to the wall segment, either a force or axial strain must be specified for degree-of-freedom Nos. 1 and 3, and either a moment or curvature must be specified for degree-of-freedom Nos. 2 and 4. There are no restrictions for example, that if DOF No. 1 has a force specified then DOF No. 3 must have a force specified. Each DOF is independent as to the type of load (force or strain) which is specified. Since each DOF can be loaded in either of two ways, there are a total of 16 combinations of forces and strains in which a load vector can be specified.

To identify the load combination, that is desired, a load code is used. The load code is a four digit number of ones and zeros with each digit corresponding in order to:

1. the normal force or strain on face 1
2. the out-of-plane moment or curvature on face 1
3. the normal force or strain on face 2
4. the out-of-plane moment or curvature on face 2

In this load code, a 0 designates a strain or curvature and a 1 designates a force or moment.)

For example, if it was desired to subject the wall segment to an axial force and moment on face 1 and an axial force and moment on face 2, the load vector could be described as

$$< N_1 \quad M_1 \quad N_2 \quad M_2 >$$

and the corresponding load code would be 1111. If the wall segment was subjected to an axial force and a curvature on face 1, and an axial strain and moment on face 2, the load vector would be

$$< N_1 \quad \phi_1 \quad \varepsilon_2^{ms} \quad M_2 >$$

and the corresponding load code would be 1001.

A.2.4 Sign Convention

(a) positive forces are tensile

(b) positive moments cause tension on the inside of the element (closest to centres of curvature)

(c) distances to concrete and steel layers (Z) are measured from the centre line along the wall thickness of the concrete. Positive displacements are measured from this centre line away from the centres of cur-

vature (towards the outside of the wall).

A.3 Output

Program output is read to units 6 and 7. Unit 6 output begins with an echo check of the input data. This is followed by the results of each load increment. These results are comprised of the specified load, the stresses and strains in each layer, a damage summary of the three layers and the overall results of the specified load.

Output on unit 7 is used mainly for program debugging. For each load increment, the specified load is first printed. Then after the successful computation of each load subincrement, the values of the real strains, stresses, equivalent uniaxial strains, elastic moduli, ultimate stresses and strains at ultimate stresses are printed for each concrete layer. This is followed by the number of iterations used to find this solution. If after 30 iterations no solution is found, some additional data is output, including the trial real strains, the error in forces and moments, the total forces, the trial real strain corrections and the reduction factor applied to the strain corrections. If after 121 iterations no solution is found, then the program is terminated. After all load subincrements are completed, the solution for the load increment is output.

All output solutions will be in terms of units consistent with those input.

APPENDIX B

LISTING OF COWSAC

The author and the University of Alberta will not be responsible for misuse of the following program or for errors in its listing.

```
      IMPLICIT REAL*8(A-H,P-Z)
      COMMON/ALPHA/WV(4),P1(4),P2(4),N1,LAM
      COMMON/BRN/B1,B2,FC,FTC,CEMOD,POISS,NTYPE,NSTYPE,
     1WIDTH,HEIGHT
      COMMON/LOTUS/QP(4),C(4,4),CC(4,4),DQP(4),DSQ(4),DQ(4)
      COMMON/DINO/CLAYER(30,100),T,NLAYER
      COMMON/UBACCO/SLAYER(30,10),FYR,ER,RCEN(10),APEAR
     1(10),NPEBAR,NRD(10)
      COMMON/JARAMA/PLAYER(30,10),FYP,EP,PCEN(10),ABEAP(10)
     1,PFORCE(10),NPN(10),NPRE,NPD(10)
      COMMON/TURBO/ALOAD(100,4),NFLAG(100),TITLE(20),
     1NINC(100)
      COMMON/ESPADA/GUE(4),PREV(4),PREV1(4)
      COMMON/BBOXER/NLOADS,NJUMP(10),NLOADT
      COMMON/E26/E11,E22,S11,S22,SLOP11,SLOP12,SLOP21,SLOP22
      COMMON/BORA/NDO,NPDO,KP,NCRP,PCRP
      COMMON/ETYPE/NPI(10),NPASS,JLP,KPT
      COMMON/ASTORN/ALOADD(4),ALOADL(5,4),NFLAGD,NFLAGL(5),
     1NPSTEP
      COMMON/CS3PT0/T1,T2,T3,ALPHAC,ALPHAS,NTHERM,NTCODE
      COMMON/TYPE35/PERR1(4),PERR2(4)
      COMMON/BAYARI/YU,PE11,PE22,PS11,PS22,E1U,E2U,EIO,EIOT
      COMMON/MUIRA/E1T,E2T,E10C,E2UC,STG1C,STG2C
      COMMON/SL280/TS11,TS22,TSLO11,TSLO22,NSUB
      COMMON/WOLPN5/AXS1,AXS2,NWORK
      DIMENSION AL(4),AL2(4)
C
      CALL TIME(0,0)
      CALL INOUT
C
      NWORK=0
      DO 10 J=1,NLAYER
      DO 10 I=1,30
      CLAYER(I,J)=0.D0
   10 CONTINUE
      DO 20 J=1,10
      DO 20 I=1,30
      SLAYER(I,J)=0.D0
      PLAYER(I,J)=0.D0
   20 CONTINUE
   30 CONTINUE
      DO 40 I=1,4
      PREV(I)=0.D0
      PREV1(I)=0.D0
   40 CONTINUE
      IF(NPEBAR.LT.1) GO TO 50
      CALL PLACES(NPEBAR,NRD,RCEN,ABEAR,SLAYER)
   50 IF(NPRE.LT.1) GO TO 60
      CALL PLACES(NPRE,NPD,PCEN,ABEAP,PLAYER)
   60 CALL PLACON
      IF(B1.LT.0.D0)B1=1.D10
      IF(B2.LT.0.D0)B2=1.D10
   70 IF(NTYPE.EQ.3) GO TO 140
      IF(EIOT.GT.0.D0) GO TO 80
      EIOT=FTC/CEMOD
   80 IF(EIO.LT.0.D0) GO TO 90
      FCP=DABS(FC*1000.D0)
      EIO=-1.D0*(FCP**.25D0)*(31.5D0-FCP**.25D0)/100000.D0
   90 DIV=CEMOD/(1.D0-POISS*POISS)
      DO 100 K=1,NLAYER
      CLAYER(20,K)=DIV
      CLAYER(21,K)=DIV
      CLAYER(27,K)=POISS
  100 CONTINUE
      AXS1=CEMOD*T*WIDTH
      AXS2=CEMOD*T*HEIGHT
      IF(NREBAR.LT.1) GO TO 120
      DO 110 K=1,NPEBAR
      SLAYER(20,K)=DIV
      SLAYER(21,K)=DIV
      SLAYER(27,K)=POISS
  110 CONTINUE
  120 IF(NPRE.LT.1) GO TO 140
      DO 130 K=1,NPRE
      PLAYER(20,K)=DIV
      PLAYER(21,K)=DIV
      PLAYER(27,K)=POISS
  130 CONTINUE
C
C     DEAD LOAD APPLICATION
C
  140 N1=NFLAGD
      IF(N1.EQ.0) GO TO 190
      N1=N1-1000
      CALL GUESS
      ND=1
      DO 150 J=1,4
      P1(J)=ALOADD(J)
  150 CONTINUE
      DO 160 J=1,4
      GUP(J)=0.D0
  160 CONTINUE
      CALL GUESS
      NDD=1
      CALL LODOUT(I,NDD)
      NPASS=0
      JLP=0
      CALL WORK
      IF(NPDO.EQ.1) GO TO 170
      CALL OUT
  170 CALL RECAP
      DO 180 I125=1,4
      P1(I125)=QP(I125)
      PREV(I125)=P2(I125)
  180 CONTINUE
      CALL FINOUT(I,NDD)
      NDD=0
C
```

```
C       PRESTRESS APPLICATION
C
 190 IF(NPRE.EQ.0) GO TO 250
     IF(KDO.EQ.999) GO TO 250
     KPT=1
     CALL PRZST
     KPT=0
     NPASS=1
     IF(NCRP.EQ.0) GO TO 200
     CALL CREEP
 200 IF(NTHERM.LT.1) GO TO 220
     CALL TEMP
     DO 210 I165=1,4
     GUE(I165)=F2(I165)
 210 CONTINUE
 220 DO 230 J=1,4
     PERM1(J)=F1(J)
     PERM2(J)=F2(J)
 230 CONTINUE
     DO 240 I85=1,4
     PREV(I85)=F2(I85)
 240 CONTINUE
 250 CONTINUE
C
C       LIVE LOAD APPLICATION
C
     I99=0
     DO 460 KIJ=1,NLOADS
     I99=I99+NJUMP(KIJ)
     XJUMP=FLOAT(NJUMP(KIJ))
     N1=NFLAG(I99)
     CALL GUES
     DO 270 J=1,4
     IF(NV(J).EQ.0) GO TO 260
     AL(J)=F1(J)
     GO TO 270
 260 AL(J)=F2(J)
 270 CONTINUE
     IF(NINC(I99).EQ.0) GO TO 290
     DO 280 J=1,4
     AL2(J)=0.D0
 280 CONTINUE
     GO TO 310
 290 DO 300 J=1,4
     AL2(J)=AL(J)
 300 CONTINUE
 310 J10=I99+1-NJUMP(KIJ)
     J11=I99-1
     X1=1.D0
     DO 330 J=J10,I99
     DO 320 JJ=1,4
     NFLAG(J)=NFLAG(I99)
 320 ALOAD(J,JJ)=X1*(ALOAD(I99,JJ)-AL2(JJ))/XJUMP
    1+AL(JJ)
 330 X1=X1+1.D0
 340 CONTINUE
     DO 450 I=J10,I99
     DO 350 JJ=1,4
     F1(JJ)=ALOAD(I,JJ)
 350 CONTINUE
     IF(I.GT.1) GO TO 370
     IF(ND.EQ.1) GO TO 370
     IF(NPRE.GT.0) GO TO 370
     DO 360 III=1,4
     GUE(III)=0.D0
 360 CONTINUE
     GO TO 390
 370 DO 380 I1=1,4
     GUE(I1)=F2(I1)
 380 CONTINUE
 390 CALL GUESS
     CALL LODOUT(I,NDD)
     CALL WORK
     IF(NPDO.EQ.1) GO TO 400
     CALL OUT
 400 CALL RECAP
     DO 410 I32=1,4
     F1(I32)=QP(I32)
 410 CONTINUE
     IF(NTHERM.NE.-1) GO TO 440
     ALOAD(I,3)=F2(3)
     I1000=I+1
     I1001=I-1
     ALOAD(I1000,3)=2.D0*F2(3)-ALOAD(I1001,3)
     WRITE(7,430)
     WRITE(7,420)F2(1),F2(3),PS11,PS22,E10,E20,SLOP11,
    1SLOP22,VU
 420 FORMAT(1X,E12.5,1X,E12.5,1X,F6.3,1X,F6.3,1X,E12.5,1X,
    1F12.5,       1X,F6.1,1X,F6.1,1X,F5.3)
 430 FORMAT(8X,'F2(1)',8X,'F2(3)',3X,'PS11',3X,'PS22',10X,
    1'E10',       10X,'E20',1X,'SLOP11',1X,'SLOP22',4X,
    2'VU')
 440 CALL PINOUT(I,NDD)
 450 CONTINUE
 460 CONTINUE
     WRITE(6,470)
 470 FORMAT(20X,///,'*** END OF PROBLEM ***')
 480 CALL TIME(3,3)
     STOP
     END
C
C
C
     SUBROUTINE INOUT
     IMPLICIT REAL*8(A-H,P-Z)
     COMMON/TURBO/ALOAD(100,4),NFLAG(100),TITLE(20),
    1NINC(100)
     COMMON/BAR/B1,B2,FC,FTC,CENOD,POISS,NTIPE,NSTIPE,
```

```
     1WIDTH,HEIGHT
      COMMON/DINO/CLAYER(30,100),T,NLAYER
      COMMON/URACCO/SLAYER(30,10),FYR,ER,PCEN(10),AREAP
     1(10),NPEBAR,NRD(10)
      COMMON/JARAMA/PLAYER(30,10),FYP,EP,PCEN(10),AREAP(10)
     1,PFORCE(10),NPN(10),NPRE,NPD(10)
      COMMON/BROXER/NLOADS,NJUMP(10),NLOADT
      COMMON/BOPA/KDO,NPDO,KP,NCRP,FCRP
      COMMON/ASTOKR/ALOADD(4),ALOADL(5,4),NFLAGD,NFLAGL(5),
     1NEPSTEP
      COMMON/CS3P30/T1,T2,T3,ALPHAC,ALPHAS,NTHERM,NTCODE
      COMMON/SL280/TS11,TS22,TSL011,TSL022,NSUB
      COMMON/BAVARI/WU,PE11,PE22,PS11,PS22,E1U,E2U,EIO,EIOT
      COMMON/MUIRA/E1T,E2T,E1UC,E2UC,SIG1C,SIG2C
C
C
      READ(5,10)TITLE
      READ(5,100)NLAYER,T,WIDTH,HEIGHT,R1,R2
      READ(5,170)NPEBAR,ER,FYR
      IF(NPEBAR.LT.1) GO TO 20
      DO 10 I=1,NPEBAR
      READ(5,120)NRD(I),AREAR(I),RCEN(I)
   10 CONTINUE
   20 READ(5,140)NFLAGD,(ALOADD(J),J=1,4)
      READ(5,110)NPRE,EP,FYP,KP,NPSTEP,KDO,NCRP,FCRP
      IF(NPRE.LT.1) GO TO 50
      DO 30 J=1,NPRE
      READ(5,120)NPD(J),AREAP(J),PCEN(J),PFORCE(J),NPN(J)
   30 CONTINUE
      IF(NPSTEP.EQ.0) GO TO 50
      DO 40 I=1,NPSTEP
      READ(5,140)NFLAGL(I),(ALOADL(I,J),J=1,4)
   40 CONTINUE
   50 READ(5,130)NLOADS,NJUMPX,NPDO,NTHERM,NEPSTE
      IF(NTHERM.EQ.-1) GO TO 60
      IF(NTHERM.LT.1) GO TO 70
   60 READ(5,160)T1,T2,T3,ALPHAC,ALPHAS,NTCODE
   70 I=0
      DO 80 KIJ=1,NLOADS
      NJUMP(KIJ)=NJUMPX
      I=I+NJUMP(KIJ)
      READ(5,160)NFLAG(I),(ALOAD(I,J),J=1,4),NINC(I)
      IF(KIJ.EQ.NLOADS) GO TO 90
      READ(5,190) NJUMPX
   80 CONTINUE
      NLOADT=I
      READ(5,150)FC,FTC,POISS,CEMOD,NTYPE,NSUB,EIO,EIOT
   90 FORMAT(20A4)
  100 FORMAT(I3,5F10.4)
  110 FORMAT(I3,2E10.5,4I3,F10.5)
  120 FORMAT(I3,3F10.4,I3)
  130 FORMAT(5I4)
  140 FORMAT(I5,4E12.7)
  150 FORMAT(4F10.4,2I5,2E12.7)
  160 FORMAT(I5,4E12.5,I5)
  170 FORMAT(I3,2E12.5)
  180 FORMAT(5E12.5,I4)
  190 FORMAT(I4)
C
C     ..........ECHO CHECK OF INPUT DATA..........
C
      WRITE(6,340)TITLE
      WRITE(6,350)NLAYER,T,WIDTH,HEIGHT,R1,R2
      IF(NPEBAR.LT.1) GO TO 210
      WRITE(6,360)NPEBAR,ER,FYR
      DO 200 I=1,NPEBAR
      WRITE(6,370)NRD(I),AREAR(I),RCEN(I)
  200 CONTINUE
      WRITE(6,430)
      WRITE(6,530)NFLAGD,(ALOADD(J),J=1,4)
  210 IF(NPRE.LT.1) GO TO 240
      WRITE(6,380)NPRE,EP,FYP,KP
      DO 220 J=1,NPRE
      WRITE(6,390)NPD(J),AREAP(J),PCEN(J),PFORCE(J),NPN(J)
  220 CONTINUE
      IF(NPSTEP.EQ.0) GO TO 240
      WRITE(6,440)
      DO 230 I=1,NPSTEP
      WRITE(6,450)NFLAGL(I),(ALOADL(I,J),J=1,4),I
  230 CONTINUE
  240 IF(NCRP.LT.1) GO TO 250
      WRITE(6,460)FCRP
  250 IF(NTHERM.LT.1) GO TO 300
      WRITE(6,470)
      GO TO (260,270,280),NTHERM
  260 WRITE(6,480)
      GO TO 290
  270 WRITE(6,490)
      GO TO 290
  280 WRITE(6,500)
  290 WRITE(6,510)T1,T2,T3,ALPHAC,ALPHAS,NTCODE
  300 IF(NEPSTE.EQ.0) GO TO 320
      WRITE(6,520)
      I=0
      DO 310 KIJ=1,NLOADS
      I=I+NJUMP(KIJ)
      WRITE(6,410)NJUMP(KIJ),NFLAG(I),(ALOAD(I,J),J=1,4),
     1NINC(I)
  310 CONTINUE
      CALL CURVE
  320 WRITE(6,400)NLOADS
      I=0
      DO 330 KIJ=1,NLOADS
      I=I+NJUMP(KIJ)
      WRITE(6,410)NJUMP(KIJ),NFLAG(I),(ALOAD(I,J),J=1,4),
     1NINC(I)
  330 CONTINUE
      WRITE(6,420)FC,FTC,POISS,CEMOD,NTYPE,NSUB,EIO,EIOT
```

```
340 FORMAT('1',5X,20A4)
350 FORMAT(//10X,'THE NUMBER OF LAYERS IS',I5,/10X,
   1'THE THICKNESS IS',8X,F10.5,/10X,'WIDTH = ',F10.5,5X,
   2'HEIGHT = ',F10.5,5X,'RADIUS 1 =',F10.5,5X,
   3'RADIUS 2 = ',F10.5)
360 FORMAT(///10X,'.....REINFORCING STEEL.....',//,11X,
   1'NO. OF LAYERS = ',2X,I4,/10X,' ELASTIC MODULUS = ',
   2E12.7,/10X,' YIELD POINT = ',3X,F10.5//10X,
   3'DIRECTION',10X,'  AREA  ',10X,'LOCATION')
370 FORMAT(10X,I5,10X,F10.5,10X,F10.5)
380 FORMAT(///10X,'.....PRESTRESSING STEEL.....',//,10X,
   1'NO. OF LAYERS   = ',I4,/10X,'ELASTIC MODULUS = ',
   2E12.7,/10X,'YIELD POINT     =  ',F10.5/10X,
   3'PRESTRESS CODE  = ',I4 //10X,'DIRECTION',10X,
   4'  AREA ',10X,'LOCATION',5X,'PRESTRESSING FORCE ',5X,
   5'PRESTRESSING ORDER')
390 FORMAT(10X,I5,10X,F10.5,10X,F10.5,10X,F10.5,10X,I3)
400 FORMAT(///10X,'NO. OF LOADS = ',I5,//5X,'LOAD NUMBER',
   15X,'LOAD CODE',7X,'N1',13X,'S1',13X,'N2',13X,'S2',
   28X,'LOAD TYPE')
410 FORMAT(8X,I5,10X,I5,4(3X,E12.5),8X,I5)
420 FORMAT(///10X,'.....CONCRETE.....'//10X,
   1'UNIAXIAL COMPRESSIVE STRENGTH '
   2,5X,F10.5/10X,'UNIAXIAL TENSILE STRENGTH ',9X,
   3F10.5/10X,    'POISSON S RATIO ',19X,F10.5/10X,
   4'ELASTIC MODULUS',20X,F10.5/10X,
   5'BIAXIAL CONCRETE MODEL '
   6,12X,I5, /10X,'NUMBER OF SUBINCREMENTS',12X,I5,
   7/10X,'STRAIN @ MAX.STRESS IN UNIAX.COMPR.',E12.5,
   8/10X,'STRAIN @MAX. STRESS IN UNIAX.TENSION',E12.5)
430 FORMAT(///10X,'*** DEAD LOAD ***'//,8X,'LOAD CODE',7X,
   1'N1',13X,  'S1',13X,'N2',13X,'S2')
440 FORMAT(///10X,'*** TARGET LOAD AFTER PRESTRESSING ***'
   1,          //8X,'LOAD CODE',7X,'N1',13X,'S1',13X,
   2'N2',13X,'S2',                  5X,'PRESTRESS STEP')
450 FORMAT(10X,I5,4(3X,E12.5),I5)
460 FORMAT(//10X,'CREEP FACTOR= ',F10.5)
470 FORMAT(//10X,'***THERMAL EFFECTS***')
480 FORMAT(/15X,'LINEAR DISTRIBUTION OF THERMAL STRAINS')
490 FORMAT(/15X,
   1'QUADRATIC DISTRIBUTION OF THERMAL STRAINS')
500 FORMAT(/15X,
   1'EXPONENTIAL DISTRIBUTION OF THERMAL STRAINS')
510 FORMAT(/10X,'CONSTANT T1=',E12.5,
   1/10X,'CONSTANT T2=',E12.5,
   2/10X,'CONSTANT T3=',E12.5,
   3/10X,'COEFFICIENT OF THERMAL EXPANSION - CONCRETE =',
   4E12.5,/10X,
5'COEFFICIENT OF THERMAL EXPANSION - STEEL    ='
   6,E12.5,/10X,'THERMAL LOAD CODE =',I4)
520 FORMAT(/5X,'---H.EPSTEIN TYPE LOADING---',
   1/8X,'LOAD CODE',7X,'N1',12X,'*1/N1',11X,'N2',12X,
   2'F2/N2',8X,     'LOAD TYPE')
530 FORMAT(10X,I5,4(3X,E12.5),8X,I5)
      RETURN
      END
C
      SUBROUTINE WORK
      IMPLICIT REAL*8(A-H,P-Z)
      COMMON/ALPHA/NV(4),P1(4),P2(4),N1,LAM
      COMMON/BMW/R1,R2,PC,PTC,CEMOD,POISS,NTYPI,NSTYPE,
     1WIDTH,HEIGHT
      COMMON/LOTUS/QP(4),C(4,4),CC(4,4),DQP(4),DSO(4),DQ(4)
      COMMON/DINO/CLAYER(30,100),T,NLAYER
      COMMON/URACCO/SLAYEP(30,10),FYR,ER,RCEN(10),AREAR
     1(10),NREBAR,NRD(10)
      COMMON/JARAMA/PLAYER(30,10),FYP,EP,PCEN(10),AREAP(10)
     1,PFORCE(10),NPW(10),NPRE,NPD(10)
      COMMON/ESPADA/GUE(4),PREV(4),PREV1(4)
      COMMON/E26/E11,E22,S11,S22,SLOP11,SLOP12,SLOP21,SLOP22
      COMMON/STYPE/NPI(10),NPASS,JLP,KPT
      COMMON/BAVARI/VU,PE11,PE22,PS11,PS22,E11,E22U,EIO,EIOT
      COMMON/MUIRA/E1T,E2T,E1UC,E2UC,SIG1C,SI
      COMMON/SL280/TS11,TS22,TSLO11,TSLO22,NS
      COMMON/CS3PTO/T1,T2,T3,ALPHAC,ALPHAS,NTEMM,NTCODE
      COMMON/WOLFW5/AXS1,AXS2,NWORK
      DIMENSION PREV3(4),SUBI(4),ERR2(4),DPLP(4),DP1(4),
     1DPLP2(4)
      DIMENSION DP2(4),CL(30,100),SL(30,10),PL(30,10)
      DIMENSION CLP(6,100),SLP(6,10),PLP(6,10
C
      CALL MONEY(NLAYER,CLAYER,NREBAR,SLAYER,NPRE,PLAYER,CL,
     1SL,PL)
C
      SUB1=0.D0
      SUB2=0.D0
      NRPST=0
   10 IF(CEMOD.LT.0.D0) NWORK=0
      IF(NTHERM.EQ.10.AND.NTYPE.EQ.3) NWORK=
      IF(NWORK.NE.0) GO TO 20
      NSC=0
      NFLAT=0
   20 IF(NTYPE.LT.3.AND.NTHERM.NE.-1) GO TO 3
      GO TO 40
   30 TA=1
      NSUBIN=1
      GO TO 250
   40 IF(NWORK.NE.0) GO TO 50
      NSUBIN=0
      C11=0.D0
      C33=0.D0
   50 IF(NTHERM.NE.-1) GO TO 90
      SUB1=1.D0
      SUB2=1.D0
      TX1=AXS1/.1D6
      TX2=AXS2/.1D6
      IF(NTHERM.EQ.-1) GO TO 80
      IF(NV(1).EQ.0.AND.NV(3).EQ.0) GO TO 2
```

```
 60 IF(NV(1).EQ.0) GO TO 70
    IF(DABS(C11).LT.TE1) GO TO 70
    SUB1=AIS1/DABS(C11)
 70 IF(NV(3).EQ.0) GO TO 140
 80 IF(DABS(C33).LT.TE2) GO TO 140
    SUB2=AIS2/DABS(C33)
    GO TO 140
 90 IF(NWORK.EQ.0) GO TO 140
    IF(NV(1).EQ.0) GO TO 100
    SUB1=(P1(1)-PREV1(1))/(C(1,1)*.140D-4)
    GO TO 110
100 SUB1=(P2(1)-PREV(1))/.14D-4
110 SUB1=DABS(SUB1)
    IF(NV(3).EQ.0) GO TO 120
    SUB2=(P1(3)-PREV1(3))/(C(3,3)*.14D-4)
    GO TO 130
120 SUB2=(P2(3)-PREV(3))/.14D-4
130 SUB2=DABS(SUB2)
140 IF(SUB1.LT.1.D0)SUB1=1.D0
    IF(SUB2.LT.1.D0)SUB2=1.D0
    IF(SUB2.GT.SUB1)  SUB1=SUB2
    IF(SUB1.GT.50.D0) SUB1=050.D0
    001=SNGL(SUB1)
    NSUBIN=INT(001)
    IF(NSUBIN.LT.NSUBIN) GO TO 150
    NSUBIN=NSUBIN
    IF(NSUBIN.GT.200) NSUBIN=200
    GO TO 170
150 NSC=NSC+1
    IF(NSC.LE.2) GO TO 170
    IF(NSUBIN.LE.2) GO TO 160
    NSUBIN=NSUBIN/2
160 NSC=0
170 IF(NSUBIN.GT.NSUBIN) NSUBIN=NSUBIN
    ALS1=0.D0
    LSG=0
    DO 190 IE=1,4
    IF(NV(IE).EQ.0) GO TO 180
    IF(DABS(P1(IE)).LT.1.D0) GO TO 190
    ALS1T=DABS((P1(IE)-PREV1(IE))/(.0100D0**N1(IE)))
    IF(ALS1T.GT.ALS1)ALS1=ALS1T
    GO TO 190
180 IF(DABS(P2(IE)).LT..1D-9) GO TO 190
    ALS1T=DABS((P2(IE)-PREV(IE))/(.0100D0**N2(IE)))
    IF(ALS1T.GT.ALS1) ALS1=ALS1T
190 CONTINUE
    OALS1=SNGL(ALS1)
    LS1=INT(OALS1)
    IF(LS1.EQ.0) GO TO 210
200 IF(NSUBIN.LT.LS1) GO TO 210
    NSUBIN=LS1
    LSG=1
210 SUB1=FLOAT(NSUBIN)
    IF(SUB1.LT.2.D0) SUB1=2.D0
    IF(NSUBIN.LT.2) NSUBIN=2
    IF(NTHERM.EQ.-1) GO TO 350
    DO 220 ID=1,4
    DELP1(ID)=P1(ID)-PREV1(ID)
    IF(NV(ID).EQ.0) DELP1(ID)=0.D0
    DP1(ID)=DELP1(ID)/SUB1
    DELP2(ID)=P2(ID)-PREV(ID)
    IF(NV(ID).EQ.1) DELP2(ID)=0.D0
    DP2(ID)=DELP2(ID)/SUB1
    PP2(ID)=0.D0
220 CONTINUE
    DO 270 IA=1,NSUBIN
230 AIA=FLOAT(IA)
    DO 240 IB=1,4
    P1(IB)=PREV1(IB)+AIA*DP1(IB)
    P2(IB)=PREV(IB)+AIA*DP2(IB)+ERR2(IB)
240 CONTINUE
    IF(NSUBIN.EQ.1.AND.NPLAT.NE.1)  NPLAT=-10
    CALL NOTE(NLAYER,CLAYER,CLP)
    CALL NOTE(NREBAR,SLAYER,SLP)
    CALL NOTE(NPRE,PLAYER,PLP)
250 NGOOD=0
    CALL WORK1(NGOOD,C11,C33,ERR2,PREV3,NPLAT)
    IF(NTYPE.LT.3) GO TO 410
    IF(IA.EQ.1.AND.NREST.EQ.3) GO TO 260
    CALL UNLOAD(NLAYER,CLAYER,CLP,NUNLOD)
    IF(NUNLOD.EQ.0) GO TO 260
    CALL UNLOAD(NREBAR,SLAYER,SLP,NUNLOD)
    CALL UNLOAD(NPRE,PLAYER,PLP,NUNLOD)
    GO TO 230
260 IF(NPLAT.NE.-20) GO TO 270
    SUB1=20.D0
    NPLAT=0
    GO TO 330
270 CONTINUE
    IF(PPLAT.NE.1) NPLAT=0
    IF(NWORK.EQ.0)GO TO 410
    IF(NPLAT.EQ.1) GO TO 410
    IF(N1.EQ.0) GO TO 410
    IF(LSG.EQ.1) GO TO 410
    IF(NSUBIN.GT.10) GO TO 410
    IF(NREST.EQ.3) GO TO 410
290 TSUB1=(P2(1)-PREV(1))/.14D-4
290 TSUP1=DABS(TSUB1)
300 TSUB2=(P2(3)-PREV(3))/.14D-4
310 TSUB2=DABS(TSUB2)
    IF(TSUB2.GT.TSUB1) TSUB1=TSUB2
    TSUB1=TSUB1/1.5D0
    IF(TSUB1.LT.SUB1) GO TO 410
    SUB1=TSUB1*2.0D0
320 CALL MONEY(NLAYER,CL,NREBAR,SL,NPRE,PL,CLAYER,SLAYER,
   1PLAYER)
330 IF(SUB1.GT.200.D0) GO TO 340
    002=SNGL(SUB1)
```

```
      NSUBIN=INT(OO2)
  340 OO3=SNGL(SUB1)
      NSUBIN=INT(OO3)
      NREST=3
      GO TO 200
  350 DO 360 LJ=1,4
      SUBI(LJ)=(P2(LJ)-PREV(LJ))/SUB1
      ERR2(LJ)=0.DO
  360 CONTINUE
      DO 400 LBJ=1,NSUBIN
  370 NGOOD=0
      ILBJ=FLOAT(LBJ)
  380 DO 390 LJ=1,4
      P2(LJ)=PREV(LJ)+ILBJ*SUBI(LJ)+ERR2(LJ)
  390 CONTINUE
      CALL WORK1(NGOOD,C11,C33,ERR2,PREV3,NPLAT)
      IF(NGOOD.EQ.5) GO TO 370
  400 CONTINUE
  410 DO 420 I80=1,4
      PREV(I80)=P2(I80)
      PREV1(I80)=QP(I80)
  420 CONTINUE
      NWORK=NWORK+1
      IF(NTHERM.EQ.10) NWORK=0
      CALL TIME(3,3)
      CALL TIME(0,0)
      RETURN
      END
      SUBROUTINE OUT
      IMPLICIT REAL*8(A-H,P-Z)
      COMMON/BNW/B1,B2,PC,PTC,CENCD,POISS,NTYPE,NSTYPE,
     1WIDTH,HEIGHT
      COMMON/DINO/CLAYER(30,100),T,NLAYER
      COMMON/JARAMA/PLAYER(30,10),PYP,EP,PCEN(10),
     1,APPAP(10),PFORCE(10),NPN(10),NPRE,NPD(10)
      COMMON/URACCO/SLAYER(30,10),PYR,ER,RCEN(10),
     1AREAR(10),NREBAR,NRD(10)
      NSTYPE=0
      CALL OUTPUT(NSTYPE,CLAYER,NLAYER,NRD)
      IF(NREBAR.EQ.0)GO TO 10
      NSTYPE=1
      CALL OUTPUT(NSTYPE,SLAYER,NREBAR,NRD)
   10 IF(NPRP.EQ.0) GO TO 20
      NSTYPE=2
      CALL OUTPUT(NSTYPE,PLAYER,NPRE,NPD)
   20 RETURN
      END
C
C
C
      SUBROUTINE PREST
      IMPLICIT REAL*8(A-H,P-Z)
      COMMON/ALPHA/BV(4),P1(4),P2(4),N1,LAM
      COMMON/BNW/B1,B2,PC,PTC,CENCD,POISS,NTYPE,NSTYPE,
     1WIDTH,HEIGHT
      COMMON/LOTUS/QP(4),C(4,4),CC(4,4),DQP(4),DS2(4),DQ(4)
      COMMON/DINO/CLAYER(30,100),T,NLAYER
      COMMON/URACCO/SLAYER(30,10),PYR,ER,RCEN(10),
     1AREAR(10),NREBAR,NRD(10)
      COMMON/JARAMA/PLAYER(30,10),PYP,EP,PCEN(10),
     1APPAP(10),PFORCE(10),NPN(10),NPRE,NPD(10)
      COMMON/TURBO/ALOAD(100,4),NFLAG(100),TITLE(20)
      COMMON/ESPADA/GUE(4),PREV(4),PREV1(4)
      COMMON/E26/E11,E22,S11,S22,SLOP11,SLOP12,SLOP21,SLOP22
      COMMON/ETYPE/NPI(10),NPASS,JLP,KPT
      COMMON/BORA/KDO,NPDO,KP
      COMMON/ASTONM/ALOADO(4),ALOADL(5,4),NFLAGO,NFLAGL(5),
     1NPSTEP
      COMMON/BAYAPI/YU,PE11,PE22,PS11,PS22,E10,E20,EIO,EIOT
      COMMON/MUIRA/E1T,E2T,E10C,E20C,SIG1C,SIG2C
      COMMON/SL280/TS11,TS22,TSLO11,TSLO22,NSUB
      COMMON/WOLFW5/AXS1,AXS2,NWORK
C
C
      DO 10 J=1,NPRE
      NPI(J)=NPN(J)
   10 CONTINUE
      WRITE(6,150)
      NPASS=0
      DO 140 JK=1,NPSTEP
      JP=1
   20 IF(NPN(JP).EQ.JK) GO TO 30
      JP=JP+1
      IF(JP.GT.NPRE) GO TO 60
      GO TO 20
   30 K=JP
      NRPD=1
      NSTYPE=2
      PLAYER(17,K)=PFORCE(K)/(APPAP(K)*EP)
      KOUNT=0
      PRAC=PLAYER(7,K)
   40 E11=PLAYER(17,K)
      CALL STEEL(NSTYPE,PYP,EP,NNRD,K,PRAC,YIELD)
      PLAYER(7,K)=PRAC
      PP=APPAP(K)*S11
      PT=(PFORCE(K)-PP)/PFORCE(K)
      IF(DABS(PT).LT..00500) GO TO 50
      PT=PFORCE(K)-PP
      DEL=PT/SLOP11
      PLAYER(17,K)=DEL+PLAYER(17,K)
      KOUNT=KOUNT+1
      IF(KOUNT.GE.10) GO TO 190
   50 JP=JP+1
      GO TO 20
   60 IF(NPSTEP.EQ.0) GO TO 90
   70 N1=NFLAGL(JK)
      CALL GUES
      DO 80 J=1,4
```

```
      P1(J)=ALOADL(JK,J)
      GUE(J)=P2(J)
   80 CONTINUE
      CALL GUESS
      GO TO 100
   90 N1=1111
      CALL GUES
  100 JLP=JK
  110 NWORK=0
      CALL WORK
      DO 130 K=1,NPRE
      IF(NPR(K).NE.JK) GO TO 130
      YER=PLAYER(3,K)
      IF(NPD(K).EQ.2) GO TO 120
      E11=(P2(1)-YER*P2(2))/(1.D0+YER/R1)
      PLAYER(17,K)=PLAYER(17,K)-E11
      GO TO 130
  120 E22=(P2(3)-YER*P2(4))/(1.D0+YER/R2)
      PLAYER(17,K)=PLAYER(17,K)-E22
  130 CONTINUE
  140 CONTINUE
  150 FORMAT('1',9X,80('*')/10X,80('*'),///,30X,
     1'RESULTS OF PRESTRESS APPLICATION',
     2///,10X,80('*'),/10X,80('*')///)
  160 IF(NPDO.EQ.1) GO TO 170
      CALL OUT
  170 CALL RECAP
      DO 180 ND=1,4
      P1(ND)=QP(ND)
  180 CONTINUE
      I=999
      CALL FINOUT(I,NDD)
      RETURN
  190 WRITE(6,200)
  200 FORMAT(///,10X,
     1'PRESTRESS NOT CONVERGING---PROGRAM TERMINATED')
      STOP
      END
      SUBROUTINE PLACES(NREBAR,NRD,RCEN,AREAR,SLAYER)
      IMPLICIT REAL*8(A-H,P-Z)
      DIMENSION RCEN(10),AREAR(10),NRD(10),SLAYER(30,10)
      COMMON/BMW/R1,R2,FC,FTC,CEMOD,POISS,NTYPE,ITYPE,
     1WIDTH,HEIGHT
C     THIS SUBROUTINE ASSIGNS THE LOCATIONS OF THE STEEL
C     LAYERS TO SLAYER
C
C     SLAYER(1,I)=STARTING COORDINATE
C     SLAYER(2,I)=ENDING COORDINATE
C     SLAYER(3,I)=MIDDLE COORDINATE
C
      DO 30 I=1,NREBAR
      IF(NRD(I).EQ.2) GO TO 20
      TSTEEL=AREAR(I)/WIDTH
   10 SLAYER(1,I)=RCEN(I)-TSTEEL/2.D0
      SLAYER(2,I)=RCEN(I)+TSTEEL/2.D0
      SLAYER(3,I)=RCEN(I)
      GO TO 30
   20 TSTEEL=AREAR(I)/HEIGHT
      GO TO 10
   30 CONTINUE
      RETURN
      END
      SUBROUTINE PLACON
      IMPLICIT REAL*8(A-H,P-Z)
      COMMON/DIMO/CLAYER(30,100),T,NLAYER
C
C     THIS SUBROUTINE FINDS THE STARTING AND ENDING
C     COORDINATES OF THE CONCRETE LAYERS
C
      XLAYER=NLAYER
      D=T/XLAYER
      DO 10 I=1,NLAYER
      XI=I
      CLAYER(1,I)=(XI-1.D0)*D-T/2.D0
      CLAYER(2,I)=XI*D-T/2.D0
      CLAYER(3,I)=(XI-0.5D0)*D-T/2.D0
   10 CONTINUE
      RETURN
      END
      SUBROUTINE GUESS
      IMPLICIT REAL*8(A-H,P-Z)
      COMMON/ESPADA/GUE(4),PREV(4),PREV1(4)
      COMMON/ALPHA/NV(4),P1(4),P2(4),N1,LAM
C
C     THIS SUBROUTINE DISCOVERS IF A LOAD OR STRAIN IS
C     SPECIFIED...   IF A LOAD IS SPECIFIED, THEN THE
C     INITIAL SPECIFIED STRAIN IS SET TO ZERO
C
C     IF NV(I)=0     THEN A STRAIN IS SPECIFIED
C     OR NV(I)=1     THEN ALOAD IS SPECIFIED
C
      DO 20 I25=1,4
      IF(NV(I25).EQ.0) GO TO 10
      P2(I25)=GUE(I25)
      GO TO 20
   10 P2(I25)=P1(I25)
   20 CONTINUE
   30 RETURN
      END
      SUBROUTINE GUES
      IMPLICIT REAL*8(A-H,P-Z)
      COMMON/ALPHA/NV(4),P1(4),P2(4),N1,LAM
C
C
C     THIS SUBROUTINE IF A LOAD OR A STRAIN IS SPECIFIED
C
C
      N2=N1
```

```
      IF(N1.GE.1000) GO TO 40
      NV(1)=0
   10 IF(N1.GE.100) GO TO 50
      NV(2)=0
   20 IF(N1.GE.10) GO TO 60
      NV(3)=0
   30 IF(N1.EQ.1) GO TO 70
      NV(4)=0
      GO TO 80
C
   40 N1=N1-1000
      NV(1)=1
      GO TO 10
   50 N1=N1-100
      NV(2)=1
      GO TO 20
   60 N1=N1-10
      NV(3)=1
      GO TO 30
   70 NV(4)=1
   80 N1=N2
      RETURN
      END
      SUBROUTINE LODOUT(I,NDD)
      IMPLICIT REAL*8(A-H,P-Z)
      COMMON/ALPHA/NV(4),F1(4),F2(4),N1,LAM
      COMMON/TYPE35/PERM1(4),PERM2(4)
      DIMENSION NSKIP(4)
      DATA NSKIP(1),NSKIP(2),NSKIP(3),NSKIP(4)/' ','N1',
     1'N2','*2'/
C
C     THIS SUBROUTINE PRINTS THE CURRENT LOAD NUMBER AND
C     THE SPECIFIED LOADS OR STRAINS
C
C
      IF(NDD.EQ.3) GO TO 130
      IF(NDD.EQ.2) GO TO 110
      IF(NDD.EQ.1) GO TO 30
      WRITE(6,20)I
      WRITE(7,10)I
   10 FORMAT(30X,'L O A D   N U M B E R ',I4)
   20 FORMAT('1',9X,100('*'),//30X,'L O A D   :   N U M B E R',
     1I4,//)
      GO TO 40
   30 WRITE(6,100)
      WRITE(7,100)
   40 DO 80 J=1,4
      IF(NV(J).EQ.0) GO TO 60
      PINC1=F1(J)-PERM1(J)
      WRITE(6,50)NSKIP(J),F1(J),PINC1
      WRITE(7,50)NSKIP(J),F1(J),PINC1
   50 FORMAT(30X,A2,5X,E12.5,5X,'(LOAD)',12X,E12.5,5X,
     1'(LOAD INCREMENT)')
      GO TO 80
   60 PINC2=F2(J)-PERM2(J)
      WRITE(6,70)NSKIP(J),F2(J),PINC2
      WRITE(7,70)NSKIP(J),F2(J),PINC2
   70 FORMAT(30X,A2,5X,E12.5,5X,'(STRAIN)',10X,E12.5,5X,
     1'(STRAIN INCREMENT)')
   80 CONTINUE
C
      WRITE(6,90)
   90 FORMAT(//10X,100('*'),//)
  100 FORMAT('1',9X,100('*'),///,30X,'DEAD LOAD RESULTS'//)
      RETURN
  110 WRITE(6,120)
      WRITE(7,120)
  120 FORMAT(//,10X,'*** CREEP RESULTS ***')
      GO TO 150
  130 WRITE(6,140)
      WRITE(7,140)
  140 FORMAT(//,10X,'*** THERMAL STRAIN RESULTS ***')
  150 DO 160 J=1,4
      PERM1(J)=F1(J)
      PERM2(J)=F2(J)
  160 CONTINUE
      GO TO 40
      END
      SUBROUTINE FINOUT(I,NDD)
      IMPLICIT REAL*8(A-H,P-Z)
      COMMON/ALPHA/NV(4),F1(4),F2(4),N1,LAM
      COMMON/TYPE35/PERM1(4),PERM2(4)
      DIMENSION NSKIP(4)
      DATA NSKIP(1),NSKIP(2),NSKIP(3),NSKIP(4)/'N1','N1',
     1'N2','*2'/
C
C     THIS SUBROUTINE OUTPUTS THE UNKNOWN AND DESIRED LOADS
C     OR STRAINS     I.E. THE PROBLEM SOLUTION
C
C
      IF(NDD.EQ.3) GO TO 140
      IF(NDD.EQ.2) GO TO 120
      IF(I.EQ.999) GO TO 80
      IF(NDD.EQ.1) GO TO 100
      WRITE(6,10)I
      WRITE(7,20)I
   10 FORMAT(//,20X,'SOLUTION TO LOAD NO. ',I3,//)
   20 FORMAT(20X,'SOLUTION TO LOAD NO. ',I3)
C
   30 DO 70 J=1,4
      IF(NV(J).EQ.0) GO TO 50
      PINC2=F2(J)-PERM2(J)
      WRITE(6,40)NSKIP(J),F2(J),PINC2
      WRITE(7,40)NSKIP(J),F2(J),PINC2
   40 FORMAT(25X,A2,5X,E12.5,5X,'(STRAIN)',10X,E12.5,5X,
     1'(STRAIN INCREMENT)')
      GO TO 70
   50 PINC1=F1(J)-PERM1(J)
```

```
      WRITE(6,60)#SKIP(J),P1(J),PINC1
      WRITE(7,60)#SKIP(J),P1(J),PINC1
   60 FORMAT(25X,A2,5X,F12.5,5X,'(LOAD)',12X,F12.5,5X,
     1'(LOAD INCREMENT)')
   70 CONTINUE
      RETURN
   80 WRITE(6,90)
      WRITE(7,90)
   90 FORMAT(//,15X,'RESULTS FROM PRESTRESS APPLICATION')
      GO TO 30
  100 WRITE(6,110)
      WRITE(7,110)
  110 FORMAT(//,15X,'RESULTS FROM DEAD LOAD APPLICATION')
      GO TO 30
  120 WRITE(6,130)
      WRITE(7,130)
  130 FORMAT(//15X,'RESULTS AFTER CREEP')
      GO TO 160
  140 WRITE(6,150)
      WRITE(7,150)
  150 FORMAT(//,15X,'RESULTS AFTER THERMAL EFFECTS')
  160 DO 170 J=1,4
      PERM1(J)=P1(J)
      PERM2(J)=P2(J)
  170 CONTINUE
      GO TO 30
      END
      SUBROUTINE TEMP
      IMPLICIT REAL*8(A-H,P-Z)
      COMMON/ALPHA/BT(4),P1(4),P2(4),N1,LAM
      COMMON/BNB/B1,B2,FC,FTC,CENOD,POISS,BTYPE,NSTYPE,
     1WIDTH,HEIGHT
      COMMON/BORA/KDO,NPDO,KP,NCRP,PCRP
      COMMON/DINO/CLAYER(30,100),T,NLAYER
      COMMON/E26/E11,E22,S11,S22,SLOP11,SLOP12,SLOP21,SLOP22
      COMMON/ESPADA/CUE(4),PREV(4),PREV1(4)
      COMMON/ETYPE/EPI(10),NPASS,JLP,KPT
      COMMON/JARARA/PLAYER(30,10),PIP,EP,PCEN(10),AREAP(10)
     1,PFORCE(10),NPB(10),NPBE,NPD(10)
      COMMON/CS3PTO/T1,T2,T3,ALPHAC,ALPHAS,NTHERM,NTCODE
      COMMON/LOTUS/QP(4),C(4,4),CC(4,4),BQP(4),DSQ(4),DQ(4)
      COMMON/URACCO/SLAYER(30,10),PYB,SB,PCEN(13),AREAS
     1(10),NREBAR,NRD(10)
C
C     1.  T1 + T2*Z + T3*Z*Z
C     2.  T1 + T2*(Z**T3)
C     3.  T1 + T2*(E** (Z*T3) )
C
C     Z IN THESE EQUATIONS IS DEFINED AS ZERO (0) ON THE
C     INSIDE SURFACE
C
      N1=NTCODE
      NDD=3
      CALL LOGOUT(I,NDD)
      TBY2=T/2.DO
C
      GO TO (10,60,110),NTHERM
C
   10 DO 20 K=1,NLAYER
      ZED=CLAYER(3,K)+TBY2
      CLAYER(24,K)=(T1+T2*ZED+T3*ZED*ZED)*ALPHAC
   20 CONTINUE
      IF(NREBAR.LT.1) GO TO 40
      DO 30 K=1,NREBAR
      ZED=SLAYER(3,K)+TBY2
      TEMDIF=T1+T2*ZED+T3*ZED*ZED
      SLAYER(24,K)=TEMDIF*ALPHAS
      SLAYER(17,K)=TEMDIF*ALPHAC
   30 CONTINUE
   40 IF(NPRE.LT.1) GO TO 160
      DO 50 K=1,NPRE
      ZED=PLAYER(3,K)+TBY2
      TEMDIF=T1+T2*ZED+T3*ZED*ZED
      PLAYER(24,K)=TEMDIF*ALPHAS
      PLAYER(16,K)=TEMDIF*ALPHAC
   50 CONTINUE
      GO TO 160
C
   60 DO 70 K=1,NLAYER
      ZED=CLAYER(3,K)+TBY2
      CLAYER(24,K)=T1+T2*ZED**T3
   70 CONTINUE
      IF(NREBAR.LT.1) GO TO 90
      DO 80 K=1,NREBAR
      ZED=SLAYER(3,K)+TBY2
      TEMDIF=T1+T2*ZED**T3
      SLAYER(24,K)=TEMDIF*ALPHAS
      SLAYER(17,K)=TEMDIF*ALPHAC
   80 CONTINUE
   90 IF(NPRE.LT.1) GO TO 160
      DO 100 K=1,NPRE
      ZED=PLAYER(3,K)+TBY2
      TEMDIF=T1+T2*ZED**T3
      PLAYER(24,K)=TEMDIF*ALPHAS
      PLAYER(16,K)=TEMDIF*ALPHAC
  100 CONTINUE
      GO TO 160
C
  110 DO 120 K=1,NLAYER
      ZED=CLAYER(3,K)+TBY2
      Y=ZED*T3
      CLAYER(24,K)=T1+T2*DEXP(Y)
  120 CONTINUE
      IF(NREBAR.LT.1) GO TO 140
      DO 130 K=1,NREBAR
      ZED=SLAYER(3,K)+TBY2
      Y=ZED*T3
      TEMDIF=T1+T2*DEXP(Y)
```

```
      SLAYER(24,K)=TENDIF*ALPHAS
      SLAYER(17,K)=TENDIF*ALPHAC
  130 CONTINUE
  140 IF(NPRE.LT.1) GO TO 160
      DO 150 K=1,NPRE
      IED=PLAYER(J,K)+TBT2
      T=IED-T)
      TENDIF=T1+T2*DEEP(T)
      PLAYER(24,K)=TENDIF*ALPHAS
      PLAYER(16,K)=TENDIF*ALPHAC
  150 CONTINUE
C
  160 NTHE=NTHERM
      NTHERM=10
      CALL GUESS
      CALL WORK
      NTHERM=NTHE
C
      IF(NPBO.EQ.1) GO TO 170
      CALL OUT
  170 DO 180 I=1,4
      P1(I)=QP(I)
      PPEV(I)=P2(I)
  180 CONTINUE
      CALL RECAP
      CALL FINOUT(I,NDD)
      NDD=0
      RETURN
      END
      SUBROUTINE CURVE
      IMPLICIT REAL*8(A-H,P-Z)
      COMMON/BROKER/NLOADS,NJUMP(10),*LOADT
      COMMON/BMW/P1,R2,PC,PTC,CEMOD,POISS,NTYPE,NSTYPE,
     1WIDTH,HEIGHT
      COMMON/DINO/CLAYER(30,100),T,NLAYER
      COMMON/JARAMA/PLAYER(30,10),PYP,EP,PCEN(10),AREAP(10)
     1,PFORCE(10),NPW(10),NPRE,NPD(10)
      COMMON/TURBO/ALOAD(100,4),NFLAG(100),TI.E(20),
     1NINC(100)
      COMMON/BRACCO/SLAYER(30,10),PYR,ER,RCEN(10),AREAR
     1(10),NPEBAR,NRD(10)
C
C     CALCULATE SECTION PROPERTIES
C
      ENP=EP/CEMOD-1.D0
      ENR=ER/CEMOD-1.D0
      AREA1=WIDTH*T
      AREA2=HEIGHT*T
      CG1=0.D0
      CG2=0.D0
      IF(NPEBAR.EQ.0) GO TO 30
      DO 20 K=1,NPEBAR
      IF(NPD(K).EQ.2) GO TO 10
      AREA1=AREA1+ENR*AREAR(K)
      CG1=CG1+AREAR(K)*ENR*RCEN(K)
      GO TO 20
   10 AREA2=AREA2+ENR*AREAR(K)
      CG2=CG2+AREAR(K)*ENR*RCEN(K)
   20 CONTINUE
   30 IF(NPRE.EQ.0) GO TO 60
      DO 50 K=1,NPRE
      IF(NPD(K).EQ.2) GO TO 40
      AREA1=AREA1+ENP*AREAP(K)
      CG1=CG1+AREAP(K)*ENP*PCEN(K)
      GO TO 50
   40 AREA2=AREA2+ENP*AREAP(K)
      CG2=CG2+AREAP(K)*ENP*PCEN(K)
   50 CONTINUE
   60 CG1=CG1/AREA1
      CG2=CG2/AREA2
      SINER1=(WIDTH*T**3)/12.D0+WIDTH*T*CG1*CG1
      SINER2=(HEIGHT*T**3)/12.D0+HEIGHT*T*CG2*CG2
      IF(NPEBAR.EQ.0) GO TO 90
      DO 80 K=1,NPEBAR
      IF(NRD(K).EQ.2) GO TO 70
      SINEP1=SINER1+AREAR(K)*ENR*(RCEN(K)-CG1)**2
      GO TO 80
   70 SINEP2=SINER2+AREAR(K)*ENR*(RCEN(K)-CG2)**2
   80 CONTINUE
   90 IF(NPRE.EQ.0) GO TO 120
      DO 110 K=1,NPRE
      IF(NPD(K).EQ.2) GO TO 100
      SINER1=SINER1+AREAP(K)*ENR*(PCEN(K)-CG1)**2
      GO TO 110
  100 SINEP2=SINEP2+AREAP(K)*ENP*(PCEN(K)-CG2)**2
  110 CONTINUE
C
  120 I=0
      DO 130 KIJ=1,NLOADS
      I=I+NJUMP(KIJ)
      ALOAD(I,2)=(ALOAD(I,2)*ALOAD(I,1))/(CEMOD*SINER1)
      ALOAD(I,4)=(ALOAD(I,4)*ALOAD(I,3))/(CEMOD*SINER2)
  130 CONTINUE
      RETURN
      END
      SUBROUTINE CREEP
      IMPLICIT REAL*8(A-H,P-Z)
      COMMON/ALPHA/HV(4),P1(4),P2(4),N1,LA*
      COMMON/BMW/P1,R2,PC,PTC,CEMOD,POISS,NTYPE,NSTYPE,
     1WIDTH,HEIGHT
      COMMON/BORA/KDO,NPDO,KP,NCRP,PCRP
      COMMON/DINO/CLAYER(30,100),T,NLAYER
      COMMON/E26/E11,E22,S11,S22,SLOP11,SLOP12,SLOP21,SLOP22
      COMMON/ESPADA/GUE(4),PREV(4),PREV1(4)
      COMMON/ETYPE/NPI(10),NPASS,JLP,KPT
      COMMON/JARAMA/PLAYER(30,10),PYP,EP,PCEN(10),AREAP(10)
     1,PFORCE(10),NPW(10),NPRE,NPD(10)
      COMMON/LOTUS/QP(4),C(4,4),CC(4,4),DQP(4),DSQ(4),DQ(4)
```

```
      COMMON/UNACCQ/SLAYER(30,10),PTR,RR,RCEN(10),AREAR
     1(10),NREBAR,NRD(10)
      DIMENSION DIFC(4),PREVC(4),CCR(2,100),SCR(2,10),
     1PCR(2,10)
C
      I=0
      N1=1111
      CALL GUES
      NDO=2
      CALL LOOOUT(I,NDO)
      DO 10 K=1,NLAYER
      CLAYER(12,K)=CLAYER(8,K)
      CLAYER(13,K)=CLAYER(9,K)
      CCR(1,K)=CLAYER(18,K)
      CCR(2,K)=CLAYER(19,K)
   10 CONTINUE
      IF(NREBAR.EQ.0) GO TO 30
      DO 20 K=1,NREBAR
      CLAYER(14,K)=SLAYER(8,K)
      CLAYER(15,K)=SLAYER(9,K)
      SCR(1,K)=SLAYER(18,K)
      SCR(2,K)=SLAYER(19,K)
   20 CONTINUE
   30 IF(NPRE.EQ.0) GO TO 50
      DO 40 K=1,NPRE
      CLAYER(16,K)=PLAYER(8,K)
      CLAYER(17,K)=PLAYER(9,K)
      PCR(1,K)=PLAYER(18,K)
      PCR(2,K)=PLAYER(19,K)
   40 CONTINUE
   50 CEMOD1=CEMOD
      CEMOD=CEMOD/FCPP
      IF(NTYPE.GE.3) CEMOD=-1.D0*CEMOD
      CALL WORK
      CEMOD=CEMOD1
      DO 70 I=1,4
      PREVC(I)=F2(I)
   70 CONTINUE
C
      DO 80 K=1,NLAYER
      CLAYER(22,K)=CLAYER(8,K)-CLAYER(12,K)
      CLAYER(23,K)=CLAYER(9,K)-CLAYER(13,K)
      CLAYER(18,K)=CCR(1,K)
      CLAYER(19,K)=CCR(2,K)
      CLAYER(8,K)=CLAYER(12,K)
      CLAYER(9,K)=CLAYER(13,K)
   80 CONTINUE
      IF(NREBAR.EQ.0) GO TO 100
      DO 90 K=1,NREBAR
      SLAYER(22,K)=SLAYER(8,K)-CLAYER(14,K)
      SLAYER(23,K)=SLAYER(9,K)-CLAYER(15,K)
      SLAYER(18,K)=SCR(1,K)
      SLAYER(19,K)=SCR(2,K)
      SLAYER(8,K)=CLAYER(14,K)
      SLAYER(9,K)=CLAYER(15,K)
   90 CONTINUE
  100 IF(NPRE.EQ.0) GO TO 120
      DO 110 K=1,NPRE
      PLAYER(22,K)=PLAYER(8,K)-CLAYER(16,K)
      PLAYER(23,K)=PLAYER(9,K)-CLAYER(17,K)
      PLAYER(18,K)=PCR(1,K)
      PLAYER(19,K)=PCR(2,K)
      PLAYER(8,K)=CLAYER(16,K)
      PLAYER(9,K)=CLAYER(17,K)
  110 CONTINUE
  120 KOUNT=0
      CALL WORK
  130 DO 140 J=1,4
      DIFC(J)=PREVC(J)-F2(J)
  140 CONTINUE
      KOUNT=KOUNT+1
      IF(KOUNT.GE.20) GO TO 280
      DO 150 K=1,NLAYER
      YER=CLAYER(3,K)
      E11=(DIFC(1)-YER*DIFC(2))/(1.D0+YER/P1)
      E22=(DIFC(3)-YER*DIFC(4))/(1.D0+YER/P2)
      CLAYER(22,K)=CLAYER(22,K)+E11
      CLAYER(23,K)=CLAYER(23,K)+E22
  150 CONTINUE
      IF(NREBAR.LE.0) GO TO 170
      DO 160 K=1,NREBAR
      YER=SLAYER(3,K)
      E11=(DIFC(1)-YER*DIFC(2))/(1.D0+YER/P1)
      E22=(DIFC(3)-YER*DIFC(4))/(1.D0+YER/P2)
      SLAYER(22,K)=SLAYER(22,K)+E11
      SLAYER(23,K)=SLAYER(23,K)+E22
  160 CONTINUE
  170 IF(NPRE.LE.0) GO TO 190
      DO 180 K=1,NPRE
      YER=PLAYER(3,K)
      E11=(DIFC(1)-YER*DIFC(2))/(1.D0+YER/P1)
      E22=(DIFC(3)-YER*DIFC(4))/(1.D0+YER/P2)
      PLAYER(22,K)=PLAYER(22,K)+E11
      PLAYER(23,K)=PLAYER(23,K)+E22
  180 CONTINUE
  190 CALL WORK
      DO 200 J=1,4
      DIF=DABS(F1(J)-OF(J))
      IF(DIF.LT.0.1D0) GO TO 200
      F1A=DABS(F1(J))
      PERCEN=DIF/(DIF+F1A)
      IF(PERCEN.GT..00500) GO TO 130
  200 CONTINUE
      IF(NPDO.EQ.1) GO TO 270
      CALL OUT
      WRITE(6,210)
  210 FORMAT(//,10X,'CREEP STRAINS',//
     110X,'LAYER NO.',20X,'CONCRETE',20X,'NEGATIVE STEEL',
```

```
     220X,          'NEGATIVE PRESTRESSING',/
     315X,3(11X,'DIREC1',11X,'DIREC2'))
      DO 260 K=1,NLAYER
      IF(K.GT.NPRE.AND.K.GT.NREBAR) GO TO 230
      IF(K.GT.NPRE) GO TO 220
      IF(K.GT.NREBAR) GO TO 240
      WRITE(6,250)K,CLAYER(22,K),CLAYER(23,K),SLAYEP(22,K),
     1SLAYER(23,K),PLAYER(22,K),PLAYER(23,K)
      GO TO 260
  220 WRITE(6,300)K,CLAYER(22,K),CLAYER(23,K),SLAYEP(22,K),
     1SLAYER(23,K)
      GO TO 260
  230 WRITE(6,310)K,CLAYER(22,K),CLAYER(23,K)
      GO TO 260
  240 WRITE(6,320)K,CLAYER(22,K),CLAYER(23,K),P.AYER(22,K),
     1PLAYER(23,K)
  250 FORMAT(10X,I5,6(5X,E12.5))
  260 CONTINUE
  270 CALL RECAP
      CALL PINOUT(I,NDD)
      NDD=0
      RETURN
  280 WRITE(6,290)
  290 FORMAT(///,20X,
     1'CREEP NOT CONVERGING---PROGRAM TERMINATED')
      CALL TIME(J,J)
      STOP
  300 FORMAT(10X,I5,4(5X,E12.5))
  310 FORMAT(10X,I5,2(5X,E12.5))
  320 FORMAT(10X,I5,2(5X,E12.5),34X,2(5X,E12.5))
      END
      SUBROUTINE LOOP(NLAYER,CLAYER,FYR,EP,NDD,NGOOD,NFLAT)
      IMPLICIT REAL*8(A-H,P-Z)
      COMMON/ALPHA/BT(4),P1(4),P2(4),N1,LAR
      COMMON/BRR/P1,B2,PC,FYC,CENOD,POISS,NTYPE,NSTYPE,
     1WIDTH,HEIGHT
      COMMON/LOTRS/QP(4),C(4,4),CC(4,4),DQP(4),DSQ(4),SQ(4)
      COMMON/E26/E11,E22,S11,S22,SLOP11,SLOP12,SLOP21,SLOP22
      DIMENSION CLAYER(30,1),NDD(10),NSKIP(3)
      COMMON/ETYPE/NPE(10),NPASS,JLP,KPT
      COMMON/DORA/KDO,NPDO,KP,KCRP,PCRP
      COMMON/DAVARI/YU,PE11,PE22,PS11,PS22,E1U,E2U,E1O,E1OT
      COMMON/RGIRA/E1T,E2T,E1UC,E2UC,SIG1C,SIG2C
      COMMON/SL280/TS11,TS22,TSLO11,TSLO22,NSUB
      COMMON/CSJPTO/T1,T2,T3,ALPHAC,ALPHAS,NTYPE,YYCODE
      DATA NSKIP(1),NSKIP(2),NSKIP(3)/' ','S','P'/
C
C       THIS SUBROUTINE LOOPS OVER ALL THE LAYERS OF THE
C       SEGMENT TO FIND THE
C       'DELTA Q' VECTOR AND THE 'C' MATRIX
C
      DO 270 K=1,NLAYER
      YER=CLAYER(3,K)
      P11=(P2(1)-YER*P2(2))/(1.DO+YER/B1)
      E22=(P2(3)-YER*P2(4))/(1.DO+YER/B2)
      AK1=1.DO+YER/B1
      AK2=1.DO+YER/B2
      NWATCH=2
      E11E=E11
      E22E=E22
      IF(NSTYPE.EQ.0) GO TO 130
      IF(NSTYPE.EQ.1) GO TO 70
      IF(JLP.LE.0) GO TO 90
      IF(NPASS.EQ.1) GO TO 10
      IF(NPE(K).GT.JLP) GO TO 90
   10 IF(NPD(K).EQ.1) GO TO 40
      IF(KPT.EQ.1.AND.KP.EQ.1) GO TO 30
   20 S22=E22+CLAYER(17,K)
      GO TO 70
   30 IF(NPE(K).EQ.JLP) E22=0.DO
      GO TO 20
   40 IF(KPT.EQ.1.AND.KP.EQ.1) GO TO 60
   50 E11=E11+CLAYER(17,K)
      GO TO 70
   60 IF(NPE(K).EQ.JLP) E11=0.DO
      GO TO 50
C
   70 FRAC=CLAYER(7,K)
      YIELD=CLAYER(16,K)
      NNPD=NPD(K)
      E11=P11-CLAYER(20,K)
      S22=E22-CLAYER(24,K)
      CALL STESL(NSTYPE,FYR,EP,NNPD,K,FRAC,YIELD)
      IF(NGOOD.LT.1) GO TO 80
      CLAYER(7,K)=FRAC
      CLAYER(12,K)=E11
      CLAYER(13,K)=E22
      CLAYER(14,K)=S11
      CLAYER(15,K)=S22
      CLAYER(16,K)=YIELD
   80 NWATCH=0
      E11=E11E
      E22=E22E
      GO TO 150
   90 EC=CLAYER(4,K)
      ET1=CLAYER(5,K)
      ET2=CLAYER(6,K)
      PE11=CLAYER(8,K)
      PE22=CLAYER(9,K)
      PS11=CLAYER(10,K)
      PS22=CLAYER(11,K)
      E1U=CLAYER(18,K)
      E2U=CLAYER(19,K)
      SLOP11=CLAYER(20,K)
      SLOP22=CLAYER(21,K)
      TSLO11=CLAYER(25,K)
      TSLO22=CLAYER(26,K)
      YU=CLAYER(27,K)
```

```
      TS11=CLAYEP(28,K)
      TS22=CLAYEP(29,K)
      NWATCH=2
      N=10-NSTYPE
      E11=E11-CLAYEP(22,K)-CLAYEP(N,K)
      E22=E22-CLAYEP(23,K)-CLAYEP(N,K)
      CALL CONCRE(LC,LT1,LT2,K)
C       IF(NGOOD.LT.1) GO TO 15
      CLAYEP(21,K)=SLOP22
      CLAYEP(20,K)=SLOP11
      CLAYEP(19,K)=E20
      CLAYEP(10,K)=E10
      CLAYEP(11,K)=S22
      CLAYEP(10,K)=S11
      CLAYEP(9,K)=E22
      CLAYEP(8,K)=E11
      CLAYEP(27,K)=VU
      IF(NGOOD.LT.1) GO TO 100
      CLAYEP(28,K)=TS11
      CLAYEP(29,K)=TS22
      CLAYEP(6,K)=LT2
      CLAYEP(5,K)=LT1
      CLAYEP(4,K)=LC
      CLAYEP(25,K)=TSLO11
      CLAYEP(26,K)=TSLO22
  100 IF(NNOD.EQ.2) GO TO 110
      S11=-S11
      S22=0.D0
      SLOP11=-SLOP11
      SLOP22=0.D0
      GO TO 120
  110 S22=-S22
      SLOP22=-SLOP22
      SLOP11=0.D0
      S11=0.D0
  120 E11=-E11
      E22=-E22
      SLOP12=0.D0
      SLOP21=0.D0
      GO TO 150
C
  130 LC=CLAYEP(4,K)
      LT1=CLAYEP(5,K)
      LT2=CLAYEP(6,K)
      PE11=CLAYEP(8,K)
      PE22=CLAYEP(9,K)
      PS11=CLAYEP(10,K)
      PS22=CLAYEP(11,K)
      E10=CLAYEP(10,K)
      E20=CLAYEP(19,K)
      SLOP11=CLAYEP(20,K)
      SLOP22=CLAYEP(21,K)
      TSLO11=CLAYEP(25,K)
      TSLO22=CLAYEP(26,K)
      VU=CLAYEP(27,K)
      TS11=CLAYEP(28,K)
      TS22=CLAYEP(29,K)
      E11=E11-CLAYEP(22,K)-CLAYEP(20,K)
      E22=E22-CLAYEP(23,K)-CLAYEP(20,K)
      CALL CONCRE(LC,LT1,LT2,K)
C       IF(NGOOD.LT.1) GO TO 12
  140 CLAYEP(8,K)=E11
      CLAYEP(9,K)=E22
      CLAYEP(10,K)=S11
      CLAYEP(11,K)=S22
      CLAYEP(10,K)=E10
      CLAYEP(19,K)=E20
      CLAYEP(20,K)=SLOP11
      CLAYEP(21,K)=SLOP22
      CLAYEP(27,K)=VU
      IF(NGOOD.LT.1) GO TO 150
      CLAYEP(4,K)=LC
      CLAYEP(5,K)=LT1
      CLAYEP(6,K)=LT2
      CLAYEP(25,K)=TSLO11
      CLAYEP(26,K)=TSLO22
      CLAYEP(28,K)=TS11
      CLAYEP(29,K)=TS22
  150 DZ=CLAYEP(2,K)-CLAYEP(1,K)
      QP(1)=QP(1)+AK2*S11*DZ*WIDTH
      QP(2)=QP(2)-YER*AK2*S11*DZ*WIDTH
      QP(3)=QP(3)+AK1*S22*DZ*HEIGHT
      QP(4)=QP(4)-YER*AK2*S22*DZ*HEIGHT
C
C  99 IF(NGOOD.LT.1) GO TO 99
  160 IF(NTHERM.EQ.-1) GO TO 170
      IF(N1.EQ.0) GO TO 220
      GO TO 180
  170 C(1,1)=C(1,1)+SLOP11*AK2*DZ*WIDTH/AK1
      C(1,3)=C(1,3)+SLOP12*DZ*WIDTH
      C(3,1)=C(3,1)+SLOP21*DZ*HEIGHT
      C(3,3)=C(3,3)+SLOP22*AK1*DZ*HEIGHT/AK2
      GO TO 220
C
  180 IF(NV(1).EQ.0) GO TO 190
      C(1,1)=C(1,1)+SLOP11*AK2*DZ*WIDTH/AK1
      C(1,2)=C(1,2)-YER*SLOP11*AK2*DZ*WIDTH/AK1
      C(1,3)=C(1,3)+SLOP12*DZ*WIDTH
      C(1,4)=C(1,4)-YER*SLOP12*DZ*WIDTH
C
  190 IF(NV(2).EQ.0) GO TO 200
      C(2,1)=C(2,1)-YER*SLOP11*AK2*DZ*WIDTH/AK1
      C(2,2)=C(2,2)+YER*YER*SLOP11*AK2*DZ*WIDTH/AK1
      C(2,3)=C(2,3)-YER*SLOP12*DZ*WIDTH
      C(2,4)=C(2,4)+YER*YER*SLOP12*DZ*WIDTH
C
  200 IF(NV(3).EQ.0) GO TO 210
      C(3,1)=C(3,1)+SLOP21*DZ*HEIGHT
```

```
      C(3,2)=C(3,2)-YER*SLOP21*DZ*HEIGHT
      C(3,3)=C(3,3)+SLOP22*AK1*DZ*HEIGHT/AK2
      C(3,4)=C(3,4)-YER*SLOP22*AK1*DZ*HEIGHT/AK2
C
  210 IF(NV(4).EQ.0) GO TO 220
      C(4,1)=C(4,1)-YER*SLOP21*DZ*HEIGHT
      C(4,2)=C(4,2)+YER*YER*SLOP21*DZ*HEIGHT
      C(4,3)=C(4,3)-YER*SLOP22*AK1*DZ*HEIGHT/AK2
      C(4,4)=C(4,4)+YER*YER*SLOP22*AK1*DZ*HEIGHT/AK2
  220 IF(NWATCH.EQ.0) GO TO 90
      IF(NGOOD.EQ.-10) GO TO 240
      IF(NGOOD.EQ.0) GO TO 270
      IF(NT.NE.1) GO TO 230
      IF(K.EQ.1) NFLAT1=0
      ETX=CEMOD/4000.D0
      IF(DABS(E1T).LT.ETX.AND.DABS(E2T).LT.ETX)
     1NFLAT1=NFLAT1+1
  230 IF(NFLAT1.EQ.NLAYER) NFLAT=1
  240 NT=NSTYPE+1
      IF(NT.NE.1) GO TO 270
      IF(NTYPE.NE.3) GO TO 250
      WRITE(7,260)NSKIP(NT),K,E11,E22,S11,S22,E1U,E2U,E1T,
     1E2T,          SIG1C,SIG2C,E1UC,E2UC
      GO TO 270
  250 WRITE(7,260)NSKIP(NT),K,E11,E22,S11,S22,E1T,E2T
  260 FORMAT(1X,A1,I3,1X,E12.5,1X,E12.5,1X,F6.3,1X,F6.3,1X,
     1E12.5,1X,    E12.5,1X,F6.0,1X,F6.0,1X,F6.3,1X,F6.3,1X,
     2E12.5,1X,E12.5)
C
  270 CONTINUE
      RETURN
C
C
      END
      SUBROUTINE MATRIX
      IMPLICIT REAL*8(A-H,P-Z)
      DIMENSION NSKIP(4)
      COMMON/ALPHA/NV(4),P1(4),P2(4),M1,LAM
      COMMON/LOTUS/QP(4),C(4,4),CC(4,4),DQP(4),DSQ(4),DQ(4)
C
C     THIS SUBROUTINE FORMULATES THE COEFFICIENT MATRIX
C     'CT' TO FIND THE UNKNOWN VECTOR 'SMALL DELTA Q'...
C
      DO 10 J=1,4
      IF(NV(J).NE.0) GO TO 20
   10 CONTINUE
      LAM=0
      GO TO 110
C
   20 LAM=1
      NSK=0
      DO 90 LLL=1,4
      IF(NV(LLL).EQ.0) GO TO 80
      DO 70 L=1,LAM
      DO 70 LL=1,LAM
      LX=L
      LLX=LL
      IF(NSK.EQ.0) GO TO 40
      DO 30 II=1,NSK
      IF(LX.GE.NSKIP(II)) LX=LX+1
      IF(LLX.GE.NSKIP(II)) LLX=LLX+1
   30 CONTINUE
C
   40 IF(L.LT.LAM.AND.LL.LT.LAM) GO TO 70
      IF(L.LT.LAM.AND.LL.EQ.LAM) GO TO 50
      GO TO 60
   50 LLX=LLL
   60 CC(L,LL)=C(LX,LLX)
   70 CONTINUE
      IF(LLL.LT.4) LAM=LAM+1
      GO TO 90
   80 NSK=NSK+1
      NSKIP(NSK)=LLL
   90 CONTINUE
      LAM=0
      DO 100 J=1,4
      LAM=LAM+NV(J)
  100 CONTINUE
C
  110 RETURN
      END
      SUBROUTINE SOLVER
      IMPLICIT REAL*8(A-H,P-Z)
      COMMON/ALPHA/NV(4),P1(4),P2(4),M1,LAM
      COMMON/LOTUS/QP(4),C(4,4),CC(4,4),DQP(4),DSQ(4),DQ(4)
      DIMENSION SQ(4)
C
C     THIS SUBROUTINE SOLVES FOR 'SMALL DELTA Q' BY GAUSSIAN
C     ELIMINATION
C
      IJ=1
      DO 30 I=1,LAM
   10 IF(NV(IJ).NE.0) GO TO 20
      IJ=IJ+1
      GO TO 10
   20 DQ(I)=DQP(IJ)
      IJ=IJ+1
   30 CONTINUE
C
C
      DO 70 I=1,LAM
      DIV=CC(I,I)
      DO 40 J=I,LAM
      IF(DABS(CC(I,I)).LT.0.00001D0) GO TO 150
   40 CC(I,J)=CC(I,J)/DIV
      DQ(I)=DQ(I)/DIV
      NI=I+1
      IF(I.EQ.LAM) GO TO 70
```

```
      DO 60 II=NI,LAM
      CCIII=CC(II,I)
      DO 50 J=I,LAM
   50 CC(II,J)=CC(II,J)-CC(I,J)*CCIII
      DQ(II)=DQ(II)-CCIII*DQ(I)
   60 CONTINUE
   70 CONTINUE
C
C     BACK SUBSTITUTE
C
      DO 100 I=1,LAM
      K=LAM+1-I
      SQ(K)=DQ(K)
      IF(K.EQ.LAM) GO TO 90
      K10=I-1
      DO 80 KK=1,K10
      KKK=LAM+1-KK
      SQ(K)=SQ(K)-CC(K,KKK)*SQ(KKK)
   80 CONTINUE
C
   90 SQ(K)=SQ(K)/CC(K,K)
  100 CONTINUE
      DO 110 I=1,4
  110 DSQ(I)=0.D0
      IJ=1
      DO 140 I=1,LAM
  120 IF(NV(IJ).NE.0) GO TO 130
      IJ=IJ+1
      GO TO 120
  130 DSQ(IJ)=SQ(I)
      IJ=IJ+1
  140 CONTINUE
C
      RETURN
C
  150 WRITE(6,160)
  160 FORMAT(10X,
     1'ZERO ELEMENT ON MAIN DIAGONAL---PROGRAM TERMINATED')
      CALL RECAP
      CALL TIME(3,3)
      STOP
C
      END
      SUBROUTINE OUTPUT(NSTYPE,CLAYER,NLAYER,NRD)
      IMPLICIT REAL*8(A-H,P-Z)
      DIMENSION CLAYER(30,1),NRD(10)
C
C
      IF(NSTYPE.NE.0) GO TO 50
      WRITE(6,10)
   10 FORMAT(//20X,'***CONCRETE LAYERS***'//10X,'LAYER NO.',
     13X,'START  COORD',4X,'END COORD',8X,'STRAIN1',10X,
     2'STRAIN2',10X,'STRESS1',10  X,'STRESS2')
   20 DO 30 K=1,NLAYER
      WRITE(6,40)K,CLAYER(1,K),CLAYER(2,K),CLAYER(8,K),
     1CLAYER(9,K),     CLAYER(10,K),CLAYER(11,K)
   40 FORMAT(14X,I3,5X,F8.4,6X,F8.4,4X,4(5X,E12.5))
      RETURN
C
C
   50 IF(NSTYPE.NE.1) GO TO 100
      WRITE(6,60)
   60 FORMAT(//20X,'***STEEL REINFORCING LAYERS***'//10X,
     1'LAYER NO.',3X,'START COORD',5X,'END COORD',7X,
     2'DIRECTION',9X,'STRAIN',11X,   'STRESS')
      DO 80 K=1,NLAYER
      NN1=NRD(K)+11
      NN2=NRD(K)+13
      WRITE(6,70)K,CLAYER(1,K),CLAYER(2,K),NRD(K),
     1CLAYER(NN1,K),          CLAYER(NN2,K)
   70 FORMAT(14X,I3,5X,F8.4,6X,F8.4,12X,I3,6X,2(5X,E12.5))
   80 CONTINUE
      WRITE(6,90)
   90 FORMAT(//20X,'***NEGATIVE CONCRETE LAYERS***'//10X,
     1'LAYER NO.',3X,'START  COORD',4X,'END COORD',8X,
     2'STRAIN1',         10X,'STRAIN2',10X,'STRESS1',10X,
     3'STRESS2')
      GO TO 20
C
C
  100 WRITE(6,110)
  110 FORMAT(//20X,'*** PRESTRESSING LAYERS ***',//,10X,
     1'LAYER NO.',     3X,'START COORD',5X,'END COORD',8X,
     2'DIRECTION',8X,'STRAIN',11X,   'STRESS')
      DO 120 K=1,NLAYER
      NN1=NRD(K)+11
      NN2=NRD(K)+13
      WRITE(6,70)K,CLAYER(1,K),CLAYER(2,K),NRD(K),
     1CLAYER(NN1,K),          CLAYER(NN2,K)
  120 CONTINUE
      WRITE(6,90)
      GO TO 20
C
      END
      SUBROUTINE CONCRE(LC,LT1,LT2,K)
      IMPLICIT REAL*8(A-H,P-Z)
      COMMON/BNN/P1,R2,PC,PTC,CEMOD,POISS,NTYPE,NSTYPE,
     1WIDTH,HEIGHT
      COMMON/E26/E11,E22,S11,S22,SLOP11,SLOP12,SLOP21,SLOP22
      COMMON/BAYARI/YU,PE11,PE22,PS11,PS22,E10,E20,EIO,EIOT
      COMMON/MUIRA/E1T,E2T,E10C,E20C,SIG1C,SIG2C
      COMMON/SL280/TS11,TS22,TSLO11,TSLO22,NSUB
C
C     THIS SUBROUTINE CALLS THE PROPER CONCRETE
C     CONSTITUTIVE EQUATION
C
      GO TO (10,20,30,40),NTYPE
   10 CALL LINELC(LC,LT1,LT2,K)
```

```
C
      GO TO 40
   20 CALL DEPEND(LC,LT1,LT2,K)
      GO TO 40
   30 CALL SAME(LC,LT1,LT2,K)
   40 RETURN
      END
C
C
C
C
C
      SUBROUTINE LINELC(LC,LT1,LT2,K)
      IMPLICIT REAL*8(A-H,P-Z)
      COMMON/BNW/P1,R2,FC,FTC,CEMOD,POISS,NTYPE,NSTYPE,
     1WIDTH,HEIGHT
      DIMENSION NSKIP(3)
      COMMON/E26/E11,E22,S11,S22,SLOP11,SLOP12,SLOP21,SLOP22
      DATA NSKIP(1),NSKIP(2),NSKIP(3)/' ','S','P'/
C
C     THIS SUBROUTINE PRESENTS THE CONCRETE CONSTITUITIVE
C      EQUATIONS IN THE FORM OF A TWO PART ELASTIC CURVE
C     WITH A TENSION CUT-OFF.  THE TWO DIRECTIONS ARE
C     CONSIDERED AS BEING INDEPENDENT.  CRACK CLOSURE BU"
C     NO CRACK HEALING.  AFTER CRUSHING, THE CONCRETE IS
C     IGNOR"D IN BOTH DIRECTIONS IN BOTH TENSION AND
C     COMPRESSION...
C
      NT=NSTYPE+1
      NS1=0
      NS2=0
      IF(LC.GT.1) GO TO 140
      IF(E11.LT.-0.003500.OR.E22.LT.-0.003500)
     1GO TO 120
      YIELD=-1.D0*FC/CEMOD
      IF(E11.LT.YIELD) GO TO 80
   10 TEN=FTC/CEMOD
      IF(E11.LE.TEN) GO TO 40
   20 S11=0.D0
      IF(LT1.GT.1) GO TO 140
      LT1=3
      SLOP11=0.D0
      NDIR=1
      WRITE(6,30)NSKIP(NT),K,NDIR
   30 FORMAT(10X,'CONCRETE LAYER ',A1,I3,
     1' HAS FRACTURED IN THE DIRECTION#',5X,I3)
      GO TO 60
   40 IF(E11.LE.0.D0) GO TO 50
      IF(LT1.LT.1) GO TO 50
      GO TO 20
   50 S11=CEMOD*E11
      SLOP11=CEMOD
   60 IF(E22.LT.YIELD) GO TO 90
      IF(E22.LE.TEN) GO TO 100
      IF(LT2.GT.1) GO TO 170
   70 S22=0.D0
      LT2=3
      SLOP22=0.D0
      NDIR=2
      WRITE(6,30)NSKIP(NT),K,NDIR
      GO TO 150
   80 S11=-1.D0*FC
      SLOP11=0.D0
      NS1=1
      GO TO 60
   90 S22=-1.D0*FC
      SLOP22=0.D0
      NS2=1
      GO TO 150
  100 IF(E22.LE.0.D0) GO TO 110
      IF(LT2.LT.1) GO TO 110
      GO TO 170
  110 S22=CEMOD*E22
      SLOP22=CEMOD
      GO TO 150
  120 LC=3
      WRITE(6,130)NSKIP(NT),K
  130 FORMAT(10X,'CONCRETE LAYER ',A1,I3,' HAS CRUSHED')
  140 S11=0.D0
      S22=0.D0
      SLOP11=0.D0
      SLOP22=0.D0
C
  150 SLOP12=0.D0
      SLOP21=0.D0
      RETURN
  160 S11=0.D0
      SLOP11=0.D0
      GO TO 60
  170 S22=0.D0
      SLOP22=0.D0
      GO TO 150
      END
C
C
C
      SUBROUTINE DEPEND(LC,LT1,LT2,K)
      IMPLICIT REAL*8(A-H,P-Z)
      COMMON/BNW/R1,R2,FC,FTC,CEMOD,POISS,NTYPE,NSTYPE,
     1WIDTH,HEIGHT
      DIMENSION NSKIP(3)
      COMMON/E26/E11,E22,S11,S22,SLOP11,SLOP12,SLOP21,SLOP22
      DATA NSKIP(1),NSKIP(2),NSKIP(3)/' ','S','P'/
C
C     THIS SUBROUTINE PRESENTS THE CONCRETE CONSTITUITIVE
C     EQUATIONS IN THE FORM OF A TWO PART ELASTIC CURVE WITH
C     A TENSION CUT-OFF.  THE TWO DIRECTIONS ARE CONSIDERED
C     AS BEING INDEPENDENT.  CRACK CLOSURE BUT NO CRACK
```

```
C     HEALING.  AFTER CRUSHING, THE CONCRETE IS IGNORED IN
C     BOTH DIRECTIONS IN BOTH TENSION AND COMPRESSION...
C
      NT=NSTYPE+1
      NS1=0
      NS2=0
      IF(LC.GT.1) GO TO 140
      IF(E11.LT.-0.0035D0.OR.E22.LT.-0.0035D0)
     1GO TO 120
      YIELD=-1.D0*FC/CEMOD
      IF(E11.LT.YIELD) GO TO 80
   10 TEN=FTC/CEMOD
      IF(E11.LE.TEN) GO TO 40
   20 S11=0.D0
      IF(LT1.GT.1) GO TO 220
      LT1=3
      SLOP11=0.D0
      NDIR=1
      WRITE(6,30)NSKIP(NT),K,NDIR
   30 FORMAT(10X,'CONCRETE LAYER ',A1,I3,
     1' HAS FRACTURED IN THE DIRECTION',5X,I3)
      GO TO 60
   40 IF(E11.LE.0.D0) GO TO 50
      IF(LT1.LT.1) GO TO 50
      GO TO 20
   50 NS1=5
      SLOP11=CEMOD
   60 IF(E22.LT.YIELD) GO TO 90
      IF(E22.LE.TEN) GO TO 100
      IF(LT2.GT.1) GO TO 230
   70 S22=0.D0
      LT2=3
      SLOP22=0.D0
      NDIR=2
      WRITE(6,30)NSKIP(NT),K,NDIR
      GO TO 150
   90 S11=-1.D0*FC
      SLOP11=0.D0
      GO TO 60
   90 S22=-1.D0*FC
      SLOP22=0.D0
      GO TO 150
  100 IF(E22.LE.0.DG) GO TO 110
      IF(LT2.LT.1) GO TO 110
      GO TO 230
  110 NS2=5
      SLOP22=CEMOD
      GO TO 150
  120 LC=3
      WRITE(6,130)NSKIP(NT),K
  130 FORMAT(10X,'CONCRETE LAYER ',A1,I3,' HAS CRUSHED')
  140 S11=0.D0
      S22=0.D0
      SLOP11=0.D0
      SLOP22=0.D0
      SLOP12=0.D0
      SLOP21=0.D0
      GO TO 210
C
  150 SLOP12=POISS*DSQRT(SLOP11*SLOP22)
      SLOP21=SLOP12
      IF(LC.GT.1) GO TO 210
      IF(NS2.NE.5) GO TO 180
      IF(LT1.LT.1) GO TO 160
      S22=CEMOD*E11
      GO TO 180
  160 YFC=-1.D0*FC
      IF(S11.LE.YFC) GO TO 170
      BOTTOM=1.D0-POISS*POISS
      S22=(SLOP22*E22+POISS*DSQRT(SLOP22*SLOP11)*E11)/BOTTOM
      GO TO 180
  170 S22=SLOP22*E22+POISS*S11
  180 IF(NS1.NE.5) GO TO 210
      IF(LT2.LT.1) GO TO 190
      S11=CEMOD*E11
      GO TO 210
  190 YFC=-1.D0*FC
      IF(S22.LE.YFC) GO TO 200
      BOTTOM=1.D0-POISS*POISS
      S11=(SLOP11*E11+POISS*DSQRT(SLOP11*SLOP22)*E22)/BOTTOM
      GO TO 210
  200 S11=SLOP11*E11+POISS*S22
  210 RETURN
  220 S11=0.D0
      SLOP11=0.D0
      GO TO 60
  230 S22=0.D0
      SLOP22=0.D0
      GO TO 150
      END
      SUBROUTINE SAENZ(LC,LT1,LT2,K)
      IMPLICIT REAL*8(A-H,P-Z)
      COMMON/BNW/R1,R2,FC,FTC,CEMOD,POISS,NTYPE,NSTYPE,
     1WIDTH,HEIGHT
      COMMON/E26/E11,E22,S11,S22,SLOP11,SLOP12,SLOP21,SLOP22
      COMMON/BAVASI/VU,PE11,PE22,PS11,PS22,E1U,E2U,EIO,EIOT
      COMMON/MUIRA/E1T,E2T,E1UC,E2UC,SIG1C,SIG2C
      COMMON/SL280/TS11,TS22,TSLO11,TSLO22,NSUB
      COMMON/BORA/KDO,NPDO,KP,NCRP,PCRP
      DIMENSION NSKIP(3)
      DATA NSKIP(1),NSKIP(2),NSKIP(3)/' ','S','P'/
C
C
      KCH=0
      EXCEM=1.D0
      PT=1.D0
      FPC=-1.D0*FC
      PSIG1=PS11
```

```
      PSIG2=PS22
      E111=PE11
      E222=PE22
      S10C=TSLO11
      E20C=TSLO22
      CEMODT=CEMOD
      IF(CEMOD.GT.0.D0) GO TO 10
      CEMOD=-1.D0*CEMOD
      EXCEM=FCRP
   10 NT=NSTYPE+1
      ESMALL=CEMOD/4000.D0
      IF(DABS(E1).LT.ESMALL.AND.DABS(E2).LT.ESMALL)
     1GO TO 20
      IF(NSUB.GT.0) GO TO 30
      ZSUB10=(E11-PE11)/.14D-4
      ZSUB20=(E22-PE22)/.14D-4
      ZSUB30=(E11+E22-PE11-PE22)/.7D-5
      ZSUB10=DABS(ZSUB10)
      IF(DABS(ZSUB20).GT.ZSUB10) ZSUB10=DABS(ZSUB20)
      IF(DABS(ZSUB30).GT.ZSUB10) ZSUB10=DABS(ZSUB30)
      OO4=SNGL(ZSUB10)
      NSUB1=INT(OO4)+1
      GO TO 40
   20 NSUB1=1
      GO TO 40
   30 NSUB1=NSUB
   40 IF(NSUB1.GT.100) NSUB1=100
      XSUB=FLOAT(NSUB1)
      KCH=0
      DE11=(E11-PE11)/XSUB
      DE22=(E22-PE22)/XSUB
C
C
      DO 480 KK=1,NSUB1
      NRUN=0
      IF(LC.GT.0) GO TO 450
   50 E1=SLOP11*(1.D0-VU*VU)
      E2=SLOP22*(1.D0-VU*VU)
   60 SCHANG=1.D0
      SIGN=1.D0
      IF(E1.GT.0.D0.AND.E2.LT.0.D0) SCHANG=-1.D0
      IF(E1.LT.0.D0.AND.E2.GT.0.D0) SCHANG=-1.D0
      IF(E1.LT.0.D0.AND.E2.LT.0.D0) SIGN=-1.D0
      IF(DABS(PS11).GT.DABS(PS22).AND.E1.LT.0.D0)
     1SIGN=-1.D0
      IF(DABS(PS22).GT.DABS(PS11).AND.E2.LT.0.D0)
     1SIGN=-1.D0
      SQ=DSQRT(SCHANG*E1*E2)
      SLOP12=VU*SIGN*SQ/(1.D0-VU*VU)
      SLOP21=SLOP12
      DSIG1=SLOP11*DE11+SLOP12*DE22
      DSIG2=SLOP21*DE11+SLOP22*DE22
      IF(E1.EQ.0.D0) GO TO 70
      DE1U=DSIG1/E1
      GO TO 80
   70 DE1U=0.D0
   80 IF(E2.EQ.0.D0) GO TO 90
      DE2U=DSIG2/E2
      GO TO 100
   90 DE2U=0.D0
  100 IF(NSUB1.GE.99) GO TO 130
      IF(KK.NE.1) GO TO 130
      IF(E1UC.EQ.0.D0) GO TO 110
      RATT1=E1U/E1UC
      IF(RATT1.GT.2.D0.OR.RATT1.LT.0.5D0) GO TO 110
      CMAX=DABS(.05D0*E1UC)
      CMAX1=-1.D0*CMAX
      IF(DE1U.GT.CMAX) KCH=1
      IF(DE1U.LT.CMAX1) KCH=1
  110 IF(E2UC.EQ.0.D0) GO TO 120
      RATT2=E2U/E2UC
      IF(RATT2.GT.2.D0.OR.RATT2.LT.0.5D0) GO TO 120
      CMAX=DABS(0.05D0*E2UC)
      CMAX1=-1.D0*CMAX
      IF(DE2U.GT.CMAX) KCH=1
      IF(DE2U.LT.CMAX1) KCH=1
  120 IF(KCH.EQ.0) GO TO 130
      NSUB1=NSUB1*5
      GO TO 40
  130 TE1U1=E1U+DE1U
      TE2U1=E2U+DE2U
  140 PSIG1=PS11
      PSIG2=PS22
  150 E1T=E1
      E2T=E2
C
C     CHECK FOR CRACK CLOSURE
C
  160 IF(TE1U1.LT.0.D0.AND.TE2U1.LT.0.D0) GO TO 210
      XXSUB=FLOAT(KK)
      E11X=PE11+XXSUB*DE11
      E22X=PE22+XXSUB*DE22
      SSIGN=1.D0
      IF(LT1.GT.-60.AND.LT2.GT.-60) GO TO 210
      IF(LT1.LE.-60.AND.LT2.LE.-60) GO TO 190
      IF(LT1.LE.-60) GO TO 180
  170 IF(TE2U1.LT.0.) GO TO 210
      IF(E1T.LT.0.D0) SSIGN=-1.D0
      EPS2=-1.D0*VU*SSIGN*DSQRT(DABS(E1T)/CEMOD)*E11X
      IF(E22X.GT.EPS2) GO TO 210
      E2U=-.1D-6
      TE2U1=-.1D-6
      GO TO 210
  180 IF(TE1U1.LT.0.D0) GO TO 210
      IF(E2T.LT.0.D0) SSIGN=-1.D0
      EPS1=-1.D0*VU*SSIGN*DSQRT(DABS(E2T)/CEMOD)*E22X
      IF(E11X.GT.EPS1) GO TO 210
      E1U=-.1D-6
```

```
      TE101=-.1D-6
      GO TO 210
  190 IF(TE101.LT.0.D0) GO TO 170
      IF(TE201.LT.0.D0) GO TO 180
      IF(E11X.GT.0.D0) GO TO 200
      E10=-.1D-6
      TE101=-.1D-6
  200 IF(E22X.GT.0.D0) GO TO 210
      E20=-.1D-6
      TE201=-.1D-6
C
C
  210 CALL FAILUR(NQUAD,KQUAD,FPC,FTC,LC,LT1,LT2,POISS,
     1TE101,TE201,R,RX,RT,PSIG1,PSIG2)
C
  220 CALL STRESS(LC,LT1,LT2,POISS,EXCEN,CENOD,SIG1,SIG2,
     1TE101,TE201,R,RX,RT,PSIG1,PSIG2,E10P,E20P,DE11,DE22)
C
C
  230 PSIG1=SIG1
      PSIG2=SIG2
  240 IF(NQUAD.EQ.3) GO TO 250
      LC=0
      IF(E1T.LT.0.D0) LC=-10
      IF(E2T.LT.0.D0) LC=-20
      IF(E1T.LT.0.D0.AND.E2T.LT.0.D0) LC=-30
  250 EMIN=CENOD/400.D0
      EMIN1=-1.D0*EMIN
  260 IF(E1T.GT.0.D0.AND.E1T.LT.EMIN) E1T=EMIN
      IF(E1T.LT.0.D0.AND.E1T.GT.EMIN1) E1T=EMIN1
      IF(E2T.GT.0.D0.AND.E2T.LT.EMIN) E2T=EMIN
      IF(E2T.LT.0.D0.AND.E2T.GT.EMIN1) E2T=EMIN1
      NRUN=NRUN+1
      IF(NRUN.EQ.2) GO TO 160
      IF(NRUN.EQ.3) GO TO 330
      DENOM=1.D0-VU*VU
  270 SCHANG=1.D0
      SIGN=+1.D0
      IF(E1T.LT.0.D0.AND.E2T.GT.0.D0) SCHANG=-1.D0
      IF(E1T.GT.0.D0.AND.E2T.LT.0.D0) SCHANG=-1.D0
      IF(E1T.LT.0.D0.AND.E2T.LT.0.D0) SIGN=-1.D0
      IF(DABS(PSIG1).GT.DABS(PSIG2).AND.E1T.LT.0.D0)
     1SIGN=-1.D0
      IF(DABS(PSIG2).GT.DABS(PSIG1).AND.E2T.LT.0.D0)
     1SIGN=-1.D0
      SQ=DSQRT(SCHANG*E1T*E2T)
      DSIG1=(E1T*DE11+VU*SIGN*SQ*DE22)/DENOM
      DSIG2=(VU*SIGN*SQ*DE11+E2T*DE22)/DENOM
      IF(E1T.EQ.0.D0) GO TO 280
      DE102=DSIG1/E1T
      GO TO 290
  280 DE102=0.D0
  290 IF(E2T.EQ.0.D0) GO TO 300
      DE202=DSIG2/E2T
      GO TO 310
  300 DE202=0.D0
  310 E10=E10+(DE10+DE102)/2.D0
      E20=E20+(DE20+DE202)/2.D0
  320 TE101=E10
      TE201=E20
      GO TO 160
  330 S11=SIG1
      S22=SIG2
      DENOM=(1.D0-VU*VU)
      IF(NQUAD.NE.3) GO TO 350
      SIGLS=1.005D0*FTC/7.5D0
      SIGLT=0.995D0*FTC/7.5D0
      IF(E1T.GE.0.D0) GO TO 340
      IF(SIG1.LT.SIGLS.AND.SIG1.GT.SIGLT) E1T=0.D0
  340 IF(E2T.GE.0.D0) GO TO 350
      IF(SIG2.LT.SIGLS.AND.SIG2.GT.SIGLT) E2T=0.D0
  350 SLOP11=E1T/DENOM
      SCHANG=1.D0
      SIGN=1.D0
      IF(E1T.GT.0.D0.AND.E2T.LT.0.D0) SCHANG=-1.D0
      IF(E1T.LT.0.D0.AND.E2T.GT.0.D0) SCHANG=-1.D0
      IF(E1T.LT.0.D0.AND.E2T.LT.0.D0) SIGN=-1.D0
      IF(DABS(PSIG1).GT.DABS(PSIG2).AND.E1T.LT.0.D0)
     1SIGN=-1.D0
      IF(DABS(PSIG2).GT.DABS(PSIG1).AND.E2T.LT.0.D0)
     1SIGN=-1.D0
      SQ=DSQRT(SCHANG*E1T*E2T)
      SLOP12=VU*SIGN*SQ/DENOM
      SLOP21=SLOP12
      SLOP22=E2T/DENOM
C
C     CHECK FOR UNLOADING ON DECLINING BRANCH
C
      E1UCI=E1UC
      E2UCI=E2UC
      IF(E1UC.EQ.0.D0) E1UCI=E1U
      IF(E2UC.EQ.0.D0) E2UCI=E2U
      IF(E1UCI.NE.0.D0) GO TO 360
      RATE1=1.D0
      GO TO 370
  360 RATE1=E1U/E1UCI
  370 IF(E2UCI.NE.0.D0) GO TO 380
      RATE2=1.D0
      GO TO 390
  380 RATE2=E2U/E2UCI
  390 TS11=RATE1
      TS22=RATE2
C
C
      IF(NQUAD.NE.1) GO TO 400
      IF(E1U.LT.E1UP.AND.E2U.LT.E2UP) GO TO 440
      GO TO 460
  400 IF(NQUAD.EQ.2) GO TO 410
```

```
      IF(NQUAD.EQ.4) GO TO 420
      IF(NQUAD.EQ.3) GO TO 460
  410 IF(E2U.GT.E2UF.AND.E1U.LT.E1UF) GO TO 440
      GO TO 460
  420 IF(E1U.GT.E1UF.AND.E2U.LT.E2UF) GO TO 440
      GO TO 460
  430 IF(LT1.GT.0.OR.LT2.GT.0) GO TO 460
      NDIR=1
      LT1=3
C     WRITE(6,501) NSKIP(NT),K,NDIR
      NDIR=2
      LT2=3
C     WRITE(6,501)NSKIP(NT),K,NDIR
      GO TO 460
  440 LC=3
C     WRITE(6,502)NSKIP(NT),K
  450 S11=0.D0
      S22=0.D0
      SLOP11=0.D0
      SLOP12=0.D0
      SLOP21=0.D0
      SLOP22=0.D0
      YU=0.D0
      GO TO 490
C
C
  460 IF(LC.GT.0) GO TO 490
  470 IF(KK.EQ.NSUB1) GO TO 480
      PS11=SIG1
      PS22=SIG2
  480 CONTINUE
  490 CPROD=CESODI
      TSLO11=E1UC
      TSLO22=E2UC
  500 RETURN
C
  510 FORMAT(10X,'CONCRETE LAYER ',A1,I3,
     1' HAS FRACTURED IN THE DIRECTION',2X,I3)
  520 FORMAT(10X,'CONCRETE LAYER ',A1,I3,' HAS CRUSHED')
C
      END
      SUBROUTINE STZEL(NSTYPE,FYR,ER,NSBD,K,FRAC,YIELD)
      IMPLICIT REAL*8(A-H,P-Z)
      COMMON/E26/E11,E22,S11,S22,SLOP11,SLOP12,SLOP21,SLOP22
      DIMENSION PL(8),SL(7)
      DATA PL(1),PL(3),PL(4),PL(5),PL(6),PL(7),PL(8)/0.D0,
     1.0004D0,      .01000,.01200,.02000,.25000,1.D0/
      DATA SL(1),SL(2),SL(3),SL(4),SL(5),SL(6),SL(7)/0.D0,
     10.777D0,      0.464D0,0.896D0,0.9099D0,0.9479D0,1.000D0/
C
C     NSTYPE=1    REINFORCING BAR
C     NSTYPE=2    PRESTRESSING WIRE
C
      GO TO (10,220),NSTYPE
C
C
C           ...REINFORCING BAR...
C
   10 ET=FYR/ER
      IF(FRAC.GT.0.1000) GO TO 60
      GO TO (20,150),NSBD
   20 IF(E11.LT.-0.1000) GO TO 100
      IF(E11.LT.(-1.D0*ET)) GO TO 110
      IF(E11.LT.ET) GO TO 130
      IF(E11.LE.0.1000) GO TO 140
C 115 WRITE(6,109)K
   30 FORMAT(10X,'STEEL LAYER',5X,I3,' HAS FRACTURED')
   40 CONTINUE
   50 FRAC=1.05D0
   60 S11=0.D0
   70 SLOP11=0.D0
   80 S22=0.D0
      SLOP21=0.D0
      SLOP22=0.D0
      SLOP12=0.D0
      GO TO 210
C
C  85 WRITE(6,111)K
   90 FORMAT(10X,'STEEL LAYER ',4X,I3,' HAS CRUSHED')
  100 FRAC=1.05D0
      GO TO 40
  110 S11=-1.D0*FYR
      IF(YIELD.GT.0.1000) GO TO 70
      YIELD=1.05D0
C     WRITE(6,140)K
  120 FORMAT(10X,'STEEL LAYER ',4X,I3,' HAS YIELDED')
      GO TO 70
  130 S11=ER*E11
      SLOP11=ER
      GO TO 80
  140 S11=FYR
      IF(YIELD.GT.0.100) GO TO 70
C     WRITE(6,140)K
      YIELD=1.05D0
      GO TO 70
C
  150 IF(E22.LT.-0.1000) GO TO 100
      IF(E22.LT.(-1.D0*ET)) GO TO 160
      IF(E22.LT.ET) GO TO 170
      IF(E22.LT.0.1000) GO TO 180
      GO TO 40
  160 S22=-1.D0*FYR
      IF(YIELD.GT.0.1000) GO TO 190
      YIELD=1.05D0
C     WRITE(6,140)K
      GO TO 190
  170 S22=ER*E22
      SLOP22=ER
      GO TO 200
```

```
180 S22=FYR
    IF(YIELD.GT.0.1D0) GO TO 190
    YIELD=1.05D0
C     WRITE(6,140)K
190 SLOP22=0.D0
200 S11=0.D0
    SLOP12=0.D0
    SLOP11=0.D0
    SLOP21=0.D0
C
210 RETURN
C
C          ...PRESTRESSING WIRE...
C
C
220 IF(FRAC.GT.0.1D0) GO TO 60
    PSIGN=1.D0
    PL(2)=0.777D0*FYR/ER
    IF(NWPD.EQ.1) EXX=E11
    IF(NWPD.EQ.2) EXX=E22
    IF(EXX.LT.0.D0) PSIGN=-1.D0
    EXX=DABS(EXX)
    DO 230 KP=1,7
    KP1=KP+1
    IF(EXX.GT.PL(KP).AND.EXX.LE.PL(KP1)) GO TO 240
230 CONTINUE
240 IF(KP.EQ.7) GO TO 250
    SLOP11=FYR*(SL(KP1)-SL(KP))/(PL(KP1)-PL(KP))
    S11=SL(KP)*FYR+SLOP11*(EXX-PL(KP))
    GO TO 260
250 IF(PSIGN.GT.0.D0) GO TO 240
    GO TO 300
260 S11=PSIGN*S11
    IF(NWPD.EQ.2) GO TO 270
    GO TO 80
270 S22=S11
    SLOP22=SLOP11
    GO TO 200
280 WRITE(6,290)K
290 FORMAT(10X,'PRESTRESS LAYER ',I3,' HAS FRACTURED')
    GO TO 50
300 WRITE(6,310)K
310 FORMAT(10X,'PRESTRESS LAYER ',I3,' HAS CRUSHED')
    GO TO 50
C
    END
C
C
    SUBROUTINE RECAP
    IMPLICIT REAL*8(A-H,P-Z)
    COMMON/BRW/R1,R2,FC,FTC,CERCD,POISS,NTYPE,NSTYPE,
   1WIDTH,HEIGHT
    COMMON/DIBO/CLAYER(30,100),T,NLAYER
    COMMON/JARAMA/PLAYER(30,10),FYP,EP,PCEN(10),AREAP(10)
   1,PFORCE(10),NPN(10),NPBE,NPD(10)
    COMMON/URACCO/SLAYER(30,10),FYR,ER,RCEN(10),AREAR
   1(10),NREBAR,NRD(10)
C
C     INSIDE CRACKING OR CRUSHING
C
    TBY2=T/2.D0
    CRIO1=0.D0
    CRIO2=0.D0
    CSHI=0.D0
    CRI1=0.D0
    CRI2=0.D0
    NOPEN=0
    NINE=8
    BONE=1.D0
    IF(NTYPE.NE.3) GO TO 10
    NINE=18
    BONE=-1.D0
 10 DO 30 K=1,NLAYER
    CLA=BONE*CLAYER(5,K)
    IF(CLA.LT.1.D0) GO TO 40
    IF(CLAYER(20,K).GT.0.D0.AND.NTYPE.EQ.1) GO TO 40
    CRI1=CLAYER(2,K)+TBY2
    IF(NOPEN.EQ.1) GO TO 30
    IF(CLAYER(NINE,K).GT.0.D0) GO TO 20
    NOPEN=1
    GO TO 30
 20 CRIO1=CLAYER(2,K)+TBY2
 30 CONTINUE
 40 NOPEN=0
    NINE=NINE+1
    DO 60 K=1,NLAYER
    CLA=BONE*CLAYER(6,K)
    IF(CLA.LT.1.D0) GO TO 70
    IF(CLAYER(21,K).GT.0.D0.AND.NTYPE.EQ.1) GO TO 70
    CRI2=CLAYER(2,K)+TBY2
    IF(NOPEN.EQ.1) GO TO 60
    IF(CLAYER(NINE,K).GT.0.D0) GO TO 50
    NOPEN=1
    GO TO 60
 50 CRIO2=CLAYER(2,K)+TBY2
 60 CONTINUE
 70 DO 90 K=1,NLAYER
    CLA=BONE*CLAYER(4,K)
    IF(CLA.GE.-1.D0.AND.CLA.LE.1.D0) GO TO 100
    IF(NTYPE.EQ.1) GO TO 80
    IF(CLAYER(25,K).LT.0.D0.AND.CLAYER(20,K).LT.0.D0)
   1GO TO 80
    IF(CLAYER(26,K).LT.0.D0.AND.CLAYER(21,K).LT.0.D0)
   1GO TO 80
    GO TO 100
 80 CSHI=CLAYER(2,K)+TBY2
 90 CONTINUE
100 WRITE(6,260)
```

```
C
C     OUTSIDE CRACKING OR CRUSHING
      TT=T-0.05D0
      CSHO=0.D0
      CRO1=0.D0
      CRO2=0.D0
      CROO1=0.D0
      CROO2=0.D0
      NOPEN=0
      NINE=NINE-1
      DO 120 K=1,NLAYER
      KK=NLAYER+1-K
      CLA=BONE*CLAYER(5,KK)
      IF(CLA.LT.1.D0) GO TO 130
      IF(CLAYER(20,KK).GT.0.D0.AND.NTYPE.EQ.1)
     1GO TO 130
      CRO1=TBI2-CLAYER(1,KK)
      IF(NOPEN.EQ.1) GO TO 120
      IF(CLAYER(NINE,KK).GT.0.D0) GO TO 110
      NOPEN=1
      GO TO 120
  110 CROO1=TBI2-CLAYER(1,KK)
  120 CONTINUE
  130 NOPEN=0
      NINE=NINE+1
      DO 150 K=1,NLAYER
      KK=NLAYER+1-K
      CLA=BONE*CLAYER(6,KK)
      IF(CLA.LT.1.D0) GO TO 160
      IF(CLAYER(21,KK).GT.0.D0.AND.NTYPE.EQ.1)
     1GO TO 160
      CRO2=TBI2-CLAYER(1,KK)
      IF(NOPEN.EQ.1) GO TO 150
      IF(CLAYER(NINE,KK).GT.0.D0) GO TO 140
      NOPEN=1
      GO TO 150
  140 CROO2=TBI2-CLAYER(1,KK)
  150 CONTINUE
  160 DO 180 K=1,NLAYER
      KK=NLAYER+1-K
      CLA=BONE*CLAYER(4,KK)
      IF(CLA.GE.-1.D0.AND.CLA.LE.1.D0) GO TO 190
      IF(NTYPE.EQ.1) GO TO 170
      IF(CLAYER(25,KK).LT.0.D0.AND.CLAYER(20,KK).LT.0.D0)
     1GO TO 170
      IF(CLAYER(26,KK).LT.0.D0.AND.CLAYER(21,KK).LT.0.D0)
     1GO TO 170
      GO TO 190
  170 CSHO=TBI2-CLAYER(1,KK)
  180 CONTINUE
C
  190 NI=1
      WRITE(6,270)CRI1,NI
      IF(CRI1.GE.TT) WRITE(6,280)
      WRITE(6,380)CRIO1,NI
      NI=2
      WRITE(6,270)CRI2,NI
      IF(CRI2.GE.TT) WRITE(6,280)
      WRITE(6,380)CRIO2,NI
      NI=1
      WRITE(6,310)CRO1,NI
      IF(CRO1.GE.TT) WRITE(6,280)
      WRITE(6,390)CROO1,NI
      NI=2
      WRITE(6,310)CRO2,NI
      IF(CRO2.GE.TT) WRITE(6,280)
      WRITE(6,390)CROO2,NI
      WRITE(6,290)CSHI
      IF(CSHI.GE.TT) WRITE(6,300)
      WRITE(6,320)CSHO
      IF(CSHO.GE.TT) WRITE(6,300)
C
C
      WRITE(6,330)
      LDAM=0
      DO 220 K=1,NREBAR
      IF(SLAYER(7,K).GE.2.D0) GO TO 200
      IF(SLAYER(16,K).GE.1.D0) GO TO 210
      GO TO 220
  200 WRITE(6,350)K
      LDAM=1
      GO TO 220
  210 WRITE(6,340)K
      LDAM=1
  220 CONTINUE
      IF(LDAM.GT.0) GO TO 230
      WRITE(6,370)
  230 LDAM=0
      WRITE(6,360)
      DO 240 K=1,NPRE
      IF(PLAYER(7,K).LT.1.D0) GO TO 240
      LDAM=1
      WRITE(6,350)K
  240 CONTINUE
      IF(LDAM.GT.0) GO TO 250
      WRITE(6,370)
  250 RETURN
  260 FORMAT(//15X,'***DAMAGE SUMMARY***',///20X,
     1'1. CONCRETE',//        30X,'DAMAGE TYPE',13X,
     2'DEPTH OF DAMAGE',10X,'DIRECTION')
  270 FORMAT(30X,'INSIDE  CRACKED',12X,F8.2,15X,I2)
  280 FORMAT('+',89X,'THROUGH CRACKING')
  290 FORMAT(30X,'INSIDE  CRUSHED',12X,F8.2)
  300 FORMAT('+',89X,'THROUGH CRUSHING')
  310 FORMAT(30X,'OUTSIDE CRACKED',12X,F8.2,15X,I2)
  320 FORMAT(30X,'OUTSIDE CRUSHED',12X,F8.2)
  330 FORMAT(//20X,'2. REINFORCING STEEL',//
     130X,'DAMAGE TYPE',10X,'LAYER NO.')
```

```
340 FORMAT(30X,'YIELD',10X,I4)
350 FORMAT(30X,'FRACTURE',15X,I4)
360 FORMAT(//20X,'3. PRESTRESSING STEEL'/
   130X,'DAMAGE TYPE',10X,'LAYER NO.')
370 FORMAT(30X,'-NO DAMAGE-')
380 FORMAT(30X,'INSIDE  CRACKED AND OPEN',3X,F8.2,15X,I2)
390 FORMAT(30X,'OUTSIDE CRACKED AND OPEN',3X,F8.2,15X,I2)
    END
    SUBROUTINE SRATIO(*,*,ERR2,NGOOD)
    IMPLICIT REAL*8(A-H,P-Z)
    COMMON/CS3PTO/T1,T2,T3,ALPHAC,ALPHAS,NTHERM,NTCODE
    COMMON/LOTUS/QP(4),C(4,4),CC(4,4),DQP(4),DSQ(4),DQ(4)
    COMMON/ALPHA/NV(4),P1(4),P2(4),N1,LAM
    COMMON/WOLFW5/AXS1,AXS2,NWORK
    COMMON/E26/E11,E22,S11,S22,SLOP11,SLOP12,SLOP21,SLOP22
    DIMENSION ERR2(4)
C     NBOUNC=0
    IF(NBOUNC.LT.0) NBOUNC=0
    IF(QP(3).NE.0.D0) GO TO 10
    RAT1=10000.D0
    GO TO 20
 10 RAT1=QP(1)/QP(3)
 20 RAT2=T1/T2
    IF(RAT2.NE.0.D0) GO TO 30
    PERT=RAT1
    GO TO 40
 30 PERT=(RAT2-RAT1)/RAT2
 40 XMIN=.01D0
    XMIN1=C(3,3)/AXS2
    IF(DABS(XMIN1).LT.XMIN) XMIN=0.005DC
    IF(DABS(PERT).LT.XMIN.AND.NGOOD.EQ.1) GO TO 110
    IF(RAT2.NE.0.D0) GO TO 50
    DQQ=-1.D0*QP(3)
    GO TO 60
 50 QQ=QP(1)/RAT2
    DQQ=QQ-QP(3)
 60 XINC1=DABS(C(3,3))/AXS2
    DSQQ2=XINC1*DQQ*C(1,1)/(C(1,1)*C(3,3)-C(1,3)*C(3,1))
    DSQQ1=-1.*C(1,3)*DSQQ2/C(1,1)
    IF(SLOP11.LT.0.D0.AND.SLOP22.GT.0.D0) GO TO 70
    GO TO 80
 70 NBOUNC=NBOUNC+1
    BOUNCE=FLOAT(NBOUNC)
    DSQQ2=DSQQ2*BOUNCE*E22*SLOP12**2/(DABS(SLOP11)*DABS(
   1SLOP22)        *5.D0)
 80 IF(NBOUNC.GT.3) GO TO 120
    GO TO 100
 90 IF(DSQQ2.LT.0.D0.AND.E22.LT.0.D0) GO TO 100
    IF(DSQQ2.GT.0.D0.AND.E22.GT.0.D0) GO TO 100
    IF(SLOP22.LT.0.D0) GO TO 120
100 ERR2(3)=ERR2(3)+DSQQ2
    ERR2(1)=ERR2(1)+DSQQ1
    IF(DABS(PERT).LT.XMIN)NGOOD=1
    RETURN 2
110 NBOUNC=0
    RETURN 1
120 WRITE(7,130)
130 FORMAT(10X,'NBOUNC IS GREATER THAN 3')
    GO TO 150
140 IF(NBOUNC.LE.1) GO TO 150
    BOUNCE=BOUNCE-1.D0
    P2(3)=P2(3)-BOUNCE*E22*SLOP12**2/(DABS(SLOP11)*DABS(
   1SLOP22)        *5.D0)
150 NBOUNC=0
    RETURN
    END
    SUBROUTINE WORK1(NGOOD,C11,C33,ERR2,PREV3,NPLAT)
    IMPLICIT REAL*8(A-H,P-Z)
    COMMON/ALPHA/NV(4),P1(4),P2(4),N1,LAM
    COMMON/BMW/B1,B2,PC,PTC,CEBOD,POISS,NTYPE,NSTYPE,
   1WIDTH,HEIGHT
    COMMON/LOTUS/QP(4),C(4,4),CC(4,4),DQP(4),DSQ(4),DQ(4)
    COMMON/DINO/CLAYER(30,100),T,NLAYER
    COMMON/UBACCO/SLAYER(30,10),FYR,ER,NCER(10),AREAR
   1(10),NREBAR,NRD(10)
    COMMON/JARAMA/PLAYER(30,10),FYP,EP,PCEN(10),AREAP(10)
   1,PFORCP(10),NPN(10),NPRE,XPD(10)
    COMMON/ESPADA/GUI(4),PREV(4),PREV1(4)
    COMMON/E26/E11,E22,S11,S22,SLOP11,SLOP12,SLOP21,SLOP22
    COMMON/ETYPE/NPX(10),NPASS,JLP,KPT
    COMMON/BAYARI/YU,PE11,PE22,PS11,PS22,E1U,E2U,EIO,EIOT
    COMMON/MUIBA/E1T,E2T,E1UC,E2UC,SIG1C,SIG2C
    COMMON/SL280/TS11,TS22,TSLO11,TSLO22,NSUB
    COMMON/CS3PTO/T1,T2,T3,ALPHAC,ALPHAS,NTHERM,NTCODE
    COMMON/WOLFW5/AXS1,AXS2,NWORK
    DIMENSION ERR2(4),PREV3(4),NCE(4)
 10 NW1=0
    NCOUNT=1
    IF(NTHERM.NE.-1.AND.N1.EQ.0) NGOOD=1
    DO 20 I2=1,4
    NW1=NW1+NV(I2)
    NCE(I2)=0
 20 CONTINUE
    NW1=2*NW1
    IF(NTYPE.GE.3) NW1=NW1+5
    NW=0
    IF(NWORK.EQ.00)NGOOD=1
 30 DO 40 KK=1,4
    QP(KK)=0.D0
    DO 40 K=1,4
 40 C(KK,K)=0.D0
    NSTYPE=0
    CALL LOOP(NLAYER,CLAYER,FYR,ER,XPD,NGOOD,*PLAT)
    IF(NGOOD.NE.1) GO TO 50
    C11=C(1,1)
    C33=C(3,3)
 50 IF(NREBAR.LT.1) GO TO 60
    NSTYPE=1
```

```
      CALL LOOP(NBREAB,SLAYER,FYP,EP,EPP,NGOOD,NFLAT)
   60 IF(NPRE.LT.1) GO TO 70
      NSTYPE=2
      CALL LOOP(NPRE,PLAYER,FYP,EP,EPP,NGOOD,NFLAT)
   70 IF(NTHERE.NE.-1) GO TO 90
   80 CALL SRATIO(&340,&350,EPP2,NGOOD)
   90 IF(N1.EQ.0)GO TO 360
      IF(NGOOD.EQ.1.AND.NWORK.GT.0) GO TO 360
      IF(NWORK.EQ.0.AND.NGOOD.EQ.2) GO TO 360
C
C
  100 DO 110 I3=1,4
      IF(NV(I3).EQ.0) GO TO 110
      W1=DABS(F1(I3)-QP(I3))
      W2=DABS(F1(I3)-PREV3(I3))
      IF(W2.GT.W1) GO TO 120
      IF(NW.GT.NW1) GO TO 370
      NW=NW+1
  110 CONTINUE
      GO TO 130
  120 NW=0
C
C
  130 BIG=DABS(F1(1))
      DO 140 I4=2,4
      IF(NV(I4).EQ.0) GO TO 140
      F1AA=DABS(F1(I4))
      IF(F1AA.GT.BIG) BIG=F1AA
  140 CONTINUE
      BIG=BIG/10000.D0
      CUMPN=0.D0
      CUMP=0.D0
      DO 170 I3=1,4
      IF(NV(I3).EQ.0) GO TO 170
      QPA=DABS(QP(I3))
      F1A=DABS(F1(I3))
      IF(QPA.LT.BIG) QPA=0.D0
      IF(QPA.LT.BIG.AND.F1A.LT.BIG) GO TO 170
      DIF=DABS(F1(I3)-QP(I3))
      IF(DIF.GT.0.5D0) GO TO 150
      PERCEN=.00100
      GO TO 160
  150 PERCEN=DIF/(F1A+DIF)
  160 CUMP=CUMP+PERCEN*PERCEN
      CUMPN=CUMPN+1.D0
  170 CONTINUE
      CUMP=DSQRT(CUMP/CUMPN)
      IF(CUMP.LT..05D0.AND.NCOUNT.GE.90) GO TO 340
      IF(CUMP.LE..00100) GO TO 340
C
C
  180 CALL MATRIX
      DO 190 I31=1,4
      DQP(I31)=F1(I31)-QP(I31)

  190 CONTINUE
      CALL SOLVER
C
C     CHECK SOLUTIONS
C
      XINC5=1.D0
      IF(NCOUNT.LE.20) GO TO 210
      DO 200 I31=1,4
      IF(NV(I31).EQ.0) GO TO 200
      IF(DABS(DQP(I31)).LT.0.5000) GO TO 200
      VW=DQP(I31)*DSQ(I31)
      IF(VW.GE.0.D0) GO TO 200
      DSQ(I31)=-1.D0*DSQ(I31)
  200 CONTINUE
C
C     FIND UNDER-RELAXATION FACTOR   -XINC-
C
  210 XINC=1.00D0
      IF(NTYPE.LT.3) GO TO 300
      IF(NFLAT.NE.1) GO TO 230
  220 XINC=0.5D0
      GO TO 290
  230 IF(DABS(C(1,1)).LT.1.D0.AND.DABS(C(3,3)).LT.1.D0)
     1GO TO 260
      IF(DABS(C(3,3)).LT.1.D0) GO TO 240
      IF(DABS(C(1,1)).LT.1.D0) GO TO 250
      XINC=(DABS(C(1,1))/AXS1+DABS(C(3,3))/AXS2)/2.D0
      GO TO 260
  240 XINC=DABS(C(1,1))/AXS1
      GO TO 260
  250 XINC=DABS(C(3,3))/AXS2
  260 IF(XINC.GT.0.50D0) XINC=0.50D0
      XNW=FLOAT(NW)
      XNW1=FLOAT(NW1)
      XINCW=1.-XNW/XNW1
      IF(XINC.GT.XINCW) XINC=XINCW
  270 IF(NWORK.EQ.0) GO TO 290
      DO 280 I40=1,4
      DSXX=DSQ(I40)*XINC5
      IF(DABS(DSXX).LT..40D-3)GO TO 290
      XINC5=.39D-3/DABS(DSQ(I40))
      GO TO 270
  280 CONTINUE
  290 XINC=2.D0*XINC
      IF(XINC.GT.0.5D0) XINC=0.5D0
      IF(NCOUNT.LT.30) GO TO 300
      FCOUNT=1./FLOAT(NCOUNT-25)
      IF(FCOUNT.LT..05D0) FCOUNT=.05D0
      IF(XINC.LT.FCOUNT) XINC=FCOUNT
  300 IF(XINC.GT.XINC5) XINC=XINC5
      DO 310 I4=1,4
      F2(I4)=F2(I4)+DSQ(I4)*XINC
      PREV3(I4)=QP(I4)
      EPP2(I4)=ERR2(I4)+XINC*DSQ(I4)
```

```
      IF(DSQ(I4).GT.0) NCE(I4)=NCE(I4)+1
  310 CONTINUE
C
C
      NCOUNT=NCOUNT+1
      IF(NFLAT.EQ.-10.AND.NCOUNT.GT.15) GO TO 330
      IF(NCOUNT.LT.30) GO TO 30
      IF(NCOUNT.EQ.30) WRITE(7,410)
      WRITE(7,400)NCOUNT,P2(1),P2(3),DQP(1),DQP(2),DQP(3),
     1DQP(4),QP(1),  QP(3),DSQ(1),DSQ(2),DSQ(3),DSQ(4),XINC
      IF(NCOUNT.LT.115)GO TO 320
      NGOOD=-10
  320 IF(NCOUNT.GT.120)GO TO 370
      GO TO 30
  330 NFLAT=-20
      GO TO 360
  340 IF(NGOOD.EQ.1.AND.NTHERN.EQ.-1) GO TO 360
      NGOOD=1
      IF(NWORK.EQ.0.AND.NGOOD.EQ.1) NGOOD=2
      GO TO 30
  350 NWORK=5
  360 WRITE(7,390)NCOUNT,(NCE(NN),NN=1,4)
      RETURN
  370 WRITE(6,380)
      WRITE(7,380)
  380 FORMAT(//20X,'***SOLUTION NOT CONVERGING***'//20X,
     1'PROGRAM TERMINATED')
  390 FORMAT(10X,'NCOUNT=',I5,'DSQ.GT.0   1.',I5,'   2.',I5,
     1'   3.',I5,'   4.',I5)
  400 FORMAT(1X,I3,1X,E12.5,1X,E12.5,1X,F7.3,1X,F7.3,1X,
     1F7.3,1X,F7.3,   1X,F8.2,1X,F8.2,1X,E10.3,1X,E10.3,1X,
     2E10.3,1X,E10.3,1X,F6.5)
  410 FORMAT(1X,'NCOUNT',1X,'P2(1)',8X,'P2(3)',6X,'DQP(1)',
     12X,'DQP(2)', 2X,'DQP(3)',2X,'DQP(4)',2X,'QP(1)',4X,
     2'QP(3)',4X,'DSQ(1)',5X,     'DSQ(2)',5X,'DSQ(3)',5X,
     3'DSQ(4)',                                5X,'XINC')
  420 CALL TIME(3,3)
      STOP
      END
      SUBROUTINE MONEY(NLAYER,CLAYER,NPEBAR,SLAYER,NPRE,
     1PLAYER,CL,SL,PL)
      IMPLICIT REAL*8(A-H,P-Z)
      DIMENSION CLAYER(30,100),SLAYER(30,10),PLAYER(30,10),
     1CL(30,100),  SL(30,10),PL(30,10)
      DO 20 K=1,NLAYER
      DO 10 KI=4,30
      CL(KI,K)=CLAYER(KI,K)
   10 CONTINUE
   20 CONTINUE
      IF(NPEBAR.LT.1) GO TO 50
      DO 40 K=1,NPEBAR
      DO 30 KI=4,30
      SL(KI,K)=SLAYER(KI,K)
   30 CONTINUE
   40 CONTINUE
   50 IF(NPRE.LT.1) GO TO 80
      DO 70 K=1,NPRE
      DO 60 KI=4,30
      PL(KI,K)=PLAYER(KI,K)
   60 CONTINUE
   70 CONTINUE
   80 RETURN
      END
      SUBROUTINE FAILUR(NQUAD,KQUAD,FPC,FTC,LC,LT1,LT2,
     1POISS,           TE1U1,TE2U1,R,RX,RT,PSIG1,PSIG2)
      IMPLICIT REAL*8(A-H,P-Z)
      COMMON/BAYARI/YU,PE11,PE22,PS11,PS22,E1U,E2U,EIO,EIOT
      COMMON/MUIRA/E1T,E2T,E1UC,E2UC,SIG1C,SIG2C
   10 IF(TE1U1.LT.0.D0.AND.TE2U1.LT.0.D0) NQUAD=1
      IF(TE1U1.LT.0.D0.AND.TE2U1.GE.0.D0) NQUAD=2
      IF(TE1U1.GE.0.D0.AND.TE2U1.LT.0.D0) NQUAD=4
      IF(TE1U1.GE.0.D0.AND.TE2U1.GE.0.D0) NQUAD=3
      IF(PSIG1.LT.0.D0.AND.PSIG2.LT.0.D0) KQUAD=1
      IF(PSIG1.LT.0.D0.AND.PSIG2.GE.0.D0) KQUAD=2
      IF(PSIG1.GE.0.D0.AND.PSIG2.LT.0.D0) KQUAD=4
      IF(PSIG1.GE.0.D0.AND.PSIG2.GE.0.D0) KQUAD=3
      GO TO (20,120,260,100),NQUAD
C
C     COMPRESSION-COMPRESSION QUADRANTS
C
   20 NEX=0
      IF(LC.LT.-5.AND.PSIG1.EQ.0.D0) GO TO 40
      IF(LC.LT.-5.AND.PSIG2.EQ.0.D0) GO TO 50
      R=TE1U1/TE2U1
      IF(NQUAD.EQ.KQUAD) R=PSIG1/PSIG2
      IF(R.GT.100.D0) R=100.D0
      IF(R.LT.0.01D0) R=0.01D0
   30 IF(R.LE.1.D0) GO TO 60
      R=1.D0/R
      NEX=1
      GO TO 40
   40 R=0.01D0
      GO TO 60
   50 R=0.01D0
      NEX=1
   60 REU=R**R*R-1.8D0*R*R+1.8D0*R
      SIG2C=(1.D0+3.65D0*R)*FPC/((1.D0+R)**2)
      SIG1C=R*SIG2C
      IF(NEX.NE.1) GO TO 70
      CHANGE=SIG1C
      SIG1C=SIG2C
      SIG2C=CHANGE
   70 E1UC=EIO*((1.D0+7.75D0*REU)/(1.D0+8.D0*REU))
      E2UC=E1UC*REU
      IF(NEX.EQ.1) GO TO 80
      CHANGE=E1UC
      E1UC=E2UC
      E2UC=CHANGE
```

```
 80 CONTINUE
    IF(R.GE.0.01D0) GO TO 370
    E1=E1T*E2T
    IF(E1.GE.0.D0) GO TO 370
    IF(NEI.EQ.1) GO TO 90
    TE1U1=E1OC*TE2U1/E2OC
    GO TO 370
 90 TE2U1=E2OC*TE1U1/E1OC
    GO TO 370
C
C     COMPRESSION-TENSION QUADRANTS
C
100 NEI=0
    IF(DABS(PSIG2).LT..1D-5) GO TO 110
    R=PSIG1/PSIG2
    GO TO 140
110 R=-100.D0
    GO TO 140
120 NEI=1
    IF(DABS(PSIG1).LT..1D-5) GO TO 130
    R=PSIG2/PSIG1
    GO TO 140
130 R=-100.D0
140 IF(NQUAD.EQ.KQUAD) GO TO 140
    IF(NQUAD.EQ.2) GO TO 160
    NEI=0
    IF(DABS(TE2U1).LT..1D-9) GO TO 150
    R=TE1U1/TE2U1
    GO TO 180
150 R=-100.D0
    GO TO 180
160 NEI=1
    IF(DABS(TE1U1).LT..1D-9) GO TO 170
    R=TP2U1/TE1U1
    GO TO 180
170 R=-100.D0
180 IF(R.LT.-100.D0) R=-100.D0
    IF(R.GT.-0.01D0) R=-0.01D0
190 SIG2C=FPC*FTC/(R*FPC+0.8D0*FTC)
    IF(R.LT.-0.04D0) GO TO 200
    SIG2CA=(1.D0+3.65D0*R)*FPC/((1.D0+R)**2)
    IF(SIG2CA.GT.SIG2C) SIG2C=SIG2CA
200 IF(SIG2C.LT.FPC) SIG2C=FPC
    SIG1C=R*SIG2C
    E1OC=EIOT*(1.D0-(1.D0-SIG1C/FTC)**4)
    E=SIG2C/FPC
    E2OC=EIO*((1.5D0*E-1.4D0)*E+0.9D0)*E
    IF(NEI.EQ.1) GO TO 210
    CHANGE=SIG1C
    SIG1C=SIG2C
    SIG2C=CHANGE
    CHANGE=E1OC
    E1OC=E2OC
    E2OC=CHANGE
210 E1=E1T*E2T
    IF(E1.GE.0.D0) GO TO 370
    IF(R.LT.-99.D0) GO TO 240
    IF(R.GT.-0.01D0) GO TO 220
    GO TO 370
220 IF(NEI.EQ.1) GO TO 230
    TE1U1=E1OC*TE2U1/E2OC
    GO TO 370
230 TE2U1=E2OC*TE1U1/E1OC
    GO TO 370
240 IF(NEI.EQ.0) GO TO 250
    TE1U1=E1OC*TE2U1/E2OC
    GO TO 370
250 TE2U1=E2OC*TE1U1/E1OC
    GO TO 370
C
C     TENSION-TENSION QUADRANTS
C
260 NEI=0
    IF(NQUAD.EQ.KQUAD) GO TO 300
    IF(TP2U1.LT..1D-9) GO TO 270
    R=TP1U1/TE2U1
    GO TO 280
270 R=100.D0
    IF(TP1U1.LT..1D-9) R=1.D0
280 IF(R.GT.1.D0) GO TO 290
    NEI=1
    R=1.D0/R
290 IF(R.GT.100.D0)R=100.D0
    GO TO 330
300 IF(PSIG2.LT..001D4) GO TO 310
    R=PSIG1/PSIG2
    GO TO 320
310 R=100.D0
    IF(PSIG1.LT..001D0) R=1.D0
320 IF(R.GE.1.D0) GO TO 330
    R=1.D0/R
    NEI=1
330 IF(R.GT.100.D0) R=100.D0
    SIG1C=FTC
    SIG2C=SIG1C/R
    RI=1.D0/R
    RT=1.D0
    E1OC=EIOT*(1.D0+0.5D0*RI-0.25D0*RI**2)
    E2OC=EIOT*(0.75D0*RI**0.33333333D0+0.5D0*RI*RI*RI)
340 IF(NEI.EQ.1) GO TO 350
    CHANGE=SIG1C
    SIG1C=SIG2C
    SIG2C=CHANGE
    CHANGE=E1OC
    E1OC=E2OC
    E2OC=CHANGE
350 CONTINUE
    E1=E2T*E2T
```

```
      IF(R1.GE.0.D0) GO TO 370
      IF(R.LE.99.D0) GO TO 370
      IF(RRR.EQ.0) GO TO 360
      TE1U1=E10C*TE2U1/E2UC
      GO TO 370
  360 TE2U1=E2UC*TE1U1/E10C
  370 RETURN
      END
      SUBROUTINE STRESS(LC,LT1,LT2,POISS,PICER,CEMOD,SIG1,
     1SIG2,          TE1U1,TE2U1,R,RE,RT,PSIG1,PSIG2,E10F,
     2E20F,DE11,DE22)
      IMPLICIT REAL*8(A-H,P-Z)
      COMMON/BAVARI/VU,PE11,PE22,PS11,PS22,E10,E20,EIO,EIOT
      COMMON/MOIRA/E1T,E2T,E10C,E20C,SIG1C,SIG2C
      E10C=PICER*E10C
      E20C=PICER*E20C
      PTC=SIG1C
      IF(SIG2C.GT.PTC) PTC=SIG2C
      IF(E10C.NE.0.D0) GO TO 10
      IF(E20C.EQ.0.D0) GO TO 40
      RAT=TE2U1/E2UC
      GO TO 20
   10 RAT=TE1U1/E10C
   20 VU1=POISS*(1.D0+1.3763D0*RAT-5.3600*RAT*RAT+8.586D0*
     1RAT*RAT        *RAT)
      IF(VU1.GT.0.5D0) VU1=0.5D0
      IF(E2UC.EQ.0.D0) GO TO 30
      RAT=TE2U1/E2UC
      VU2=POISS*(1.D0+1.3763D0*RAT-5.3600*RAT*RAT+8.586D0*
     1RAT*RAT        *RAT)
      IF(VU2.GT.0.5D0) VU2=0.5D0
      VU=DSQRT(VU1*VU2)
      GO TO 50
   30 VU=VU1
      GO TO 50
   40 VU=0.5D0
   50 SIG1F=0.25D0*SIG1C
      SIG2F=0.25D0*SIG2C
      E10F=4.D0*E10C
      E20F=4.D0*E20C
   60 IF(E10C.GT.0.D0.AND.LT1.LE.-60) GO TO 110
      IF(E10C.EQ.0.D0) GO TO 70
      IF(TE1U1.GT.E10C.AND.E10C.GT.0.D0) GO TO 80
      ES=SIG1C/E10C
      RE=CEMOD/ES
      RP=SIG1C/SIG1F
      RESP=E10F/E10C
      P=RE*(RP-1.D0)/((RESP-1.D0)**2)-1.D0/RESP
      RAT=TE1U1/E10C
      DENOM=1.+RAT*((R+RE-2.D0)+RAT*((1.D0-2.D0*R)+RAT*P))
      SIG1=CEMOD*TE1U1/DENOM
      E1T=CEMOD*(1.D0+RAT*RAT*(2.D0*R-1.D0-2.D0*R*RAT))/(
     1DENOM          *DENOM)
      IF(TE1U1.LT.E10C.AND.E10C.LT.0.D0) GO TO 250
      GO TO 140
   70 SIG1=0.D0
      E1T=CEMOD
      IF(LC.EQ.-10) E1T=0.D0
      IF(LC.EQ.-30) E1T=0.D0
      GO TO 140
C
C     TENSILE DECLINING BRANCH
C
   80 IF(LT1.LT.-40.AND.R.LT.90.D0) GO TO 120
      IF(LT1.GT.-10) LT1=-10
      IF(E10C.GT.E20C) GO TO 90
      E10G=30.D0*E2UC
      SIG1G=SIG1C/7.5D0
      SIG1L=SIG2C/7.5D0
      SIG1T=E1T*DE11+PSIG1
      GO TO 100
   90 E10G=30.D0*E10C
      SIG1G=SIG1C/7.5D0
      SIG1L=SIG1G
      SIG1T=0.D0
      IF(DABS(PSIG1).LT.DABS(PSIG2)) SIG1T=E1T*DE11+PSIG1
  100 P1T=(SIG1G-SIG1C)/E10G
      SIG1=SIG1C+E1T*(TE1U1-E1UC)
      IF(SIG1.LT.SIG1T) SIG1=SIG1T
      IF(SIG1.LT.SIG1L) GO TO 120
      E10F=E10G
      GO TO 140
  110 LT1=-60
      SIG1=0.D0
      E1T=0.D0
      GO TO 140
  120 IF(R.GT.7.D0) GO TO 130
      E1T=0.D0
      SIG1=SIG1L
      IF(LT1.GT.-50) LT1=-50
      GO TO 140
  130 SIG1=PTC/7.5D0
      E1T=CEMOD/400.D0
C
  140 IF(E2UC.GT.0.D0.AND.LT2.LE.-60) GO TO 230
      IF(E2UC.EQ.0.D0) GO TO 150
      IF(TE2U1.GT.E2UC.AND.E2UC.GT.0.D0) GO TO 160
      ES=SIG2C/E2UC
      RF=SIG2C/SIG2F
      RESP=E2UF/E2UC
      RE=CEMOD/ES
      P=RF*(RP-1.D0)/((RESP-1.D0)**2)-1.D0/RESP
      RAT=TE2U1/E2UC
      DENOM=1.D0+RAT*((R+RE-2.D0)+RAT*((1.D0-2.D0*R)+RAT*P))
      SIG2=CEMOD*TE2U1/DENOM
      E2T=CEMOD*(1.D0+RAT*RAT*(2.D0*R-1.D0-2.D0*R*RAT))/(
     1DENOM          *DENOM)
      IF(TE2U1.LT.E2UC.AND.E2UC.LT.0.D0) GO TO 260
```

```
      GO TO 240
  150 SIG2=0.D0
      E2T=CEMOD
      IF(LC.EQ.-20) E2T=0.D0
      IF(LC.EQ.-30) E2T=0.D0
      GO TO 240
C
C     TENSILE DECLING BRANCH
C
  160 IF(LT2.LT.-40.AND.R.LT.90.D0) GO TO 200
      IF(LT2.GT.-10) LT2=-10
      IF(E1UC.GT.E2UC) GO TO 180
  170 E2UG=30.D0*E2UC
      SIG2G=SIG2C/7.5D0
      SIG2L=SIG2G
      SIG2T=0.D0
      IF(DABS(PSIG1).GT.DABS(PSIG2)) SIG2T=E2T*DE22+PSIG2
      GO TO 190
  180 E2UG=30.D0*E1UC
      SIG2G=SIG2C/7.5D0
      SIG2L=SIG1C/7.5D0
      SIG2T=E2T*DE22+PSIG2
  190 E2T=(SIG2G-SIG2C)/E2UG
      SIG2=SIG2C+E2T*(TE2U1-E2UC)
      IF(SIG2.LT.SIG2T) SIG2=SIG2T
      IF(SIG2.LT.SIG2L) GO TO 200
      E2UP=E2UG
      GO TO 240
  200 IF(R.GT.7.D0) GO TO 210
      E2T=0.D0
      SIG2=SIG2L
      IF(LT2.GT.-50) LT2=-50
      GO TO 220
  210 SIG2=FTC/7.5D0
      E2T=CEMOD/400.D0
  220 RETURN
  230 LT2=-60
      E2T=0.D0
      SIG2=0.D0
  240 RETURN
  250 IF(DABS(PSIG1).GT.DABS(PSIG2)) GO TO 140
      SIG1T=E1T*DE11+PSIG1
      IF(SIG1.GT.SIG1T) SIG1=SIG1T
      GO TO 140
  260 IF(DABS(PSIG2).GT.DABS(PSIG1)) RETURN
      SIG2T=E2T*DE22+PSIG2
      IF(SIG2.GT.SIG2T) SIG2=SIG2T
      RETURN
      END
      SUBROUTINE NOTE(NLAYER,CLAYER,CLP)
      IMPLICIT REAL*8(A-H,P-Z)
      DIMENSION CLAYER(30,1),CLP(6,1)
C
      IF(NLAYER.LE.0) GO TO 20
      DO 10 K=1,NLAYER
      CLP(1,K)=CLAYER(28,K)
      CLP(2,K)=CLAYER(29,K)
      CLP(3,K)=CLAYER(20,K)
      CLP(4,K)=CLAYER(21,K)
      CLP(5,K)=CLAYER(25,K)
      CLP(6,K)=CLAYER(26,K)
   10 CONTINUE
C
   20 RETURN
      END
      SUBROUTINE UNLOAD(NLAYER,CLAYER,CLP,NUNLOD)
      IMPLICIT REAL*8(A-H,P-Z)
      DIMENSION CLAYER(30,1),CLP(6,1)
      NUNLOD=0
      IF(NLAYER.LE.0) GO TO 30
C
      DO 20 K=1,NLAYER
      IF(CLAYER(4,K).GT.0.D0) GO TO 20
      IF(CLP(3,K).GT.0.D0.OR.CLP(4,K).GT.0.D0)
     1GO TO 10
      RATE1P=CLP(1,K)
      RATE2P=CLP(2,K)
      RATE1=CLAYER(28,K)*1.05D0
      RATE2=CLAYER(29,K)*1.05D0
      E1UC=CLP(5,K)
      E2UC=CLP(6,K)
      IF(RATE1.GE.RATE1P.OR.RATE2.GE.RATE2P) GO TO 10
      CLAYER(30,K)=CLAYER(30,K)+10.D0
C      IF(CLAYER(30,K).LT.15.D0) GO TO 200
      IF(E1UC.GE.0.D0) CLAYER(5,K)=-65.D0
      IF(E2UC.GE.0.D0) CLAYER(6,K)=-65.D0
      IF(E1UC.LT.0.D0.OR.E2UC.LT.0.D0) CLAYER(4,K)=3.D0
      NUNLOD=1
   10 CLAYER(30,K)=0.D0
   20 CONTINUE
C
   30 RETURN
      END
```

APPENDIX C

SAMPLE INPUT AND OUTPUT

C.1 Sample Input

The following is the input deck for example segment UD1 as discussed in Chapter 4.

```
      1     PROGRAM TEST   UD1H   EXAMPLE WALL SEGMENT
      2     24,24.,12.,12.,1632.,1632.,
      3     4,29600.,60.,
      4     1,1.1,-9.3,
      5     1,1.1,9.3,
      6     2,1.27,-7.9,
      7     2,1.69,7.9,
      8     2111,-15.4,-302.0,21.9,-46.7,
      9     2,29600.,255.,1,2,0,1,2.5,
     10     1,2.33,0.,374.,1,
     11     2,2.33,0.,200.,2,
     12     1111,.6,-1258.8,72.8,-46.7,
     13     1111,.6,-1258.8,72.8,-165.1,
     14     1,26,0,1,1,
     15     26.,-3.17,0.,.65E-5,.65E-5,1010,
     16     1010,650.,19.7132,-532.,-3.9332,1,
     17     5.00,.424,.15,4120.,3,-25,1.,.000126,
END OF FILE
```

C.2 Sample Output

The following is a partial listing of the output for example segment UD1 as discussed in Chapter 4. This output was generated using the input deck of the previous section of this appendix and includes the data echo check, and the solutions to the dead load, prestressing, creep effects, temperature effects and the first live load.

PROGRAM TEST OD1N 20-06-78 REVISED 78.11.27

THE NUMBER OF LAYERS IS 24
THE THICKNESS IS 24.00000
WIDTH = 12.00000 HEIGHT = 12.00000 RADIUS 1 =1632.00000 RADIUS 2 = 1632.00000

.....REINFORCING STEEL.....

NO. OF LAYERS = 4
ELASTIC MODULUS = .2960000E+05
YIELD POINT = 60.00000

DIRECTION	AREA	LOCATION
1	1.10000	-9.30000
1	1.10000	9.30000
2	1.27000	-7.90000
2	1.69000	7.90000

*** DEAD LOAD ***

LOAD CODE	N1	M1	N2	M2
2111	-0.15400E+02	-0.30200E+03	0.21900E+02	-0.46700E+02

.....PRESTRESSING STEEL.....

NO. OF LAYERS = 2
ELASTIC MODULUS = .2960000E+05
YIELD POINT = 255.00000
PRESTRESS CODE = 1

DIRECTION	AREA	LOCATION	PRESTRESSING FORCE	PRESTRESSING ORDER
1	2.33000	0.0	374.00000	1
2	2.33000	0.0	200.00000	2

*** TARGET LOAD AFTER PRESTRESSING ***

LOAD CODE	N1	M1	N2	M2	PRESTRESS STEP
1111	0.60000E+00	-0.12588E+04	0.72800E+02	-0.46700E+02	1
1111	0.60000E+00	-0.12588E+04	0.72800E+02	-0.16510E+03	2

CREEP FACTOR= 2.50000

THERMAL EFFECTS

LINEAR DISTRIBUTION OF THERMAL STRAINS

CONSTANT T1= 0.26000E+02
CONSTANT T2=-0.31700E+01
CONSTANT T3= 0.0
COEFFICIENT OF THERMAL EXPANSION - CONCRETE = 0.65000E-05
COEFFICIENT OF THERMAL EXPANSION - STEEL = 0.65000E-05
THERMAL LOAD CODE =1010

---*.EPSTEIN TYPE LOADING---

LOAD CODE	M1	M1/N1	N2	M2/N2	LOAD TYPE
26	1010	0.65000E+03	0.19713E+02	-0.53200E+03	-0.39332E+01 1

NO. OF LOADS = 1

LOAD NUMBER	LOAD CODE	N1	M1	N2	M2	LOAD TYPE
26	1010	0.65000E+03	0.20733E-03	-0.53200E+03	0.33937E-04	1

.....CONCRETE.....

UNIAXIAL COMPRESSIVE STRENGTH	5.00000
UNIAXIAL TENSILE STRENGTH	0.42400
POISSON S RATIO	0.15000
PLASTIC MODULUS	4120.00000
BIAXIAL CONCRETE MODEL	3
NUMBER OF SUBINCREMENTS	-25
STRAIN @ MAX.STRESS IN UNIAX.COMPR.	0.10000E+01
STRAIN @MAX.STRESS IN UNIAX.TENSION	0.12600E-03

****

DEAD LOAD RESULTS

N1	-15.40000	(LOAD)	-15.40000	(LOAD INCREMENT)
N1	-302.00000	(LOAD)	-302.00000	(LOAD INCREMENT)
N2	21.90000	(LOAD)	21.90000	(LOAD INCREMENT)
N2	-46.70000	(LOAD)	-46.70000	(LOAD INCREMENT)

****

CONCRETE LAYERS

LAYER NO.	START COORD	END COORD	STRAIN1	STRAIN2	STRESS1	STRESS2
1	-12.0000	-11.0000	-0.64408E-04	0.18758E-04	-0.29276E+00	0.32584E-01
2	-11.0000	-10.0000	-0.59923E-04	0.18753E-04	-0.27213E+00	0.35984E-01
3	-10.0000	-9.0000	-0.55443E-04	0.18748E-04	-0.25067E+00	0.39508E-01
4	-9.0000	-8.0000	-0.50969E-04	0.18744E-04	-0.22863E+00	0.43128E-01
5	-8.0000	-7.0000	-0.46500E-04	0.18739E-04	-0.20629E+00	0.46819E-01
6	-7.0000	-6.0000	-0.42037E-04	0.18734E-04	-0.18392E+00	0.50553E-01
7	-6.0000	-5.0000	-0.37579E-04	0.18729E-04	-0.16168E+00	0.54308E-01
8	-5.0000	-4.0000	-0.33126E-04	0.18725E-04	-0.13970E+00	0.58072E-01
9	-4.0000	-3.0000	-0.28680E-04	0.18720E-04	-0.11806E+00	0.61834E-01
10	-3.0000	-2.0000	-0.24238E-04	0.18715E-04	-0.96777E-01	0.65588E-01
11	-2.0000	-1.0000	-0.19802E-04	0.18711E-04	-0.75875E-01	0.69331E-01
12	-1.0000	-0.0	-0.15372E-04	0.18706E-04	-0.55346E-01	0.73059E-01
13	-0.0	1.0000	-0.10947E-04	0.18701E-04	-0.35177E-01	0.76772E-01
14	1.0000	2.0000	-0.65269E-05	0.18697E-04	-0.15352E-01	0.80469E-01
15	2.0000	3.0000	-0.21126E-05	0.18692E-04	0.44685E-02	0.83498E-01
16	3.0000	4.0000	0.22962E-05	0.18687E-04	0.21313E-01	0.84556E-01
17	4.0000	5.0000	0.66957E-05	0.18683E-04	0.41139E-01	0.85280E-01
18	5.0000	6.0000	0.11098E-04	0.18678E-04	0.61362E-01	0.88615E-01
19	6.0000	7.0000	0.15491E-04	0.18673E-04	0.80426E-01	0.91309E-01
20	7.0000	8.0000	0.19878E-04	0.18669E-04	0.98716E-01	0.94694E-01
21	8.0000	9.0000	0.24260E-04	0.18664E-04	0.11815E+00	0.98999E-01
22	9.0000	10.0000	0.28637E-04	0.18660E-04	0.13765E+00	0.10260E+00
23	10.0000	11.0000	0.33008E-04	0.18655E-04	0.15719E+00	0.10551E+00
24	11.0000	12.0000	0.37374E-04	0.18650E-04	0.17673E+00	0.10780E+00

STEEL REINFORCING LAYERS

LAYER NO.	START COORD	END COORD	DIRECTION	STRAIN	STRESS

1	-9.3458	-9.2542	1	-0.54548E-04	-0.16146E+01
2	9.2542	9.3458	1	0.27762E-04	0.82175E+00
3	-7.9529	-7.8471	2	0.18741E-04	0.55473E+00
4	7.8296	7.9704	2	0.18667E-04	0.55254E+00

NEGATIVE CONCRETE LAYERS

LAYER NO.	START COORD	END COORD	STRAIN1	STRAIN2	STRESS1	STRESS2
1	-9.3458	-9.2542	-0.54548E-04	0.18747E-04	-0.24629E+00	0.40225E-01
2	9.2542	9.3458	0.27762E-04	0.18660E-04	0.13374E+00	0.10193E+00
3	-7.9529	-7.8471	-0.48287E-04	0.18741E-04	-0.21524E+00	0.45335E-01
4	7.8296	7.9704	0.21631E-04	0.18667E-04	0.10648E+00	0.96501E-01

*** PRESTRESSING LAYERS ***

LAYER NO.	START COORD	END COORD	DIRECTION	STRAIN	STRESS
1	-0.0971	0.0971	1	0.0	0.0
2	-0.0971	0.0971	2	0.0	0.0

NEGATIVE CONCRETE LAYERS

LAYER NO.	START COORD	END COORD	STRAIN1	STRAIN2	STRESS1	STRESS2
1	-0.0971	0.0971	-0.13158E-04	0.18704E-04	-0.45217E-01	0.74917E-01
2	-0.0971	0.0971	-0.13158E-04	0.18704E-04	-0.45217E-01	0.74917E-01

DAMAGE SUMMARY

1. CONCRETE

DAMAGE TYPE	DEPTH OF DAMAGE	DIRECTION
INSIDE CRACKED	0.0	1
INSIDE CRACKED AND OPEN	0.0	1
INSIDE CRACKED	0.0	2
INSIDE CRACKED AND OPEN	0.0	2
OUTSIDE CRACKED	0.0	1
OUTSIDE CRACKED AND OPEN	0.0	1
OUTSIDE CRACKED	0.0	2
OUTSIDE CRACKED AND OPEN	0.0	2
INSIDE CRUSHED	0.0	
OUTSIDE CRUSHED	0.0	

2. REINFORCING STEEL

DAMAGE TYPE	LAYER NO.

-NO DAMAGE-

3. PRESTRESSING STEEL
DAMAGE TYPE LAYER NO.
-NO DAMAGE-

RESULTS FROM DEAD LOAD APPLICATION				
N1	-0.13158E-04	(STRAIN)	-0.13158E-04	(STRAIN INCREMENT)
M1	-0.44170E-05	(STRAIN)	-0.44170E-05	(STRAIN INCREMENT)
N2	0.18704E-04	(STRAIN)	0.18704E-04	(STRAIN INCREMENT)
M2	-0.67886E-08	(STRAIN)	-0.67886E-08	(STRAIN INCREMENT)

****

****

RESULTS OF PRESTRESS APPLICATION

****

****

CONCRETE LAYERS

LAYER NO.	START COORD	END COORD	STRAIN1	STRAIN2	STRESS1	STRESS2
1	-12.0000	-11.0000	-0.55489E-03	-0.47489E-04	-0.21820E+01	-0.57334E+00
2	-11.0000	-10.0000	-0.53267E-03	-0.48049E-04	-0.21039E+01	-0.56305E+00
3	-10.0000	-9.0000	-0.51047E-03	-0.48608E-04	-0.20249E+01	-0.55259E+00
4	-9.0000	-8.0000	-0.48831E-03	-0.49167E-04	-0.19457E+01	-0.54175E+00
5	-8.0000	-7.0000	-0.46617E-03	-0.49725E-04	-0.18655E+01	-0.53051E+00
6	-7.0000	-6.0000	-0.44405E-03	-0.50282E-04	-0.17849E+01	-0.51901E+00
7	-6.0000	-5.0000	-0.42197E-03	-0.50838E-04	-0.17037E+01	-0.50716E+00
8	-5.0000	-4.0000	-0.39991E-03	-0.51394E-04	-0.16220E+01	-0.49500E+00
9	-4.0000	-3.0000	-0.37788E-03	-0.51949E-04	-0.15397E+01	-0.48252E+00
10	-3.0000	-2.0000	-0.35587E-03	-0.52504E-04	-0.14567E+01	-0.46974E+00
11	-2.0000	-1.0000	-0.33390E-03	-0.53058E-04	-0.13734E+01	-0.45670E+00
12	-1.0000	-0.0	-0.31195E-03	-0.53611E-04	-0.12892E+01	-0.44343E+00
13	-0.0	1.0000	-0.29002E-03	-0.54163E-04	-0.12047E+01	-0.42998E+00
14	1.0000	2.0000	-0.26813E-03	-0.54715E-04	-0.11196E+01	-0.41636E+00
15	2.0000	3.0000	-0.24626E-03	-0.55266E-04	-0.10327E+01	-0.40197E+00
16	3.0000	4.0000	-0.22441E-03	-0.55816E-04	-0.94769E+00	-0.38892E+00
17	4.0000	5.0000	-0.20260E-03	-0.56366E-04	-0.86198E+00	-0.37494E+00
18	5.0000	6.0000	-0.18081E-03	-0.56915E-04	-0.77511E+00	-0.36174E+00
19	6.0000	7.0000	-0.15905E-03	-0.57464E-04	-0.68837E+00	-0.34800E+00
20	7.0000	8.0000	-0.13731E-03	-0.58011E-04	-0.60045E+00	-0.33540E+00
21	8.0000	9.0000	-0.11560E-03	-0.58558E-04	-0.51272E+00	-0.32224E+00
22	9.0000	10.0000	-0.93915E-04	-0.59105E-04	-0.42893E+00	-0.30957E+00
23	10.0000	11.0000	-0.72258E-04	-0.59651E-04	-0.33603E+00	-0.29620E+00
24	11.0000	12.0000	-0.50627E-04	-0.60196E-04	-0.24513E+00	-0.28163E+00

STEEL REINFORCING LAYERS

LAYER NO.	START COORD	END COORD	DIRECTION	STRAIN	STRESS
1	-9.3458	-9.2542	1	-0.59604E-03	-0.14979E+02
2	9.2542	9.3459	1	-0.44250E-04	-0.29082E+01

3	-7.9529	-7.8871	2	-0.49501E-04	-0.14652E+01
4	7.8296	7.9704	2	-0.58230E-04	-0.17236E+01

NEGATIVE CONCRETE LAYERS

LAYER NO.	START COORD	END COORD	STRAIN1	STRAIN2	STRESS1	STRESS2
1	-9.3458	-9.2542	-0.50604E-03	-0.43720E-04	-0.20091E+01	-0.55044E+00
2	9.2542	9.3458	-0.98250E-04	-0.58996E-04	-0.44043E+00	-0.31106E+00
3	-7.9529	-7.8871	-0.47502E-03	-0.49501E-04	-0.18975E+01	-0.53501E+00
4	7.8296	7.9704	-0.12862E-03	-0.58230E-04	-0.57017E+00	-0.33009E+00

*** PRESTRESSING LAYERS ***

LAYER NO.	START COORD	END COORD	DIRECTION	STRAIN	STRESS
1	-0.0971	0.0971	1	0.53596E-02	0.15d64E+03
2	-0.0971	0.0971	2	0.28999E-02	0.858d7E+02

NEGATIVE CONCRETE LAYERS

LAYER NO.	START COORD	END COORD	STRAIN1	STRAIN2	STRESS1	STRESS2
1	-0.0971	0.0971	-0.30098E-03	-0.53887E-04	-0.12469E+01	-0.43670E+00
2	-0.0971	0.0971	-0.30098E-03	-0.53887E-04	-0.12469E+01	-0.43670E+00

DAMAGE SUMMARY

1. CONCRETE

DAMAGE TYPE	DEPTH OF DAMAGE	DIRECTION
INSIDE CRACKED	0.0	1
INSIDE CRACKED AND OPEN	0.0	1
INSIDE CRACKED	0.0	2
INSIDE CRACKED AND OPEN	0.0	2
OUTSIDE CRACKED	0.0	1
OUTSIDE CRACKED AND OPEN	0.0	1
OUTSIDE CRACKED	0.0	2
OUTSIDE CRACKED AND OPEN	0.0	2
INSIDE CRUSHED	0.0	
OUTSIDE CRUSHED	0.0	

2. REINFORCING STEEL

DAMAGE TYPE	LAYER NO.
-NO DAMAGE-	

3. PRESTRESSING STEEL
DAMAGE TYPE LAYER NO.
-NO DAMAGE-

RESULTS FROM PRESTRESS APPLICATION

N1	-0.30098E-03	(STRAIN)	-0.30098E-03	(STRAIN INCREMENT)
M1	-0.21739E-04	(STRAIN)	-0.21739E-04	(STRAIN INCREMENT)
N2	-0.53887E-04	(STRAIN)	-0.53887E-04	(STRAIN INCREMENT)
M2	0.58546E-06	(STRAIN)	0.58546E-06	(STRAIN INCREMENT)

*** CREEP RESULTS ***

N1	0.60279	(LOAD)	0.0	(LOAD INCREMENT)
M1	-1258.69328	(LOAD)	0.0	(LOAD INCREMENT)
N2	72.76355	(LOAD)	0.0	(LOAD INCREMENT)
M2	-164.67404	(LOAD)	0.0	(LOAD INCREMENT)

****

CONCRETE LAYERS

LAYER NO.	START COORD	END COORD	STRAIN1	STRAIN2	STRESS1	STRESS2
1	-12.0000	-11.0000	-0.47732E-03	-0.44777E-04	-0.19050E+01	-0.53121E+00
2	-11.0000	-10.0000	-0.45818E-03	-0.45041E-04	-0.18356E+01	-0.52056E+00
3	-10.0000	-9.0000	-0.43906E-03	-0.45304E-04	-0.17654E+01	-0.50975E+00
4	-9.0000	-8.0000	-0.41997E-03	-0.45566E-04	-0.16954E+01	-0.49858E+00
5	-8.0000	-7.0000	-0.40090E-03	-0.45829E-04	-0.16243E+01	-0.48704E+00
6	-7.0000	-6.0000	-0.38185E-03	-0.46091E-04	-0.15532E+01	-0.47526E+00
7	-6.0000	-5.0000	-0.36283E-03	-0.46353E-04	-0.14815E+01	-0.46315E+00
8	-5.0000	-4.0000	-0.34383E-03	-0.46614E-04	-0.14095E+01	-0.45076E+00
9	-4.0000	-3.0000	-0.32486E-03	-0.46875E-04	-0.13370E+01	-0.43807E+00
10	-3.0000	-2.0000	-0.30590E-03	-0.47136E-04	-0.12641E+01	-0.42511E+00
11	-2.0000	-1.0000	-0.28697E-03	-0.47397E-04	-0.11910E+01	-0.41192E+00
12	-1.0000	-0.0	-0.26807E-03	-0.47657E-04	-0.11171E+01	-0.39852E+00
13	-0.0	1.0000	-0.24918E-03	-0.47917E-04	-0.10431E+01	-0.38497E+00
14	1.0000	2.0000	-0.23032E-03	-0.48176E-04	-0.96860E+00	-0.37128E+00
15	2.0000	3.0000	-0.21149E-03	-0.48435E-04	-0.89247E+00	-0.35683E+00
16	3.0000	4.0000	-0.19269E-03	-0.48694E-04	-0.81844E+00	-0.34378E+00
17	4.0000	5.0000	-0.17388E-03	-0.48953E-04	-0.74380E+00	-0.32982E+00
18	5.0000	6.0000	-0.15512E-03	-0.49211E-04	-0.66813E+00	-0.31666E+00
19	6.0000	7.0000	-0.13637E-03	-0.49469E-04	-0.59273E+00	-0.30301E+00
20	7.0000	8.0000	-0.11765E-03	-0.49727E-04	-0.51630E+00	-0.29055E+00

21	8.0000	9.0000	-0.98950E-04	-0.49984E-04	-0.44018E+00	-0.27757E+00
22	9.0000	10.0000	-0.80273E-04	-0.50241E-04	-0.36815E+00	-0.26520E+00
23	10.0000	11.0000	-0.61619E-04	-0.50498E-04	-0.28709E+00	-0.25231E+00
24	11.0000	12.0000	-0.42988E-04	-0.50754E-04	-0.20794E+00	-0.23822E+00

STEEL REINFORCING LAYERS

LAYER NO.	START COORD	END COORD	DIRECTION	STRAIN	STRESS
1	-9.3458	-9.2542	1	-0.10863E-02	-0.32154E+02
2	9.2542	9.3458	1	-0.20926E-03	-0.61941E+01
3	-7.9529	-7.8471	2	-0.14076E-03	-0.41664E+01
4	7.8296	7.9704	2	-0.12892E-03	-0.38161E+01

NEGATIVE CONCRETE LAYERS

LAYER NO.	START COORD	END COORD	STRAIN1	STRAIN2	STRESS1	STRESS2
1	-9.3458	-9.2542	-0.43524E-03	-0.45356E-04	-0.17514E+01	-0.50754E+00
2	9.2542	9.3458	-0.84007E-04	-0.50190E-04	-0.37726E+00	-0.26661E+00
3	-7.9529	-7.8471	-0.40852E-03	-0.45724E-04	-0.16526E+01	-0.49166E+00
4	7.8296	7.9704	-0.11017E-03	-0.49830E-04	-0.49067E+00	-0.28532E+00

*** PRESTRESSING LAYERS ***

LAYER NO.	START COORD	END COORD	DIRECTION	STRAIN	STRESS
1	-0.0971	0.0971	1	0.50153E-02	0.14845E+03
2	-0.0971	0.0971	2	0.28190E-02	0.83442E+02

NEGATIVE CONCRETE LAYERS

LAYER NO.	START COORD	END COORD	STRAIN1	STRAIN2	STRESS1	STRESS2
1	-0.0971	0.0971	-0.25862E-03	-0.47787E-04	-0.10801E+01	-0.39173E+00
2	-0.0971	0.0971	-0.25862E-03	-0.47787E-04	-0.10801E+01	-0.39173E+00

CREEP STRAINS

LAYER NO.	CONCRETE		NEGATIVE STEEL		NEGATIVE PRESTRESSING	
	DIREC1	DIREC2	DIREC1	DIREC2	DIREC1	DIREC2
1	-0.71403E-03	-0.98707E-04	-0.85104E-03	-0.78439E-04	-0.38665E-03	-0.87028E-04
2	-0.68538E-03	-0.97684E-04	-0.12525E-03	-0.77696E-04	-0.38665E-03	-0.87028E-04
3	-0.65676E-03	-0.96663E-04	-0.81105E-03	-0.95032E-04		
4	-0.62813E-03	-0.95643E-04	-0.16861E-03	-0.79693E-04		
5	-0.59963E-03	-0.94624E-04				
6	-0.57112E-03	-0.93607E-04				

7	-0.54265E-03	-0.92591E-04
8	-0.51421E-03	-0.91576E-04
9	-0.48580E-03	-0.90562E-04
10	-0.45743E-03	-0.89550E-04
11	-0.42909E-03	-0.88538E-04
12	-0.40079E-03	-0.87528E-04
13	-0.37252E-03	-0.86520E-04
14	-0.34429E-03	-0.85512E-04
15	-0.31609E-03	-0.84506E-04
16	-0.28793E-03	-0.83501E-04
17	-0.25980E-03	-0.82497E-04
18	-0.23170E-03	-0.81494E-04
19	-0.20364E-03	-0.80493E-04
20	-0.17561E-03	-0.79493E-04
21	-0.14762E-03	-0.78494E-04
22	-0.11966E-03	-0.77496E-04
23	-0.91740E-04	-0.76500E-04
24	-0.63849E-04	-0.75504E-04

DAMAGE SUMMARY

1. CONCRETE

DAMAGE TYPE	DEPTH OF DAMAGE	DIRECTION
INSIDE CRACKED	0.0	1
INSIDE CRACKED AND OPEN	0.0	1
INSIDE CRACKED	0.0	2
INSIDE CRACKED AND OPEN	0.0	2
OUTSIDE CRACKED	0.0	1
OUTSIDE CRACKED AND OPEN	0.0	1
OUTSIDE CRACKED	0.0	2
OUTSIDE CRACKED AND OPEN	0.0	2
INSIDE CRUSHED	0.0	
OUTSIDE CRUSHED	0.0	

2. REINFORCING STEEL

DAMAGE TYPE	LAYER NO.
-NO DAMAGE-	

3. PRESTRESSING STEEL

DAMAGE TYPE	LAYER NO.
-NO DAMAGE-	

RESULTS AFTER CREEP

M1	-0.64527E-03	(STRAIN)	0.0	(STRAIN INCREMENT)
M1	-0.46755E-04	(STRAIN)	0.0	(STRAIN INCREMENT)
M2	-0.13481E-03	(STRAIN)	0.0	(STRAIN INCREMENT)
M2	-0.66628E-06	(STRAIN)	0.0	(STRAIN INCREMENT)

*** THERMAL STRAIN RESULTS ***

M1	0.60279	(LOAD)	0.0	(LOAD INCREMENT)
M1	-1258.69328	(LOAD)	0.0	(LOAD INCREMENT)
M2	72.76355	(LOAD)	0.0	(LOAD INCREMENT)
M2	-164.67404	(LOAD)	0.0	(LOAD INCREMENT)

****

CONCRETE LAYERS

LAYER NO.	START COORD	END COORD	STRAIN1	STRAIN2	STRESS1	STRESS2
1	-12.0000	-11.0000	-0.72695E-03	-0.27687E-03	-0.28391E+01	-0.14822E+01
2	-11.0000	-10.0000	-0.68715E-03	-0.25648E-03	-0.27042E+01	-0.13957E+01
3	-10.0000	-9.0000	-0.64737E-03	-0.23609E-03	-0.25693E+01	-0.13075E+01
4	-9.0000	-8.0000	-0.60762E-03	-0.21571E-03	-0.24263E+01	-0.12174E+01
5	-8.0000	-7.0000	-0.56789E-03	-0.19532E-03	-0.22830E+01	-0.11254E+01
6	-7.0000	-6.0000	-0.52818E-03	-0.17493E-03	-0.21374E+01	-0.10315E+01
7	-6.0000	-5.0000	-0.48850E-03	-0.15454E-03	-0.19889E+01	-0.93571E+00
8	-5.0000	-4.0000	-0.44884E-03	-0.13415E-03	-0.18378E+01	-0.83806E+00
9	-4.0000	-3.0000	-0.40920E-03	-0.11376E-03	-0.16840E+01	-0.73855E+00
10	-3.0000	-2.0000	-0.36959E-03	-0.93375E-04	-0.15274E+01	-0.63725E+00
11	-2.0000	-1.0000	-0.33000E-03	-0.72986E-04	-0.13682E+01	-0.53420E+00
12	-1.0000	-0.0	-0.29043E-03	-0.52597E-04	-0.12059E+01	-0.42951E+00
13	-0.0	1.0000	-0.25089E-03	-0.32207E-04	-0.10412E+01	-0.32324E+00
14	1.0000	2.0000	-0.21137E-03	-0.11817E-04	-0.87410E+00	-0.21458E+00
15	2.0000	3.0000	-0.17187E-03	0.85736E-05	-0.70514E+00	-0.10449E+00
16	3.0000	4.0000	-0.13240E-03	0.28964E-04	-0.55989E+00	0.18331E-02
17	4.0000	5.0000	-0.92946E-04	0.49355E-04	0.34622E+00	0.93623E-02
18	5.0000	6.0000	-0.53518E-04	0.69746E-04	-0.30203E-02	0.28890E+00
19	6.0000	7.0000	-0.14114E-04	0.90138E-04	0.41609E-01	0.35643E+00
20	7.0000	8.0000	0.25268E-04	0.11053E-03	0.20283E+00	0.40037E+00
21	8.0000	9.0000	0.64627E-04	0.13092E-03	0.33791E+00	0.42360E+00
22	9.0000	10.0000	0.10396E-03	0.15131E-03	0.36744E+00	0.41997E+00
23	10.0000	11.0000	0.14328E-03	0.17171E-03	0.41705E+00	0.41215E+00
24	11.0000	12.0000	0.18257E-03	0.19210E-03	0.41251E+00	0.40684E+00

STEEL REINFORCING LAYERS

LAYER NO.	START COORD	END COORD	DIRECTION	STRAIN	STRESS
1	-9.3458	-9.2542	1	-0.12905E-02	-0.38198E+02
2	9.2542	9.3458	1	-0.29155E-04	-0.86298E+00
3	-7.9529	-7.8471	2	-0.29850E-03	-0.88357E+01
4	7.8296	7.9704	2	0.39593E-04	0.11719E+01

NEGATIVE CONCRETE LAYERS

LAYER NO.	START COORD	END COORD	STRAIN1	STRAIN2	STRESS1	STRESS2
1	-9.3458	-9.2542	-0.63942E-03	-0.23202E-03	-0.25385E+01	-0.12897E+01
2	9.2542	9.3458	0.96098E-04	0.14723E-03	0.38750E+00	0.42050E+00
3	-7.9529	-7.8471	-0.58378E-03	-0.20347E-03	-0.23404E+01	-0.11624E+01
4	7.8296	7.9704	0.41015E-04	0.11863E-03	0.25612E+00	0.41512E+00

*** PRESTRESSING LAYERS ***

LAYER NO.	START COORD	END COORD	DIRECTION	STRAIN	STRESS
1	-0.0971	0.0971	1	0.50033E-02	0.14810E+03
2	-0.0971	0.0971	2	0.28244E-02	0.83601E+02

NEGATIVE CONCRETE LAYERS

LAYER NO.	START COORD	END COORD	STRAIN1	STRAIN2	STRESS1	STRESS2
1	-0.0971	0.0971	-0.27066E-03	-0.42402E-04	-0.11237E+01	-0.37665E+00
2	-0.0971	0.0971	-0.27066E-03	-0.42402E-04	-0.11237E+01	-0.37665E+00

DAMAGE SUMMARY

1. CONCRETE

DAMAGE TYPE	DEPTH OF DAMAGE	DIRECTION
INSIDE CRACKED	0.0	1
INSIDE CRACKED AND OPEN	0.0	1
INSIDE CRACKED	0.0	2
INSIDE CRACKED AND OPEN	0.0	2
OUTSIDE CRACKED	3.00	1
OUTSIDE CRACKED AND OPEN	3.00	1
OUTSIDE CRACKED	4.00	2
OUTSIDE CRACKED AND OPEN	4.00	2
INSIDE CRUSHED	0.0	
OUTSIDE CRUSHED	0.0	

2. REINFORCING STEEL

DAMAGE TYPE	LAYER NO.
-NO DAMAGE-	

3. PRESTRESSING STEEL

DAMAGE TYPE	LAYER NO.
-NO DAMAGE-	

RESULTS AFTER THERMAL EFFECTS

N1	-0.73557E-03	(STRAIN)	0.0		(STRAIN INCREMENT)
M1	-2523.38282	(LOAD)		0.0	(LOAD INCREMENT)
N2	-0.20769E-03	(STRAIN)	0.0		(STRAIN INCREMENT)
M2	-1361.97139	(LOAD)		0.0	(LOAD INCREMENT)

****

LOAD NUMBER 1

N1	26.12155	(LOAD)	25.00000	(LOAD INCREMENT)
M1	-0.38781E-04	(STRAIN)	0.79742E-05	(STRAIN INCREMENT)
N2	52.47508	(LOAD)	-20.46154	(LOAD INCREMENT)
M2	0.63900E-06	(STRAIN)	0.13053E-05	(STRAIN INCREMENT)

****

CONCRETE LAYERS

LAYER NO.	START COORD	END COORD	STRAIN1	STRAIN2	STRESS1	STRESS2
1	-12.0000	-11.0000	-0.60612E-03	-0.27152E-03	-0.24324E+01	-0.14485E+01
2	-11.0000	-10.0000	-0.57442E-03	-0.25245E-03	-0.23194E+01	-0.13644E+01
3	-10.0000	-9.0000	-0.54273E-03	-0.23338E-03	-0.22043E+01	-0.12792E+01
4	-9.0000	-8.0000	-0.51105E-03	-0.21431E-03	-0.20879E+01	-0.11925E+01
5	-8.0000	-7.0000	-0.47939E-03	-0.19523E-03	-0.19691E+01	-0.11044E+01
6	-7.0000	-6.0000	-0.44775E-03	-0.17615E-03	-0.18487E+01	-0.10150E+01
7	-6.0000	-5.0000	-0.41612E-03	-0.15707E-03	-0.17263E+01	-0.92412E+00
8	-5.0000	-4.0000	-0.38450E-03	-0.13799E-03	-0.16020E+01	-0.83194E+00
9	-4.0000	-3.0000	-0.35289E-03	-0.11891E-03	-0.14759E+01	-0.73844E+00
10	-3.0000	-2.0000	-0.32130E-03	-0.99824E-04	-0.13477E+01	-0.64368E+00
11	-2.0000	-1.0000	-0.28972E-03	-0.80737E-04	-0.12177E+01	-0.54770E+00
12	-1.0000	-0.0	-0.25815E-03	-0.61649E-04	-0.10855E+01	-0.45062E+00
13	-0.0	1.0000	-0.22660E-03	-0.42558E-04	-0.95152E+00	-0.35249E+00
14	1.0000	2.0000	-0.19506E-03	-0.23466E-04	-0.81591E+00	-0.25245E+00
15	2.0000	3.0000	-0.16354E-03	-0.43716E-05	-0.67875E+00	-0.15145E+00
16	3.0000	4.0000	-0.13203E-03	0.14724E-04	-0.55135E+00	-0.54669E-01
17	4.0000	5.0000	-0.10053E-03	0.33822E-04	0.31213E+00	-0.31888E-02
18	5.0000	6.0000	-0.69044E-04	0.52942E-04	0.48518E-02	0.19745E+00
19	6.0000	7.0000	-0.37572E-04	0.72023E-04	0.16527E-02	0.28975E+00
20	7.0000	8.0000	-0.61139E-05	0.91127E-04	0.40797E-02	0.38090E+00
21	8.0000	9.0000	0.25331E-04	0.11023E-03	0.16443E+00	0.47953E+00
22	9.0000	10.0000	0.56763E-04	0.12934E-03	0.0	0.0
23	10.0000	11.0000	0.88182E-04	0.14845E-03	0.0	0.0
24	11.0000	12.0000	0.11959E-03	0.16756E-03	0.0	0.0

STEEL REINFORCING LAYERS

LAYER NO.	START COORD	END COORD	DIRECTION	STRAIN	STRESS

1	-9.3458	-9.2542	1	-0.11874E-02	-0.35148E+02
2	9.2542	9.3458	1	-0.74775E-04	-0.22133E+01
3	-7.9529	-7.8471	2	-0.29789E-03	-0.88176E+01
4	7.8296	7.9704	2	0.19676E-04	0.58240E+00

NEGATIVE CONCRETE LAYERS

LAYER NO.	START COORD	END COORD	STRAIN1	STRAIN2	STRESS1	STRESS2
1	-9.3458	-9.2542	-0.53639E-03	-0.22956E-03	-0.21812E+01	-0.12619E+01
2	9.2542	9.3458	0.50478E-04	0.12552E-03	0.0	0.0
3	-7.9529	-7.8471	-0.49206E-03	-0.20286E-03	-0.20167E+01	-0.11397E+01
4	7.8296	7.9704	0.64658E-05	0.98769E-04	0.25217E-01	0.37446E+00

*** PRESTRESSING LAYERS ***

LAYER NO.	START COORD	END COORD	DIRECTION	STRAIN	STRESS
1	-0.0971	0.0971	1	0.50315E-02	0.14893E+03
2	-0.0971	0.0971	2	0.28147E-02	0.83314E+02

NEGATIVE CONCRETE LAYERS

LAYER NO.	START COORD	END COORD	STRAIN1	STRAIN2	STRESS1	STRESS2
1	-0.0971	0.0971	-0.24238E-03	-0.52104E-04	-0.10186E+01	-0.40177E+00
2	-0.0971	0.0971	-0.24238E-03	-0.52104E-04	-0.10186E+01	-0.40177E+00

DAMAGE SUMMARY

1. CONCRETE

DAMAGE TYPE	DEPTH OF DAMAGE	DIRECTION
INSIDE CRACKED	0.0	1
INSIDE CRACKED AND OPEN	0.0	1
INSIDE CRACKED	0.0	2
INSIDE CRACKED AND OPEN	0.0	2
OUTSIDE CRACKED	0.00	1
OUTSIDE CRACKED AND OPEN	0.00	1
OUTSIDE CRACKED	0.00	2
OUTSIDE CRACKED AND OPEN	0.00	2
INSIDE CRUSHED	0.0	
OUTSIDE CRUSHED	0.0	

2. REINFORCING STEEL

DAMAGE TYPE	LAYER NO.

-NO DAMAGE-

3. PRESTRESSING STEEL
DAMAGE TYPE
-NO DAMAGE-

LAYER NO.

SOLUTION TO LOAD NO. 1

N1	-0.70729E-03	(STRAIN)	0.28280E-04	(STRAIN INCREMENT)
M1	-2018.99212	(LOAD)	504.39070	(LOAD INCREMENT)
N2	-0.21739E-03	(STRAIN)	-0.57019E-05	(STRAIN INCREMENT)
M2	-1154.50689	(LOAD)	207.46450	(LOAD INCREMENT)